

**A Thesis Submitted for the Degree of PhD at the University of Warwick**

**Permanent WRAP URL:**

<http://wrap.warwick.ac.uk/130208>

**Copyright and reuse:**

This thesis is made available online and is protected by original copyright.

Please scroll down to view the document itself.

Please refer to the repository record for this item for information to help you to cite it.

Our policy information is available from the repository home page.

For more information, please contact the WRAP Team at: [wrap@warwick.ac.uk](mailto:wrap@warwick.ac.uk)

**COMPLEXATION OF EARLY- AND POST-  
TRANSITION METAL HALIDES WITH AZA-,  
OXA-, AND THIAMACROCYCLIC LIGANDS**

**Miles T. Lakin**

A thesis submitted for  
the degree of  
Doctor of Philosophy

Department of Chemistry  
University of Warwick

March 1993

To Marie and the kids

## CONTENTS

CONTENTS .....	i
LIST OF TABLES .....	iv
LIST OF FIGURES .....	vii
ACKNOWLEDGEMENTS .....	xii
DECLARATION .....	xiii
SUMMARY .....	xiv
PUBLICATIONS .....	xv
ABBREVIATIONS .....	xvi

### CHAPTER I

INTRODUCTION .....	- 1 -
1-1 BACKGROUND .....	- 2 -
1-2 CHARACTERISTICS OF MACROCYCLIC LIGANDS .....	- 3 -
1-3 POLYAZAMACROCYCLES .....	- 15 -
1-4 POLYOXAMACROCYCLES .....	- 21 -
1-5 POLYPHOSPHAMACROCYCLES .....	- 29 -
1-6 POLYTHIAMACROCYCLES .....	- 31 -
1-7 SYNTHESIS OF MACROCYCLIC LIGANDS .....	- 39 -

## CHAPTER 2

### SOME COORDINATION CHEMISTRY OF GROUP 15 TRIHALIDES

WITH THIAMACROCYCLIC LIGANDS . . . . .	- 45 -
2-1 SULFUR MACROCYCLE COMPLEXES OF P-BLOCK ELEMENTS . . . . .	- 46 -
2-2 SULFUR MACROCYCLE COMPLEXES OF ARSENIC, ANTIMONY, AND BISMUTH TRICHLORIDE . . . . .	- 48 -
2-3 TRENDS IN THIAETHER BONDING TO TERVALENT ANTIMONY AND BISMUTH . . . . .	- 72 -
2-4 CONFORMATIONAL CHANGES UPON THIAMACROCYCLE COMPLEXATION OF GROUP 15 TRICHLORIDES . . . . .	- 79 -
2-5 CONCLUSIONS . . . . .	- 87 -
2-6 EXPERIMENTAL . . . . .	- 88 -

## CHAPTER 3

### INVESTIGATIONS INTO THE COMPLEXATION OF EARLY TRANSITION

METAL HALIDES BY THIAMACROCYCLIC LIGANDS . . . . .	- 103 -
3-1 INTRODUCTION . . . . .	- 104 -
3-2 RESULTS AND DISCUSSION . . . . .	- 108 -
3-3 CONCLUSIONS . . . . .	- 121 -
3-4 EXPERIMENTAL . . . . .	- 122 -

## CHAPTER 4

### REACTIONS OF GROUP 15 TRIHALIDES WITH AZAMACROCYCLIC

LIGANDS	- 127 -
4-1 INTRODUCTION	- 128 -
4-2 RESULTS AND DISCUSSION	- 134 -
4-3 CONCLUSIONS	- 165 -
4-4 EXPERIMENTAL	- 166 -

## CHAPTER 5

### STABILISATION OF ANHYDROUS GROUP 3 CATIONIC SPECIES

BY OXAMACROCYCLIC LIGANDS	- 174 -
5-1 INTRODUCTION	- 175 -
5-2 RESULTS AND DISCUSSION	- 183 -
5-3 CONCLUSIONS AND FUTURE WORK	- 211 -
5-4 EXPERIMENTAL	- 213 -

REFERENCES	- 221 -
------------	---------

APPENDIX	- 233 -
----------	---------

## LIST OF TABLES

Table 1.1	Thermodynamics of formation of $M^{2+}$ complexes with $N_4$ ligands at 25 °C in $H_2O$ . . . . .	- 7 -
Table 1.2	Kinetic data for $Cu^{II}$ reacting with tetrathiaethers in 80% methanol at 25°, $\mu = 0.10 \text{ moldm}^{-3}$ ( $HClO_4$ ). . . . .	- 9 -
Table 2.1	Reported thiamacrocyclic complexes of p-block compounds. . . . .	- 47 -
Table 2.2	Summary of reactions undertaken between selected polythiamacrocycles and arsenic, antimony and bismuth trichloride. . . . .	- 48 -
Table 2.3	Physical and spectroscopic properties of $MCl_3 \cdot S$ -macrocyclic complexes ( $M = Sb, Bi$ ) and the free ligands. . . . .	- 49 -
Table 2.4	Change in chemical shift ( $-CH_2CH_2-$ ) of $MCl_3 \cdot S$ -macrocyclic complexes ( $M = Sb, Bi$ ) from that recorded for the free ligand ( $\Delta\delta$ ). . . . .	- 51 -
Table 2.5	Selected bond lengths (Å) and angles (°) for $SbCl_3 \cdot 9S3$ . . . . .	- 54 -
Table 2.6	Selected bond lengths (Å) and angles (°) for $18S6 \cdot 2SbCl_3$ . . . . .	- 58 -
Table 2.7	Selected bond lengths (Å) and angles (°) for $BiCl_3 \cdot 12S4$ . . . . .	- 62 -
Table 2.8	Selected bond lengths (Å) and angles (°) for $BiCl_3 \cdot 15S5 \cdot \frac{1}{2}MeCN$ . . . . .	- 66 -
Table 2.9	Selected bond lengths (Å) and angles (°) for $BiCl_3 \cdot 18S6$ . . . . .	- 71 -
Table 2.10	Structurally characterised Group 15-crown ether complexes. . . . .	- 73 -
Table 2.11	Comparison of standard van der Waals and covalent $M-X$ separations (Å) ( $M = Sb, Bi$ ; $X = O, S, Cl$ ). . . . .	- 75 -
Table 2.12	Selected mean distances (Å) and angles (°) about the metal atom in antimony and bismuth trichlorides and their thiamacrocyclic complexes. . . . .	- 76 -

Table 2.13	Mean bond lengths (Å), mean bond angles (°), and torsion angles (°) for selected thiamacrocycles and the ligands of group 15 trichloride-thiamacrocyclic complexes. . . . .	- 80 -
Table 2.14	Strain energy calculations (kcal.mol <sup>-1</sup> ) for various thiamacrocycles and for the ligands in group 15 trichloride-thiamacrocyclic complexes. . . . .	- 82 -
Table 2.15	Estimated macrocycle distortion energy upon complexation for the thiamacrocycle complexes of antimony and bismuth trichloride. . . . .	- 85 -
Table 2.16	Crystallographic data for SbCl <sub>3</sub> ·9S3 . . . . .	- 93 -
Table 2.17	Crystallographic data for (SbCl <sub>3</sub> ) <sub>2</sub> ·18S6 . . . . .	- 95 -
Table 2.18	Crystallographic data for BiCl <sub>3</sub> ·12S4. . . . .	- 97 -
Table 2.19	Crystallographic data for BiCl <sub>3</sub> ·15S5·½MeCN. . . . .	- 99 -
Table 2.20	Crystallographic data for BiCl <sub>3</sub> ·18S6. . . . .	- 101 -
Table 3.1	Summary of transition metals complexed by homoleptic polythiaether macrocycles. . . . .	- 105 -
Table 3.2	Selected bond lengths (Å) and angles (°) for VOCl <sub>2</sub> (9S3). . . . .	- 120 -
Table 3.3	Crystallographic data for VOCl <sub>2</sub> ·9S3. . . . .	- 125 -
Table 4.1	Diagrammatic representations and nomenclature used to classify the five distinct isomers of cyclam and its tetra-N-substituted derivatives. . . . .	- 131 -
Table 4.2	Bond lengths (Å) and angles (°) for the compound [H <sub>2</sub> (TMC)][Sb <sub>2</sub> OCl <sub>4</sub> ] <sup>2</sup> . . . . .	- 139 -
Table 4.3	Comparison of mean interatomic distances (Å) for [Sb <sub>2</sub> OCl <sub>4</sub> ] <sup>2-</sup> based species. . . . .	- 142 -
Table 4.4	Comparison of interatomic distances (Å) and angles (°) for [Sb <sub>2</sub> OCl <sub>4</sub> ] <sup>2-</sup> based species. . . . .	- 142 -



Table 4.5	Bond lengths (Å) and angles (°) for the compound [H <sub>2</sub> (TMC)][As <sub>4</sub> O <sub>2</sub> Cl <sub>10</sub> ] <sup>2-</sup> . . . . .	146 -
Table 4.6	Comparison of interatomic distances (Å) for [As <sub>2</sub> OCln] <sup>3-</sup> based species. . . . .	149 -
Table 4.7	Basicity constants of selected tetramines at 25-0 °C. . . . .	150 -
Table 4.8	Bond lengths (Å) and angles (°) for tetra-N-methylcyclam. . . . .	153 -
Table 4.9	Selected bond lengths (Å) of neutral and protonated TMC and cyclam structures. . . . .	161 -
Table 4.10	Strain energy calculations (kcal mol <sup>-1</sup> ) for the solid state isomers of TMC and its diprotonated cations. . . . .	162 -
Table 4.11	Crystallographic data for [H <sub>2</sub> (TMC)][As <sub>4</sub> O <sub>2</sub> Cl <sub>10</sub> ]. . . . .	168 -
Table 4.12	Crystallographic data for [H <sub>2</sub> (TMC)][Sb <sub>2</sub> OCln]. . . . .	170 -
Table 4.13	Crystallographic data for tetramethylcyclam. . . . .	172 -
Table 5.1	Summary of reactions conducted between rare earth trichlorides, crown ethers and antimony pentachloride. . . . .	183 -
Table 5.2	Bond lengths (Å) and angles (°) for [SbCl <sub>2</sub> (18O6)][SbCl <sub>4</sub> ]. . . . .	194 -
Table 5.3	Ionic radius comparison (Å) for M <sup>3+</sup> (M = Sc, Y, La, Yb). . . . .	200 -
Table 5.4	Bond lengths (Å) and angles (°) for [ScCl <sub>2</sub> (Bz15O5)][SbCl <sub>4</sub> ]. . . . .	207 -
Table 5.5	Crystallographic data for [ScCl <sub>2</sub> (18O6)][SbCl <sub>4</sub> ]. . . . .	217 -
Table 5.6	Crystallographic data for [ScCl <sub>2</sub> (Bz15O5)][SbCl <sub>4</sub> ]. . . . .	219 -

## LIST OF FIGURES

Figure 1.1	Log $K$ vs cation radius for $M^{2+} + L \rightarrow [ML]^{2+}$ ( $H_2O$ , $25^\circ C$ ); $L =$ dicyclohexyl18O6 isomer A ( $\circ$ ), and isomer B ( $\blacksquare$ ). From ref. 19.	- 10 -
Figure 1.2	Variation of complex stability as a function of macrocyclic ring size.	- 13 -
Figure 1.3	Derivation of minimum strain energy forms for five- and six-membered chelate rings.	- 14 -
Figure 1.4	The nickel(II) mediated Schiffs base condensation of Curtis.	- 15 -
Figure 1.5	An early macrocycle synthesis of the type used by Busch to elucidate the <i>kinetic template effect</i> .	- 16 -
Figure 1.6	Dibenzo[b,i]-1,4,8,11-tetraazacyclotetradec-2,4,6,9,11-hexaenato(2-) macrocyclic dianion.	- 18 -
Figure 1.7	Side view of TMTAA showing the saddle shape.	- 19 -
Figure 1.8	Structure of monoprotonated 1,4,7-trimethyl-1,4,7-triazacyclononane.	- 20 -
Figure 1.9	Selected classes of polyoxamacrocycle.	- 22 -
Figure 1.10	Pedersen's reaction that lead to the first synthesis of a crown ether.	- 21 -
Figure 1.11	Structure of 18O6 ( $C_i$ point symmetry).	- 24 -
Figure 1.12	Structure of 18O6 when complexed to $K^+$ ( $D_{3h}$ point symmetry).	- 25 -
Figure 1.13	[2.2.2]-cryptand and 18-crown-6.	- 26 -
Figure 1.14	The nitrogen configurations of macrobicyclic ligands.	- 27 -
Figure 1.15	Crystal structure of [222] cryptand.	- 27 -
Figure 1.16	The first homoleptic tetraphosphine macrocycle.	- 29 -

Figure 1.17	Representation of the first crystallographically characterised polyphosphamacrocyclic. . . . .	- 30 -
Figure 1.18	Molecular structure of 1,4,7-trithiacyclononane. . . . .	- 34 -
Figure 1.19	Molecular structure of 1,4,7,10-tetrathiacyclododecane. . . . .	- 35 -
Figure 1.20	Molecular structure of 1,4,8,11-tetrathiacyclotetradecane. . . . .	- 36 -
Figure 1.21	Molecular structure of 1,4,7,10,13-pentathiacyclopentadecane. . . . .	- 37 -
Figure 1.22	Molecular structure of 1,4,7,10,13,16-hexathiacyclooctadecane. . . . .	- 38 -
Figure 1.23	Preparation of 1,4,7-trithiacyclononane. . . . .	- 40 -
Figure 1.24	Preparation of 1,4,8,11-tetrathiacyclotetradecane. . . . .	- 41 -
Figure 1.25	Preparation of 1,4,7-triazacyclononane. . . . .	- 42 -
Figure 1.26	Preparation of 1,4,8,12-Tetraazacyclopentadecane. . . . .	- 43 -
Figure 1.27	Preparation of dibenzo-18-crown-6 and dicyclohexyl-18-crown-6. . . . .	- 44 -
Figure 2.1	Molecular structure of $\text{SbCl}_3 \cdot 9\text{S}_3$ . . . . .	- 53 -
Figure 2.2	Two representations of the antimony coordination sphere in $\text{SbCl}_3 \cdot 9\text{S}_3$ . . . . .	- 55 -
Figure 2.3	Molecular structure of $18\text{S}6 \cdot 2\text{SbCl}_3$ . . . . .	- 57 -
Figure 2.4	The antimony coordination sphere in the complex $18\text{S}6 \cdot 2\text{SbCl}_3$ . . . . .	- 59 -
Figure 2.5	Molecular structure of $\text{BiCl}_3 \cdot 12\text{S}_4$ . . . . .	- 61 -
Figure 2.6	Diagram showing the coordination sphere around the bismuth atom in $\text{BiCl}_3 \cdot 12\text{S}_4$ , viewed normal to the $\text{S}_4$ plane. . . . .	- 63 -
Figure 2.7	Molecular structure of $\text{BiCl}_3 \cdot 15\text{S}_5$ . . . . .	- 65 -
Figure 2.8	Two views of the bicapped trigonal prismatic coordination sphere about bismuth in the compound $\text{BiCl}_3 \cdot 15\text{S}_5$ (molecule 1 shown). . . . .	- 67 -
Figure 2.9	Molecular structure of $\text{BiCl}_3 \cdot 18\text{S}_6$ . . . . .	- 69 -

Figure 2.10	The bismuth coordination sphere in $\text{BiCl}_3 \cdot 18\text{S6}$ viewed (a) perpendicular to the three-fold axis and (b) down the three-fold axis.	- 70 -
Figure 3.1	Postulated structures for the complex $\text{TiCl}_4 \cdot 9\text{S3}$ .	- 111 -
Figure 3.2	Infrared spectra of $[\text{TiCl}_4(\text{MeCN})_2]$ and $\text{TiCl}_4 \cdot 9\text{S3}$ (upper and lower spectrum respectively).	- 112 -
Figure 3.3	Postulated structure of the complex $\text{TiCl}_3 \cdot 9\text{S3}$ .	- 114 -
Figure 3.4	Infrared spectra of $[\text{TiCl}_3(\text{MeCN})_2]$ and $\text{TiCl}_3 \cdot 9\text{S3}$ (upper and lower spectrum respectively).	- 115 -
Figure 3.5	Two views of the molecule $[\text{VOCl}_2(9\text{S3})]$ .	- 119 -
Figure 4.1	Representation of the two nickel(II)-TMC isomers; 'all Me's up' - (A), and 'two up two down' with $C_2$ axis bisecting ethyl links - (B).	- 129 -
Figure 4.2	Two views of the oxo-bridged anion $[\text{Sb}_2\text{O}_7\text{Cl}_4]^{3-}$ .	- 138 -
Figure 4.3	Perspective view of the centrosymmetric anion $[\text{Sb}_2\text{O}_7\text{Cl}_6]^{4-}$ .	- 141 -
Figure 4.4	Relationship between bridging and terminal As-Cl bond lengths in the anion of $[\text{H}_2(\text{TMC})][\text{As}_4\text{O}_7\text{Cl}_{10}]$ .	- 144 -
Figure 4.5	Structure of the polyarsa-anion $[\text{As}_4\text{O}_7\text{Cl}_{10}]^{2-}$ .	- 145 -
Figure 4.6	Perspective view of the oxo-bridged anionic anion in the compound $[\text{cp}_2\text{Fe}]_2[\text{As}_4\text{O}_7\text{Cl}_{10}]$ .	- 148 -
Figure 4.7	Perspective view of the oxo-bridged arsenic anion in $[\text{Hpy}]_2[\text{As}_2\text{OCl}_4]$ .	- 148 -
Figure 4.8	Location of methyl groups relative to the $N_4$ plane for molecules 1 and 2 of tetramethylcyclam.	- 151 -
Figure 4.9	Views of TMC molecules 1 and 2 with atomic numbering.	- 152 -
Figure 4.10	Two views of the cation $(R\bar{S}R\bar{S})$ in the compound $[\text{H}_2(\text{TMC})][\text{As}_4\text{O}_7\text{Cl}_{10}]$ .	- 156 -

Figure 4.11	Two views of the cation (RRSS) in the compound [H <sub>2</sub> (TMC)][Sb <sub>2</sub> OCln]. . . . .	157 -
Figure 4.12	Directionality of assumed nitrogen lone pairs in the mesodentate conformations of a) TMC (RSSR), and b) TMC (RRSS). . . . .	160 -
Figure 4.13	Strain energy v. H-bond N-N separation in RSRS [H <sub>2</sub> (TMC)] <sup>2+</sup> . . . .	163 -
Figure 5.1	Schematic representation of 1) bridged-intermediate, 2) self-ionisation, limiting case mechanisms for halide abstraction by antimony pentachloride. . . . .	179 -
Figure 5.2	Likely structure of the complexes [M(18O6)(MeCN) <sub>3</sub> ] <sup>1+</sup> , M = Y, La (donor nitrogen atoms only shown for MeCN molecules). . . . .	186 -
Figure 5.3	<sup>1</sup> H NMR spectra obtained by reaction of scandium(III) chloride/18O6 with one, two and three equivalents antimony pentachloride. . . . .	188 -
Figure 5.4	<sup>1</sup> H NMR spectrum of [ScCl <sub>2</sub> (18O6)][SbCl <sub>5</sub> ] at 213 K (acetone-d <sub>6</sub> ). . .	189 -
Figure 5.5	<sup>1</sup> H NMR spectrum of [ScCl <sub>2</sub> (18O6)][SbCl <sub>5</sub> ] at 183 K (in acetone-d <sub>6</sub> ). .	190 -
Figure 5.6	Molecular structure of the cation [ScCl <sub>2</sub> (18O6)] <sup>+</sup> (molecule 1). . . .	193 -
Figure 5.7	<sup>1</sup> H NMR spectra obtained by reaction of scandium(III) chloride/15O5 with one, two and three equivalents of antimony pentachloride. . . .	197 -
Figure 5.8	<sup>12</sup> C and <sup>1</sup> H NMR spectra obtained for the compound [ScCl <sub>2</sub> (Bz15O5)][SbCl <sub>5</sub> ]. . . . .	198 -
Figure 5.9	The [YbCl <sub>2</sub> (15O5)] <sup>+</sup> cation - likely to be isostructural with [ScCl <sub>2</sub> (15O5)] <sup>+</sup> . . . . .	199 -
Figure 5.10	Molecular structure of [ScCl <sub>2</sub> (Bz15O5)] <sup>+</sup> , viewed down onto O <sub>4</sub> plane. . . . .	204 -
Figure 5.11	Molecular structure of [ScCl <sub>2</sub> (Bz15O5)] <sup>+</sup> , viewed parallel to O <sub>3</sub> plane. . . . .	205 -

Figure 5.12 Diagrams showing a) scandium coordination geometry, b)  
hexachloroantimonate(V), in the compound  $[\text{ScCl}_2(\text{Bz}15\text{O}5)][\text{SbCl}_6]$ . - 206 -

Figure 5.13  $^1\text{H}$  NMR spectra resulting from the reaction of scandium(III) chloride  
and 12O4 with a) one, b) three equivalents antimony pentachloride. - 210 -

## ACKNOWLEDGEMENTS

My deepest thanks must go to that eternal optimist Gerald Willey, whose indefatigable enthusiasm must serve as a model to us all. I am extremely grateful to Dr. N. W. Alcock for taking the trouble to train me in the use of the diffractometer. I must thank Dr. C. J. Samuel for introducing me to 'chemistry by computer'. Finally, funding of the studentship by the SERC is gratefully acknowledged.

## DECLARATION

The work submitted in this thesis is my own and was conducted in the Chemistry Department at the University of Warwick. The studies involving TMC and the trichlorides of arsenic, antimony, and bismuth were conducted with the assistance of Mr. A. Assad, whilst under my direction of his final year project.



## SUMMARY

Reaction of  $MCl_3$  ( $M = As, Sb, Bi$ ) with the homoleptic polythiamacrocycles 9S3, 12S4, 15S5, and 18S6 has lead to the isolation of the molecular adducts  $SbCl_3 \cdot 9S3$  (1),  $SbCl_3 \cdot 15S5$  (2),  $(SbCl_3)_2 \cdot 18S6$  (3),  $BiCl_3 \cdot 9S3 \cdot \frac{1}{2}MeCN$  (4),  $BiCl_3 \cdot 12S4$  (5),  $BiCl_3 \cdot 15S5 \cdot \frac{1}{2}MeCN$  (6),  $BiCl_3 \cdot 18S6$  (7). The solid state structures of (1), (3), (5), (6), and (7) have been determined by single crystal X-ray diffraction methods; weak metal-sulfur bonding being confirmed. Trends in complex stability have been appraised in terms of bound-ligand strain energy using Molecular Mechanics calculations.

Investigations into the coordination chemistry of  $MCl_3$  ( $M = Sc, Ti, V$ ) and  $TiCl_4$  with 9S3 have lead to the formation of  $TiCl_4 \cdot 9S3$  (8),  $TiCl_3 \cdot 9S3$  (9), and  $[VOCl_2(9S3)]$  (10). The latter, an unexpected oxidation product, has been structurally characterised using single crystal X-ray diffraction; facial binding by the 9S3 yields a distorted octahedral vanadium coordination geometry.

Reaction of  $MCl_3$  ( $M = As, Sb, Bi$ ) with TMC has lead to hydrolysis of the metal halide. Mediation of the hydrolysis reaction has permitted the compounds  $[H_2(TMC)][Sb_2OCl_4]$  (11), and  $[H_2(TMC)][As_2O_7Cl_{10}]$  (12) to be deposited in a crystalline form. The nature of (11) and (12) has been established using single crystal X-ray diffraction techniques. The anions have been compared with other, closely related, species. The diprotonated cations of TMC exhibit the sequential stereochemistry RRSS (11) and RSRs (12). The single crystal X-ray structure of the parent macrocycle, TMC, has been determined and found to comprise of independent molecules with sequential stereochemistry RSSR and RRSS. Geometric and strain energy trends have been considered for the neutral and protonated forms of TMC and cyclam.

The use of antimony pentachloride as a halide abstraction agent from  $MCl_3$  ( $M = Sc, Y, La$ ) has facilitated the generation of a variety of cationic species, depending upon the reaction stoichiometry used. These cations have been stabilised using the macrocycles 12O4, 15O5, Bz15O5 and 18O6 to allow isolation of the compounds  $[ScCl_2(MeCN)(12O4)][SbCl_4]$  (13),  $[ScCl_2(15O5)][SbCl_4]$  (14),  $[ScCl_2(Bz15O5)][SbCl_4]$  (15),  $[ScCl_2(18O6)][SbCl_4]$  (16),  $[Y(MeCN)_3(12O4)][SbCl_4]$  (17),  $[Y(MeCN)_3(18O6)][SbCl_4]$  (18),  $[La(MeCN)_3(12O4)][SbCl_4]$  (19), and  $[La(MeCN)_3(18O6)][SbCl_4]$  (20). The single crystal X-ray structures of (15) and (16) both show a pentagonal bipyramidal geometry around scandium with the crown ether providing an equatorial girdle and the two chlorine atoms assuming the axial positions.

## PUBLICATIONS

Parts of the work reported in this thesis have been published or accepted for publication in the scientific literature:

- 1) "Crown thioether complexes of p-block elements: Crystal and molecular structures of  $\text{SbCl}_4 \cdot 9\text{S3}$ ,  $2\text{SbCl}_4 \cdot 18\text{S6}$ ."  
G. R. Willey, M. T. Lakin, M. Ravindran, and N. W. Alcock, *J. Chem. Soc., Chem. Commun.*, 1991, 271.
- 2) "Unexpected crown thioether complexation of Vanadium(IV): Isolation and structural characterisation of  $[\text{VOCl}_2(9\text{S3})]$  ( $9\text{S3} = 1,4,7\text{-trithiacyclononane}$ )."  
G. R. Willey, M. T. Lakin, and N. W. Alcock, *J. Chem. Soc., Chem. Commun.*, 1991, 1414.
- 3) "Synthesis and crystallographic studies of crown thioether complexes of bismuth(III)."  
G. R. Willey, M. T. Lakin, and N. W. Alcock, *J. Chem. Soc., Dalton Trans.*, 1992, 591.
- 4) "Synthesis and molecular structure of the adduct Trichlorobismuth-(1,4,7,10,13,16-hexathiaclooctadecane)."  
G. R. Willey, M. T. Lakin, and N. W. Alcock, *J. Chem. Soc., Dalton Trans.*, 1992, 1339.
- 5) "Unusual crown ether encapsulation of a chloro-scandium(III) cation. Structure of threaded  $[\text{ScCl}_2(18\text{crown6})][\text{SbCl}_4]$ ."  
G. R. Willey, M. T. Lakin, and N. W. Alcock, *J. Chem. Soc., Chem. Commun.*, 1992, 1619.
- 6) "Group 15-azamacrocyclic chemistry. A study of the reactions of 1,4,8,11-tetramethyl-1,4,8,11-tetraazacyclotetradecane with  $\text{MCl}_3$  ( $\text{M} = \text{As}, \text{Sb}$ ): Crystal and molecular structure of  $[(\text{TMC})_2][\text{As}_2\text{O}_7\text{Cl}_{10}]$  (I) and  $[(\text{TMC})_2][\text{Sb}_2\text{O}_7\text{Cl}_8]$  (II). [ $\text{TMC} = 1,4,8,11\text{-tetramethyl-1,4,8,11-tetraazacyclotetradecane}$ ]."  
G. R. Willey, A. Asab, M. T. Lakin, and N. W. Alcock, *J. Chem. Soc., Dalton Trans.*, 1993, 365.
- 7) "Energy and structural relationships for a tetraazamacrocyclic in its neutral and protonated forms: The conformation of 1,4,8,11-tetramethyl-1,4,8,11-tetraazacyclotetradecane."  
G. R. Willey, M. T. Lakin, N. W. Alcock and C. J. Samuel, submitted for publication in *J. Incl. Phenom.*, 1993.

## ABBREVIATIONS

9S3	1,4,7-trithiacyclononane
12S4	1,4,7,10-tetrathiacyclododecane
14S4	1,4,8,11-tetrathiacyclotetradecane
16S4	1,5,9,13-tetrathiacyclohexadecane
20S4	1,6,11,16-tetrathiacycloicosane
15S5	1,4,8,11,13-pentathiacyclopentadecane
18S6	1,4,7,10,13,16-hexathiacyclooctadecane
THT	tetrahydrothiophene
edt	ethane-1,2-dithiolate
pdt	propane-1,3-dithiolate
12O4	1,4,7,10-tetraoxacyclododecane
15O5	1,4,8,11,13-pentaoxacyclopentadecane
18O6	1,4,7,10,13,16-hexaoxacyclooctadecane
24O8	24-crown-9
30O10	30-crown-10
Bz15O5	Benzo-15-crown-5
TMC	1,4,8,11-tetramethyl-1,4,8,11-tetraazacyclotetradecane
cyclam	1,4,8,11-tetraazacyclotetradecane
2,3,2-tet	1,4,8,11-tetrazaundecane
py	pyridine
cp	cyclopentadienyl
MeCN	acetonitrile
DMSO	dimethylsulfoxide
THF	tetrahydrofuran
I.R.	infra-red
NMR	nuclear magnetic resonance
u.v./vis.	ultra violet/visible
$\lambda$	wavelength
$\nu$	frequency

## **CHAPTER ONE**

### **INTRODUCTION**

## BACKGROUND

The foundations of modern coordination chemistry were conceived by Alfred Werner, with a flash of inspiration, according to contemporary accounts, one night in 1892.<sup>1</sup> These innovative concepts were published in his most famous paper 'Beitrag zur Konstitution anorganischer Verbindungen'<sup>2</sup> (Contribution to the Constitution of Inorganic Compounds). He was just 26 years old and would go on to receive the 1913 Nobel Prize in chemistry for "his work on the linkage of atoms in molecules, by which he has thrown fresh light on old problems and opened new fields of research, particularly in inorganic chemistry".<sup>3</sup>

Werner was first to synthesise and recognise the significance of metal chelate compounds. The application of his coordination theory to complexes suggested the existence of chelate rings and their significance to the stereochemistry of coordination compounds. From this beginning, the high relative stability of chelate compounds became qualitatively established.

Remarkably, although suitable synthetic macrocyclic ligands had been prepared as early as 1936,<sup>4</sup> it was not until the early 1960's that the first systematic studies of these multidentate chelating ligands were conducted.<sup>5</sup> Since that time, macrocyclic chemistry has seen such great expansion that a wide variety of applications have emerged, e.g. ion selective electrodes,<sup>6</sup> anion activation in organic syntheses,<sup>7</sup> and modelling of biologically active molecules. The significance of macrocyclic ligands was acknowledged in 1987 when the Nobel Prize in chemistry was awarded to three leading exponents in the field; Charles Pedersen, Donald Cram and Jean-Marie Lehn.<sup>8</sup>

The work described in this thesis has applied polyaza-, polythia-, and polyoxamacrocycles to a variety of novel circumstances thereby extending the range of their known utility.

A macrocyclic ligand is generally defined as a cyclic compound with nine or more members (including hetero atoms) and with three or more donor atoms available for binding. Those macrocycles in common use predominantly have two or three methylene linkages between donor groups. The intense interest in macrocycles as complexing agents can be attributed to the extraordinary stability of their cation complexes, up to ten times that of acyclic analogues, and their peculiar ability to selectively bind certain cations in preference to others. Additionally, they can provide coordination spheres around metal ions that are not obtainable by other routes so leading to unique structural, kinetic, thermodynamic, electronic and redox properties. With careful design of the macrocycle, it is possible to tailor the properties of a complexed ion to match predetermined requirements.

Macrocycles are known to bind a wide variety of species including metal ions, neutral polar molecules, protonated amines, and, in special cases, anions. The factors influencing the formation and thermodynamic stabilities of complexes between macrocycles and ions have been identified:<sup>9</sup>

- 1) Relative sizes of the ion and macrocyclic cavity.
- 2) The physical placement of the binding sites.
- 3) Steric hindrance in the ring.
- 4) The number of binding sites in the ring.
- 5) The types of binding site in the ring.
- 6) Solvation of the ion and donor sites.
- 7) Electric charge on the ion.

The first two factors have been the attention of many detailed studies and will be considered further. The other five factors are self-explanatory. An introduction to six features, pertinent to this general overview of macrocyclic chemistry, will now follow.

## The Chelate Effect

Before moving to an examination of the macrocyclic effect, it is first worth considering the basis for the superior binding power of chelating ligands. The thermodynamic chelate effect (c.e.) for an  $n$ -dentate chelating ligand refers to the thermodynamics of the reaction where the chelating ligand replaces  $n$  unidentate analogues about a metal centre. It is defined as the ratio of stability constants for the chelate complex,  $M(\text{chel})$ , to that of the closest unidentate analogue,  $M(L)_n$ :

$$\log \text{c.e.} = \log K_{M(\text{chel})} - \log K_{M(L)_n}$$

This is equivalent to the equilibrium constant for the reaction:



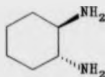
$$K = \frac{[M(\text{chel})][L]^n}{[M(L)_n][\text{chel}]} = \text{c.e.}$$

The various factors that can be considered when rationalising the chelate effect include:

- 1) Poorer solvation of chelate donor atoms
- 2) The *electrostatic* penalty of moving donor atoms into close proximity is largely paid during the synthesis of chelate ligands.

- 3) Chelates may have a *conformation* pre-organised for complexation.

e.g.



Ring imposes gauche arrangement of donor atoms.

Donor atoms may be gauche or anti.

- 4) The increased translational *entropy* following the liberation of unidentate ligands into solution.

### The Macrocyclic Effect

Although the chelate effect has been recognised since the time of Werner, the superiority of macrocyclic ligands over their linear counterparts was first reported by Margerum in 1969.<sup>10,11</sup> The macrocyclic effect (m.e.) is defined as the ratio of stability constants for the macrocyclic complex,  $M(\text{macr})$  to its closest acyclic analogue,  $M(\text{lin})$ :

$$\log \text{m.e.} = \log K_{M(\text{macr})} - \log K_{M(\text{lin})}$$

This is equivalent to the equilibrium constant for the reaction:



$$K = \frac{[M(\text{macr})][\text{lin}]}{[M(\text{lin})][\text{macr}]} = \text{m.e.}$$




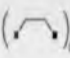




Despite the almost universal occurrence of the macrocyclic effect, its specific thermodynamic origin is subject to some controversy. Some specimen results are given in Table 1.1 to illustrate the conflicting nature of the reports.

The results of Hinz and Margerum show a macrocyclic effect of some  $7 \log K$  units. Their work lead to the proposition that this macrocyclic effect is enthalpic in origin and to the rejection of an explanation in terms of changes in translational entropy. Conversely, the investigations of Paoletti *et al* into copper(II) systems produced the conclusion that only entropic contributions were important. The debate has continued with many papers being published. Examination of a more contemporary report<sup>12</sup> shows that some of the earlier thermodynamic measurements may have been somewhat erroneous but confirms that enthalpy is the major contributor to the macrocyclic effect. The following factors should be considered to underlie the influence of each term:

- 1) A favourable entropic term can be interpreted as the loss of possible conformations upon complexation of an acyclic ligand. For a macrocycle, the existing conformational constraints lead to a reduced loss of entropy upon complexation.
- 2) A favourable enthalpic term can be ascribed to the pre-organisation of cyclic ligands with the donor atoms presented at optimal positions and orientations towards the metal ion so as to maximise orbital overlap, whilst simultaneously remaining in a low energy conformation.
- 3) The poor solvation of the donor atoms in the restricted cavities of macrocycles will augment the enthalpic term of the macrocyclic effect.

Table 1.1 Thermodynamics of formation of  $M^{2+}$  complexes with  $N_6$  ligands at 25 °C in  $H_2O$ .

Ligand	Metal ion	$\log K$	$\Delta H / kJmol^{-1}$	$T\Delta S / kJmol^{-1}$
 2,3,2-tet	$Ni^{2+}$	15.3	-70	17
 cyclam	$Ni^{2+}$	22.2	-130	-3
 Me <sub>2</sub> -cyclam	$Ni^{2+}$	21.9	-117	10
 en	$Cu^{2+}$	19.7	-105	7.1
 2,2,2-tet	$Cu^{2+}$	20.1	-90	24
 cyclen	$Cu^{2+}$	24.8	-77	64

When examining investigations into the macrocyclic effect it should be recalled that the 2° donors of the cyclic compounds will be stronger donors than the 1° donors often found in the acyclic analogues, i.e. inductive effects upon addition of bridging groups.

### Kinetic Contributions to the Macrocyclic Effect


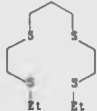
The term "*multiple juxtapositional fixedness*" has been used to describe the stability of macrocyclic complexes from a kinetic viewpoint.<sup>13</sup> The results shown in Table 1.2 clearly illustrate the far greater decomposition rate of the acyclic ligands.<sup>14</sup>

It is hypothesised that the straight-chain ligand is able to undergo sequential S<sub>N</sub>1 replacements of the ligand donor atoms commencing at one end. In contrast, the relative rigidity of the complexed cyclic ligands is thought to result in an apparent increase in the difficulty of sequentially cleaving the metal-donor atom bonds. This concept can accommodate the elevated stability of macrocyclic ligands in cases where the metal ion is bound outside the ring cavity.

### The Reverse Macrocyclic Effect

Contrary to findings for the chelate effect, the stability of a macrocyclic complex is not always superior to that of the open-chain analogue. A reverse macrocycle effect has been witnessed for the relative stability of [Hg(16S4)]<sup>2+</sup>.<sup>15</sup> The molecule has minimal strain energy in the 16-membered ring, as witnessed by the small average deviation from the strain-free values of the torsion angles. Nevertheless, the mercury(II) ion is more strongly bound

**Table 1.2** Kinetic data for  $\text{Cu}^{\text{II}}$  reacting with tetrathiaethers in 80% methanol at  $25^\circ$ ,  $\mu = 0.10 \text{ mol dm}^{-3}$  ( $\text{HClO}_4$ ).

Ligand	$k_f / \text{s}^{-1}$	$k_r / \text{s}^{-1}$
 14S4	$2.8 \times 10^4$	9
 Bu <sub>4</sub> TTU	$4.1 \times 10^4$	$3.0 \times 10^4$

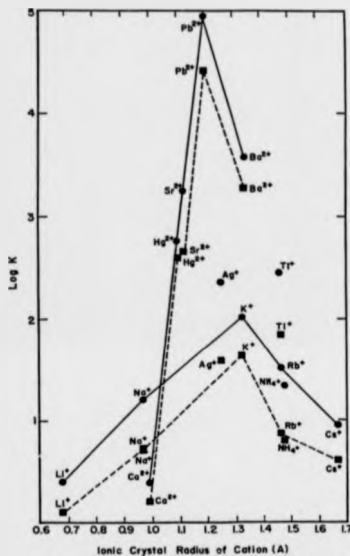
by the acyclic tetrathia ligands 3,6,10,13-tetrathiapentadecane and 2,5,9,12-tetrathiatridecane than to the macrocyclic compounds 14S4, 15S4, 16S4, 18S4 and 20S4.

### Relative Sizes of the Ion and the Macrocyclic Cavity

The concept of size-match selectivity is most strongly supported by the formation constants of crown ethers for a given cavity diameter. Extensive studies have been conducted for the

reaction of mono- and dications with the two isomers of dicyclohexyl-1806 in aqueous solution<sup>16,17</sup>. The results are shown graphically in Figure 1.1.

**Figure 1.1** Log  $K$  vs cation radius for  $M^{n+} + L \rightarrow [ML]^n$  ( $H_2O$ ,  $25^\circ C$ );  $L$  = dicyclohexyl1806 isomer A ( $\circ$ ), and isomer B ( $\blacksquare$ ). From ref. 19.



It is clear from these results that there are optimum radii for both monovalent and divalent cations. The change of log  $K$  with cation radius is smaller in the case of the monovalent ions. For the case of lead(II) and calcium(II) the difference in stability constants with dicyclohexyl-

18O6 is approximately  $10^3$ . Neither ligand isomer has measurable affinity in water for either cadmium(II) or zinc(II), but both have a high affinity for mercury(II). An exhaustive compilation of  $\log K$ ,  $\Delta H$ , and  $\Delta S$  data for coronand and cryptand complexes with alkali, alkaline earth, transition-metal, post transition-metal and organic cations has been prepared<sup>18</sup>. It has been suggested that a primary reason for the lower stability of complexes formed between dicyclohexyl-18O6 and cations larger than the optimum size is that these cations are too large to "fit" into the ligand cavity. Other factors can also rationalise the observations *i.e.* changes in metal-oxygen bond strength and cation solvation energies. Many early works propounded the concept of oxa-crown cavity/cationic radius matching to explain the selectivity patterns observed.<sup>19</sup> However, as noted by Myers,<sup>20</sup> the size of an ion is environment dependent; standard ionic radii are not applicable to the situation pertaining in an ether oxygen cavity. Additionally, he pointed out that the calculated cavities were often based on van der Waals radii and that the cation should be expected to penetrate into the outer electron shells of the ligands. Thus, the macrocyclic cavities are underestimated. Using the corrected radii of Myers, a more rigorous explanation of the observed trends is facilitated.

A "goodness of fit" parameter has been introduced by Lindoy *et al.*<sup>21</sup> This factor is given by the following equation:

$$\text{goodness of fit} = \frac{R_A}{R_P}$$

Where  $R_A$  is the bonding cavity radius (hole size less effective covalent radii of the donor set), and  $R_P$  is the Pauling covalent radius of the metal in its given oxidation state and spin. This approach suffers from the disadvantage of requiring an existing structural data set of a series of compounds which show systematic alteration in their structural parameters. Within

the confines of nickel(II) complexes these workers were able to present several trends dependent upon macrocyclic structure and cavity hole size.

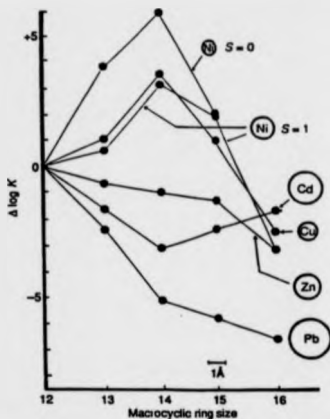
The "ion-in-hole" model provides, at best, only a starting framework for the general prediction of the relative binding capacities of metal cations with cyclic multidentate ligands. Those cations with non-ideal radii are able to perturb the ligand, perhaps at the expense of increase conformational energy, and thereby optimise ligand-metal interactions.

### Chelate Ring Geometry

The decrease in complex stability on moving from a five- to six-membered chelate ring has traditionally been considered as an entropic effect.<sup>22,23</sup> Contemporary studies by Hancock have shown this to be erroneous and that the phenomenon is, in all cases studied, enthalpic in its origin.<sup>24</sup> The decrease in complex stability is strongly related to the size of the metal ion, with larger metal ions showing larger decreases in complex stability upon chelate ring size expansion (see Figure 1.2).<sup>25</sup>

Figure 1.2

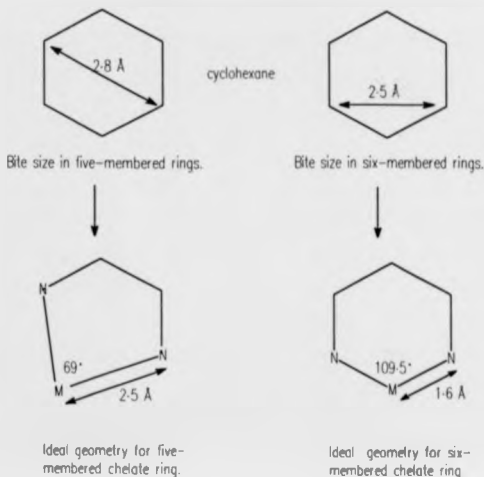
Variation of complex stability as a function of macrocyclic ring size for a variety of metal ions with the  $N_4$  macrocycles 12N4 through 16N4. The variation has been represented as the change in complex stability,  $\Delta \log K$ , relative to  $\log K$ , for the complex with 12N4 for each metal ion. The metal ions are shown inside circles proportional to their ionic radii (square-planar  $\text{Cu}^{2+}$ , octahedral all others). Reproduced from Ref. 24.



By considering the low-strain chair form of cyclohexane it is possible to rationalise the increase in complex stability for small metal ions relative to large metal ions upon change of chelate ring size from five to six members. The strain-free conformer of cyclohexane has all torsion angles at  $60^\circ$  and all C-C-C angles at  $109.5^\circ$ . Applying this model to the five ligand atoms of an  $sp^3$  hybridised chelating ligand, it is evident that the ideal metal ion for coordination has a metal-donor bond length of  $1.6 \text{ \AA}$  and a donor-metal-donor angle of  $109.5^\circ$ . Similarly, a four-membered chelate ligand requires a metal-donor bond length of  $2.5 \text{ \AA}$  and donor-metal-donor bond angle of  $69^\circ$ . These concepts are illustrated in Figure 1.3.



**Figure 1.3** Derivation of minimum strain energy forms for five- and six-membered chelate rings.



A rapid increase in strain energy is produced as the metal ion departs from this ideal size and geometry.<sup>24</sup> To cite one example of the insights afforded by this model: the large lead(II) ion decreases in complex stability as the size of the macrocyclic ring increases along the series 12N4 to 16N4 thus contradicting any simple size-match selectivity. It is now apparent why a large metal ion such as lead(II) does not coordinate well in six-membered chelate rings. Hancock has found his model to work equally for oxa-, aza-, thia- and mixed-donor macrocycles in addition to acyclic and cryptand ligands.

## POLYAZAMACROCYCLES

The systematic development of macrocyclic ligands began in the early 1960's with the work of N. Curtis and D. H. Busch. The compounds they produced using Schiff base and template-assisted condensation reactions opened the door to the macrocyclic coordination chemistry of transition metal ions.

Curtis' report demonstrated the condensation reaction of acetone with a 1,2-diamine complex of nickel(II) to form a polydentate macrocyclic ligand<sup>27</sup> that could not be isolated from the metal ion (see Figure 1.4).

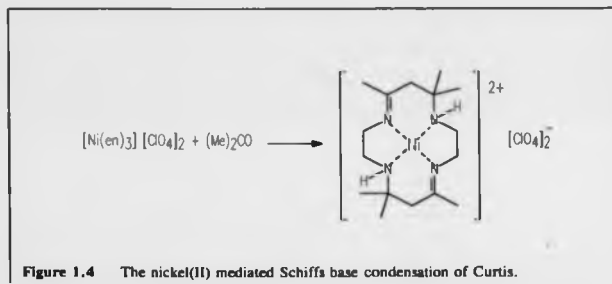
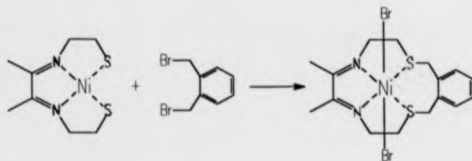


Figure 1.4 The nickel(II) mediated Schiff's base condensation of Curtis.

The term *Kinetic template reaction* was first coined by Busch,<sup>28</sup> who carefully set out to establish the role of the metal ion in the formation of macrocyclic complexes. The reaction scheme from one of his early papers is illustrated in Figure 1.5.



**Figure 1.5** An early macrocycle synthesis of the type used by Busch to elucidate the *kinetic template effect*.

Synthetic macrocycles can be constructed so as to mimic metal binding to compounds of biological interest. In metalloproteins the transition metals are often incorporated via the nitrogen centres of amino acids and so polyazamacrocycles can function as model compounds of low molecular weight. In particular, macrocyclic tetramines have attracted most interest as a consequence of them offering the following attributes:

- 1) The thermodynamic and kinetic stability of their transition metal complexes.
- 2) Their ability to exert stereochemical and electronic control over transition metal coordination spheres.
- 3) Their close relation to the haem proteins, chlorophyll and other biologically significant molecules.

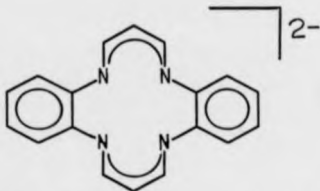
- 4) Their relative simplicity, so allowing insights into the mechanism of transition metal complexation by polyaza ring systems.

The nickel(II) complex of cyclam was reported in 1965 by Bosnich, Poon and Tobe,<sup>28</sup> using a preparation for the macrocycle that had been reported nearly 30 years previously.<sup>4</sup> The interest generated by this publication has led to the synthesis of a multitude of derivatives with differing ring size, nitrogen substituents, carbon substituents and degrees of unsaturation. The chemistry of these macrocycles is sensitive to pH and hydrogen bonding effects due to the amine groups present. Cyclam has been described as the "ultimate prototypic macrocyclic ligand".<sup>30</sup>

Coordinated secondary and tertiary nitrogen atoms become chiral centres leading to isomerism in certain cases. The differing internal strain energy leads to selection of a favoured form for a given metal coordination geometry. Tetraaza macrocycles usually exhibit an approximately coplanar N<sub>4</sub> donor set when bound in a square planar or *trans*-octahedral coordination geometry.

### **Tetramethyltetraazaannulene and its compounds**

The structure of the parent to this class of compounds is shown in Figure 1.6. The anion is obtained by deprotonation of the 1,8-dihydro[14]annulene. With sixteen  $\pi$ -electrons, this molecule is antiaromatic (c.f. porphyrins which satisfy the  $(4n+2)$   $\pi$ -electron rule). Nevertheless, for all coordination compounds of this molecule as a dianion, the six-membered rings are fully delocalised with equal C-C and C-N bond lengths. Comparison of bond lengths suggests that the five-membered chelate rings are not incorporated into the delocalisation.



**Figure 1.6** Dibenzo[b,i]-1,4,8,11-tetraazacyclotetradec-2,4,6,9,11-hexaenato(2-) macrocyclic dianion.

Substitution of methyl groups onto carbon atoms 5, 7, 12 and 14 yields a compound (TMTAA) whose macrocycle complexes are more readily handled than those of the parent ligand. This difference in properties is due to the four methyl groups interacting with the aromatic rings to render a "saddle shape" to the ligand. The concomitant loss of planarity has little bearing on the coordinative ability of the molecule, but greatly improves solubility. Marginal solubility is characteristic of planar, totally conjugated systems such as porphyrin and phthalocyanine, and the simple dibenzo parent macrocycle.

The structure of TMTAA (see Figure 1.7) shows similar bond lengths around the macrocycle to those of its metal-ion derivatives.<sup>31</sup> This suggests the presence of electron delocalisation in the diimine moiety. Consideration of bond tautomerism *i.e.* exchange of N-H and N...H bonds and of the amine lone pair occupying a *p* orbital permits rationalisation of this observation. One structural difference between the free amine and metal-ion chelates concerns the N...N separation across the benzenoid groups. For the neutral free ligand this is 2.71 Å, but reduces to *e.g.* 2.57 Å for the iron(II) compound.<sup>32</sup> A consequence of the saddle shape is the coordination of metal ions to one side of the N<sub>4</sub> donor plane. The metal-N<sub>4</sub> plane

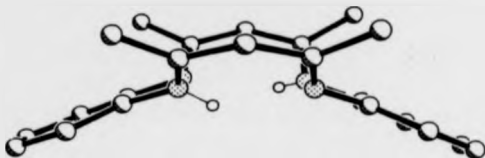


Figure 1.7 Side view of TMTAA showing the saddle shape.

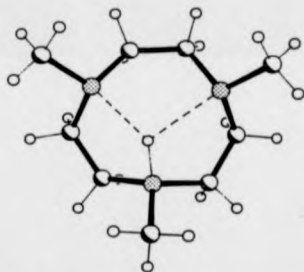
distance ranges from 0.435 Å for  $\text{Cr}(\text{TMTAA})\text{Cl}$ ,<sup>33</sup> to 1.07 Å for  $\text{Zr}(\text{TMTAA})\text{Cl}_2$ .<sup>34</sup> The chemistry of TMTAA has been the subject of a recent review.<sup>35</sup>

### 1,4,7-Triazacyclononane and its compounds

The chemistry of the triazamacrocycles has received comparatively little attention in comparison to the extensive studies directed at the complexes of the tetradentate azamacrocycles. However, since the late 1970's interest has slowly developed in these ligands, leading to a review in 1987.<sup>36</sup> Recent interest has focused on the derivatives of triazamacrocycles as magnetic contrast enhancement agents,<sup>37</sup> metal ion selective probes for <sup>31</sup>P NMR spectroscopy,<sup>38</sup> and tumor imaging and radiotherapeutic agents.<sup>39</sup>

9N3 and Me<sub>9</sub>N3, its tri-N-methyl substituted derivative, are found to bind very strongly to main group and transition metals. Their inherent geometry predisposes these compounds to

occupy a triangular face of the metal-ion coordination sphere. In all cases investigated, the thermodynamic stabilities of 1:1 complexes exceed those of their linear analogue (diethylenetriamine). Larger triazamacrocyclic rings, cyclodecane, cycloundecane, and cyclododecane, exhibit reduced thermodynamic stability. The kinetic stability of 9N3 and its substituted analogues can be remarkable. For some complexes treatment with hot concentrated sulfuric acid does not lead to the expected ligand dissociation or formation of metal hydroxides. These macrocycles exhibit a conspicuous indifference to the oxidation state of the metal substrate; the readily prepared, air stable tricarbonyl complex  $(9N3)Mo(CO)_3$ , upon reaction with 30% hydrogen peroxide, yields  $(9N3)MoO_3$ , a change in oxidation state from 0 to 6.<sup>38</sup> Although 9N3 has yet to be structurally characterised, the monoprotonated cation of Me<sub>9</sub>N3 has been reported (see Figure 1.8).<sup>40</sup>



**Figure 1.8** Structure of 1,4,7-trimethyl-1,4,7-triazacyclononane.

## POLYOXAMACROCYCLES

Synthetic polyoxa-macrocycles have been the subject of considerable interest since the publication, by Pedersen in 1967,<sup>41</sup> of synthetic procedures for the preparation of over fifty cyclic polyethers. Subsequently the field has blossomed to encompass a wide variety of ligand categories such as podandocoronands, spherands, calixarenes, catenands and cryptands (Figure 1.9).

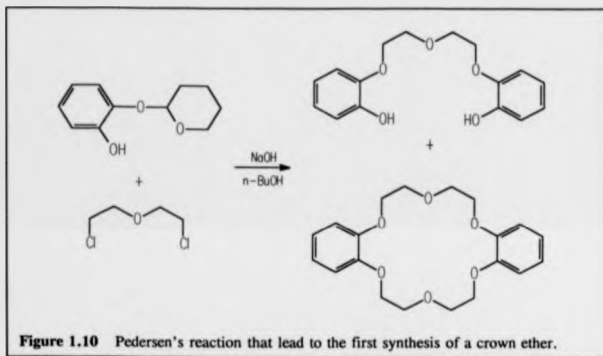
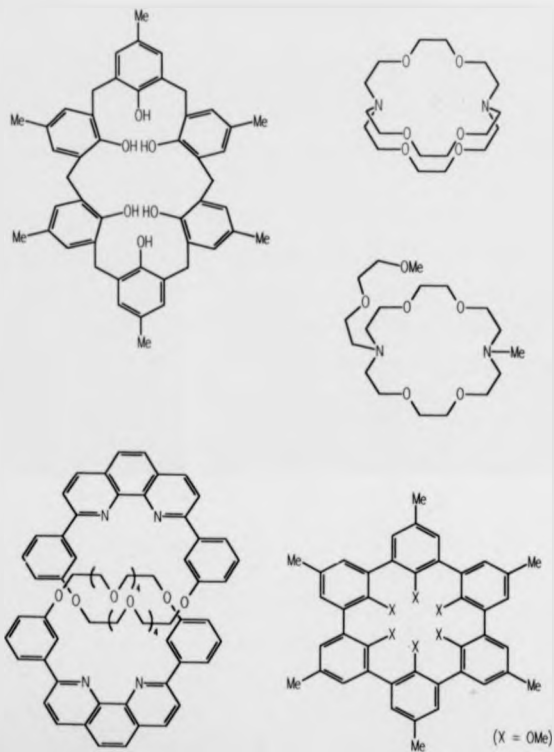


Figure 1.10 Pedersen's reaction that lead to the first synthesis of a crown ether.

Pedersen had attempted to prepare an acyclic multidentate ligand (see Figure 1.10) for subsequent use as a complexing agent for the vanadyl cation. His initial endeavours produced some silky, fibrous crystals in just 0.4% yield. Careful study of this unexpected product combined with continued deductive experimentation lead to the isolation of dibenzo-18-crown-6 with a yield of 40%. Pedersen expanded the range of these new compounds in order to





**Figure 1.9** Selected classes of polyoxamacrocycle.

understand the limits of possible ring size, heteroatom content and other features. Additionally, he sought to identify the nature of the substrates that could be bound by these novel ring compounds.

In contrast to macrocycles incorporating the other common donor centres, polyether macrocycles are often endodentate in their binding mode. Nevertheless, in suitable circumstances a variety of forms may be observed, *e.g.* 1) more than one acceptor centre within the ring was reported for  $[\text{K}_2(\text{SCN})_2(\text{DB-24O8})]$ ,<sup>42</sup> and 2) substrate binding outside of the ring cavity as seen for  $[\text{Na}(\text{Bz-15O5})]$ .<sup>43</sup> Generally, it is observed that when the cation is seemingly too small for the available cavity, more than one may be bound by the ligand, or the ligand may wrap about the cation to better accommodate the required bond lengths and coordination number. When the cation is too large, two crowns may be used to form a 'sandwich' complex.

The oxygen macrocycles form very stable complexes with cations of the alkali and alkaline-earth metals. These pre-transition metals play an important part in biochemical processes, *e.g.*  $\text{Na}^+$  and  $\text{K}^+$  for nerve impulse propagation,  $\text{Mg}^{2+}$  and  $\text{Ca}^{2+}$  for structure. As a consequence of their closed-shell electronic structure, Group I and II metal cations do not exhibit strong stereochemical requirements in complex formation. This contrasts with the transition metals where the stereochemistry of their organic ligand complexes is highly dependent upon the differing electronic configuration of the ions.

## 18-crown-6

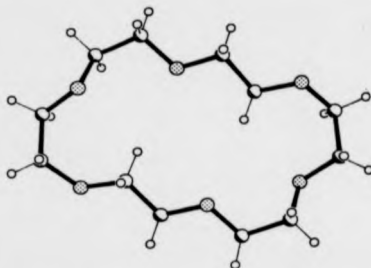


Figure 1.11 Structure of 18O6 ( $C_3$  point symmetry).

This eighteen-membered-ring polyether, without further functionalisation, can be considered as the parent compound of all coronands. A search of the Cambridge Crystallographic Database reveals over 350 structural determinations involving this ligand and its derivatives. Inspection of these reports shows that the types of substrate bound by the macrocycle are legion.

The crystal structure of the free ligand is shown in Figure 1.11.<sup>44,45</sup> The molecule enjoys  $C_3$  symmetry and shows the central void partially filled by two methylene groups. This conformation, [99], results from the presence of two pseudo-corners.<sup>46</sup> There are four *gauche* and two *anti* O-C-C-O torsion angles; reorganisation of the *anti* angles is a prerequisite for *hexakis* chelation. Spectroscopic, I.R. and NMR studies in solution suggest that the  $C_3$  conformation is retained in non-polar solvents.<sup>47</sup>

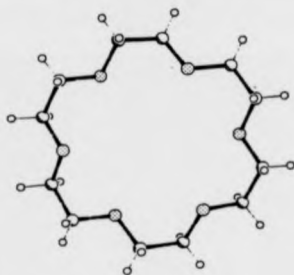


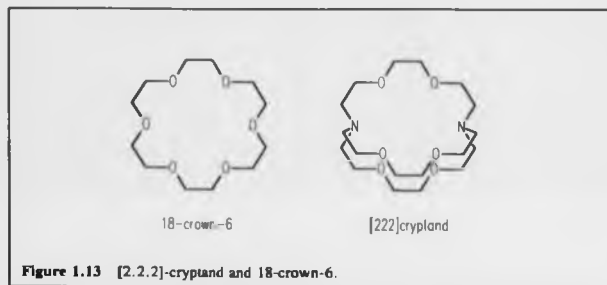
Figure 1.12 Structure of 18O6 when complexed to  $K^+$  ( $D_{3h}$  point symmetry).

When complexed with a potassium, rubidium or caesium ion, 18O6 adopts the  $D_{3h}$  conformation shown in Figure 1.12. Molecular Mechanical calculations have shown the  $D_{3h}$  conformer to be about 1 kcal mol<sup>-1</sup> less stable than  $C_1$  whilst within a medium of low dielectric constant.<sup>48</sup> On moving to a more polar environment the  $D_{3h}$  form becomes relatively more stable. Simulated encapsulation of a potassium ion by 18O6 found the  $D_{3h}$  conformer to be the most stable (as seen in the crystal structure of this complex). The preference for this conformer, despite the fact that it does not have the lowest energy metal-crown interactions, is ascribed to the low strain energy of the ligand in this conformation.

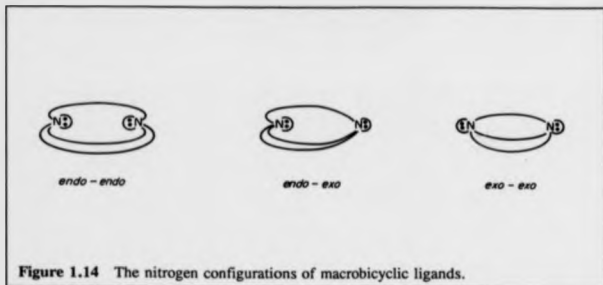
The reaction of 18O6 with Group 4 chlorides has produced some interesting results. Titanium tetrachloride reacts to form the adduct  $TiCl_4 \cdot 18O6$ , in which the crown ether functions as a bidentate ligand.<sup>49</sup> When reacted with zirconium tetrachloride, in THF/toluene, 18O6 undergoes a ring-opening reaction followed by chloride transfer from zirconium to the

hydrocarbon tail. The resulting ligand,  $\text{CH}_3\text{Cl}(\text{-CH}_2\text{-O-CH}_2)_5\text{-CH}_2\text{-O}$ , binds the zirconium centre using the oxide together with four of the neutral ether oxygen atoms.<sup>30</sup> For titanium trichloride, oxygen atoms bond directly with the metal centre. However, the complex formed,  $\text{TiCl}_3 \cdot 18\text{O}6 \cdot \text{H}_2\text{O}$ , also exhibits second-sphere interactions between the coordinated water molecule and macrocycle oxygens. This is achieved by that portion of the crown not bound directly to the titanium bending back towards the metal species.<sup>31</sup>

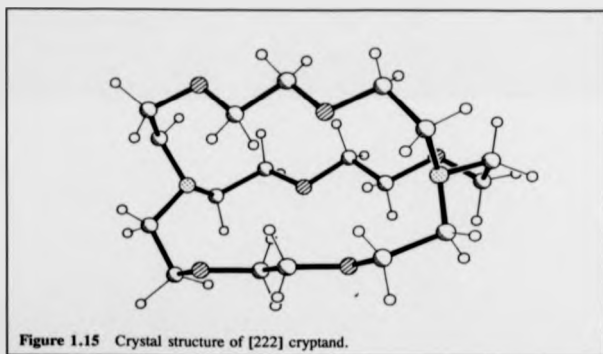
### Cryptands



Simultaneous with the work of Pedersen, Jean-Marie Lehn developed the bicyclic, nitrogen bridgehead, polyether macrocycles, known as *cryptands*.<sup>32,33</sup> Their close relation to the monocycles of Pedersen is readily seen in Figure 1.13. As shown for solutions of diazabicycloalkanes,<sup>34</sup> the ligand in macrobicyclic complexes may exist in three forms differing by the configuration of the bridgehead nitrogens: *exo-exo*, *exo-endo*, *endo-endo* (see Figure 1.14). These forms may interconvert rapidly via nitrogen inversion. For complexes the *endo-endo* form is strongly favoured since both nitrogen atoms can then participate in



metal-ligand interactions. The crystal structure of the cryptand [2.2.2] (see Figure 1.15)<sup>11</sup> and those of its cryptates show the *endo-endo* form to be expressed exclusively.



The free ligand [2.2.2] is elongated to yield a shape reminiscent of a rugby ball. As with the uncomplexed crown ethers, guest-free cryptands fill the vacant cavity somewhat by rotating

a methylene group inward and extending along one axis. With all O-C-C-O torsion angles *anti*, some oxygen lone pairs are directed out of the cavity and thereby available for interaction with other species. The N-N distance (6.871(4) Å) is very close to that found in the *exo-exo* bisborohydride derivative (6.759(5) Å).

Cryptates typically exhibit a N-N separation of 4.97 to 6.07 Å. Comparison of this molecular dimension in a number of compounds reveals a progressive opening up of the molecular cavity along the series [2.2.2 M<sup>+</sup>], where M<sup>+</sup> = Na<sup>+</sup>,<sup>56</sup> K<sup>+</sup>,<sup>57</sup> Rb<sup>+</sup>,<sup>58</sup> Cs<sup>+</sup>.<sup>59</sup> These studies show adaptation of the cryptand cavity to the effective ionic radius of the metal ion. A simple cryptand:metal ion association is not always observed. For instance, the solid state structure of the lead(II) thiocyanate complex with [222]cryptand shows that the cation resides within the *endo-endo* form of the ligand. However, the lead centre is coordinated by the two anions, one through sulfur the other nitrogen, in addition to the ten cryptand heteroatoms.<sup>60</sup> In solution, <sup>133</sup>Cs NMR studies for the complex of [222]cryptand with Cs<sup>+</sup> indicate the existence of two types of 1:1 complex.<sup>41</sup> At low temperatures an *inclusive* complex predominates with the cation inside the ligand cavity and insulated from the solvent. At higher temperatures, an *exclusive* complex forms where the cation is only partially accommodated within the cavity and is accessible to solvent molecules.

Despite the well established use of phosphines in the coordination chemistry of the transition metals, there has been little development in their use as donor centres for macrocyclic ligands. It is known that phosphine ligands stabilise low oxidation states and have found use in the development of catalytic systems for a variety of reactions.<sup>62</sup> Therefore, macrocyclic derivatives would appear to be a fertile area for investigation. The scarcity of reports must be seen as a consequence of the low yield, multistage syntheses required for the preparation of polyphosphamacrocycles.

The first homoleptic tetraphosphine macrocycle was reported in 1977 and is shown diagrammatically in Figure 1.16.<sup>63</sup> Using nickel(II) as a template ion the complex was obtained in 40% yield. The action of aqueous cyanide ions liberated the free macrocycle as an air-sensitive oil in 50% yield.

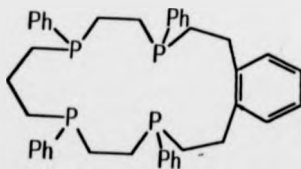


Figure 1.16 The first homoleptic tetraphosphine macrocycle.



The study of phosphorus macrocycles is complicated by the possible conformations that can exist. The barrier to phosphine inversion is approximately  $146 \text{ kJmol}^{-1}$  although some conformations are remarkably stable.<sup>64</sup> As an example, the ligand represented in Figure 1.17 is chosen.<sup>65</sup>

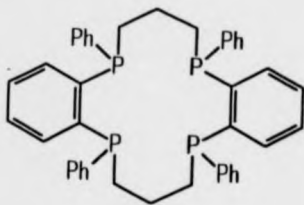


Figure 1.17 Representation of the first crystallographically characterised polyphosphamacrocycle.

This molecule was synthesised using a high dilution technique to effect ring closure. Of the five possible isomers (three *meso* and two *dl* pairs), the synthesis favours the high melting point ( $214-6^\circ\text{C}$ ) form. The phenyl groups of this conformer exhibit a *trans*, relationship across the  $P_4$  plane, as demonstrated by the x-ray crystal structure.

A macrocyclic ring compound incorporating sulfur donor atoms was first reported by Mansfield in 1886 following his reaction of sodium sulfide with ethylene bromide to produce 9S3.<sup>66</sup> Very little further work was published in the area until 1969, when Rosen and Busch prepared 14S4 in 7.5% yield so stimulating interest in the field of its coordination chemistry.<sup>67</sup> Using a related synthetic methodology, the same workers were able to prepare 12S3, 12S4, 13S4 in yields of between 3 and 16%.<sup>68</sup> Simultaneously, Black and McLean reported the synthesis of 18S6 with a 31% yield.<sup>69</sup> With the publication of these synthetic methods, the co-ordination chemistry of sulfur macrocycles was set to blossom. In 1980 Butler and Kellog greatly increased synthetic yields with the introduction of caesium carbonate to mediate ring formation and thereby curtail polymer formation.<sup>70,71,72</sup> The technique found widespread utility. 1979 saw the reported preparation of Bz<sub>3</sub>-9S3, a thiamacrocycle functionalised by incorporation of aromatic rings in the  $-CH_2CH_2-$  backbone.<sup>73</sup> Developments in the functionality of the basic thiaether rings have continued, *e.g.* the ditopic sulfur macrocycle, 2,5,8,17,20,23-hexathia[9](1,2)[9](6,5)cyclophane which contains two 11S3 rings connected by an *o*-xylyl spacing unit.<sup>74</sup>

### Thiaether coordination

Aspects of thiaether chemistry have been the subject of several reviews.<sup>75,76,77,78,79</sup> It is generally observed that the simple thiaethers (R<sub>2</sub>S) are poor ligands; a problem surmounted by the use of polythiaether macrocycles. Cyclic thiaethers have now been shown to bind a wide range of transition metal ions to form stable complexes. An appraisal of the nature of

thiaether donor- bonding merits consideration of 1) non-bonded lone pair effects, 2)  $\pi$ -bonding, 3) charge neutralisation.

#### 1) Non-bonded lone pair effects

Coordinative power decreases along the series  $R_3P > R_2S > RCl$ . This can, in some part, be ascribed to the stereoelectronic repulsion resulting from the increasing number of non-bonding electron pairs on the donor atom and metal-based electrons.

#### 2) $\pi$ -bonding

Historically, the  $\pi$ -acidity of second-row donor atoms was attributed to metal  $\rightarrow$  donor- $d$ -orbital back-bonding. Subsequent calculations have shown the  $3d$  orbitals to be energetically unattainable. Recent studies have reconciled experiment with theory for phosphine donor complexes. The  $M \rightarrow P$   $\pi$ -bonding employs  $P-X \sigma^*$  orbitals ( $X$  = phosphine substituent) for electron acceptance.<sup>80</sup> It is likely that a similar rationalisation can be invoked for thiaether  $\pi$ -bonding. A further factor, not applicable to group 15 donors, is the existence of a second non-bonded electron pair. In consequence,  $\pi$ -donation to empty metal  $d$  orbitals of suitable symmetry, warrants consideration. Currently, there is little experimental evidence to support this notion.<sup>79</sup>

Evidence for the existence of  $\pi$ -acidity in thiaether donor bonds has been exhaustively reviewed.<sup>81</sup> Properties examined include vibrational spectroscopy, stabilisation of low-spin states, nephelauxetic effects, thermal stability, photoelectron spectroscopy and redox potentials.

### 3) Charge neutralisation

The  $\sigma$ -donating ability of a Lewis base is affected by its electronegativity, its size (for matching of orbital energies and orbital overlap with the acceptor), dipole moment, and polarisability. The poor  $\sigma$ -donor ability of the thiaethers is manifest in the widespread coordination by "non-coordinating" species to metal centres whose coordination sphere is primarily thiaether, e.g.  $[\text{Pb}(\text{9S3})_2(\text{ClO}_4)_2]$  where two monodentate perchlorate anions remain bound to the lead(II) centre.<sup>82</sup>

The *crown* thiaethers provide an excellent means of imposing a homoleptic thiaether environment around metal ions in which the coordinative properties of the ligand have often been found not to match the typical stereochemical preferences of the cation. This has permitted the study of metal ion properties when bound in unusual coordination geometries. In part, this can be ascribed to the enthalpic cost imposed by *exo* to *endo* reorganisation required for metal ion encapsulation. In the brief summary of the properties of some sulfur macrocycles that follows, the examples included demonstrate the great structural variety of their complexes. The polythiaether macrocycles and their complexes have been the subject of recent reviews.<sup>83,84,85,81</sup>

### 1,4,7-trithiacyclononane

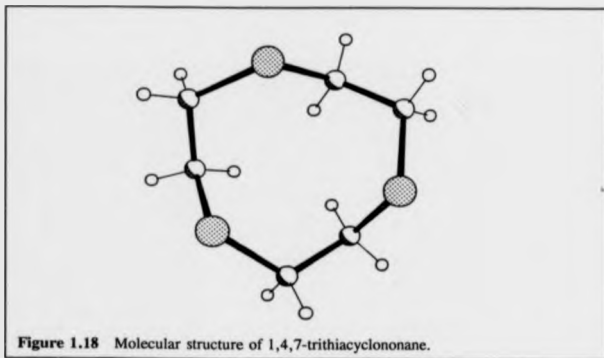
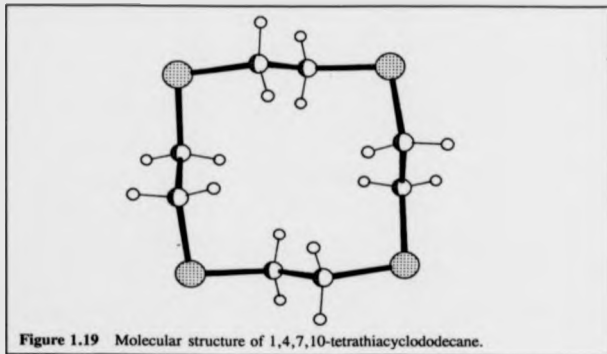


Figure 1.18 Molecular structure of 1,4,7-trithiacyclononane.

A [333] conformation with  $C_3$  point symmetry was confirmed by the crystal structure reported in 1980.<sup>66</sup> The endodentate geometry adopted by the ligand contrasts with other polythiaether macrocycles where the sulfur lone pairs are directed out of the ring cavity. Bond lengths are C-S, 1.820(5), 1.823(5) Å; C-C, 1.510(6) Å; with a non-bonded S...S contact of 3.451(2) Å some 0.25 Å less than the sum of the van der Waals radii of sulfur. 9S3 is atypical of sulfur macrocycles, being preorganised for coordination to the face of a metal ion. Photoelectron spectroscopy confirms that the [333] conformation is retained in the gas phase.<sup>67</sup> Oxidation of 9S3 leads to bicyclic sulfonium cation formed via transannular C-S bond formation and C-H bond cleavage. Interestingly, a recent publication showed 9S3 coordinated to Re(VII), challenging the view that thiaether coordination is the preserve of low substrate oxidation states.<sup>68</sup> Despite a predominance of facial, tridentate coordination for this ligand, other modes have been characterised, for example:

- 1)  $[\text{Cu}(\text{9S3})_2]^{2+}$  <sup>89</sup> - bis(tridentate).
- 2)  $[\text{Cu}_2((\text{S3})_2)]^{2+}$  <sup>90</sup> - tridentate (x2), bidentate ligand bridging binuclear.
- 3)  $[\text{IrH}(\text{9S3})_2]^{2+}$  <sup>91</sup> - bidentate, tridentate.

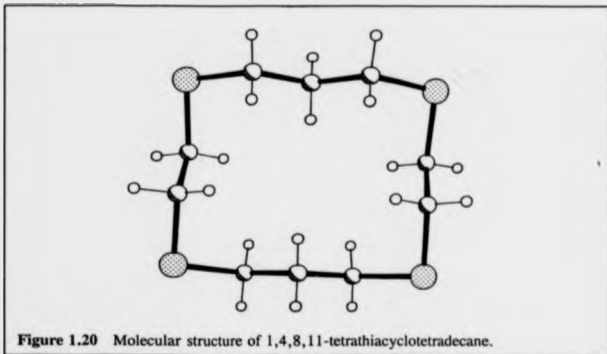
### 1,4,7,10-tetrathiacyclododecane



The [3333] conformation of 12S4 was confirmed with the crystal and molecular structure determination by Robinson *et al* in 1988.<sup>92</sup> All sulfur atoms are located at the corner of a square and all eight C-S bonds adopt gauche placements. An approximate  $D_4$  symmetry is apparent. Semi-empirical molecular-mechanics calculations show the crystal coordinates to represent an essentially strain-free structure.<sup>91</sup> The range of coordinative modes exhibited by for this ligand is illustrated by:

- 1)  $[\text{Al}(\text{CH}_3)_3(12\text{S4})]^{+}$  <sup>93</sup> - monodentate.
- 2)  $[\text{Re}(\text{CO})_5(12\text{S4})]^{+}$  <sup>93</sup> - tridentate.
- 3)  $[\text{Cu}(12\text{S4})(\text{OH}_2)]^{2+}$  <sup>94</sup> - tetradentate.

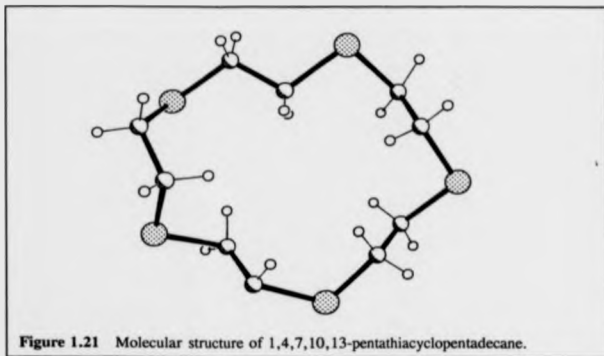
### 1,4,8,11-tetrathiacyclotetradecane



The structure, reported in 1976 by DeSimone *et al.*, revealed that 14S4 crystallises in three conformations; all with similar *exo* conformations and the sulfur atoms occupying the corners of quadrilateral molecules.<sup>97</sup> This is entirely in accord with the tendency for S4 macrocycles to partake in exodentate co-ordination; endodentate ion encapsulation requires extensive ligand reorganisation. The  $\alpha$  form contains one, and the  $\beta$  form two independent molecules. The coordinative versatility of this molecule is best demonstrated by example:

- 1)  $[(\text{HgCl}_2)_2(14\text{S}4)]^{\infty}$  - tetradentate, ligand bridging, binuclear.
- 2)  $[\text{Hg}(\text{H}_2\text{O})(14\text{S}4)]^{2+ \infty}$  - tetradentate.
- 3)  $[\text{HgI}_2(14\text{S}4)]^{\infty}$  - bidentate, ligand bridging, polymeric.

### 1,4,7,10,13-pentathiacyclopentadecane

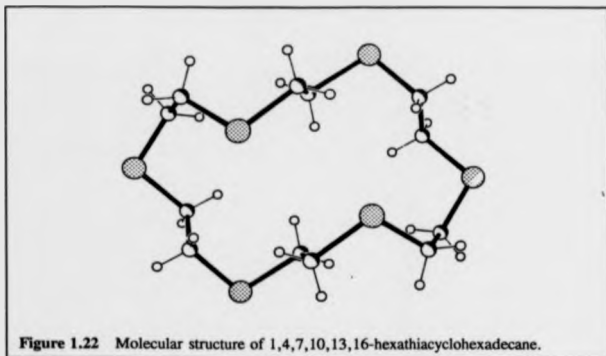


In common with other macrocyclic polythiaethers the crystal structure of this compound shows that an *exo* conformation is adopted with all sulfur atoms pointing out of the ring cavity.<sup>101</sup> The ring adopts an irregular  $C_1$  symmetry. The structural chemistry of this ligand has been less fully explored than for many other common thiamacrocycles. Reports include:

- |  |   |
|--|---|
| 1) $[\text{ReBr}(\text{CO})_4(15\text{S}5)]^{102}$               | - bidentate.  |
| 2) $[\text{Cu}(15\text{S}5)]^{+ 103}$                            | - tetradentate.   |
| 3) $[(15\text{S}5)\text{Cd}(\text{ClO}_4)(\text{OH}_2)]^{+ 104}$ | - pentadentate.   |
| 4) $[\text{Ag}_2(15\text{S}5)_2]^{2+ 105}$                       | - tetradentate / pentadentate, asymmetric<br>bridging ligands, binuclear. |



# 1,4,7,10,13,16-hexathiacyclooctadecane



In contrast to the solid state structures of the sulfur macrocycles with a smaller ring size (except 9S3), the single-crystal X-ray structure of this compound shows that whilst four of the six sulfur atoms adopt the expected exodentate geometry, the remaining two are directed into the macrocyclic cavity. All C-S bonds in 18S6 adopt *gauche* configurations. Examples of structurally characterised complexes incorporating this ligand cover:

- 1)  $[\text{Cu}_2(\text{CH}_3\text{CN})_2(18\text{S}6)]^{2+}$  <sup>106</sup> - hexadentate (2x3) bridging ligand, binuclear.
- 2)  $[\text{Co}(18\text{S}6)]^{2+}$  <sup>107</sup> - hexadentate (meso isomer).
- 3)  $[\text{CuCl}(18\text{S}6)]_n$  <sup>108</sup> - bidentate bridging ligand, tetradentate bridging ligand, polymeric.

## SYNTHESIS OF MACROCYCLIC LIGANDS

An ideal synthetic methodology would endeavour to optimise the following criteria:

- 1) production of the target macrocycle in high yield
- 2) generation of a form readily purified and isolated from side-products
- 3) utilisation of readily available starting materials
- 4) employment of a straightforward experimental procedure
- 5) low financial expenditure

The prime focus in the preparation of macrocyclic compounds is to secure closure of the correctly sized ring, thereby suppressing production of ring homologues and polymeric materials. Three major strategies have emerged:

1) Richman-Atkins<sup>99</sup> - the Richman-Atkins approach promotes cyclisation between one reagent having two terminal  $\text{NH}_2$  groups converted into *p*-toluenesulfonamide sodium salts,  $-(\text{Ts})\text{N}^-\text{Na}^+$ , and a second reagent with two alcohol groups converted into *p*-toluenesulfonate ester groups,  $-\text{OTs}$ . The sodium salts benefit from enhanced nucleophilicity over tosylated amines and the sulfonate esters are more effective leaving groups than halides. A dipolar, aprotic solvent is required.

2) Template<sup>110</sup> - By coordinating the linear precursors around a metal ion, so defining their orientation, the template effect ensures that the target ring is obtained in high yield.

3) High Dilution<sup>111</sup> - Maintenance of unusually low reactant concentrations limits the occurrence of further oligomerisation. The entropic terms favouring chain growth over cyclisation become less statistically favoured at high dilution.

There are many review articles<sup>112,113,114,115,116,117</sup> pertaining to the synthesis of macrocyclic ligands and so it is intended to simply highlight the field with a few selected examples.

### 1,4,7-trithiacyclononane

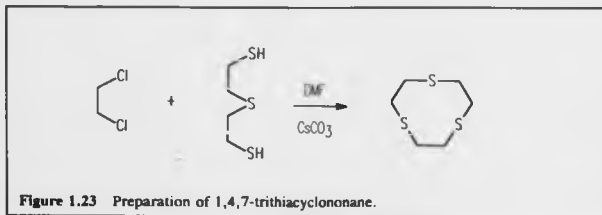


Figure 1.23 Preparation of 1,4,7-trithiacyclononane.

Although 9S3 has been prepared by a number of routes, some in high yield,<sup>118</sup> the technique shown in Figure 1.23 benefits from its single step approach.<sup>119</sup> The use of caesium carbonate to mediate cyclisation reactions was first introduced by Kellogg and co-workers.<sup>70</sup> The caesium ions promote ring formation by means of very weak ion-pairing, thereby generating an exceptionally nucleophilic thiolate anion. High reactivity ensures low reactant concentrations so leading to the desired intramolecular reaction. A DMF solution of 2-mercaptoethyl sulfide and 1,2-dichloroethane is added dropwise to a DMF suspension of

caesium carbonate under a dinitrogen atmosphere. After heating at 100°C for twelve hours, conventional work-up and vacuum sublimation leads to the pure macrocycle in 50% yield.

### 1,4,8,11-tetrathiacyclotetradecane

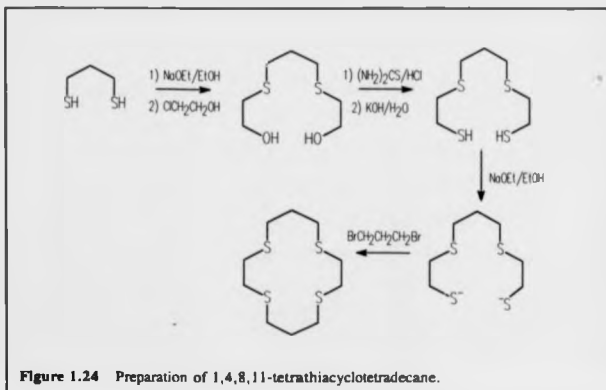
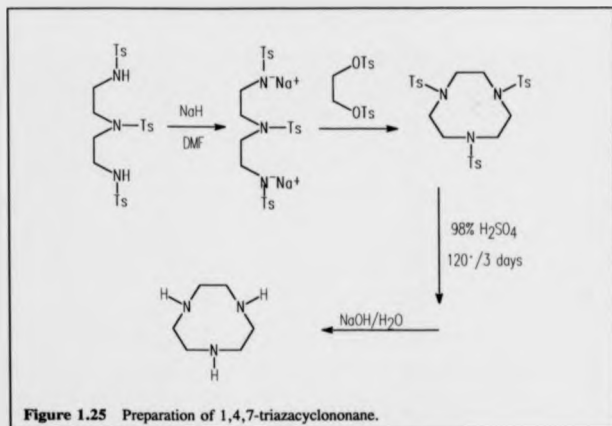


Figure 1.24 Preparation of 1,4,8,11-tetrathiacyclotetradecane.

Historically, the development of polythiamacrocylic chemistry was hindered by the low synthetic yields obtained from the preparative techniques then available. The synthesis of 14S4 in 1969 serves to illustrate this with a yield of just 7.5%.<sup>47</sup> Using an analogous procedure (see Figure 1.24) combined with high dilution conditions the yield was boosted to 55%.<sup>120</sup> The sodium salt of 1,4,8,11-tetrathiaundecane is prepared by addition of sodium ethoxide to the dithiol. Dropwise addition, over three hours, of a dilute solution (0.18 mol dm<sup>-3</sup>) dibromoethane to the resulting mixture produces the desired macrocycle in 55% yield after purification by vacuum sublimation.

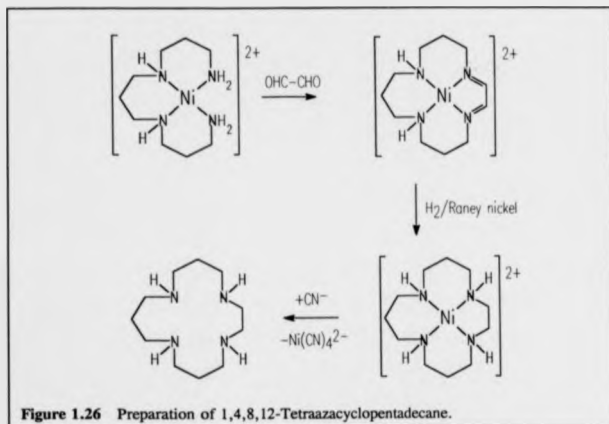
# 1,4,7-triazacyclononane<sup>121</sup>



**Figure 1.25** Preparation of 1,4,7-triazacyclononane.

This synthesis provides an example of the Richman-Atkins procedure. The mechanism is quite general and can be used to prepare 9- to 21-membered saturated macrocycles containing three to seven donor atoms (nitrogen and/or oxygen). Polymeric side products are negligible and so do not pose a problem. The overall reaction scheme is shown in Figure 1.25. The tosylated derivatives are obtained by reaction of the diamine and the diol with *p*-toluenesulfonyl chloride. Addition of sodium hydride (50% oil suspension) to the di(*p*-toluenesulfonyl)ethane-1,2-diamine yields the disodium salt to which the di(*p*-toluenesulfonyloxy)ethane can be introduced. The hydrolysis step of the cyclic tritosylate is efficiently achieved in concentrated sulfuric acid at 120 °C for three days. Final purification is best accomplished using column chromatography.

**1,4,8,12-tetraazacyclopentadecane<sup>123</sup>**



**Figure 1.26** Preparation of 1,4,8,12-Tetraazacyclopentadecane.

The most commonly used method of ring closure via the template effect invokes the Schiffs base condensation of a diketone with the metal-coordinated primary amine groups of an acyclic multidentate ligand. This preparation is shown schematically in Figure 1.26. N,N'-bis(3-aminopropyl)-1,3-propanediamine is added to an aqueous solution of nickel(II) chloride, followed by aqueous glyoxal. Hydrogen reduction takes place over Raney nickel during 24 hours. Addition of NaCN effects decomplexation of the nickel ion. Conventional work-up procedures then afford the free ligand in 48% yield.

Dibenzo-18-crown-6 and dicyclohexyl-18-crown-6<sup>123</sup>

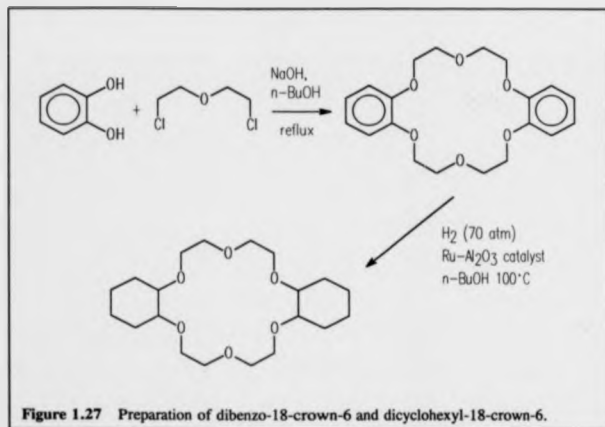


Figure 1.27 Preparation of dibenzo-18-crown-6 and dicyclohexyl-18-crown-6.

The formation of the eighteen-membered ring is facilitated by the presence of the sodium ions in this example of a template synthesis. The dicyclohexyl-18-crown-6 formed contains a mixture of all stereoisomers. The overall procedure is shown in Figure 1.27. Treatment of catechol with base forms the dianion. Dropwise addition of 2,2'-dichlorodiethyl ether to this nucleophile results in a 'quadruple Williamson' reaction. Work up, by extraction, precipitation with acetone and recrystallisation delivers the product in 40% yield. Hydrogenation of the aromatic derivative requires an autoclave. Purification, including an acid-washed alumina column, leads to the desired compound as a diastereoisomeric mixture in 60% yield.

## **CHAPTER TWO**

### **SOME COORDINATION CHEMISTRY OF GROUP 15 TRIHALIDES WITH THIAMACROCYCLIC LIGANDS**



## 2.1 SULFUR MACROCYCLE COMPLEXES OF P-BLOCK ELEMENTS

Despite many reports concerning the binding of crown thiaethers to transition metal ions, relatively few investigations have examined the action of these compounds upon p-block metal centres. The five studies reported prior to the investigations described in this thesis are summarised in the Table 2.1.<sup>94,124,125,132,83</sup> Inspection of the table shows that whilst Group 13 has received most attention, gallium is conspicuous in its absence. A further feature is the existence of just one example from outside group 13, lead(II) perchlorate. Within this limited selection, some typical features of thiamacrocyclic binding are observed:

- 1) 9S3, being pre-organised for facial coordination, has found most success to-date.
- 2) Coordination is maintained between the cationic centre and its counterion.

The requirement for a systematic enquiry into the binding mode of sulfur macrocycles with the other group 14 elements, together with those of group 15 and 16, is self-evident. Following the recent reports concerning the coordination of group 15 trihalides by the crown ethers,<sup>126,127,128,129,130</sup> an analogous investigation using the crown thiaethers was a natural development. If similar coordination modes were exhibited, a direct comparison between oxygen and sulfur crown macrocycles ('hard' and 'soft' donors respectively) would be possible.

Table 2.1 Reported thiamacrocycle complexes of p-block compounds.

P-BLOCK COMPOUND	MACROCYCLE	STRUCTURE
$\text{AlMe}_3$	1254	Polymeric compound with 1:1 stoichiometry. $\mu^2$ -bridging macrocycle produces trigonal bipyramidal geometry at aluminium with sulfur atoms in the axial positions.
$\text{AlMe}_3$	1454	Each ring sulfur is bound to one $\text{Al}(\text{Me})_3$ to produce a tetranuclear compound. An approximately tetrahedral geometry exists around the aluminium atoms.
$\text{InCl}_2$	953	not determined
$\text{TiPF}_6$	953	Facial co-ordination of 953 to each $\text{Ti}^+$ . Additional $2^+$ bonding present to one sulfur of another ring and to four fluorine atoms from $\text{PF}_6^-$ anions.
$\text{Pb}(\text{ClO}_4)_2$	953	Two 953 rings together with two monodentate $\text{ClO}_4^-$ surround $\text{Pb}(\text{II})$ in a distorted square antiprism.

After a description of the spectroscopic results obtained, this chapter will examine the molecular structure of each compound for which this has been determined. Structural trends involving the metal centre will then be considered and, where relevant, compared to analogous oxa-crown complexes. Finally, ligand conformational preferences will be scrutinised.

## 2:2 SULFUR MACROCYCLE COMPLEXES OF ARSENIC,

## ANTIMONY, AND BISMUTH TRICHLORIDE

The four polythiamacrocycles used to conduct these studies were selected in view of their ease of synthesis (9S3) or economical commercial purchase (12S4, 15S5, 18S6). All are homologues of the  $(-CH_2-CH_2-S-)_n$  basic unit with  $n = 3, 4, 5, 6$ . A summary of the reactions attempted is shown in Table 2.2. The complexes were obtained by direct addition of the macrocycle to the metal trihalide. Acetonitrile was found to be most efficacious as the solvent medium. Where successful, the adduct was produced in almost quantitative yield.

**Table 2.2** Summary of reactions undertaken between selected polythiamacrocycles and arsenic, antimony and bismuth trichloride.

ligand	Metal trichloride		
	AsCl <sub>3</sub>	SbCl <sub>3</sub>	BiCl <sub>3</sub>
9S3	no adduct isolated	crystal structure determined	spectroscopic characterisation
12S4	no adduct isolated	no adduct isolated	crystal structure determined
15S5	no adduct isolated	spectroscopic characterisation	crystal structure determined
18S6	no adduct isolated	crystal structure determined	crystal structure determined



For each ligand with arsenic trichloride, and for 12S4 with antimony trichloride, the macrocycle was recovered without reaction. However, on a sole occasion, a very few, extremely sensitive needle crystals were obtained from reaction between arsenic trichloride and 9S3. The only characterisation, the melting point of 176°C, suggested these to be a novel compound. Numerous attempts failed to repeat this preparation. Of the seven compounds isolated, the adduct between 15S5 and antimony trichloride was anomalous in its far greater air/moisture sensitivity; problems were experienced even under the dinitrogen atmosphere. Relevant spectroscopic and other data for all the complexes isolated are given in Table 2.3.

Perhaps the most noticeable difference between the bismuth and antimony complexes is the presence of a pale yellow coloration in the case of the former. Examination of the U. V./visible electronic spectra shows little change in  $\lambda_{\text{max}}$  values from those recorded for the parent trihalides. However, a slight trailing into the visible region, no doubt, accounts for the coloration of the bismuth complexes. There is an apparent difference between antimony and bismuth in the number of i.r. bands assigned to  $\nu(\text{M-Cl})$  (three and two respectively) and yet both exist as pyramidal  $\text{MCl}_3$  units of similar geometry (later confirmed crystallographically). This is due to an additional Bi-Cl band falling below the  $200\text{ cm}^{-1}$  cutoff of the spectrometer. That the melting points of the bismuth complexes are in each case higher than those of the corresponding antimony analogue may indicate an enhanced thermal stability. Certainly, this would concur with the trend suggested by NMR spectroscopy.

#### NMR

The shifts quoted relate to the  $-\text{CH}_2-\text{CH}_2-$  backbone of the macrocycle. Each complex shows a characteristic singlet, which is a consequence of there being negligible energetic barriers between ligand conformers. A reduction in temperature to 233 K failed to 'freeze' this

fluxionality. There is little change in shift upon complexation from that of the free ligand in the same medium ( $\Delta\delta$ ), as shown in Table 2.4. This suggests minimal interaction between macrocycle and substrate whilst in acetonitrile solution. The sole exception is  $\text{BiCl}_3 \cdot 15\text{S5}$  where the change is somewhat more pronounced. Despite the limited magnitude observed,  $\Delta\delta$  is unfailingly upfield in direction, for all seven complexes. This is commensurate with an explanation invoking simple inductive effects. The general trend of a greater  $\Delta\delta$  in respect of the bismuth complexes is consistent with there being a stronger interaction between the heavier group 15 metal and polythiamacrocycles.

**Table 2.4** Change in chemical shift ( $-\text{CH}_2\text{-CH}_2-$ ) of  $\text{MCl}_3 \cdot \text{S}$ -macrocycle complexes ( $\text{M}=\text{Sb, Bi}$ ) from that recorded for the free ligand ( $\Delta\delta$ ).

Metal halide	SbCl <sub>3</sub>			BiCl <sub>3</sub>			
Ligand	9S3	15S5	18S6	9S3	12S4	15S5	18S6
Δδ	0.01	0.01	0.01	0.04	0.04	0.12	0.03

These characterisations offer little indication as to the nature of the bonding between the trihalide and the macrocycle. As a consequence, five of the seven compounds isolated have been the subject of an x-ray structural determination. Each will now be considered individually before moving on to assess the more general trends observed.

## MOLECULAR STRUCTURE OF $\text{SbCl}_2 \cdot 1,4,7\text{-TRITHIACYCLONONANE}$

Each antimony centre is irregularly bound by the three sulfur donors of one macrocycle together with one sulfur from a second macrocycle with an overall 1:1 stoichiometry. The polymeric chain structure, with one bridging sulfur from each ligand, is shown in Figure 2.1. Bond lengths and angles are shown in Table 2.5. The Sb-Cl distances to this seven coordinate metal centre (mean 2.417 Å) remain very similar to those seen for antimony trichloride itself. It is of interest to note that the bridging bond of the  $\mu^2$ -sulfur atom, 3.171(3) Å, is one of the shortest. A similar [3+1] binding mode by 9S3 was observed in the trimeric cation  $[\text{Ag}_3(9\text{S3})_3]^{1+}$ , where, again, the shortest metal-sulfur bond is observed for the bridging sulfur atom to the metal centre of an adjoining unit.<sup>131</sup> The S-S contacts within each ring (3.39 to 3.43 Å) are similar to those seen in the free ligand (3.45 Å). The bridging sulfur has a shortest inter-ring S-S contact of 3.53 Å. The antimony atom lies 2.66 Å from the  $\text{S}_3$  plane and 2.07 Å below the mean  $\text{S}_6$  plane. The  $\angle$ 's S-Tl-S of 67° in the ion  $[\text{Tl}(9\text{S3})]^+$  were considered particularly small.<sup>132</sup> The  $\angle$ 's S-Sb-S found here are smaller still, ranging between 60.62 and 62.94°.

Two views of the antimony coordination sphere are shown in Figure 2.2. A void suitable for accommodation of the electron lone pair is evident opposite Cl3. However, this could simply be a corollary of the steric constraint imposed by the coordinated macrocycles.

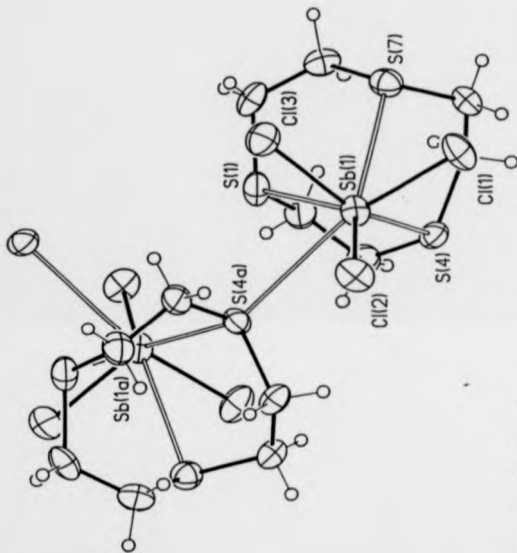


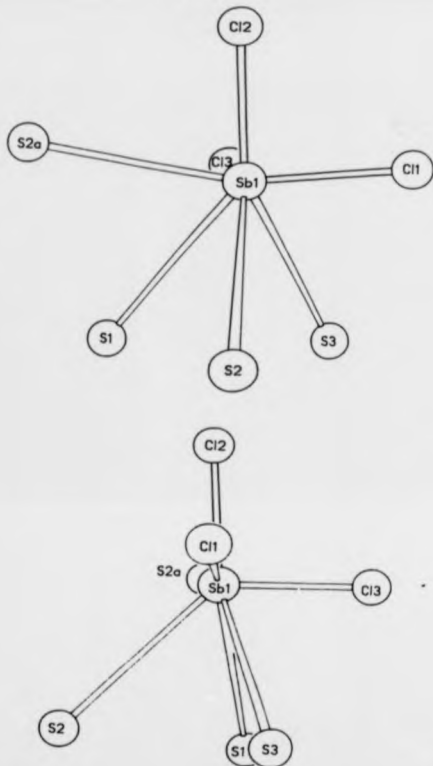
Figure 2.1 Molecular structure of  $\text{SbCl}_3 \cdot 9\text{S}_3$ .



Table 2.5 Selected bond lengths (Å) and angles (°) for SbCl<sub>3</sub>·9S<sub>3</sub>.

Bond lengths (Å)			
Sb(1)-Cl(1)	2.451(3)	Sb(1)-Cl(2)	2.426(2)
Sb(1)-Cl(3)	2.374(4)	Sb(1)-S(1)	3.409(3)
Sb(1)-S(4)	3.396(3)	Sb(1)-S(7)	3.156(3)
Sb(1)-S(4a)	3.171(3)	S(1)-C(2)	1.808(10)
S(1)-C(9)	1.799(10)	C(2)-C(3)	1.902(14)
C(3)-S(4)	1.821(11)	S(4)-C(5)	1.810(10)
C(5)-C(6)	1.522(13)	C(6)-S(7)	1.813(9)
S(7)-C(8)	1.811(11)	C(8)-C(9)	1.524(14)

Bond angles (deg.)	
Cl(1)-Sb(1)-Cl(2)	86.8(1)
Cl(1)-Sb(1)-Cl(3)	99.3(1)
Cl(2)-Sb(1)-Cl(3)	91.9(1)
Cl(1)-Sb(1)-S(1)	132.3(1)
Cl(2)-Sb(1)-S(1)	140.7(1)
Cl(3)-Sb(1)-S(1)	78.9(1)
Cl(1)-Sb(1)-S(4)	93.1(1)
Cl(2)-Sb(1)-S(4)	133.1(1)
Cl(3)-Sb(1)-S(4)	134.0(1)
S(1)-Sb(1)-S(4)	60.6(1)
Cl(1)-Sb(1)-S(7)	70.7(1)
Cl(2)-Sb(1)-S(7)	154.1(1)
Cl(3)-Sb(1)-S(7)	79.8(1)
S(1)-Sb(1)-S(7)	62.0(1)
S(4)-Sb(1)-S(7)	62.9(1)
Cl(1)-Sb(1)-S(4a)	162.2(1)
Cl(2)-Sb(1)-S(4a)	76.9(1)
Cl(3)-Sb(1)-S(4a)	88.3(1)
S(1)-Sb(1)-S(4a)	64.8(1)
S(4)-Sb(1)-S(4a)	93.0(1)
S(7)-Sb(1)-S(4a)	126.8(1)
S(1)-C(2)-C(3)	114.7(7)
C(2)-C(3)-S(4)	117.4(7)
C(3)-S(4)-C(5)	104.0(4)
S(4)-C(5)-C(6)	113.4(6)
C(5)-C(6)-S(7)	116.5(7)
C(6)-S(7)-C(8)	103.2(4)
S(7)-C(8)-C(9)	112.3(7)
S(1)-C(9)-C(8)	116.7(7)
C(9)-S(1)-C(2)	102.7(5)



**Figure 2.2** Two representations of the antimony coordination sphere in  $\text{SbCl}_3 \cdot 9\text{S}_3$ .

MOLECULAR STRUCTURE OF  $\text{SbCl}_3 \cdot 1,4,7,10,13,16$ -  
HEXATHIACYCLOOCTADECANE

A centrosymmetric binuclear complex is formed with an antimony trichloride unit lying on each side of the ring plane. The structure is shown in Figure 2.3. Bond length and angles are given in Table 2.6. The two antimony atoms, related by an inversion centre, are separated by a distance of 8.32 Å which precludes interaction between them. Three consecutive sulfur atoms bind to each metal centre to yield an irregular *fac*-octahedral geometry. The sulfur coordination pattern could be described as [2+1] with one Sb-S bond (3.460(3) Å) far longer than the other two (2.968(2), 3.061(3) Å). A similar [2+1] Sb-S bonding mode has been reported twice before; for  $\text{SbCl}_3(\text{EtNH}\cdot\text{CS}\cdot\text{CS}\cdot\text{NHEt})_2$ <sup>133</sup> and  $\text{SbCl}_3(1,4\text{-dithiacycloheptane})$ .<sup>134</sup> Weak binding by the sulfur atoms is confirmed by comparison of the mean Sb-Cl distance with that for Sb-S; an increase of 0.745 Å (31%) is observed. The geometry of the  $\text{SbCl}_3$  unit is little changed from that of the parent trihalide as would be expected with the sulfur atoms only weakly bound. The antimony atom lies 2.11 Å above the  $\text{S}_3$  plane. The *cis* S...S atoms distances are 3.39 and 3.54 Å. The transannular S...S distances are 6.10, 7.08, and 8.64 Å. For comparison, this measurement in the free macrocycle is 3.88, 7.45, and 8.99 Å. Figure 2.4 shows the coordination sphere about antimony, grossly distorted from an idealised octahedron. A void exists between the atoms labelled Cl3, Cl1, S3a and S2 that could accommodate a stereochemically active lone pair. However, the distortion could also be a consequence of the geometric constraints imparted by the ring onto the donor sulfur atoms.

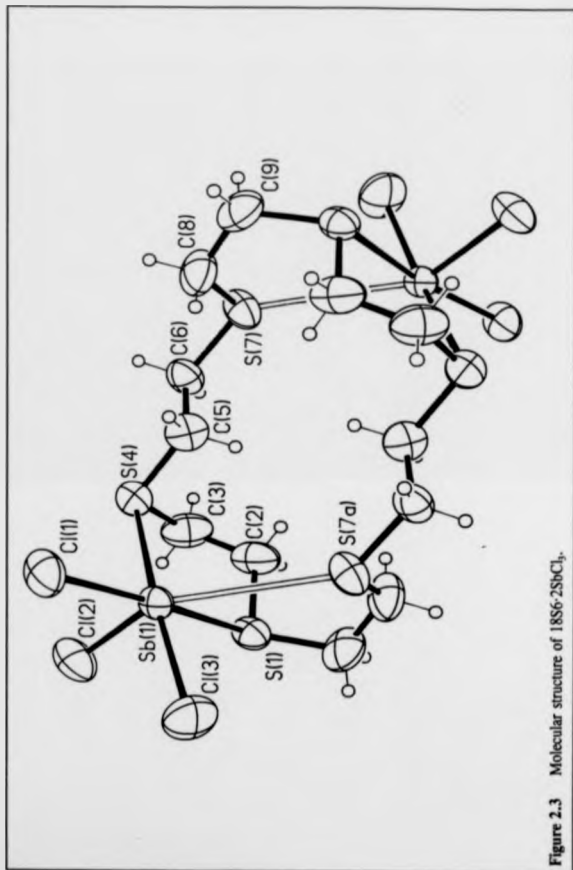


Figure 2.3 Molecular structure of 18S6-2SbCl<sub>3</sub>.

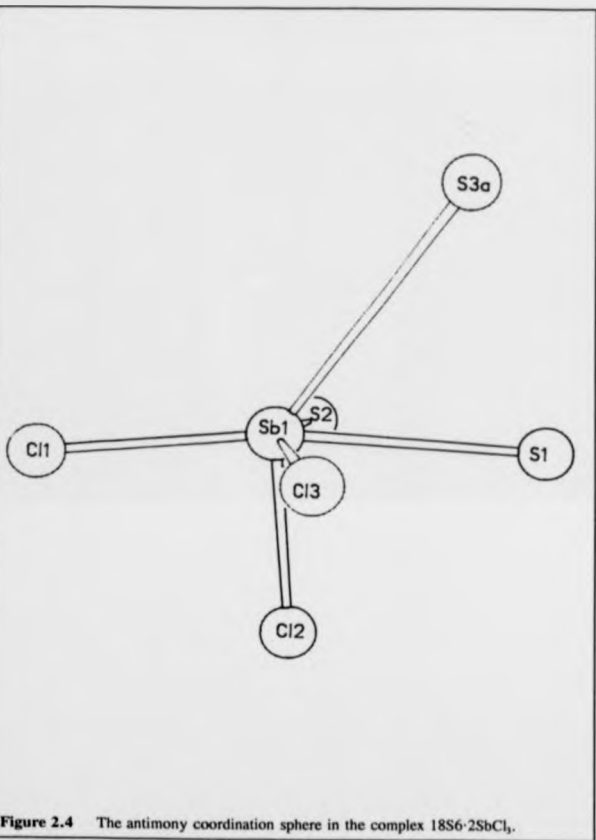
Table 2.6 Selected bond lengths (Å) and angles (°) for 18S6-2SbCl<sub>3</sub>.

Bond lengths (Å)

Sb(1)-Cl(1)	2.471(2)	Sb(1)-Cl(2)	2.381(3)
Sb(1)-Cl(3)	2.402(3)	Sb(1)-S(1)	2.968(2)
Sb(1)-S(4)	3.061(3)	S(1)-C(2)	1.803(10)
S(1)-C(9a)	1.810(7)	C(2)-C(3)	1.509(9)
C(3)-S(4)	1.815(8)	S(4)-C(5)	1.803(8)
C(5)-C(6)	1.492(12)	C(6)-S(7)	1.818(8)
S(7)-C(8)	1.790(8)	C(8)-C(9)	1.502(12)
C(9)-S(1a)	1.810(7)		

Bond angles (deg.)

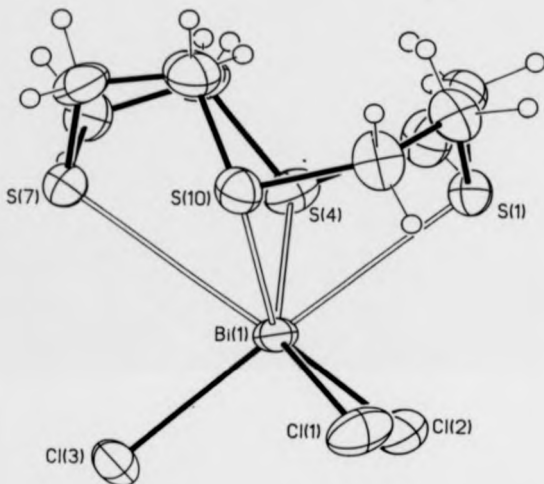
Cl(1)-Sb(1)-Cl(2)	89.1(1)	Cl(1)-Sb(1)-Cl(3)	95.6(1)
Cl(2)-Sb(1)-Cl(3)	90.6(1)	Cl(1)-Sb(1)-S(1)	167.5(1)
Cl(2)-Sb(1)-S(1)	79.9(1)	Cl(3)-Sb(1)-S(1)	90.6(1)
Cl(1)-Sb(1)-S(4)	100.2(1)	Cl(2)-Sb(1)-S(4)	79.0(1)
Cl(3)-Sb(1)-S(4)	160.9(1)	S(1)-Sb(1)-S(4)	71.9(1)
Sb(1)-S(1)-C(2)	103.9(2)	Sb(1)-S(1)-C(9a)	114.5(3)
C(2)-S(1)-C(9a)	102.1(4)	S(1)-C(2)-C(3)	113.4(7)
C(2)-C(3)-S(4)	116.4(7)	Sb(1)-S(4)-C(3)	103.3(3)
Sb(1)-S(4)-C(5)	98.4(3)	C(3)-S(4)-C(5)	102.9(4)
S(4)-C(5)-C(6)	113.1(6)	C(5)-C(6)-S(7)	113.7(5)
C(6)-S(7)-C(8)	101.5(4)	S(7)-C(8)-C(9)	112.0(6)
C(8)-C(9)-S(1a)	117.8(5)		



## MOLECULAR STRUCTURE OF $\text{BiCl}_3 \cdot 1,4,7,10\text{-TETRATHIACYCLODODECANE}$

The bismuth atom is coordinated to all four sulfur of the macrocycle to yield a structure with an overall half-sandwich topology (see Figure 2.5 and Table 2.7). The bismuth atom is located centrally above the ring centroid. The four sulfur atoms are coplanar with a maximum deviation from the  $S_4$  plane of just 0.01 Å. The mean  $S_4$  plane intersects the  $\text{Cl}_2$  plane at an angle of  $8.4^\circ$ . An approximate  $C_4$  symmetry is exhibited by the macrocycle conformation in this complex.

The sulfur atoms of the free macrocycle are exodentate and occupy the corner positions of a [3333] conformation. Use of all four donor atoms to chelate bismuth trichloride has necessitated significant reorganisation by the ligand. In the solid state, the macrocycle shows *cis* S-S contacts ranging between 4.44 and 4.46 Å. In the present structure this distance is reduced to between 3.36 and 3.45 Å, within the van der Waals radius of sulfur. Some indication of the ring cavity dimension is given by the *trans* S-S distance. For 1254 this lies in a range 6.25 to 6.35 Å, diminished to between 4.77 and 4.92 Å for  $\text{BiCl}_3 \cdot 1254$ . The bismuth lone pair may be directed through the centre of the crown cavity (see Figure 2.6).



**Figure 2.5** Molecular structure of  $\text{BiCl}_3 \cdot 12\text{S}_4$ .



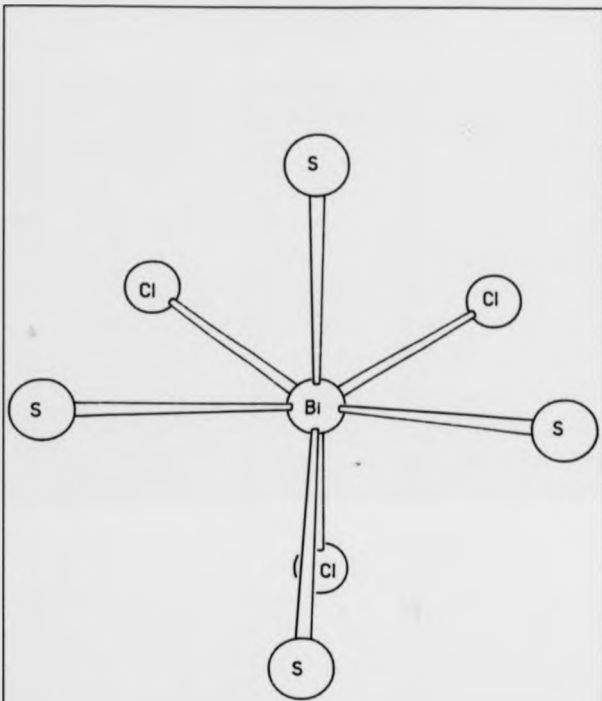
Table 2.7 Selected bond lengths (Å) and angles (°) for BiCl<sub>3</sub>·12S4.

Bond lengths (Å)

Bi(1)-Cl(1)	2.569(4)	Bi(1)-Cl(2)	2.569(3)
Bi(1)-Cl(3)	2.575(3)	Bi(1)-S(1)	2.996(3)
Bi(1)-S(4)	3.072(3)	Bi(1)-S(10)	2.987(3)
S(1)-C(2)	1.814(11)	S(1)-C(12)	1.820(10)
S(4)-C(3)	1.777(11)	S(4)-C(5)	1.804(10)
S(7)-C(6)	1.818(12)	S(7)-C(8)	1.812(12)
S(10)-C(9)	1.796(12)	S(10)-C(11)	1.796(11)
C(2)-C(3)	1.521(17)	C(5)-C(6)	1.502(14)
C(8)-C(9)	1.490(17)	C(11)-C(12)	1.475(14)

Bond angles (deg.)

Cl(1)-Bi(1)-Cl(2)	90.9(1)	Cl(1)-Bi(1)-Cl(3)	91.4(1)
Cl(1)-Bi(1)-Cl(3)	94.3(1)	Cl(1)-Bi(1)-S(1)	85.6(1)
Cl(1)-Bi(1)-S(1)	84.3(1)	Cl(3)-Bi(1)-S(1)	176.7(1)
Cl(1)-Bi(1)-S(4)	152.7(1)	Cl(2)-Bi(1)-S(4)	75.9(1)
Cl(3)-Bi(1)-S(4)	113.0(1)	S(1)-Bi(1)-S(4)	69.6(1)
Cl(1)-Bi(1)-S(10)	76.9(1)	Cl(2)-Bi(1)-S(10)	152.1(1)
Cl(3)-Bi(1)-S(10)	110.8(1)	S(1)-Bi(1)-S(10)	69.9(1)
S(4)-Bi(1)-S(10)	103.8(1)	Bi(1)-S(1)-C(2)	109.3(4)
Bi(1)-S(1)-C(12)	109.6(3)	C(2)-S(1)-C(12)	100.8(5)
Bi(1)-S(4)-C(3)	104.4(4)	Bi(1)-S(4)-C(5)	108.9(4)
C(3)-S(4)-C(5)	103.1(5)	C(6)-S(7)-C(8)	102.1(5)
Bi(1)-S(10)-C(9)	104.1(4)	Bi(1)-S(10)-C(11)	102.3(3)
C(9)-S(10)-C(11)	103.6(5)	S(1)-C(2)-C(3)	111.2(7)
S(4)-C(3)-C(2)	116.9(7)	S(4)-C(5)-C(6)	109.4(7)
S(7)-C(6)-C(5)	117.0(9)	S(7)-C(8)-C(9)	116.3(7)
S(10)-C(9)-C(8)	112.4(7)	S(10)-C(11)-C(12)	118.3(9)
S(1)-C(12)-C(11)	114.1(7)		

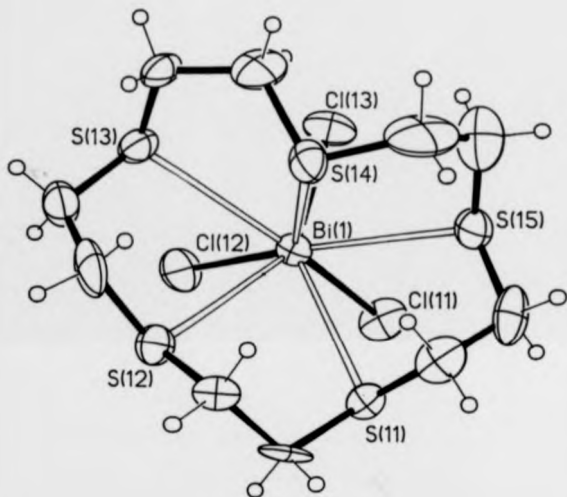


**Figure 2.6** Diagram showing the coordination sphere around the bismuth atom in  $\text{BiCl}_5 \cdot 12\text{S}_4$ , viewed normal to the  $\text{S}_4$  plane.

# MOLECULAR STRUCTURE OF $\text{BiCl}_3 \cdot 1,4,7,10,13\text{-}$ PENTATHIACYCLOPENTADECANE

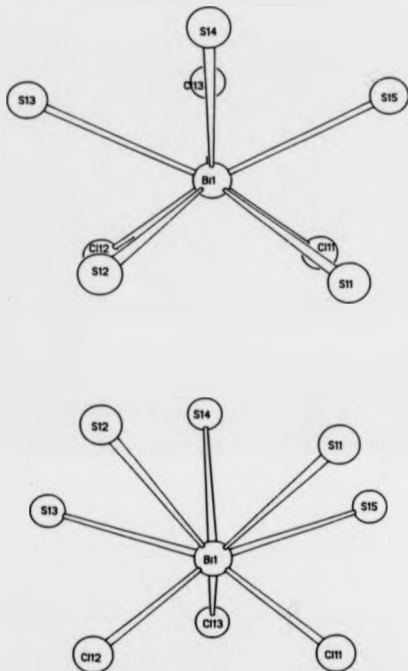
This orthorhombic unit cell contains two independent  $\text{BiCl}_3 \cdot 15\text{S}$  molecular adducts together with an acetonitrile molecule trapped as a lattice solvate. The independent  $\text{BiCl}_3 \cdot 15\text{S}$  molecules show essentially the same mode of metal coordination. Figure 2.7 shows the structure of molecule 1. Bond lengths and angles are provided in Table 2.8. Variations in geometry about the bismuth atom in each molecule are without chemical significance. All five sulfur atoms bind to the pyramidal bismuth trichloride unit to form a molecule with half-sandwich topology. The macrocycle has undergone an *exo* to *endo* conformational change as a consequence of the penta-chelation. The  $\text{S}_5$  plane is poorly defined in this molecule, mean deviation 0.56 Å molecule 1 (0.58 Å molecule 2). Closest 1,3-S...S contacts are 3.32 Å molecule 1 (3.29 Å molecule 2). An indication of the macrocyclic cavity size is given by the range of 1,4-S...S contacts; 3.924 - 5.617 Å molecule 1 (4.282 - 5.589 Å molecule 2).

For this molecular adduct the best insight into the nature of the structure is obtained by comparison with the eight-coordinate parent trihalide; a biccapped trigonal prism is again observed in the present compound. Figure 2.8 highlights the geometry about bismuth with views looking at a trigonal and a rectangular face. Confluence with the bismuth trichloride structure is evident from the 'one short two long' pattern of primary Bi-Cl bond lengths and  $\angle \text{S}_{(\text{topping})}\text{-Bi-S}_{(\text{topping})}$  of  $123.9^\circ$  ( $127.0^\circ \angle \text{Cl}_{(\text{topping})}\text{-Bi-Cl}_{(\text{topping})}$  in  $\text{BiCl}_3$ ). Clearly, in this instance, the bismuth lone pair must be little altered from that in the free halide *i.e.* holding a  $\psi$ -tetrahedral location.



**Figure 2.7** Molecular structure of  $\text{BiCl}_5 \cdot 15\text{S}_5$ .





**Figure 2.8** Two views of the bicapped trigonal prismatic coordination sphere about bismuth in the compound  $\text{BiCl}_3 \cdot 1.5\text{S}_5$  (molecule 1 shown).

MOLECULAR STRUCTURE OF  $\text{BiCl}_3 \cdot 1,4,7,10,13,16$ -  
HEXATHIACYCLOHEXADECANE

The pyramidal  $\text{BiCl}_3$  unit of this molecule is bonded to all six sulfur atoms of the crown thiaether and has the bismuth atom located on a crystallographic three-fold axis (see Figure 2.9 and Table 2.9). The bismuth atom enjoys a coordination geometry of nine [3:3:3], arising from the three chlorine atoms, and two sets of three sulfur atoms (S(1), S(1a), S(1b) - set A; S(2), S(2a), S(2b) - set B). The three planes so described are, of course, required to be parallel.

Metal-sulfur bond distances are 3.225(4) Å (Set A) and 3.146(4) Å (Set B). The arrangement of sulfur and chlorine atoms about the bismuth centre is illustrated in Figure 2.10. The three chlorine atoms are very nearly eclipsed by the sulfur atoms of set A (7.3° stagger) and therefore the bismuth coordination geometry of nine approximates to a tricapped (rectangular faces) trigonal prism. The bismuth coordination geometry is related to that seen in the structure of the parent halide, where again the bismuth atom sits, displaced from centre, in a trigonal prism. In this compound, however, only two of the rectangular faces are capped by further atoms. Even closer analogy is possible with the structure of lead(II) chloride. This nine-coordinate lead compound shows trigonal prismatic coordination with all three rectangular faces capped by chlorine atoms. The bismuth atom lies at a distance of nearly 2 Å from the set A S<sub>3</sub> plane and is displaced by just 0.5 Å out of the Set B S<sub>3</sub> plane.

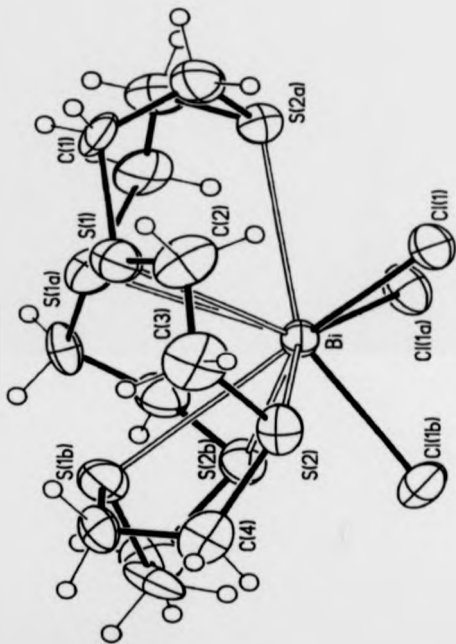
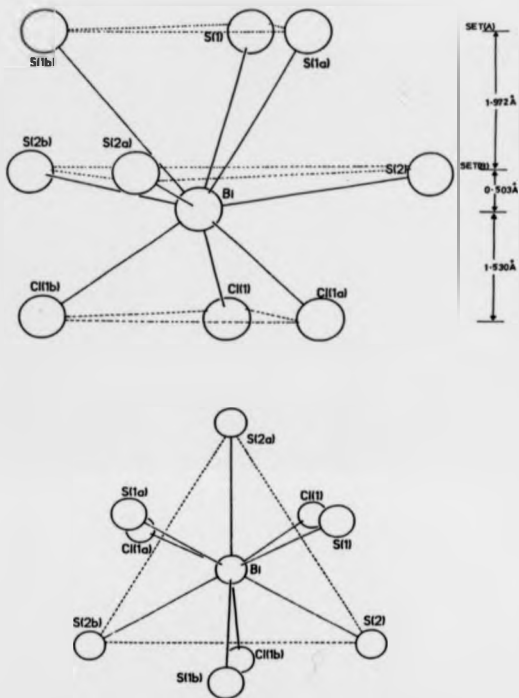


Figure 2.9 Molecular structure of  $\text{BiCl}_3 \cdot 18\text{S}_6$ .





**Figure 1.11** The bismuth coordination sphere in  $\text{BiCl}_3 \cdot 18\text{S6}$  viewed (a) perpendicular to the three-fold axis and (b) down the three-fold axis.

Table 2.9 Selected bond lengths (Å) and angles (°) for BiCl<sub>3</sub>·18S6.

Bond lengths (Å)

Bi-S(1)	3.225(4)	Bi-S(2)	3.146(4)
Bi-Cl(1)	2.607(4)	Bi-S(1a)	3.225(4)
Bi-S(1b)	3.225(4)	Bi-S(2a)	3.146(4)
Bi-S(2b)	3.146(4)	Bi-Cl(1a)	2.607(4)
Bi-Cl(1b)	2.607(4)	S(1)-C(1)	1.838(18)
S(1)-C(2)	1.790(17)	S(2)-C(3)	1.838(18)
S(2)-C(4)	1.810(16)	C(1)-C(4a)	1.510(21)
C(2)-C(3)	1.510(23)	C(4)-C(1a)	1.510(21)

Bond angles (deg.)

S(1)-Bi-S(2)	62.4(1)	S(1)-Bi-Cl(1)	86.3(1)
S(2)-Bi-Cl(1)	75.7(1)	S(1)-Bi-S(1a)	67.5(1)
S(2)-Bi-S(1a)	120.6(1)	Cl(1)-Bi-S(1a)	130.6(1)
S(1)-Bi-S(1b)	67.5(1)	S(2)-Bi-S(1b)	65.6(1)
Cl(1)-Bi-S(1b)	139.9(1)	S(1a)-Bi-S(1b)	67.5(1)
S(1)-Bi-S(2a)	65.6(1)	S(2)-Bi-S(2a)	117.5
Cl(1)-Bi-S(2a)	68.8(1)	S(1a)-Bi-S(2a)	62.4(1)
S(1b)-Bi-S(2a)	120.6(1)	S(1)-Bi-S(2b)	120.6(1)
S(2)-Bi-S(2b)	117.5	Cl(1)-Bi-S(2b)	152.9(1)
S(1a)-Bi-S(2b)	68.6(1)	S(1b)-Bi-S(2b)	62.4(1)
S(2a)-Bi-S(2b)	117.5	S(1)-Bi-Cl(1a)	139.9(1)
S(2)-Bi-Cl(1a)	152.9(1)	Cl(1)-Bi-Cl(1a)	89.0(1)
S(1a)-Bi-Cl(1a)	86.3(1)	S(1b)-Bi-Cl(1a)	130.6(1)
S(2a)-Bi-Cl(1a)	75.7(1)	S(2b)-Bi-Cl(1a)	68.8(1)
S(1)-Bi-Cl(1b)	130.6(1)	S(2)-Bi-Cl(1b)	68.8(1)
S(1a)-Bi-Cl(1b)	89.0(1)	S(1a)-Bi-Cl(1b)	139.9(1)
S(1b)-Bi-Cl(1b)	86.3(1)	S(2a)-Bi-Cl(1b)	152.9(1)
S(2b)-Bi-Cl(1b)	75.7(1)	Cl(1a)-Bi-Cl(1b)	89.0(1)
Bi-S(1)-C(1)	110.3(5)	Bi-S(1)-C(2)	100.6(5)
C(1)-S(1)-C(2)	100.1(7)	Bi-S(2)-C(3)	112.6(6)
Bi-S(2)-C(4)	109.4(5)	C(3)-S(2)-C(4)	101.7(7)
S(1)-C(1)-C(4a)	116.1(10)	S(1)-C(2)-C(3)	108.3(11)
S(2)-C(3)-C(2)	111.5(11)	S(2)-C(4)-C(1a)	114.9(11)

## 2-3 TRENDS IN THIAETHER BONDING TO TERVALENT ANTIMONY AND BISMUTH

Certain mean dimensions about the metal atom of the  $MCl_3$  S-macrocyclic adducts have been gathered in order that general patterns or trends may become apparent (Table 2.12). During the discussion, reference will be made to analogous oxygen-donor complexes. Consequently, the nature of these complexes will first be briefly reviewed. Additionally, before embarking upon this discussion, the nature of the parent antimony and bismuth trihalides in the crystalline state will be summarised and standard antimony(III) and bismuth(III) bond lengths tabulated.

### Complexes of group 15 trichlorides with oxygen crown ethers

The donor-acceptor compounds formed between the pnictide trihalides and the common oxygen-donor macrocycles have been structurally characterised.<sup>126,127,128,129,130</sup> The results are summarised in Table 2.10. The half-sandwich structure adopted almost exclusively, shows endodentate coordination by all ligand donor atoms and their adherence to either a true or approximate plane (greatest deviation 0.5 Å). The pyramidal  $MCl_3$  units show only slight change from the free metal halide.

For 12O4 and 15O5 simple 1:1 half-sandwich adducts are the only structure found with arsenic, antimony, and bismuth trichloride as substrate. With 18O6 as the complexing agent, no product was isolable with  $AsCl_3$ , and a simple half-sandwich was formed with  $SbCl_3$ . A total of three compounds have been isolated by reaction of  $BiCl_3$  and 18O6. The first and

second comprise half-sandwich adducts, an additional water molecule within the ring for the second. The third form involves halide transfer between two bismuth centres to yield the ions  $[\text{BiCl}_2 \cdot 18\text{O}6]^+$  and  $[\text{Bi}_2\text{Cl}_4]^2-$ .

**Table 2.10** Structurally characterised Group 15-crown ether complexes.

Metal Halide	Macrocycle (L)		
	12O4	15O5	18O6
$\text{AsCl}_3$	1:1	1:1	no complex
$\text{SbCl}_3$	1:1	1:1	1:1
$\text{BiCl}_3$	1:1	1:1	1) 1:1 2) 1:1·H <sub>2</sub> O 3) $2[\text{BiCl}_2\text{L}]^+ [\text{Bi}_2\text{Cl}_4]^{2-}$

For the half-sandwich complexes the trends can be summarised as follows:-

- 1) As the ring size increases, (12 → 15 → 18), the metal- $\text{O}_{\text{inner plane}}$  decreases.
- 2) As the metal radius increases, the metal- $\text{O}_{\text{inner plane}}$  decreases.
- 3) The M-O contacts are very long; some 0.3 - 0.7 Å greater than the associated M-Cl distance.
- 4) A very slight lengthening of the M-Cl bond by up to 0.05 Å is observed.
- 5) A systematic diminution of the Cl-M-Cl angle is apparent as the ligand size increases.

## The structures of antimony and bismuth trichloride in the crystalline state

### 1) Antimony trichloride

The metal coordination geometry can be described in terms of a bicapped trigonal prism with an eight-coordinate metal centre.

M-Cl bond lengths are:

- 2.340, 2.368, 2.368 Å - primary coordination.
- 3.609, 3.736, 3.736 Å - secondary coordination, prism atoms.
- 3.457, 3.457 Å - secondary coordination, capping atoms.

Bond angles for the primary coordinated chlorine atoms are:

95.70, 95.70, 90.98°, mean 94.13°.

### 2) Bismuth trichloride

This compound is isostructural with antimony trichloride. The M-Cl distances in this bicapped trigonal prism are:

- 2.468, 2.513, 2.518 Å - primary coordination.
- 3.224, 3.398, 3.450 Å - secondary coordination, prism atoms.
- 3.216, 3.256 - secondary coordination, capping atoms.

Notice the stronger secondary bonding in the bismuth structure. Bond angles about bismuth involving the three primary coordinated chlorine atoms are:

94.9, 93.2, 84.45°, mean 90.85°.

Standard bond lengths of antimony(III) and bismuth(III)

Table 2.11 Comparison of standard van der Waals and covalent M-X separations (Å) (M = Sb, Bi; X = O, S, Cl).

M	X	covalent	van der Waals
Sb	O	2.02	3.57
	S	2.40	3.85
	Cl	2.35	3.80
Bi	O	2.21	3.67
	S	2.59	3.95
	Cl	2.54	3.90

Reference to the standard M-X (M = Sb, Bi; X = O, S, Cl) covalent and van der Waals separations<sup>111</sup> (see Table 2.11) allows a qualitative notion of the relative strength of the bonding involved in the adducts under consideration.

## Discussion

**Table 2.12** Selected mean distances (Å) and angles (°) about the metal atom in antimony and bismuth trichlorides and their thiamacrocycle complexes.

Compound	Coordination number	M-Cl (mean)	∠ Cl-M-Cl (mean)	M-S (mean)	M-S <sub>6</sub> (mean plane)
SbCl <sub>3</sub>	8	2.359	94.13	n/a	n/a
SbCl <sub>3</sub> ·9S3	7	2.417	92.7	3.283	2.07
(SbCl <sub>3</sub> ) <sub>2</sub> ·18S6	6	2.418	91.8	3.163	2.11
BiCl <sub>3</sub>	8	2.50	90.85	n/a	n/a
BiCl <sub>3</sub> ·12S4	7	2.571	92.2	3.065	1.87
BiCl <sub>3</sub> ·15S5 (molecule 1)	8	2.567	91.2	3.168	1.66
BiCl <sub>3</sub> ·15S5 (molecule 2)	8	2.563	90.8	3.196	1.71
BiCl <sub>3</sub> ·18S6	9	2.607	89.0	3.186	1.54

The M-S distances, although within van der Waals separation, are significantly larger than the primary M-Cl contacts. Ergo, they must be considerably weaker. This is borne out by the relatively small perturbations to the MCl<sub>3</sub> unit and entirely consistent with deductions made from NMR regarding the solution state binding. The difference between standard oxygen and

sulfur radii varies between 0.38 (covalent) and 0.28 Å (van der Waals). Comparison with the  $\text{MCl}_3$ -oxaether donor bond lengths ( $\text{M} = \text{Sb, Bi}$ ) suggests that the sulfur macrocycles are slightly the more strongly bound.

Contrast between the bismuth and antimony adducts shows that whilst the mean Bi-S distance is around 20% larger than that of Bi-Cl in the same complex, for antimony this increase is about 35%. For the related oxygen macrocyclic complexes the same  $\text{As} < \text{Sb} < \text{Bi}$  order of M-macrocyclic bonding is observed.

For the bismuth-thiamacrocyclic adducts there is an increase in the M-Cl bond of at least 0.06 Å, about 3%, above that seen in the parent trihalide. For the antimony compounds this increase is slightly less at about 2.5%. A maximum M-Cl elongation of 1% is seen for the oxygen macrocycle-group 15 trichloride complexes, indicating a smaller metal-ether donor interaction.

The  $\angle \text{Cl-M-Cl}$  angles show a systematic decrease as the size of the ligand/coordination number increases for both the oxygen and sulfur macrocycles. For the bismuth complexes, not all the angles are less than those observed in the parent halide. That this is probably related to the secondary Bi-Cl interactions already present in the solid chloride is substantiated by the very similar angles observed for the bicapped trigonal prismatic (isostructural)  $\text{BiCl}_4^+1555$ .

Correlation of the metal-S (oxygen) distances necessitates caution in view of the structural diversity shown by these compounds. For the half-sandwich bismuth complexes with 12S4 and 1555 (two molecules) direct comparison with the oxygen analogues, 1:87 / 1:84, 1:66



/ 1·61, and 1·71 / 1·61 respectively, suggests superior binding by thiaether macrocycles. For the antimony complexes with 12O4 and 9S3 (both seven coordinate) this parameter, 2·00 / 2·07 respectively, again serves to illustrate the relative weakness of the oxamacrocyclic chelation.

## 2.4 CONFORMATIONAL CHANGES UPON THIAMACROCYCLE COMPLEXATION OF GROUP 15 TRICHLORIDES

Comparison of the bound macrocycle geometry to that shown by the parent ligand facilitates the investigation of ring reorganisation concomitant with complex formation. Mean C-C and C-S bond lengths together with torsion angles are given in Table 2.13 for the five structurally characterised compounds and the parent macrocycles.

### Bond lengths

No systematic trend exists for either C-C or C-S bonds. The more outlying mean bond lengths are a result of individual distances being subject to disorder. This is most pronounced in the structures reported for  $\text{BiCl}_4 \cdot 15\text{S}5$  (molecule 2) and 18S6, both with C-C bonds around 1.35 Å. The stoicism observed is in accord with the general maxim that bond length (and valence angle) variation is energetically expensive and produces small geometric changes compared to adjustments in dihedral angles.<sup>13b</sup>

### Torsion angles

With the exception of 9S3, the thiamacrocycles used in these studies adhere to the *gauche* C-C-S-C and *anti* S-C-C-S dihedral angle preferences outlined by Cooper *et al.*<sup>13b</sup> This trend is ascribed to the repulsive *gauche* effect arising from 1,4-S-S interactions.<sup>13b</sup> The cyclisation constraints of the medium-sized 9S3 ring do not permit the torsional flexibility exhibited by the larger congeners.

Table 2.13 Mean bond lengths (Å), mean bond angles (°), and torsion angles (°) for selected thiamacrocyclics and the ligands of group 15 trichloride-thiamacrocyclic complexes.

Ligand description	Compound									
	953	SiCl <sub>3</sub> , 953	1254	SiCl <sub>3</sub> , 1254	1555	BiCl <sub>3</sub> , 1555 (monomer 1)	BiCl <sub>3</sub> , 1555 (monomer 2)	1856	SiCl <sub>3</sub> , 1856	BiCl <sub>3</sub> , 1856
mean C-C (Å)	1.510	1.516	1.511	1.497	1.478	1.498	1.463	1.433	1.501	1.510
mean C-S (Å)	1.822	1.810	1.815	1.805	1.854	1.791	1.798	1.854	1.807	1.817
C-C torsion (°)	58.5	-54.3	-173.1	85.1	-171.9	64.9	64.0	-78.9	67.7	60.6
	58.5	-56.4	-172.7	87.2	174.4	85.0	56.8	-174.6	-176.9	55.8
	58.5	-55.8	-174.1	-56.8	-83.9	-87.8	-53.0	176.2	-56.5	60.6
C-S torsion (°)	-131.1	130.4	73.7	-157.4	-121.9	177.5	-168.4	73.3	-175.2	80.4
	35.1	-58.3	72.5	64.3	81.0	-172.6	87.2	84.2	62.8	176.7
	35.1	129.3	72.2	-160.1	82.8	161.0	-53.8	-178.3	75.6	-138.5
C-S torsion (°)	-131.1	130.4	73.7	-157.4	-121.9	177.5	-168.4	73.3	-175.2	80.4
	35.1	-58.3	72.5	64.3	81.0	-172.6	87.2	84.2	62.8	176.7
	35.1	129.3	72.2	-160.1	82.8	161.0	-53.8	-178.3	75.6	-138.5
C-S torsion (°)	-131.1	130.4	73.7	-157.4	-121.9	177.5	-168.4	73.3	-175.2	80.4
	35.1	-58.3	72.5	64.3	81.0	-172.6	87.2	84.2	62.8	176.7
	35.1	129.3	72.2	-160.1	82.8	161.0	-53.8	-178.3	75.6	-138.5

For all of the mononuclear complexes under discussion a *gauche* placement at C-C bonds is observed, as must be the case to produce five-membered chelate rings. In the case of the binuclear complex  $(\text{SbCl}_4)_2 \cdot 18\text{S6}$  there are in effect two sets of  $-\text{SCH}_2\text{-CH}_2\text{SCH}_2\text{-CH}_2\text{S}-$  groups within which the *gauche* C-C requirement is obeyed. The apparent anomaly applies only to the two C-C bonds linking the two half molecules. That these have chosen to remain *anti* is entirely in keeping with the predictions of Cooper.

### Molecular modelling

That thiamacrocycles bond only weakly to the pyramidal  $\text{MCl}_4$  centres of antimony and bismuth trichloride would seem incongruous with the extensive ligand reorganisation upon adduct formation. In particular, the remarkable 'S' profile of the macrocycle seen in  $\text{BiCl}_4 \cdot 18\text{S6}$  provokes further investigation. Therefore, with a view to quantifying the relative energies of the macrocycles when free and when complexed, molecular mechanics calculations have been applied. The results obtained are given in Table 2.14. Although the use of molecular mechanics calculations in coordination chemistry has been reviewed,<sup>139</sup> previous reports concerning molecular mechanics calculations of macrocyclic thiaethers are extremely scarce.<sup>140,141</sup> The force field used (MMX<sup>142</sup>) is not able to reliably model secondary bonded group 15 molecules. However, atoms not associated with the macrocycle were not relevant to the modest aims of this enquiry and so were simply removed from the crystallographic coordinate data. The use of this simple device to probe thiamacrocycle conformations has been used previously.<sup>141</sup>

**Table 2.14** Strain energy calculations (kcal.mol<sup>-1</sup>) for various thiamacrocycles and for the ligands in group 15 trichloride-thiamacrocyclic complexes.

Compound	Experimental Structure	Minimised Structure	Global Minimum	Mean atomic deviation /Å
9S3	14.57	12.65	12.42	0.042
12S4	8.73	6.30	6.29	0.032
15S5	21.26	7.32	5.29	0.324
18S6	51.80	8.57	5.14	0.196
SbCl <sub>3</sub> , 9S3	14.42	12.65	12.42	0.040
(SbCl <sub>3</sub> ) <sub>2</sub> , 18S6	13.06	6.49	5.14	0.171
BiCl <sub>3</sub> , 12S4	16.34	11.02	6.29	0.057
BiCl <sub>3</sub> , 15S5 (molecule 1)	23.84	9.35	5.29	0.159
BiCl <sub>3</sub> , 15S5 (molecule 2)	50.40	8.85	5.29	0.187
BiCl <sub>3</sub> , 18S6	17.72	11.08	5.14	0.274

**KEY**

Experimental structure: Crystallographic coordinates of main atoms, hydrogen and lone pair positions minimised.

Minimised structure: Minimised structure without constraints.

Global minimum: Lowest energy structure found for the molecule.

Mean atomic deviation: Mean atomic movement comparing experimental with minimised structures.

Consideration of the energy difference ( $\Delta_i$ ) between the experimental and minimised structures shows this to embody the 'smoothing' out of irregular geometries arising from the X-ray diffraction technique. Examination of individual bond lengths in the reported structures correlates well with this energy difference:

- 1) 18S6 and  $\text{BiCl}_3 \cdot 15\text{S5}$  (molecule 1) both have two  $sp^2$  C-C bond lengths reported at c. 1.35 Å,  $\Delta_i = 50 \text{ kcal.mol}^{-1}$ .
- 2) 15S5 has two C-C bond lengths c. 1.45 Å and  $\text{BiCl}_3 \cdot 15\text{S5}$  (molecule 2) has three C-S bond lengths of less than 1.75 Å,  $\Delta_i = 15 \text{ kcal.mol}^{-1}$ .
- 3) Bond geometries are far less 'anomalous' in the other compounds, as expected  $\Delta_i$  ranges from 6.5  $\text{kcal.mol}^{-1}$  for  $\text{BiCl}_3 \cdot 18\text{S6}$  down to just 1.8  $\text{kcal.mol}^{-1}$  for  $\text{SbCl}_3 \cdot 9\text{S3}$ .

The free ligands 9S3 and 12S4 are found to exist at a conformation in the solid state that is, energetically, almost identical to that found as the global minimum for the molecule. In the case of the more flexible 15S5 and 18S6 a small energy difference exists, 2.03 and 3.43  $\text{kcal.mol}^{-1}$  respectively, which must be a consequence of small intermolecular crystal packing forces.

Comparison of the experimental structure energies with those of the relevant global minimum is clearly not warranted in view of the abnormal bond geometries present in the former. Taking the minimised crystallographic coordinates alleviates this problem but leaves open the question regarding the physical reality of the X-ray diffraction measurements. Using this protocol, energy differences between the minimised structures and global minima should

represent a minimum case; any part of  $\Delta$ , that does indeed represent a physical reality will not be included. The strain energy difference between the minimised crystal coordinates and the global minimum will be termed the distortion energy. This parameter is given in Table 2.15 for each complex under discussion. The following comments are pertinent:

- 1) The minimised structure  $\text{SbCl}_3 \cdot 9\text{S3}$  has a strain energy virtually identical to that of the global minimum. This serves to demonstrate that the existence of a bridging sulfur atom in this complex has made a negligible alteration to the strain energy of the ligand.
- 2) Distortion energies of 3.56, 4.06 and 4.73  $\text{kcal.mol}^{-1}$  are calculated for the bismuth complexes incorporating 15S5 (molecule 1), 15S5 (molecule 2) and 12S4 respectively. For ligands containing four or five donor atoms these, rather small, energetic penalties are readily overcome by the multidentate bonding mode.
- 3) The seemingly most severe bound-ligand conformation is that observed for  $\text{BiCl}_3 \cdot 18\text{S6}$ . Although the largest difference is indeed seen between the minimised structure and global minimum, at 5.94  $\text{kcal.mol}^{-1}$  this yields a burden of just 1  $\text{kcal.mol}^{-1}$  upon each Bi-S bond. Again, this presents no significant restraint to ligand reorganisation upon complex formation.
- 4) That the  $(\text{SbCl}_3)_2 \cdot 18\text{S6}$  ring conformation has an energy close (1.35  $\text{kcal.mol}^{-1}$ ) to that of the global minimum must reflect the latitude allowed by complexing two antimony trichloride centres within an open topology. It is tempting to suggest that the increased

strength of bismuth-thiaether bonds allows this ligand to move into the higher energy, fully encapsulating geometry seen in  $\text{BiCl}_3 \cdot 18\text{S}6$ .

**Table 2.15** Estimated macrocycle distortion energy upon complexation for the thiamacrocycle complexes of antimony and bismuth trichloride.

Compound	$\text{SbCl}_3 \cdot 9\text{S}3$	$(\text{SbCl}_3)_2 \cdot 18\text{S}6$	$\text{BiCl}_3 \cdot 15\text{S}5$ (molecule 2)	$\text{BiCl}_3 \cdot 15\text{S}5$ (molecule 1)	$\text{BiCl}_3 \cdot 12\text{S}4$	$\text{BiCl}_3 \cdot 18\text{S}6$
Distortion Energy /kcal mol <sup>-1</sup>	0.23	1.35	3.56	4.06	4.73	5.94

Having made a tentative quantification of the relative conformational energies of the free and unbound ligands, it seems appropriate to contemplate the failure to obtain certain complexes. These were  $\text{SbCl}_3 \cdot 12\text{S}4$  and all complexes involving arsenic trichloride. Indeed, a pattern does emerge, although this may be entirely fortuitous. It presupposes the relative thiaether binding strength  $\text{Bi} > \text{Sb} > \text{As}$ . The following considerations serve to demonstrate:

**1) Structures obtained incorporating antimony trichloride**

9S3 imposes almost no conformational penalty upon complexation. 18S6 is unusual in being able to offer a low energy conformation involving two trichloride units.

**2) Compound isolated but relatively sensitive**

15S5 is able to offer bismuth trichloride a conformation with a distortion energy of 3.5 - 4.0 kcal.mol<sup>-1</sup>. Antimony trichloride is barely able to accommodate this and so an adduct of greater sensitivity was formed.



3) **Compound not formed**

The distortion energy entailed in complex formation with 12S4 is simply too great for antimony trichloride to surmount, even with tetradentate ligation. In the case of the bismuth trichloride adduct the distortion energy has risen to nearly 5 kcal.mol<sup>-1</sup>.

On this basis, it might be reasonable to assume that the weakness of any prototypical arsenic-thiaether bond is unable to overcome the ligand reorganisation penalty (distortion energy). The sole exception to this would be 9S3, where, it should be noted, a small crop of very sensitive crystals was obtained on one occasion.

## CONCLUSIONS

- 1) With regard to the trihalides of antimony and bismuth, molecular complexes are readily formed with a variety of homoleptic polythiamacrocyclics. Adducts involving arsenic trichloride have, so far, resisted isolation.
- 2) A wide variety of molecular topology is observed for these thiamacrocyclic compounds, whereas the analogous oxamacrocyclic complexes exhibit, almost exclusively, a simple half-sandwich form. The complexes formed between bismuth trichloride and the macrocycles 15S5 and 18S6 are closely related to the extended, secondary structure seen in the halide itself.
- 3) Bonding between the thiamacrocyclics and the trichlorides of antimony and bismuth is extremely weak with mean M-S distances greater than 3.0 Å. In acetonitrile solution, an almost negligible alteration in chemical shift is observed.
- 4) The strength of bonding between the trivalent chlorides and the thiaether donors follows the order Bi > Sb > As, exactly that seen for the macrocyclic polyether adducts.
- 5) The M-S (M = As, Sb, Bi) bonding appears somewhat stronger than the M-O bonding in the analogous crown ether adducts.
- 6) The observed trends in isolation and properties of the complexes, correlate well with strain energy calculations using the conformation of the coordinated macrocycles.

## EXPERIMENTAL

Acetonitrile, dichloromethane, diethyl ether, and hexane were obtained from Fisons Scientific Ltd., Loughborough. Acetonitrile was purified following the recommended procedure,<sup>143</sup> stored over  $P_4O_{10}$  and distilled under dinitrogen immediately prior to use. Dichloromethane and hexane were dried over powdered calcium hydride before use. Diethyl ether was dried over a sodium/potassium alloy. These solvents were freshly distilled under dry dinitrogen before use. All manipulations were conducted under a dinitrogen atmosphere using standard Schlenk techniques.

Arsenic trichloride and bismuth trichloride were used as supplied from BDH Chemicals Ltd., Poole. Antimony trichloride was sublimed under vacuum before use.

The macrocycles 12S4, 15S5 and 18S6 were supplied by Aldrich Chemical Co. Ltd., Gillingham, and used without further purification. 9S3 was prepared by the method of Rawle.<sup>144</sup> Other reagents were obtained from Aldrich Chemical Co. Ltd., and used as supplied, except for 1,4,7-trithiaheptane which was distilled prior to use.

#### Synthesis of $SbCl_3 \cdot 9S3$

Dropwise addition of an acetonitrile solution of 9S3 (0.26 g, 1.46 mmol) to an ice-cold solution of antimony trichloride (0.33 g, 1.46 mmol) in acetonitrile results in a clear solution. After warming to 50 °C and stirring for 1 day, slow concentration of this solution provided colourless needle crystals (0.44 g, 74%) directly suitable for diffraction studies. M.p. 163-

164°C (decomp.). Anal. calc. for  $C_6H_{12}SbCl_3S_3$ : C, 17.64; H, 2.96; Cl, 26.04%. Found: C, 18.01; H, 3.18; Cl, 27.02%.  $^1H$  NMR (400 MHz,  $CD_3CN$ )  $\delta$ , ppm: 3.11 [12 H, s,  $CH_2$  (ligand)]. I.R. (CaI plates, nujol):  $\nu(SbCl)$  260, 290, 320  $cm^{-1}$ ;  $\nu$ (ligand) 817, 887, 925  $cm^{-1}$ . U.v./vis  $\lambda_{max}$  (MeCN) 34 990  $cm^{-1}$ .

#### Synthesis of $BiCl_3 \cdot 9S3$

An acetonitrile solution of 9S3 (0.20g, 1.11 mmol) was slowly introduced to a solution of bismuth trichloride (0.35 g, 1.11 mmol) in the same solvent at a temperature of 0°C. The resulting solution was kept at 50°C and stirred for 24 h. Removal of the solvent under vacuum produced a fine white powder which was washed with diethyl ether. Subsequent recrystallisation from acetonitrile yielded a crop of pale yellow crystalline material (0.47 g, 85%). M.p. 223-224 °C (decomp.). Anal. calc. for  $C_{14}H_{27}Bi_2Cl_6NS_4$ : C, 16.29; H, 2.64; Cl, 20.60%. Found: C, 16.71; H, 2.62; Cl, 16.71%.  $^1H$  NMR (400 MHz,  $CD_3CN$ )  $\delta$ , ppm: 3.14 [12 H, s,  $CH_2$  (ligand)]. I.R. (CaI plates, nujol):  $\nu(BiCl)$  220, 262  $cm^{-1}$ ;  $\nu$ (ligand) 820, 882, 924  $cm^{-1}$ . U.v./vis  $\lambda_{max}$  (MeCN) 34 990  $cm^{-1}$ .

#### Synthesis of $BiCl_3 \cdot 12S4$

A solution of 12S4 (0.13 g, 0.52 mmol) in acetonitrile (70  $cm^3$ ) was added to an ice-cold solution of bismuth trichloride (0.16 g, 0.52 mmol) in acetonitrile (40  $cm^3$ ) over a period of 30 min. The resulting clear solution was held at 50 °C for 24 h and, following filtration, was allowed to cool slowly to room temperature. Small pale yellow crystals of the product (0.19 g, 66%) were obtained of a quality suitable for diffraction studies. M.p. 193-194 °C. Anal. calc. for  $C_6H_{18}BiCl_3S_4$ : C, 17.30; H, 2.90%. Found: C, 17.45; H, 2.95%.  $^1H$  NMR (400 MHz,  $CD_3CN$ )  $\delta$ , ppm: 2.76 [16 H, s,  $CH_2$  (ligand)]. I.R. (CaI plates, nujol):  $\nu(BiCl)$  228, 245  $cm^{-1}$ ;  $\nu$ (ligand) 832, 919, 1404  $cm^{-1}$ . U.v./vis  $\lambda_{max}$  (MeCN) 35 080  $cm^{-1}$ .

#### Synthesis of $\text{SbCl}_3 \cdot 15\text{S5}$

15S5 (0.303 g, 1.01 mmol) in acetonitrile (40  $\text{cm}^3$ ) was added dropwise to an acetonitrile solution (30  $\text{cm}^3$ ) of antimony trichloride (0.230 g, 1.01 mmol). After stirring the clear solution overnight, the solvent was removed in *vacuo* and the resulting white powder washed with hexane (2 x 10  $\text{cm}^3$ ) and diethyl ether (1 x 3  $\text{cm}^3$ ). The solid was then dissolved again in acetonitrile and passed through a fine sinter before the solvent volume was reduced to c. 10  $\text{cm}^3$ . Standing for 2 days at  $-25^\circ\text{C}$  produced a crop of well formed colourless crystals (0.23 g, 43%). These proved to be uncharacteristically sensitive to momentary exposure to the atmosphere. M.p.  $154\text{--}156^\circ\text{C}$  (decomp.). Anal. calc. for  $\text{C}_{10}\text{H}_{10}\text{SbCl}_3\text{S}_5$ : C, 22.72; H, 3.81; Cl, 20.12%. Found: C, 22.79; H, 3.85; Cl, 20.05%.  $^1\text{H}$  NMR (400 MHz,  $\text{CD}_3\text{CN}$ )  $\delta$ , ppm: 2.77 [24 H, s,  $\text{CH}_2$  (ligand)]. I.R. (CsI plates, nujol):  $\nu(\text{SbCl})$  263, 291, 312  $\text{cm}^{-1}$ ;  $\nu(\text{ligand})$  1017, 1262, 1413  $\text{cm}^{-1}$ . U.v./vis  $\lambda_{\text{max}}$  (MeCN) 34 990  $\text{cm}^{-1}$ .

#### Synthesis of $\text{BiCl}_3 \cdot 15\text{S5}$

Dropwise addition of 15S5 (0.25 g, 0.84 mmol) in acetonitrile (50  $\text{cm}^3$ ) to and ice-cold solution of bismuth trichloride (0.27 g, 0.84 mmol) in acetonitrile (50  $\text{cm}^3$ ) produced a white cloudy suspension which was stirred for 24 h at  $50^\circ\text{C}$ . Removal of the solvent gave a white solid which was washed with hexane (4 x 20  $\text{cm}^3$ ) and diethyl ether (2 x 20  $\text{cm}^3$ ). Recrystallisation from acetonitrile-dichloromethane provided the product as pale yellow lath crystals (0.44 g, 82%). M.p.  $172\text{--}174^\circ\text{C}$ . Anal. calc. for  $\text{C}_{22}\text{H}_{14}\text{Bi}_2\text{Cl}_6\text{NS}_{10}$ : C, 20.75; H, 3.40; N, 1.10%. Found: C, 20.60; H, 3.45; N, 1.05%.  $^1\text{H}$  NMR (400 MHz,  $\text{CD}_3\text{CN}$ )  $\delta$ , ppm: 2.88 [20 H, s,  $\text{CH}_2$  (ligand)]. I.R. (CsI plates, nujol):  $\nu(\text{BiCl})$  226, 254  $\text{cm}^{-1}$ ;  $\nu(\text{ligand})$  1016, 1260, 1404  $\text{cm}^{-1}$ . U.v./vis  $\lambda_{\text{max}}$  (MeCN) 35 140  $\text{cm}^{-1}$ .

#### Synthesis of $(\text{SbCl}_2)_2 \cdot 18\text{S6}$

To an acetonitrile solution ( $30 \text{ cm}^3$ ) of antimony trichloride ( $0.191 \text{ g}$ ,  $0.836 \text{ mmol}$ ) was added, dropwise, a solution of 18S6 ( $0.302 \text{ g}$ ,  $0.836 \text{ mmol}$ ) in acetonitrile ( $60 \text{ cm}^3$ ). The flocculent white precipitate formed dissolved fully at  $50^\circ\text{C}$  and was kept at this temperature for 2 hours before filtration through a fine sinter at *c.*  $70^\circ\text{C}$ . After cooling to room temperature, the solvent was removed *in vacuo* and the white solid washed with hexane ( $3 \times 10 \text{ cm}^3$ ). Recrystallisation was effected from dichloromethane at  $-25^\circ\text{C}$  to produce a crop of colourless, nugget-shaped crystals ( $0.43 \text{ g}$ ,  $54\%$ ). M.p.  $147\text{--}150^\circ\text{C}$  (decomp.). Anal. calc. for  $\text{C}_{17}\text{H}_{24}\text{Sb}_2\text{Cl}_4\text{S}_6$ : C,  $21.30$ ; H,  $3.60$ ; Cl,  $15.75\%$ . Found: C,  $21.95$ ; H,  $3.35$ ; Cl,  $15.15\%$ .  $^1\text{H}$  NMR ( $400 \text{ MHz}$ ,  $\text{CD}_3\text{CN}$ )  $\delta$ , ppm:  $2.84$  [ $24 \text{ H}$ , s,  $\text{CH}_2$  (ligand)]. I.R. (CsI plates, nujol):  $\nu(\text{SbCl})$   $212, 240 \text{ cm}^{-1}$ ;  $\nu(\text{ligand})$   $832, 1140, 1422 \text{ cm}^{-1}$ . U.v./vis  $\lambda_{\text{max}}$  (MeCN)  $34\,990 \text{ cm}^{-1}$ .

#### Synthesis of $\text{BiCl}_2 \cdot 18\text{S6}$

A solution of 18S6 ( $0.28 \text{ g}$ ,  $0.77 \text{ mmol}$ ) in acetonitrile ( $50 \text{ cm}^3$ ) was added dropwise to a cold solution of bismuth trichloride ( $0.24 \text{ g}$ ,  $0.77 \text{ mmol}$ ) in acetonitrile ( $60 \text{ cm}^3$ ) and the resulting slurry was heated at  $60^\circ\text{C}$  with stirring for 48 h. On cooling, the pale yellow precipitate was filtered off *in vacuo*, washed with hexane ( $3 \times 15 \text{ cm}^3$ ) and diethyl ether ( $2 \times 20 \text{ cm}^3$ ), and then redissolved in the minimum of hot acetonitrile. The resulting solution was layered with an equal volume of diethyl ether to yield the product by slow deposition of pale yellow blocks ( $0.41 \text{ g}$ ,  $79\%$ ). M.p.  $175\text{--}178^\circ\text{C}$  (decomp.). Anal. calc. for  $\text{C}_{17}\text{H}_{24}\text{BiCl}_2\text{S}_6$ : C,  $21.30$ ; H,  $3.60$ ; Cl,  $15.75\%$ . Found: C,  $21.95$ ; H,  $3.35$ ; Cl,  $15.15\%$ .  $^1\text{H}$  NMR ( $400 \text{ MHz}$ ,  $\text{CD}_3\text{CN}$ )  $\delta$ , ppm:  $2.84$  [ $24 \text{ H}$ , s,  $\text{CH}_2$  (ligand)]. I.R. (CsI plates, nujol):  $\nu(\text{BiCl})$   $212, 240 \text{ cm}^{-1}$ ;  $\nu(\text{ligand})$   $832, 1140, 1422 \text{ cm}^{-1}$ . U.v./vis  $\lambda_{\text{max}}$  (MeCN)  $34\,990 \text{ cm}^{-1}$ .

#### Attempted synthesis of arsenic trichloride-thiamacrocylic complexes

Solutions (acetonitrile and dichloromethane were used) of the thiamacrocycles 9S3, 12S4, 15S5 and 18S6 were added to arsenic trichloride in the same solvent. With just one exception, attempts to recrystallise/precipitate the adduct were not successful, the free ligand alone was recovered. On a sole occasion a very few colourless, sensitive, needle crystals were obtained using 9S3 in acetonitrile. Their melting point, 176 °C, suggested the formation of a novel adduct. Insufficient material was present to allow further characterisation.

#### Molecular Modelling

Calculations were conducted using the program PCMODEL version 3.2<sup>143</sup> running on an IBM compatible personal computer with an 80386 processor. The force field was MMX<sup>142</sup> which is an extension of Allinger's MM2.<sup>144</sup> The crystallographic coordinates of the macrocyclic main atoms were read in and fixed. The hydrogen atoms and lone pairs were added, and the structure was minimised to move the hydrogens and lone pairs optimised rather than idealised positions. This was termed the *experimental structure*. The fixed atom constraint was then relaxed and the structure reminimised to produce the *minimised structure*. Geometric comparison by a least squares fitting of the heavy atoms for a pair of structures was conducted and the mean atomic deviation calculated. For each macrocycle a global minimum was sought using the RANDMZ command in PCMODEL. This was allowed to find and minimise 1000 trial structures. The strain energy difference between the minimised structure and the global minimum was termed the *distortion energy*.

**Table 2.16** Crystallographic data for SbCl<sub>3</sub>·9S3

Formula	C <sub>6</sub> H <sub>12</sub> S <sub>3</sub> ·SbCl <sub>3</sub>
M <sub>r</sub>	408.5
Crystal class	orthorhombic
Space group	P2 <sub>1</sub> 2 <sub>1</sub> 2 <sub>1</sub>
a / Å	7.733(3)
b / Å	10.241(4)
c / Å	16.329(5)
α / °	
β / °	
γ / °	
V / Å <sup>3</sup>	1293.1(6)
Z	4
D <sub>x</sub> / g cm <sup>-3</sup>	2.10
Mo-K <sub>α</sub> radiation, λ / Å	0.71069
μ <sub>(Mo-K<sub>α</sub>)</sub> / cm <sup>-1</sup>	32.0
T / K	290
F <sub>(000)</sub>	792
Final R	0.033
Unique observed (I/σ(I) ≥ 2.0) reflections	1181



### Crystal Structure determination of $\text{SbCl}_5 \cdot 9\text{S}_3$

A colourless lath crystal was mounted in a Lindemann capillary. Data were collected with a Siemens R3m four circle diffractometer in  $\omega$ - $2\theta$  mode. Maximum  $2\theta$  was  $50^\circ$  with scan range  $\pm 0.6^\circ(\omega)$  around the  $K_{\alpha 1}$ - $K_{\alpha 2}$  angles, scan speed  $2.15^\circ(\omega) \text{ min}^{-1}$ , depending on the intensity of a 2s pre-scan; backgrounds were measured at each end of the scan for 0.25 of the scan time. The  $hkl$  ranges were 0/9, 0/12, 0/19. Three standard reflections were monitored every 200 reflections, and no decrease during data collection. Unit cell dimensions and standard deviations were obtained by least-squares fit to 15 reflections ( $18 < 2\theta < 22^\circ$ ). The 1386 reflections collected were processed using profile analysis to give 1361 unique reflections, of which 1181 were considered observed ( $I/\sigma(I) > 2.0$ ). These were corrected for Lorentz, polarization and absorption effects (the last by the Gaussian method); minimum and maximum transmission factors were 0.84 and 0.79. Crystal dimensions were  $0.060 \times 0.077 \times 0.50 \text{ mm}$ . Systematic reflection conditions  $h00 \ h = 2n$ ,  $0k0 \ k = 2n$ ,  $00l \ l = 2n$ , indicate space group  $P2_12_12_1$ . Heavy atoms were located by the Patterson interpretation section of SHELXTL and the light atoms then found by successive Fourier syntheses. Anisotropic thermal parameters were used for all non-H atoms. Hydrogen atoms were given fixed isotropic thermal parameters,  $U = 0.08 \text{ \AA}^2$ . They were inserted at calculated positions and not refined. The absolute structure of the individual crystal chosen was checked by refinement of a  $\delta F$  multiplier (refined value =  $1.10(10)$ ). Final refinement was on  $F$  by least squares methods refining 118 parameters. Largest positive and negative peaks on a final difference Fourier synthesis were of height  $+0.5, -0.9 \text{ e. \AA}^{-3}$ . A weighting scheme of the form  $W = 1/(\sigma^2(F) + gF^2)$  with  $g = 0.00086$  was used and shown to be satisfactory by a weight analysis. Final  $R = 0.033$ ,  $R_w = 0.040$ ,  $S = 0.9584$ ;  $R_{\text{int}} = 0.039$ . Maximum shift/error in final cycle was 0.002. Computing was conducted on a DEC Microvax-II with SHELXTL PLUS.<sup>147</sup> Scattering factors in the analytical form and anomalous dispersion factors were taken from reference 148.

**Table 2.17** Crystallographic data for  $(\text{SbCl}_2)_2 \cdot 18\text{S6}$

Formula	$\text{C}_{12}\text{H}_{24}\text{S}_6 \cdot 2\text{SbCl}_2$
$M_r$	816.9
Crystal class	triclinic
Space group	$P\bar{1}$
$a/\text{\AA}$	8.291(4)
$b/\text{\AA}$	8.450(3)
$c/\text{\AA}$	11.587(6)
$\alpha/^\circ$	98.69(6)
$\beta/^\circ$	102.29(4)
$\gamma/^\circ$	115.86(3)
$V/\text{\AA}^3$	685.8(6)
$Z$	1
$D_x/\text{g cm}^{-3}$	1.98
Mo-K $\alpha$ radiation, $\lambda/\text{\AA}$	0.71069
$\mu_{\text{(Mo-K}\alpha\text{)}}/\text{cm}^{-1}$	32.0
$T/\text{K}$	290
$F_{000}$	
Final $R$	0.038
Unique observed ( $I/\sigma(I) \geq 2.0$ ) reflections	2006

### Crystal structure determination of $(\text{SbCl}_2)_2 \cdot 18\text{S6}$

A colourless plate crystal was mounted in a Lindemann capillary to avoid hydrolysis. Data were collected with a Siemens R3m four circle diffractometer in  $\omega$ - $2\theta$  mode. Maximum  $2\theta$  was  $50^\circ$  with scan range  $\pm 0.70^\circ(\omega)$  around the  $K_{\alpha 1}$ - $K_{\alpha 2}$  angles, scan speed  $2.15^\circ(\omega) \text{ min}^{-1}$ , depending on the intensity of a 2s pre-scan; backgrounds were measured at each end of the scan for 0.25 of the scan time. The  $hkl$  ranges were 0/10, -11/11, -14/14. Three standard reflections were monitored every 200 reflections, and showed a significant decrease during the final stages of data collection. The data were rescaled to correct for this. Unit cell dimensions and standard deviations were obtained by least-squares fit to 15 reflections ( $26 < 2\theta < 28^\circ$ ). The reflections collected were processed using profile analysis to give 2465 unique reflections ( $R_{\text{int}} =$ ), of which 2006 were considered observed ( $I/\sigma(I) > 2.0$ ). These were corrected for Lorentz, polarization and absorption effects (the last by the Gaussian method); minimum and maximum transmission factors were 0.88 and 0.62. Crystal dimensions were 0.30 x 0.24 x 0.15 mm. No systematic reflection conditions indicate space groups  $P1$  and  $P1$ .  $P1$  was selected and deemed correct by successful refinement. Heavy atoms were located by the Patterson interpretation section of SHELXTL and the light atoms then found by successive Fourier syntheses. Anisotropic thermal parameters were used for all non-H atoms. Hydrogen atoms were given fixed isotropic thermal parameters,  $U = 0.08 \text{ \AA}^2$ , inserted at calculated positions and not refined. Final refinement was on  $F$  by least squares methods refining 118 parameters. Largest positive and negative peaks on a final difference Fourier synthesis were of height  $\pm 0.7 \text{ e.\AA}^{-3}$ . A weighting scheme of the form  $W = 1/(\sigma^2(F) + gF^2)$  with  $g = 0.00025$  was used and shown to be satisfactory by a weight analysis. Final  $R = 0.38$ ,  $R_w = 0.40$ ,  $S =$ ;  $R_{\text{all reflections}} =$ . Maximum shift/error in final cycle was 0.01. Computing was conducted on a DEC Microvax-II with SHELXTL PLUS.<sup>147</sup> Scattering factors in the analytical form and anomalous dispersion factors taken from reference 148.

**Table 2.18** Crystallographic data for  $\text{BiCl}_3 \cdot 12\text{S}_4$ .

Formula	$\text{C}_2\text{H}_{18}\text{BiCl}_3\text{S}_4$
$M_r$	555.8
Crystal class	monoclinic
Space group	$\text{P}2_1/n$
$a/\text{\AA}$	7.985(4)
$b/\text{\AA}$	12.956(7)
$c/\text{\AA}$	15.278(9)
$\alpha/^\circ$	
$\beta/^\circ$	101.47(4)
$\gamma/^\circ$	
$V/\text{\AA}^3$	1549
$Z$	4
$D_x/\text{g cm}^{-3}$	2.38
Mo-K $\alpha$ radiation, $\lambda/\text{\AA}$	0.71069
$\mu_{\text{(Mo K}\alpha\text{)}}/\text{cm}^{-1}$	123.6
$T/\text{K}$	290
$F_{(000)}$	1048.0
Final $R$	0.037
Unique observed ( $I/\sigma(I) \geq 2.0$ ) reflections	2099

#### Crystal structure determination of $\text{BiCl}_3 \cdot 12\text{S}_4$

A suitable irregular crystal was mounted in a Lindemann capillary to avoid decomposition. Data were collected with a Siemens R3m four circle diffractometer in  $\omega$ - $2\theta$  mode. Maximum  $2\theta$  was  $50^\circ$  with scan range  $\pm 1.4^\circ(\omega)$  around the  $K_{\alpha 1}$ - $K_{\alpha 2}$  angles, scan speed  $5.29^\circ(\omega) \text{ min}^{-1}$ , depending on the intensity of a  $2\theta$  pre-scan; backgrounds were measured at each end of the scan for 0.25 of the scan time. The  $hkl$  ranges were 0-9, 0-15, -18 to 18. Three standard reflections were monitored every 200 reflections, and showed a slight decrease during data collection. The data were rescaled to correct for this. Unit cell dimensions and standard deviations were obtained by least-squares fit to 15 reflections ( $15 < 2\theta < 18^\circ$ ). Reflections collected were processed using profile analysis to give 2741 unique reflections ( $R_{\text{int}} = 0.039$ ); 2099 were considered observed ( $I/\sigma(I) > 2.0$ ). These were corrected for Lorentz, polarization and absorption effects (by the Gaussian method); minimum and maximum transmission factors were 0.58 and 0.28. Crystal dimensions were  $0.17 \times 0.12 \times 0.35 \text{ mm}$ . Systematic reflection conditions  $h0l \ h+l = 2n$ ,  $0k0 \ k = 2n$  indicate space group  $p2_1/n$ . Heavy atoms were located by the Patterson interpretation section of SHELXTL and the light atoms then found by successive Fourier syntheses. Anisotropic thermal parameters were used for all non-H atoms. Hydrogen atoms were given fixed isotropic thermal parameters,  $U = 0.08 \text{ \AA}^2$ , inserted at calculated positions and not refined. Final refinement was on F by least squares methods refining 146 parameters including an anisotropic extinction parameter. Largest positive and negative peaks on a final difference Fourier synthesis were of height 1.5 and  $-1.1 \text{ e. \AA}^{-3}$  with all significant peaks near bismuth. A weighting scheme of the form  $W = 1/(\sigma^2(F) + gF^2)$  with  $g = 0.00050$  was used and shown to be satisfactory by a weight analysis. Final  $R = 0.037$ ,  $R_w = 0.040$ . Maximum shift/error in final cycle was 0.1. Computing was conducted on a DEC Microvax-II with SHELXTL PLUS.<sup>147</sup> Scattering factors in the analytical form and anomalous dispersion factors taken from reference 148.

**Table 2.19** Crystallographic data for  $\text{BiCl}_3 \cdot 15.55 \cdot \frac{1}{2} \text{MeCN}$ .

Formula	$\text{C}_{10}\text{H}_{20}\text{BiCl}_3\text{S}_5 \cdot \frac{1}{2} \text{CH}_3\text{CN}$
$M_r$	636.4
Crystal class	orthorhombic
Space group	Pbca
$a / \text{\AA}$	16.972(9)
$b / \text{\AA}$	15.418(8)
$c / \text{\AA}$	30.60(2)
$\alpha / ^\circ$	
$\beta / ^\circ$	
$\gamma / ^\circ$	
$V / \text{\AA}^3$	8007
$Z$	16
$D_c / \text{g cm}^{-3}$	2.11
Mo-K $\alpha$ radiation, $\lambda / \text{\AA}$	0.71069
$\mu_{(\text{Mo-K}\alpha)} / \text{cm}^{-1}$	96.8
$T / \text{K}$	290
$F_{(000)}$	4880.0
Final R	0.0545
Unique observed ( $I/\sigma(I) \geq 2.0$ ) reflections	2951

#### Crystal structure determination of $\text{BiCl}_3 \cdot 15.55 \cdot \frac{1}{2} \text{MeCN}$

To avoid hydrolysis, the crystal was mounted in a Lindemann capillary. Data were collected with a Siemens R3m four circle diffractometer in  $\omega$ - $2\theta$  mode. Maximum  $2\theta$  was  $45^\circ$  with scan range  $\pm 1.4^\circ(\omega)$  around the  $K_{\alpha 1}$ - $K_{\alpha 2}$  angles, scan speed  $5.29^\circ(\omega) \text{ min}^{-1}$ , depending on the intensity of a  $2\theta$  pre-scan; backgrounds were measured at each end of the scan for 0.25 of the scan time. The  $hkl$  ranges were 0-16, 0-18, 0-33. Three standard reflections were monitored every 200 reflections, and showed a slight decrease during data collection. The data were rescaled to correct for this. Unit cell dimensions and standard deviations were obtained by least-squares fit to 15 reflections ( $18 < 2\theta < 20^\circ$ ). The reflections collected were processed using profile analysis to give 4957 unique reflections of which 2951 were considered observed ( $I/\sigma(I) > 2.0$ ). These were corrected for Lorentz, polarization and absorption effects (by the Gaussian method); minimum and maximum transmission factors were 0.27 and 0.19. Crystal dimensions were  $0.36 \times 0.33 \times 0.12 \text{ mm}$ . Systematic reflection conditions  $0kl \ k = 2n$ ,  $h0l \ l = 2n$ ,  $hko \ h = 2n$  indicate space group  $\text{Pbca}$ . Heavy atoms were located by the Patterson interpretation section of SHELXTL and the light atoms then found by successive Fourier syntheses which also revealed one molecule of MeCN. Anisotropic thermal parameters were used for all non-H atoms. Hydrogen atoms were given fixed isotropic thermal parameters,  $U = 0.08 \text{ \AA}^2$ , inserted at calculated positions and not refined. Final refinement was on F by least squares methods refining 366 parameters. Largest positive and negative peaks on a final difference Fourier synthesis were of height  $\pm 1.0 \text{ e. \AA}^{-3}$ . A weighting scheme of the form  $W = 1/(\sigma^2(F) + gF^2)$  with  $g = 0.0062$  was used and shown to be satisfactory by a weight analysis. Final  $R = 0.055$ ,  $R_w = 0.051$ . Maximum shift/error in final cycle was 0.2. Computing was conducted on a DEC Microvax-II with SHELXTL PLUS.<sup>147</sup> Scattering factors in the analytical form and anomalous dispersion factors were taken from reference 148.

**Table 2.20** Crystallographic data for  $\text{BiCl}_3 \cdot 18\text{S}_6$ .

Formula	$\text{C}_{12}\text{H}_{24}\text{BiCl}_3\text{S}_6$
$M_r$	676.0
Crystal class	cubic
Space group	$\text{Pa}\bar{3}$
$a/\text{\AA}$	16.381(5)
$b/\text{\AA}$	
$c/\text{\AA}$	
$\alpha/^\circ$	
$\beta/^\circ$	
$\gamma/^\circ$	
$V/\text{\AA}^3$	4395.6
$Z$	8
$D_x/\text{g cm}^{-3}$	2.04
Mo-K $\alpha$ radiation, $\lambda/\text{\AA}$	0.71069
$\mu_{\text{Mo K}\alpha}/\text{cm}^{-1}$	8.95
$T/\text{K}$	290
$F_{000}$	2608
Final $R$	0.044
Unique observed ( $I/\sigma(I) \geq 2.0$ ) reflections	825



#### Crystal structure determination of $\text{BiCl}_3 \cdot 18\text{S6}$

A large colourless block crystal was mounted in a Lindemann tube to prevent hydrolysis. Data were collected with a Siemens R3m four circle diffractometer in  $\omega$ - $2\theta$  mode. Maximum  $2\theta$  was  $50^\circ$  with scan range  $\pm 0.7^\circ(\omega)$  around the  $K_{\alpha 1}$ - $K_{\alpha 2}$  angles, scan speed  $2.5\text{--}15^\circ(\omega) \text{ min}^{-1}$ , depending on the intensity of a 2s pre-scan; backgrounds were measured at each end of the scan for 0.25 of the scan time. The  $hkl$  ranges were 0-19 on each axis. Three standard reflections were monitored every 200 reflections, and showed no significant decrease during data collection. Unit cell dimensions and standard deviations were obtained by least-squares fit to 15 reflections ( $15 < 2\theta < 20^\circ$ ). The 4357 reflections collected were processed using profile analysis to give 1312 unique reflections ( $R_{\text{int}} = 0.063$ ), of which 825 were considered observed ( $I/\sigma(I) > 2.0$ ). These were corrected for Lorentz, polarization and absorption effects (by the Gaussian method); minimum and maximum transmission factors were 0.10 and 0.27. Crystal dimensions were  $0.36 \times 0.33 \times 0.36 \text{ mm}$ . Systematic reflection conditions:  $0kl$ ,  $l = 2n$ , indicate space group  $Pa\bar{3}$ . The structure was solved by direct methods using SHELXTL (TREF) To locate a probable position for the bismuth atom, lying on a three-fold axis. The light atoms were then found successive Fourier syntheses. Anisotropic thermal parameters were used for all non-H atoms. Hydrogen atoms were given fixed isotropic thermal parameters,  $U = 0.08 \text{ \AA}^2$ , inserted at fixed positions and not refined. Final refinement was on F by least squares methods refining 67 parameters. Largest positive and negative peaks on a final difference Fourier synthesis were of height  $\pm 1.5$  and  $-1.2 \text{ e. \AA}^{-3}$ , the former apparently a bismuth diffraction ripple. A weighting scheme of the form  $W = 1/(\sigma^2(F) + gF^2)$  with  $g = 0.005$  was used and shown to be satisfactory by a weight analysis. Final  $R = 0.044$ ,  $R_w = 0.067$ ,  $S = 0.76$ . Maximum shift/error in final cycle was  $0.02:1$ . Computing was conducted on a DEC Microvax-II with SHELXTL PLUS.<sup>147</sup> Scattering factors in the analytical form and anomalous dispersion factors taken from International Tables.<sup>148</sup>

## **CHAPTER THREE**

# **INVESTIGATIONS INTO THE COMPLEXATION OF EARLY TRANSITION METAL HALIDES BY THIAMACROCYCLIC LIGANDS**

## INTRODUCTION

Having examined the range of known thiamacrocyclic complexes as a prelude to the work with the group 15 trichlorides, it became apparent that the earlier transition metals had been the subject of very few reports. As shown in Table 3.1, every metal in the first, second and third transition series from group 6 to group 12 has been successfully coordinated by a crown-thiaether ligand. Of the groups 3, 4 and 5, only niobium(V) has been complexed by a polythiamacrocyclic and unequivocally characterised by single crystal X-ray diffraction studies. With respect to the lanthanides and actinides, only one isolated, spectroscopic study has been reported.

**Thiaether macrocycle complexes of niobium pentachloride**

The strong Lewis acid niobium pentachloride has been complexed by the tetrathiamacrocycles 14S4, 16S4, and 20S4 in halide:ligand stoichiometries of 2:1 and 4:1.<sup>149,150,151</sup> As suggested by the stoichiometry, these highly reactive complexes involve *exo* coordination of the niobium pentachloride molecules to the macrocycle. The single crystal X-ray structure of  $[(\text{NbCl}_5)_2(14\text{S}4)]$  shows that in this centrosymmetric adduct an exodentate 14S4 macrocycle bridges two niobium pentachloride units by acting as a monodentate ligand to each. The octahedral niobium centres are coordinated by five chloride ions (mean Nb-Cl = 2.31 Å) and one thiaether sulfur atom (Nb-S = 2.72 Å). An interesting feature of the niobium coordination sphere is the bending of the four equatorial chloride ions toward the thiaether together with a shortening of the bond between niobium and the chloride *trans* to the sulfur atom.

Table 3.1 Summary of transition metals complexed by homoleptic polythiaether macrocycles.

Sc	None	Ti	None	V	None	Cr	✓	Mn	✓	Fe	✓	Co	✓	Ni	✓	Cu	✓	Zn	✓
Y	None	Zr	None	Nb	✓	Mo	✓	Tc	None	Ru	✓	Rh	✓	Pd	✓	Ag	✓	Cd	✓
La	None	Hf	None	Ta	None	W	✓	Re	✓	Os	✓	Ir	✓	Pt	✓	Au	✓	Hg	✓

#### Lanthanide complexes of thiaether macrocycles

A study reported in 1980 found that the homoleptic polythiaether 18S6 fails to coordinate lanthanide(III) perchlorates in acetonitrile.<sup>152</sup> The use of mixed oxa/thia ligands met greater success in this medium. In dichloromethane complexes with stoichiometry  $\text{Ln}[\text{ClO}_4]_3 \cdot 18\text{S6} \cdot \text{H}_2\text{O}$  ( $\text{Ln} = \text{Sm}, \text{Eu}, \text{or Yb}$ ) were formed although no structural data was obtained. Since the compounds were decomposed by acetonitrile and were almost insoluble in dichloromethane and other non-coordinating solvents, only solid state measurements could be obtained. Conclusive evidence for lanthanide-thiaether interaction came from the electronic spectra. Infra-red spectra suggested the presence of additional coordination by perchlorate. The material formed from dichloromethane was transformed into a mixture of the ligand and hydrated lanthanide perchlorate when exposed to air for a few minutes.

The dearth of publications pertaining to thiamacrocyclic complexes of the early transition metals stimulated this investigation using the ligand 9S3 and the chlorides of scandium(III), titanium(IV), titanium(III), and vanadium(III). The oxidation states of these metal ions represent the electronic configurations  $d^0$ ,  $d^0$ ,  $d^1$ , and  $d^1$  respectively. There exists a fundamental mismatch in terms of the *hard* acid character of the early transition metals and the *soft* bases of the thiaether macrocycles.<sup>153</sup> It has been suggested that this stems from the inability of the early transition metals to function effectively as  $\pi$ -donors to the sulfur ligands. However, with the exception of scandium(III), thiaether coordination of these metal ions was confirmed by several studies during the 1960's. No single crystal X-ray structure determinations were undertaken and so no quantitative information regarding the metal-thiaether bond geometry is available. The use of macrocyclic thiaethers would, possibly, promote the formation of the compounds in a crystalline form amenable to single crystal structure determination. 9S3 was selected in view of its preorganised conformation, ready for

facial coordination to a metal centre; *i.e.* minimal enthalpic penalty of ligand reorganisation upon complexation. Before considering the results obtained, the work reported for the earliest first row transition metal, the  $d^3$  ion chromium(III), will first be summarised.

#### Thiaether macrocycle complexes of chromium

The complex  $[\text{Cr}(\text{9S3})\text{Cl}_2]$  has been prepared by the action of 9S3 with a)  $[\text{Cr}(\text{H}_2\text{O})_6]\text{Cl}_3$  in acetonitrile, and b)  $[\text{Cr}(\text{THF})_6\text{Cl}_2]$  in dioxane.<sup>134</sup> The thiaether complex is inert and sparingly soluble in common solvents. Stirring in trifluoromethanesulphonic acid results in the replacement of chloride by triflate to form the complex  $[\text{Cr}(\text{9S3})(\text{CF}_3\text{SO}_3)_2]$  where infrared spectroscopy has shown the triflate ions to be coordinated in a monodentate fashion. Donor solvents such as acetonitrile, acetone, and THF are able to replace the labile triflate ions. Heating solid  $[\text{Cr}(\text{H}_2\text{O})_6][\text{ClO}_4]_3$  with solid 9S3 in the absence of a solvent produced the chromium(III) *hexakis*-thiaether complex  $[\text{Cr}(\text{9S3})_3][\text{ClO}_4]_3$ . This very explosive compound was found to decompose in solution within a few seconds. These results show that the *hard* chromium(III) ion can be complexed by 9S3. However, despite the  $d^3$  electronic configuration to facilitate metal-ligand back-bonding, the macrocycle is only weakly bound and is unable to displace the triflate ion from the metal coordination sphere. Neutral monodentate ligands are exchanged for the macrocyclic thiaether.

#### Scandium trichloride

Being a  $d^0$  species, scandium trichloride is unable to partake in metal-ligand  $\pi$ -donation and any adduct formed would have to rely on the very weak  $\sigma$ -donor capability of 9S3. That the ligand was recovered without reaction confirms that the interaction is simply inadequate to permit isolation of a molecular adduct. No thiaether complexes have been reported for either scandium, yttrium or lanthanum.<sup>76</sup> For the heavier, and therefore softer, Rare Earth metal ions, an interaction with thiaether donors has been reported.<sup>152</sup>

#### Titanium tetrachloride

The  $d^0$  electronic configuration of this metal species would normally be considered *hard* and so particularly ill-suited for the isolation of a complex with the thiamacrocycle 9S3. However, this notion has been challenged in view of the well characterised complexes with tetrahydrothiophene,<sup>155</sup> 1,4-dithiane,<sup>156</sup> and dimethylthiaether,<sup>157</sup> together with the unexpected report that the ambidentate ligand, thioxane, coordinates to titanium tetrachloride through its sulfur rather than oxygen atom.<sup>158</sup> The marked preference shown by titanium-chloro species for coordination by six donor atoms also warranted consideration. With four positions already occupied by chloride ions, the potential denticity of the 9S3 could be limited to just two.

Using acetonitrile as the reaction medium, slow solvent diffusion lead to a yellow, dendritic crystalline material after standing at room temperature for between two and seven days. Regrettably, despite numerous syntheses, a crystal amenable to X-ray diffraction studies was not produced. Numerous other solvents were used in an effort to induce a change in the

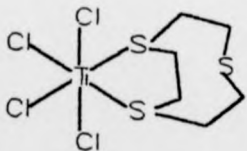
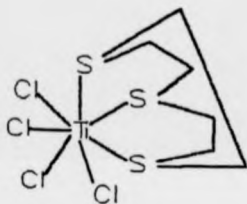
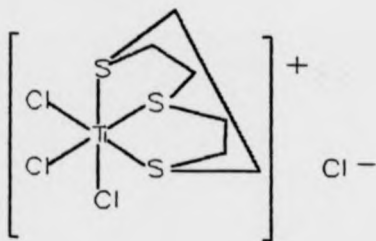
crystalline habit, but without success. Elemental analysis confirmed a 1:1 stoichiometry between the metal halide and the macrocycle in the crystalline material. The infrared spectra of the  $[\text{TiCl}_4 \cdot 9\text{S3}]$  compound and  $[\text{TiCl}_4(\text{MeCN})_2]$  are compared in Figure 3.2 to demonstrate the change in environment about the titanium centre upon thiaether coordination. The single strong band seen for the acetonitrile adduct concurs with the prediction for a  $D_{3h}$  *trans*-octahedral metal coordination geometry. If the titanium centre in the thia complex has remained six-coordinate, the enforced *cis* placement of the sulfur atoms leads to a  $C_{2v}$  point symmetry. For  $C_{2v}$ , Group Theory predicts four  $\nu(\text{Ti-Cl})$  and two  $\nu(\text{Ti-S})$  infrared active bands. Examination of the spectrum shows that there are indeed six distinct bands in the low frequency region. Although unequivocal distinction between  $\nu(\text{Ti-Cl})$  and  $\nu(\text{Ti-S})$  bands is not justified, the band at  $440 \text{ cm}^{-1}$  appears within the range previously assigned to a metal-sulfur stretching vibration.<sup>19</sup> However, that six bands are observed in the far infrared region may be entirely fortuitous. If, for simplicity, oligomeric species are ignored, a total of three limiting-case structures can be assigned to the complex  $\text{TiCl}_4 \cdot 9\text{S3}$ . These are illustrated in Figure 3.1 and described below:

- 1)  $[\text{TiCl}_4(9\text{S3})]^+ \text{Cl}^-$  - Thiaether donors show little propensity towards displacement of anionic ligands. This would seem even less likely in the present case where titanium(IV) is the Lewis acid centre. In addition, the  $C_{2v}$  point group of this cation should have just four  $\nu(\text{Ti-Cl/S})$ ; six bands are observed.
- 2)  $[\text{TiCl}_4(9\text{S3})]$  tridentate macrocycle - Although seven-coordination about titanium is unusual in comparison to authentic six-coordinate molecules, there have been thirty-seven structural characterisations recorded on the Cambridge Crystallographic Database and so this geometry can not be considered a rarity (*c.f.* 221 six-coordinate



structure determinations). An example of a seven-coordinate titanium-chloro species is the molecule  $[\text{TiLCl}_2(\text{NMeNMe}_2)]$  where  $\text{L} = \text{tris}(\text{pyrazolyl})\text{borate}$ .<sup>160</sup>

- 3)  $[\text{TiCl}_4(9\text{S}3)]$  bidentate macrocycle - Whilst meeting the stereochemical preferences of the metal, this formulation reduces the benefits bestowed by using the tridentate macrocyclic ligand. However, in view of the well-established thiaether coordination of titanium tetrachloride, a bidentate chelate binding mode may be sufficient for 9S3. An example of 9S3 exhibiting only bidentate chelation is given by the square-planar complex  $[\text{Pt}(9\text{S}3)_2]^{2+}$ .<sup>161</sup> The bidentate macrocycle adopts a conformation in which the unbound donor points away from the platinum ion. However, strain energy calculations using PCMODEL<sup>145</sup> show this conformation to have negligible distortion energy (0.04 kcal.mol<sup>-1</sup>) above the global minimum.<sup>162</sup> Clearly, from the standpoint of ligand conformational strain energy, this bidentate form is readily accessible.



**Figure 3.1** Postulated structures for the complex  $\text{TiCl}_4 \cdot 9\text{S}_3$ .

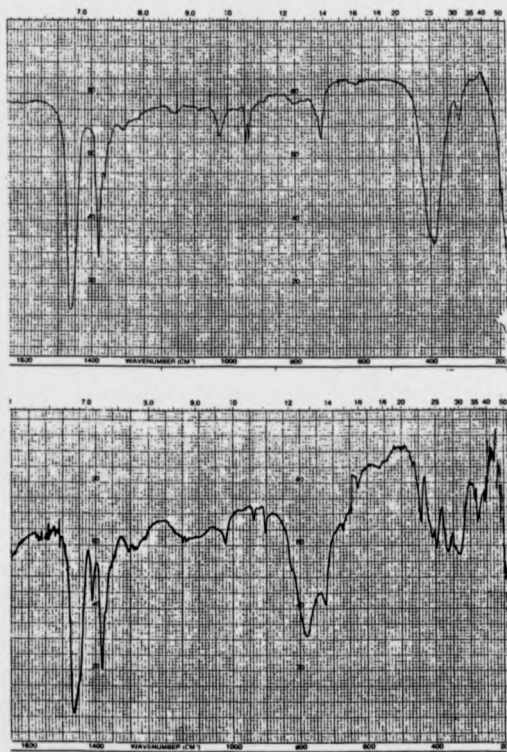


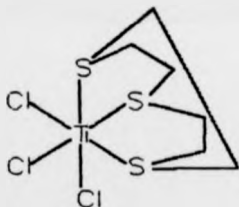
Figure 3.2 Infrared spectra of  $[\text{TiCl}_4(\text{MeCN})_2]$  and  $\text{TiCl}_4 \cdot 9\text{S}_3$  (upper and lower spectrum respectively).

### Titanium trichloride

On first consideration the trivalent chloride of titanium would seem to be well suited for complexation by 9S3. The  $d^1$  electronic configuration and oxidation state of three make this metal species much *softer* than titanium(IV) and it is generally considered to exhibit borderline *hard/soft* behaviour. The presence of just three chloride ions is ideal for facial binding by 9S3 to form a molecular adduct with octahedral geometry. The acyclic thiaether complexes of titanium trichloride are considered less well-defined than those of titanium(IV) chloride.<sup>155</sup> For example, the *bis* dimethylthiaether complex of titanium trichloride decomposes on heating to 50 °C whereas the same adduct of titanium tetrachloride can be sublimed unchanged *in vacuo*.

Introduction of 9S3 in acetonitrile to titanium trichloride in the same solvent produced an instantaneous change in colour from royal blue to purple. Shortly afterwards, a fine purple precipitate began to be deposited and after leaving overnight, the solution became clear. Elemental analysis of the precipitate confirmed a 1:1 formulation of  $TiCl_3 \cdot 9S3$ . Regrettably crystalline material could not be obtained despite using a number of different solvents and different methods to reduce the rate of contact between the two reagents. The change in colour from blue to purple upon introduction of the macrocycle solution to that of the titanium trichloride was monitored by recording the electronic spectrum within five minutes of the addition. The spectrum observed was compatible with the presence of an octahedral  $d^1$  metal ion. The d-d  $\lambda_{max}$  observed for the macrocyclic complex was 549 nm. This is, as expected from observation of the colour change, at a higher energy to the 577 nm recorded for the free trihalide in an acetonitrile solution.

The infrared spectrum of  $\text{TiCl}_3 \cdot 9\text{S}_3$  is compared with that of the *trans*-acetonitrile adduct of titanium trichloride in Figure 3.4. The spectrum of the acetonitrile adduct reveals one sharp band at  $418\text{ cm}^{-1}$  which has been assigned to the  $\delta(\text{CCN})$  bending mode.<sup>163</sup> The other bands, below  $400\text{ cm}^{-1}$ , are broad and poorly resolved. Clark has described this region as comprising just two well-defined  $\nu(\text{Ti-Cl})$  bands, consistent with  $C_{2v}$  symmetry for the molecule *i.e.* a *mer*-octahedral geometry around titanium.<sup>164</sup> If the species  $\text{TiCl}_3 \cdot 9\text{S}_3$  has, as expected, formed a neutral, monomeric six-coordinate adduct, facial binding by  $9\text{S}_3$  will produce a  $C_{3v}$  point symmetry about the titanium centre. This leads to the prediction of two  $\nu(\text{Ti-Cl})$ , and two  $\nu(\text{Ti-S})$  infrared-active bands. Examination of the spectrum shows that there are a total of four strong bands below  $400\text{ cm}^{-1}$ , entirely in accord with the group theoretical predictions. This structure is shown diagrammatically in Figure 3.3.



**Figure 3.3** Postulated structure of the complex  $\text{TiCl}_3 \cdot 9\text{S}_3$ .

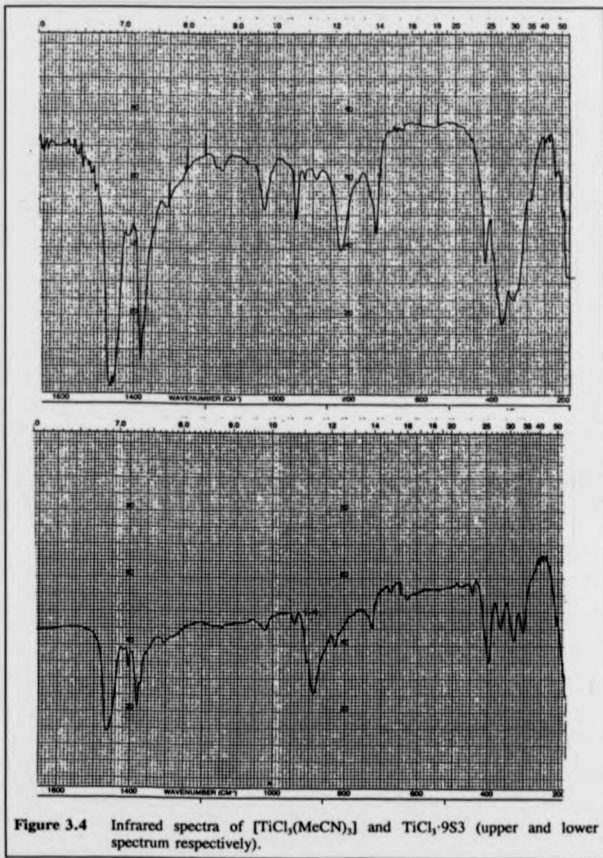


Figure 3.4 Infrared spectra of  $[\text{TiCl}_3(\text{MeCN})_3]$  and  $\text{TiCl}_3 \cdot 9\text{S}_3$  (upper and lower spectrum respectively).

### Vanadium trichloride

In view of the previously reported thiaether complexes of vanadium trichloride together with its relation to chromium(III) chloride, it was felt that adduct formation with 9S3 would be highly probable. The  $d^2$  electronic configuration and oxidation state of three make this metal species much *softer* than titanium(III). Again, The presence of just three chloride ions is ideal for facial binding by 9S3. Thiaether complexes of vanadium trichloride are known for the ligands dimethylthiaether,<sup>164</sup> diethylthiaether,<sup>165</sup> and tetrahydrothiophene,<sup>166</sup> but no structural determinations have been conducted. More recently, the crystal structures of two organometallic-vanadium(I) thiaether complexes were reported.<sup>167, 175</sup>

An acetonitrile solution of 9S3 was added to a suspension of vanadium trichloride in the same solvent with no immediate sign of reaction. With still no sign of reaction after stirring for three days, the solution was intermittently brought to reflux during the following seven days. Eventually, beautiful, jewel-like azure-blue crystals were observed in the blue solution. Intermittent reflux was continued until reaction was deemed complete. Elemental analysis of the crystals discounted the expected formulation of  $VCl_3 \cdot 9S3$  and was found to be consistent with the vanadium(IV) compound  $VOCl_2 \cdot 9S3$ . Spectroscopic evidence concurred with oxidation of the tervalent vanadium starting material. The single crystal X-ray diffraction study showed conclusively that oxidation to form the vanadyl ion had taken place, presumably a consequence of adventitious water/oxygen entering the reaction vessel during the repeated periods of reflux. This oxidation must be considered unexpected in view of the subsequent thiaether chelation.

### MOLECULAR STRUCTURE OF $\text{VOCl}_2(\text{9S3})$

The macrocycle is facially bound, *via* all three sulfur atoms, to a neutral  $\text{VOCl}_2$  moiety so producing the half-sandwich compound shown in Figure 3.5. The resulting six-coordination about the vanadium(IV) centre shows approximately octahedral geometry. Bond lengths and angles are listed in Table 3.2. Although the unit cell of this compound contains two independent molecules, the very slight variations in molecular dimensions are without chemical significance.

Distortions from an idealised octahedral geometry about the vanadium atom are confirmed by consideration of the  $\angle \text{S-V-S}$  (mean  $81.2^\circ$ ). This reduction, imposed by the steric requirements of the macrocycle, leads to an increase in the other *cis* angles, *i.e.*  $\angle \text{Cl-V-Cl}$  (mean  $94.9^\circ$ ) and  $\angle \text{O-V-Cl}$  (mean  $105.0^\circ$ ). This constriction-dilation effect has been observed in other compounds, *e.g.*  $[\text{ReO}_4(\text{9S3})]^+$  where  $\angle \text{S-Re-S}$  (mean) =  $79.5^\circ$  and  $\angle \text{O-Re-O}$  (mean) =  $107.4^\circ$ .<sup>168</sup> The two planes defined by  $\text{S}_3$  and  $\text{Cl}_2\text{O}$  intersect at an angle of  $6.3^\circ$ , using molecule 1 as an example. Again using molecule 1, the vanadium atom is displaced above the mean plane defined by  $\text{Cl}(11)$ ,  $\text{Cl}(12)$ ,  $\text{S}(11)$  and  $\text{S}(17)$ , by  $0.350 \text{ \AA}$ , towards the vanadyl oxygen.

The two chlorine atoms of the complex serve to neutralise the formal charge present on the  $\text{VO}^{2+}$  moiety. Complexes of the  $\text{VOCl}_2$  molecule generally adopt a five-coordinate, square pyramidal geometry. The vanadium-chlorine distances (mean  $2.295 \text{ \AA}$ ) are typical for square pyramidal complexes  $[\text{VOCl}_2\text{L}_2]$  where, for example,  $\text{L} = \text{Ph}_3\text{PO}$  (mean  $\text{V-Cl} = 2.31 \text{ \AA}$ ),<sup>169</sup>  $\text{L} = \text{NMe}_3$  (mean  $\text{V-Cl} = 2.25 \text{ \AA}$ ),<sup>170</sup> and  $\text{L} = (\text{Me}_2\text{N})\text{CO}$  (mean  $\text{V-Cl} = 2.34 \text{ \AA}$ ).<sup>171</sup> For the six-coordinate complex under study, a slight elongation of the vanadium-chlorine distance might be anticipated. Its absence is concomitant with only weak binding by



the thiamacrocyclic co-ligand. The V=O bond length in  $\text{VOCl}_2(9\text{S}3)$  (e.g. 1.579 Å in molecule 1) is near the lower end of the range observed for vanadyl complexes (1.55 to 1.68 Å).<sup>172</sup> When compared to other related vanadyl-S donor complexes this V=O bond length is unusually short, e.g.  $[\text{VO}(\text{edt})_2]^2$  (edt = ethane-1,2-dithiolato), V=O 1.625(2) Å, and  $[\text{VO}(\text{pdt})_2]^2$  (pdt = propane-1,3-dithiolato), V=O 1.628(2) Å.<sup>173</sup>

Turning to the vanadium-sulfur bond lengths, an irregular [2+1] configuration is evident. The lengthening of the vanadium-donor distance (V-S = 2.634 Å) *trans* to the V=O bond is quite general in six-coordinate oxo-vanadium chemistry. To cite the further example of  $[\text{VO}(\text{DMSO})_3]^2+$ ,<sup>174</sup> here the *cis* V-O distances average 2.034 Å whilst V-O of the *trans* ligand is extended to 2.18 Å. In the present compound, the V-S bonds *trans* to chlorine (mean 2.470 Å) are some 0.18 Å larger than the V-Cl bonds (mean 2.295 Å); standard covalent radii differ by only 0.03 Å between chlorine and sulfur.<sup>135</sup> The structurally characterised vanadium(II)-thiaether complex  $[\text{cpV}(\text{CO})_2(\text{THT})]$  (where THT = tetrahydrothiophene) has a vanadium-sulfur distance of 2.479(3) Å.<sup>175</sup> Yet again, this indicates weak vanadium-sulfur bonding in  $[\text{VOCl}_2(9\text{S}3)]$ ; the ionic radii of vanadium(II) and vanadium(IV) differ by 0.21 Å.<sup>176</sup> Consideration of the thiolato-vanadium distances (mean) in the compounds  $[\text{VO}(\text{edt})_2]$  (2.378 Å),  $[\text{VS}(\text{SPh})_4]$  (2.391 Å),<sup>177</sup> and  $[\text{VSe}(\text{edt})_2]$  (2.364 Å),<sup>177</sup> confirms the reduced nucleophilicity of the thiaether donor. These distances conspire to preclude the existence of a significant  $\pi$  interaction between vanadium and the 9S3 ligand. The weakness of the  $\sigma$  binding, especially pronounced in the *trans* V-S, engenders an increase in the V=O bond order.

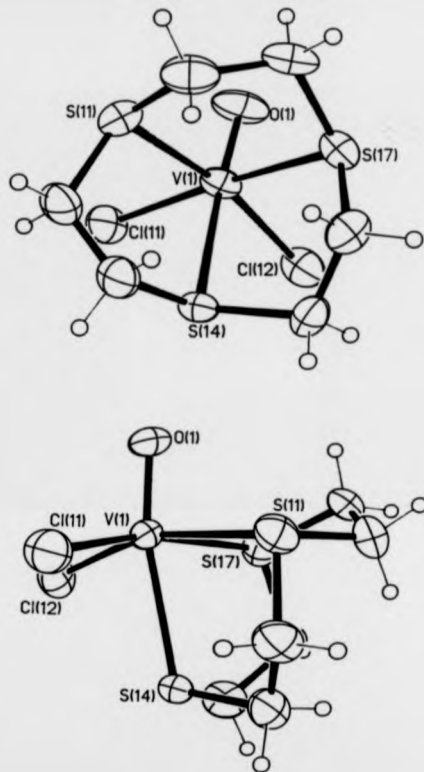


Figure 3.5 Two views of the molecule  $[\text{VOCl}_2(9\text{S}3)]$ .

Table 3.2 Selected bond lengths (Å) and angles (°) for  $\text{VOCl}_3(9\text{S}3)$ .

Bond lengths (Å)

V(1)-O(1)	1.579(5)	V(1)-Cl(11)	2.297(3)
V(1)-Cl(12)	2.288(2)	V(1)-S(11)	2.476(3)
V(1)-S(14)	2.624(2)	V(1)-S(17)	2.473(2)
S(11)-C(12)	1.781(8)	S(11)-C(19)	1.780(8)
C(12)-C(13)	1.488(11)	C(13)-S(14)	1.789(8)
S(14)-C(15)	1.796(8)	C(15)-C(16)	1.492(11)
C(16)-S(17)	1.817(7)	S(17)-C(18)	1.787(8)
C(18)-C(19)	1.529(13)	V(2)-O(2)	1.578(5)
V(2)-Cl(21)	2.303(2)	V(2)-Cl(22)	2.293(2)
V(2)-S(21)	2.471(2)	V(2)-S(24)	2.644(2)
V(2)-S(27)	2.458(2)	S(21)-C(22)	1.792(7)
S(21)-C(29)	1.788(7)	C(22)-C(23)	1.512(11)
C(23)-S(24)	1.791(8)	S(24)-C(25)	1.797(8)
C(25)-C(26)	1.495(11)	C(26)-S(27)	1.810(8)
S(27)-C(28)	1.814(7)	C(28)-C(29)	1.501(11)

Bond angles (deg.)

O(1)-V(1)-Cl(11)	104.6(2)	O(1)-V(1)-Cl(12)	104.9(2)
Cl(11)-V(1)-Cl(12)	94.9(1)	O(1)-V(1)-S(11)	94.0(2)
Cl(11)-V(1)-S(11)	86.0(1)	Cl(12)-V(1)-S(11)	160.2(1)
O(1)-V(1)-S(14)	167.5(2)	Cl(11)-V(1)-S(14)	85.6(1)
Cl(12)-V(1)-S(14)	80.9(1)	S(11)-V(1)-S(14)	79.4(1)
O(1)-V(1)-S(17)	88.9(2)	Cl(11)-V(1)-S(17)	163.6(1)
Cl(12)-V(1)-S(17)	90.4(1)	S(11)-V(1)-S(17)	83.8(1)
S(14)-V(1)-S(17)	79.9(1)	V(1)-S(11)-C(12)	104.7(3)
V(1)-S(11)-C(19)	105.4(3)	C(12)-S(11)-C(19)	102.3(4)
S(11)-C(12)-C(13)	116.1(6)	C(12)-C(13)-S(14)	111.8(6)
V(1)-S(14)-C(15)	106.7(3)	V(1)-S(14)-C(15)	102.1(3)
C(13)-S(14)-C(15)	103.6(4)	S(14)-C(15)-C(16)	114.3(6)
C(15)-C(16)-S(17)	113.0(5)	V(1)-S(17)-C(18)	109.7(3)
V(1)-S(17)-C(18)	99.0(3)	C(16)-S(17)-C(18)	102.9(4)
S(17)-C(18)-C(19)	114.1(6)	S(11)-C(19)-C(18)	112.4(6)
O(2)-V(2)-Cl(21)	105.1(2)	O(2)-V(2)-Cl(22)	105.2(2)
Cl(21)-V(2)-Cl(22)	95.1(1)	O(2)-V(2)-S(21)	87.2(2)
Cl(21)-V(2)-S(21)	90.2(1)	Cl(22)-V(2)-S(21)	164.7(1)
O(2)-V(2)-S(24)	166.1(2)	Cl(21)-V(2)-S(24)	80.2(1)
Cl(22)-V(2)-S(24)	86.8(1)	S(21)-V(2)-S(24)	79.9(1)
O(2)-V(2)-S(27)	93.8(2)	Cl(21)-V(2)-S(27)	160.0(1)
Cl(22)-V(2)-S(27)	85.9(1)	S(21)-V(2)-S(27)	84.3(1)
S(24)-V(2)-S(27)	79.9(1)	V(2)-S(21)-C(22)	110.2(3)
V(2)-S(21)-C(29)	98.9(3)	C(22)-S(21)-C(29)	102.3(4)
S(21)-C(22)-C(23)	113.0(5)	C(22)-C(23)-S(24)	114.7(5)
V(2)-S(24)-C(25)	101.3(2)	V(2)-S(24)-C(25)	106.1(2)
C(23)-S(24)-C(25)	103.3(4)	S(24)-C(25)-C(26)	111.7(5)
C(25)-C(26)-S(27)	115.6(5)	V(2)-S(27)-C(28)	109.0(3)
V(2)-S(27)-C(28)	105.2(3)	C(26)-S(27)-C(28)	101.7(4)
S(27)-C(28)-C(29)	112.1(5)	S(21)-C(29)-C(28)	115.4(5)

## CONCLUSIONS

**TiCl<sub>4</sub>·9S<sub>3</sub>**

The target compound has been successfully synthesised in the crystalline state. Unfortunately, the crystals proved to be unsuitable for a diffraction study and sensitive to hydrolysis upon attempted recrystallisation.

**TiCl<sub>3</sub>·9S<sub>3</sub>**

Again the target compound was isolated in the solid state but with no indication of crystallinity. Recrystallisation lead to hydrolysis of the compound.

**VCl<sub>3</sub>·9S<sub>3</sub>**

Somewhat unexpectedly the complex isolated was the vanadium(IV) species [VOCl<sub>2</sub>(9S<sub>3</sub>)], a consequence of the vanadium trichloride being oxidised. The gem-like crystals obtained exhibited good resistance to hydrolysis and facilitated full characterisation by single-crystal X-ray diffraction. The presence of weak V-S bonding is reflected in the short V=O distance.

## EXPERIMENTAL

All procedures were conducted using standard Schlenk techniques and an inert dinitrogen atmosphere except where stated to the contrary. Toluene and THF were pre-dried by standing over sodium wire for 7 days and then refluxed over a sodium/potassium alloy for 24 h under dinitrogen before use. Other solvents were prepared as outlined in chapter 2.

'Analar' grade scandium trichloride hydrate, titanium trichloride, titanium tetrachloride, and vanadium trichloride were obtained from Aldrich Chemical Co. Gillingham. The titanium trichloride was used directly without further purification. Titanium trichloride and vanadium trichloride were converted into their acetonitrile adducts by soxhlet extraction before use. Scandium trichloride hydrate was dehydrated by the method of Manzer<sup>178</sup> which forms the *tris*-THF adduct. This was converted into the acetonitrile adduct by twice recrystallising from acetonitrile.

**Attempted synthesis of  $\text{ScCl}_3 \cdot 9\text{S3}$** 

An acetonitrile solution (20 cm<sup>3</sup>) of 9S3 (0.151 g, 0.839 mmol) was carefully layered over a solution of scandium trichloride (0.196 g, 0.839 mmol) in acetonitrile (40 cm<sup>3</sup>). After twelve days no change was observed in the clear solution. It was then heated at reflux for two hours, allowed to cool to room temperature, and the solvent volume slowly reduced under vacuum. Eventually, small colourless crystals were deposited. These were found to be the free, unreacted macrocycle. M.pt. 81-2°C. Mass spec. *m/e* 181. I.R. no signal below 450 cm<sup>-1</sup>.

### Synthesis of $\text{TiCl}_4 \cdot 9\text{S3}$

Acetonitrile was introduced into a U-tube apparatus until the arms were approximately 1/4 full. An acetonitrile solution ( $20 \text{ cm}^3$ ) of titanium tetrachloride ( $0.527 \text{ g}$ ,  $0.278 \text{ mmol}$ ) was introduced to one arm of the apparatus with minimal agitation, likewise an acetonitrile solution ( $20 \text{ cm}^3$ ) of 9S3 ( $0.050 \text{ g}$ ,  $0.278 \text{ mmol}$ ) was passed into the other arm. After standing for 2 days a yellow crystalline material had formed at the interface between the two solutions. The dendritic nature of the crystalline material precluded successful single crystal X-ray diffraction studies. Recrystallisation from acetonitrile lead to the formation of an intractable fine white precipitate, tentatively ascribed to titanium-oxy species. The solvents toluene, diethyl ether, THF and dioxane were used for both recrystallisation and as media for the complexation reaction without success. M.p.  $> 260^\circ\text{C}$  (decomp.  $220\text{--}225^\circ\text{C}$ ). Anal. calc. for  $\text{C}_6\text{H}_{12}\text{Cl}_4\text{S}_3\text{Ti}$ : C, 19.47; H, 3.27%. Found: C, 19.48; H, 3.16%. I.R. (CsI plates, nujol):  $\nu(\text{TiCl})$  274, 326, 361, 392, 407, 440  $\text{cm}^{-1}$ ;  $\nu(\text{ligand})$  779, 904, 1408  $\text{cm}^{-1}$ . U.v./vis  $\lambda_{\text{max}}$  (MeCN) 34 990  $\text{cm}^{-1}$ .

### Synthesis of $\text{TiCl}_4 \cdot 9\text{S3}$

To a stirred, sky blue, acetonitrile ( $30 \text{ cm}^3$ ) solution of  $[\text{TiCl}_4(\text{MeCN})_2]$  ( $0.15 \text{ g}$ ,  $0.541 \text{ mmol}$ ), was added a colourless acetonitrile solution ( $10 \text{ cm}^3$ ) of 9S3 ( $0.15 \text{ g}$ ,  $0.541 \text{ mmol}$ ). Almost immediately the blue colour changed to a deep purple. Approximately 15 minutes after addition of the 9S3 a fine purple powder was deposited. After the reactants were warmed to  $50^\circ\text{C}$  for 1 h, and allowed to stand overnight, the purple powder settled to the bottom of the vessel to leave a colourless supernatant liquor. The solid was isolated by filtration from the liquid phase. directly suitable for diffraction studies. Removal of the filtered solvent under vacuum left no involatile material. M.p.  $163\text{--}164^\circ\text{C}$  (decomp.). Anal. calc. for  $\text{C}_6\text{H}_{12}\text{Cl}_4\text{S}_3\text{Ti}$ : C, 21.54; H, 3.61%. Found: C, 21.87; H, 3.39%. I.R. (CsI plates,

nujol):  $\nu(\text{TiCl})$  295, 322, 356, 391  $\text{cm}^{-1}$ ;  $\nu(\text{ligand})$  823, 888, 1402  $\text{cm}^{-1}$ . U.v./vis  $\lambda_{\text{max}}$  (MeCN) 549  $\text{cm}^{-1}$ .

### Synthesis of $\text{VOCl}_2 \cdot 9\text{S3}$

A solution of 9S3 (0.78 g, 4.3 mmol) in acetonitrile (25  $\text{cm}^3$ ) was added dropwise to a chilled (0 °C) and stirred solution of vanadium trichloride (1.20 g, 4.3 mmol) in acetonitrile (50  $\text{cm}^3$ ) maintained under an atmosphere of anhydrous dinitrogen. The resulting deep blue solution was stirred and intermittently heated at reflux during a period of one week. Slow removal of the solvent under *vacuo* resulted in the deposition of an azure blue semicrystalline solid which was collected by filtration, washed with hexane (2 x 15  $\text{cm}^3$ ) and diethyl ether (2 x 20  $\text{cm}^3$ ) and dried *in vacuo*. Recrystallisation from acetonitrile afforded beautiful, deep-blue needle crystals of the product (0.66 g, 48%) directly suitable for diffraction studies. M.p. >260 °C (decomp.). Anal. calc. for  $\text{C}_6\text{H}_{12}\text{Cl}_2\text{OS}_3\text{V}$ : C, 22.65; H, 3.80; Cl, 22.28%. Found: C, 22.79; H, 3.83; Cl, 22.38%. I.R. (CsI plates, nujol):  $\nu(\text{VCl})$  356  $\text{cm}^{-1}$ ;  $\nu(\text{V=O})$  962  $\text{cm}^{-1}$ ;  $\nu(\text{ligand})$  830, 900, 1409  $\text{cm}^{-1}$ . U.v./vis  $\lambda_{\text{max}}$  (MeCN) 11 060 (sh), 13 440 (sh), 14 750, and 26 590  $\text{cm}^{-1}$ .

**Table 3.3** Crystallographic data for  $\text{VOCl}_2 \cdot 9\text{S}_3$ .

Formula	$\text{C}_4\text{H}_{12}\text{Cl}_2\text{OS}_3\text{V}$
$M_r$	318.2
Crystal class	monoclinic
Space group	$\text{P}2_1/\text{c}$
$a/\text{\AA}$	12.328(6)
$b/\text{\AA}$	12.667(6)
$c/\text{\AA}$	14.960(11)
$\alpha/^\circ$	
$\beta/^\circ$	90.44(5)
$\gamma/^\circ$	
$V/\text{\AA}^3$	2337(2)
$Z$	8
$D_c/\text{g cm}^{-3}$	1.81
Mo-K $\alpha$ radiation, $\lambda/\text{\AA}$	0.71069
$\mu_{(\text{Mo-K}\alpha)}/\text{cm}^{-1}$	18.2
$T/\text{K}$	290
$F_{000}$	1288
Final R	0.052
Unique observed ( $I/\sigma(I) \geq 2.0$ ) reflections	2457



#### Crystal structure determination of $[\text{VOCl}_2(\text{9S3})]$ .

A pale blue-green prism was fixed onto a quartz fibre. Data were collected with a Siemens R3m four circle diffractometer in  $\omega$ - $2\theta$  mode. Maximum  $2\theta$  was  $50^\circ$  with scan range  $\pm 0.65^\circ(\omega)$  around the  $K_{\alpha 1}$ - $K_{\alpha 2}$  angles, scan speed  $4.29^\circ(\omega) \text{ min}^{-1}$ , depending on the intensity of a 2s pre-scan; backgrounds were measured at each end of the scan for 0.25 of the scan time. The  $hkl$  ranges were 0/14, 0/15, -17/17. Three standard reflections were monitored every 200 reflections and no significant decrease during data collection. Unit cell dimensions and standard deviations were obtained by least-squares fit to 15 reflections ( $21 < 2\theta < 26^\circ$ ). Reflections collected were processed using profile analysis to give 4106 unique reflections ( $R_{\text{int}} = 0.049$ ), of which 2457 were considered observed ( $I/\sigma(I) > 2.0$ ). These were corrected for Lorentz, polarization and absorption effects (the last by the Gaussian method); minimum and maximum transmission factors were 0.83 and 0.86. Crystal dimensions were  $0.50 \times 0.14 \times 0.16 \text{ mm}$ . Systematic reflection conditions  $h0l: l = 2n$ ,  $0k0: k = 2n$ , indicate space group  $P2_1/c$ . The structure was solved by direct methods using SHELXTL (TREF). Anisotropic thermal parameters were used for all non-H atoms. Hydrogen atoms were given fixed isotropic thermal parameters,  $U = 0.08 \text{ \AA}^2$ . Those defined by the molecular geometry were inserted at calculated positions and not refined. Final refinement was on F by least squares methods refining 235 parameters. Largest positive and negative peaks on a final difference Fourier synthesis were of height  $\pm 0.5 \text{ e.\AA}^{-3}$ . A weighting scheme of the form  $W = 1/(\sigma^2(F) + gF^2)$  with  $g = 0.00082$  was used and shown to be satisfactory by a weight analysis. Final  $R = 0.052$ ,  $R_w = 0.060$ ,  $S = 1.19$ ;  $R_{\text{int}}(\text{reflections}) = .$  Maximum shift/error in final cycle was 0.4. Computing was conducted on a DEC Microvax-II with SHELXTL PLUS.<sup>147</sup> Scattering factors in the analytical form and anomalous dispersion factors taken from reference 148.

**CHAPTER FOUR**

**REACTIONS OF GROUP 15 TRIHALIDES WITH  
AZAMACROCYCLIC LIGANDS**

## INTRODUCTION

Following the successful complexation of group 15 trihalides using polyoxa- and polythiamacrocyclic ligands, a corresponding course of research was initiated with polyazamacrocycles. The use of tertiary amine centres was expected to permit an exploration of the nitrogen  $\rightarrow$  MCl<sub>3</sub> (M = As, Sb, Bi) donor/acceptor interaction; secondary amines undergo a condensation reaction to liberate hydrogen chloride. No previous work has been reported in this area. The group 15-thiamacrocyclic complexes are described in Chapter Two together with a summary of the analogous oxamacrocyclic compounds.

The quadridentate saturated azamacrocycle, TMC, was selected as the most suitable ligand to start these investigations. This compound was deemed to offer the following attractions:

- 1) A well established, economical synthetic route.
- 2) A readily handled, low melting point solid as its physical state.
- 3) A good compromise for ring size, *c.f.* 9N3, 18N6.

TMC was first reported by Barefield and Wagner<sup>179</sup> who achieved tetra N-methylation of the parent secondary amine, cyclam, by reflux in a formic acid/formaldehyde mixture. Early work with this macrocycle found that reaction with  $[\text{Ni}(\text{H}_2\text{O})_6]^{2+}$  in aqueous ethanol produces the complex (A) with all methyl groups directed toward the same side of the ring (see Figure 4.1). This isomer was studied by X-ray diffraction with an azide ion to complete a square pyramidal metal geometry.<sup>180</sup> Tetra N-methylation of the preformed nickel(II) cyclam complex has been achieved using methyl iodide in dimethylsulfoxide.<sup>181</sup> In this instance, the isomer (B) with a C<sub>2</sub> axis bisecting the two ethyl linkages is formed and has

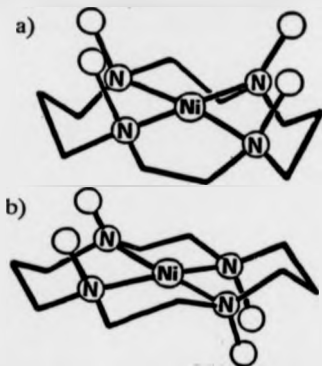


Figure 4.1 Representation of the two nickel(II) TMC isomers; 'all Me's up' - (A), and 'two up two down' with  $C_2$  axis bisecting ethyl links - (B).

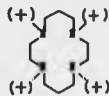

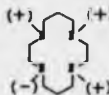

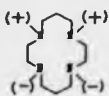

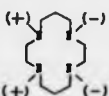



been structurally characterised.<sup>182</sup> In the presence of suitable donor molecules the (A) and (B) isomeric forms yield five- and six-coordinate adducts respectively. For several years it was believed that these two isomers were not interconvertible; the 'all methyls up' structure being the least thermodynamically stable but arising from a low energy, kinetically favoured, pathway because it is the conformation adopted by the free ligand.<sup>183,184</sup> Later work by Moore and co-workers has shown that the two isomers interconvert easily in the presence of strongly coordinating solvents.<sup>185</sup> An isomer with a 'three up and one down' methyl arrangement has been suggested as the intermediate form used to effect the interconversion.<sup>185,186</sup>

### Stereochemical nomenclature of cyclam and tetra-N-methylcyclam

In their seminal report concerning the use of cyclam to form macrocyclic complexes of cobalt(III), Bosnich and co-workers recognised that the cyclic ligand exhibits a number of distinct configurations and that identification of the ring configuration is necessary to permit the full characterisation of any complex. This arises from the coordination of each nitrogen lone pair which suppresses inversion, so leading to an asymmetric centre at each nitrogen atom. For cyclic tetradentate ligands with tetrahedral donor atoms (*e.g.* cyclam and TMC) the sixteen possible arrangements reduce to five distinct combinations, not enantiomerically related. These are presented in Table 4.1 together with the trivial nomenclature of Bosnich *et al* and non-ring nitrogen substituent bond directionality *e.g.* above the  $N_4$  plane (+) and below the plane (-). Bosnich and co-workers suggested that the directionality of the N-H bonds in cyclam should be used as a ready means to identify the configuration at each nitrogen. However, this simple device does not function where there is no Lewis acid bound within the cavity of the macrocycle. A general and unequivocal stereochemical description of the macrocycle is provided by the sequential absolute nitrogen configurations. These descriptions, equally applicable to cyclam (N-H) and TMC (N-CH<sub>3</sub>), are included in Table 4.1. The following criteria were used to prepare the table:

- 1) the sequential stereochemical labelling of the nitrogen atoms around the ring **MUST** follow the IUPAC-required 1,4,8,11 pattern. There are many instances in the literature where the non-systematic 1,5,8,12 sequence has been used for stereochemical descriptions of cyclam and TMC *e.g.* reference 185.

**Table 4.1** Diagrammatic representations and nomenclature used to classify the five distinct isomers of cyclam and its tetra-N-substituted derivatives.

Trivial Name	N-Me/H Bond Direction	N-Configuration	Systematic Sequential Configuration
Trans I			RSRS
Trans II			RRRS*
Trans III			RRSS*
Trans IV			RSSR*
Cis V			RRRR

\* commonly described as RRRR

† commonly described as RSSR

‡ commonly described as RRRS

- 2) in a metal complex the macrocycle has to adopt an endodentate geometry *i.e.* the lone pairs are directed towards the  $N_4$  centroid. In those instances where the lone pairs are not thus constrained, the directionality of the N-CH<sub>3</sub>/H bond is *NOT* characterised by the sequential absolute nitrogen configuration. TMC itself provides an example of a structure containing two independent molecules, both with the same N-Me bond directionality, but one existing as an RSSR isomer and the other as RRSS.
- 3) for any given sequential configuration, the sequence with the most R in advance of S is chosen. Thus the *trans*(II) structure could be described as SRRR, RSRR, RRSR or RRRS, but the latter is adopted.
- 4) to assign the RS configuration, the nitrogen lone pair is given lowest priority. When a metal is present, the nitrogen-metal bond takes highest priority, reversing the R or S assignment. This does not perturb the effective sequential absolute-N-configuration.

#### The structural chemistry of TMC

A search of the Cambridge Crystallographic database retrieved a total of 31 structures incorporating TMC. The transition metal ions found in 29 of these compounds are:

Fe<sup>II</sup>, Fe<sup>III</sup>, Ru<sup>II</sup>, Ru<sup>IV</sup>, Os<sup>II</sup>, Co<sup>II</sup>, Rh<sup>III</sup>, Ni<sup>II</sup>, Pd<sup>II</sup>, Cu<sup>II</sup>, Ag<sup>II</sup>, Zn<sup>II</sup>, Cd<sup>II</sup>.

In addition, the two p-block Lewis acids aluminium and gallium trimethyl have been bound.<sup>187,188</sup> For both of these each donor atom of the macrocycle is bonded to one metal

centre to produce an approximately tetrahedral metal geometry. The resulting tetranuclear complex exhibits an exodentate macrocyclic conformation. Returning to the transition metal complexes, about 70% of the structures enjoy the Trans I (RSRS) and 20% the Trans III (RRSS) configurations. Of particular interest are the two structures with the RRRS configuration originally postulated as an intermediate structure in the Trans I / Trans III interconversion with nickel(II).<sup>185</sup> The two compounds,  $[\text{Ru}(\text{TMC})(\text{MeCN})\text{N}_3][\text{PF}_6]$ <sup>189</sup> and  $[\text{Ru}(\text{TMC})(\text{MeCN})\text{O}][\text{PF}_6]$ ,<sup>190</sup> are both six-coordinate about the central metal ion. Ten (35%) of all TMC structural characterisations involve nickel(II). The RSRS configuration has been observed in  $[\text{Ni}(\text{TMC})\text{N}_3][\text{ClO}_4]$ ,  $[\text{Ni}(\text{TMC})(\text{DMF})][\text{CF}_3\text{SO}_3]_2$ ,<sup>191</sup>  $[\text{Ni}(\text{TMC})(\text{O}_2\text{COME})][\text{ClO}_4]$ ,<sup>192</sup>  $[\text{Ni}(\text{TMC})][\text{CF}_3\text{SO}_3]_2$ ,<sup>193</sup>  $[\text{Ni}(\text{TMC})(\text{MeCN})][\text{ClO}_4]_2$ ,<sup>194</sup> and  $[\text{Ni}(\text{TMC})][\text{ClO}_4]_2$ ,<sup>195</sup> while for the compounds  $[\{\text{Ni}(\text{TMC})\text{N}_3\}_2(\mu\text{-N}_3)]$ ,<sup>196</sup>  $[\text{Ni}(\text{TMC})(\text{O}_2\text{COME})_2]$ ,<sup>197</sup>  $[\text{Ni}(\text{TMC})][\text{CF}_3\text{SO}_3]_2$ , and  $[\text{Ni}(\text{TMC})(\text{H}_2\text{O})_2][\text{Cl}]_2$ ,<sup>197</sup> the RRSS isomer has been found.



## RESULTS AND DISCUSSION

Dropwise addition of a solution of TMC in acetonitrile to arsenic, antimony, or bismuth trichloride, in the same solvent, produced an immediate flocculent white precipitate. Attempts to check this uncontrolled precipitation by allowing the reagents to diffuse together through a layer of pure solvent were unsuccessful. The chemical analyses of these white solids were not consistent with a well-defined species nor were they consistent between different experimental runs. Examination of the infrared spectra suggested the presence of  $\nu(\text{N}^+\text{-H})$ , *i.e.* protonation of the macrocycle. This was thought to arise from release of hydrogen chloride subsequent to hydrolysis of metal-chlorine bonds. It was also noticed that after standing for five days, a few crystalline flecks appeared in the white precipitate of the arsenic congener. Applying the most stringent anhydrous conditions and removing the supernatant liquid as soon as the white precipitate was formed, *i.e.* a reaction time of between one and two minutes, seemed the most likely method to obtain a sample of the initial adduct with the *minimum* hydrolysis. Elemental analysis of the arsenic and bismuth congeners adhered closely with the formulation  $[(\text{TMC})_2(\text{MCl})_3]$ . Regretfully, the infrared spectra still showed the presence of protonated amine groups, so suggesting that the hydrolysis had not been avoided. If the macrocycle is assumed to be of the diprotonated form, no potential molecular structure has yet been found compatible with the 2:3 macrocycle:MCl<sub>3</sub> stoichiometry suggested by the elemental analyses. Further progress with these anhydrous systems was stymied by the onset of hydrolysis before further spectroscopic evidence could be garnered.

In an effort to *enhance* the postulated hydrolysis reaction various methods were used to increase the amount of water available to the reagents. These included both permanent and temporary exposure to the open atmosphere, use of undried solvent, and direct addition of

water to the reaction mixture; all without success. Finally, crystals were produced in good yield by introducing approximately four equivalents water into the *closed* dinitrogen atmosphere above the white precipitate. In the case of the arsenic and antimony congeners, the white powder had mostly become crystalline during the course of seven to ten days. In the case of the reaction using bismuth trichloride, only a very few needle crystals were observed by microscope amongst the white precipitate, even after allowing the reaction mixture to stand for two months. It would seem that the limited gaseous diffusion of moisture into the reaction solvent produced a concentration of water suited to a controlled rate of metal halide hydrolysis. Meticulous separation of the crystalline material from the remaining white precipitate produced a sample of material whose elemental analysis was consistent with the formulation (based on one protonated TMC ion)  $C_{14}H_{14}As_4Cl_{10}N_4O_2$  and  $C_{14}H_{14}Cl_4N_4OSb_2$  for the arsenic- and antimony-derived products respectively.

Attempts to recrystallise the products from a variety of rigorously dried solvents proved to be unsuccessful. The precipitation of further ill-defined white powder was considered to arise from additional, uncontrolled hydrolysis. Fortunately, crystals suitable for single crystal X-ray diffraction studies were retrieved from both crystalline products so obviating the need for continued speculation regarding the molecular nature of these two compounds. The molecular structures of the arsenic- and antimony-derived crystals were obtained following successful refinement of the diffraction data. These studies provided conclusive evidence that, in both cases, hydrolysis had taken place to yield the diprotonated cationic form of the tetraazamacrocyclic together with an oxo-bridged counter anion. These compounds have the formulae:





This discussion will now consider the oxy-chloro anions separately before examining the protonated and neutral structures of TMC.

More specifically, the anions will be appraised with regard to each individual structure before embarking upon a detailed comparison with other, closely related species.

The cations will be considered in relation to:

- a) The molecular structure of the parent ligand.
- b) The neutral and protonated forms of the unsubstituted, secondary parent amine, cyclam.
- c) Molecular mechanical strain energy calculations.

## MOLECULAR STRUCTURE OF THE ANION $[\text{Sb}_2\text{OCl}_4]^-$

The structure of the anion  $[\text{Sb}_2\text{OCl}_4]^-$  is shown in Figure 4.2, and the molecular dimensions given in Table 4.2. This species comprises an oxo-bridged  $\text{Cl}_2\text{Sb-O-SbCl}_2$  unit with further association by two doubly-bridging chloride ions. The  $\text{Sb}_2\text{OCl}_4$  unit (not known to exist separately) is derived from two antimony trichloride molecules by replacement of two chloride ions, one from each antimony, by a symmetrically-bridging oxide ion. The long  $\text{Sb}-\text{Cl}_{(\text{bridging})}$ , ( $\text{Cl}_{\text{br}}$ ), distances (mean 2.888 Å) can be regarded as secondary bonds with primary bonds for  $\text{Sb}-\text{O}$  (mean 1.943 Å) and  $\text{Sb}-\text{Cl}_{(\text{terminal})}$ , ( $\text{Cl}_{\text{tr}}$ , (mean 2.428 Å)). The  $\angle \text{Sb-O-Sb}$  of  $117^\circ$  reduces the  $\text{Sb}-\text{Sb}$  contact to 3.312 Å (c.f. a 4.1 Å van der Waals separation). The two  $\text{Sb}(\text{Cl}_2)_2$  planes lie orthogonal to the  $\text{Sb}_2\text{O}$  plane leading to an approximate  $C_{2v}$  symmetry for the ion. The pseudo two-fold axis passes through the mid-point of the vector between the two bridging chlorine atoms and the bridging oxygen atom. The four chlorine atoms around each antimony are virtually coplanar, with a maximum deviation from the best plane of just 0.006 Å. The antimony atoms are displaced from this plane, away from the oxo-bridge, by 0.284 and 0.277 Å.

In terms of geometric polyhedra the ion can be described in two ways; firstly by face sharing between two  $\text{SbCl}_4\text{O}$  square pyramids, or, if the antimony 5s lone pair is stereochemically active, between two  $\psi$ -octahedral  $:\text{SbCl}_4\text{O}$ . The atoms are arranged such that the bridging chlorines are *trans* to terminal chlorines and the oxygen atom is *trans* to either a vacant coordination site or the antimony lone pair.

The square pyramidal geometry seen around each antimony atom is necessarily distorted as a consequence of the bridging by two chlorine atoms. The observed geometry could be ascribed to the presence of a stereochemically active lone pair, or simply an effect of the overall geometric requirements of the three bridging atoms around each antimony.

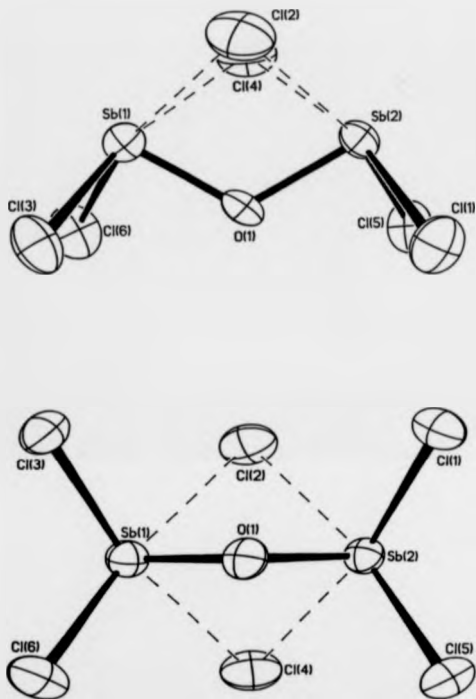


Figure 4.2 Two views of the oxo-bridged anion  $[\text{Sb}_2\text{OCl}_6]^-$ .

Table 4.2 Bond lengths (Å) and angles (°) for the compound  $[H_7(TMC)][Sb_2OCl_6]$ .

Bond lengths (Å)

Sb(1)-Cl(2)	2.900(5)	Sb(1)-Cl(3)	2.431(5)
Sb(1)-Cl(4)	2.920(5)	Sb(1)-Cl(6)	2.425(5)
Sb(1)-O(1)	1.941(7)	Sb(2)-Cl(1)	2.423(5)
Sb(2)-Cl(2)	2.865(5)	Sb(2)-Cl(4)	2.868(5)
Sb(2)-Cl(5)	2.432(5)	Sb(2)-O(1)	1.944(7)
N(11)-C(11)	1.452(13)	N(11)-C(12)	1.461(15)
N(11)-C(17a)	1.479(18)	N(12)-C(14)	1.508(14)
N(12)-C(15)	1.496(12)	N(12)-C(16)	1.473(13)
C(12)-C(13)	1.521(22)	C(13)-C(14)	1.500(16)
C(16)-C(17)	1.488(16)	C(17)-N(11a)	1.479(18)
N(21)-C(21)	1.485(16)	N(21)-C(22)	1.492(15)
N(21)-C(27)	1.485(11)	N(22)-C(24)	1.480(14)
N(22)-C(25)	1.445(16)	N(22)-C(26)	1.475(11)
C(22)-C(23)	1.522(13)	C(23)-C(24)	1.507(13)
C(26)-C(27a)	1.499(15)	C(27)-C(26a)	1.499(15)

Bond angles (deg.)

Cl(2)-Sb(1)-Cl(3)	90.9(1)	Cl(2)-Sb(1)-Cl(4)	80.5(1)
Cl(3)-Sb(1)-Cl(4)	165.8(1)	Cl(2)-Sb(1)-Cl(6)	167.2(1)
Cl(3)-Sb(1)-Cl(6)	89.9(1)	Cl(4)-Sb(1)-Cl(6)	96.1(1)
Cl(2)-Sb(1)-O(1)	76.3(2)	Cl(3)-Sb(1)-O(1)	91.1(2)
Cl(4)-Sb(1)-O(1)	76.0(2)	Cl(6)-Sb(1)-O(1)	90.9(2)
Cl(1)-Sb(2)-Cl(2)	91.1(1)	Cl(1)-Sb(2)-Cl(4)	166.5(1)
Cl(2)-Sb(2)-Cl(4)	82.0(1)	Cl(1)-Sb(2)-Cl(5)	90.7(1)
Cl(2)-Sb(2)-Cl(5)	167.6(1)	Cl(4)-Sb(2)-Cl(5)	93.6(1)
Cl(1)-Sb(2)-O(1)	89.9(2)	Cl(2)-Sb(2)-O(1)	77.2(2)
Cl(4)-Sb(2)-O(1)	77.3(2)	Cl(5)-Sb(2)-O(1)	90.6(2)
Sb(1)-Cl(2)-Sb(2)	70.2(1)	Sb(1)-Cl(4)-Sb(2)	69.9(1)
Sb(1)-O(1)-Sb(2)	117.1(4)	C(11)-N(11)-C(12)	110.3(9)
C(11)-N(11)-C(17a)	110.0(10)	C(11)-N(11)-C(17a)	110.1(8)
C(14)-N(12)-C(15)	111.1(9)	C(14)-N(12)-C(16)	111.9(8)
C(15)-N(12)-C(16)	112.1(8)	N(11)-C(12)-C(13)	113.9(9)
C(12)-C(13)-C(14)	113.5(11)	N(12)-C(14)-C(13)	113.8(10)
N(12)-C(16)-C(17)	114.2(9)	C(16)-C(17)-N(11a)	112.2(9)
C(21)-N(21)-C(22)	110.5(8)	C(21)-N(21)-C(27)	110.3(8)
C(22)-N(21)-C(27)	110.0(9)	C(24)-N(22)-C(25)	109.0(8)
C(24)-N(22)-C(26)	109.4(8)	C(25)-N(22)-C(26)	111.1(8)
N(21)-C(22)-C(23)	112.3(9)	C(22)-C(23)-C(24)	112.3(7)
N(22)-C(24)-C(23)	113.3(9)	N(22)-C(26)-C(27a)	113.5(9)
N(21)-C(27)-C(26a)	114.5(9)		

## COMPARISON OF $[\text{Sb}_2\text{OCl}_4]^-$ WITH RELATED OXYCHLOROANIONS

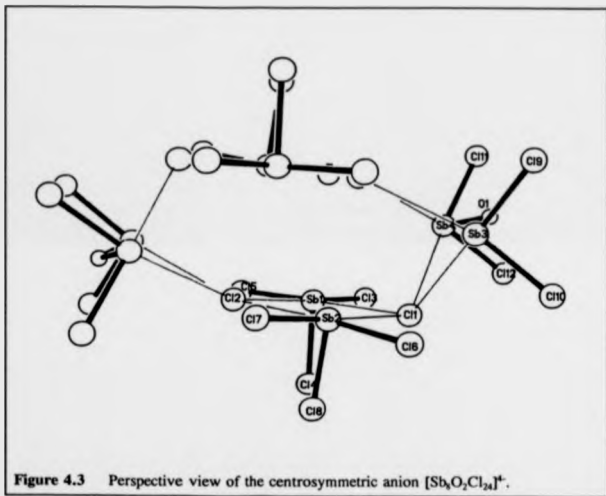
The anion in  $[\text{H}_2(\text{TMC})][\text{Sb}_2\text{OCl}_4]$ , MILSB, shows some subtle modifications to the almost identical anion reported by Sowerby *et al* in  $[\text{Hpy}]_2[\text{Sb}_2\text{OCl}_4]$ .<sup>100</sup> (where py = pyridine). The anion in this compound will be referred to as SOWSB. A related antimonate(III),  $[\text{Fe}(\text{cp})_2][\text{Sb}_2\text{OCl}_4]$ , has been characterised by Rheingold *et al*.<sup>100</sup> The anion in this compound will be termed RHEINSB during the following discussion. The relation of RHEINSB to MILSB/SOWSB is most readily appreciated by inspection of Figure 4.3. It is an octanuclear aggregate that can be considered as a hydrolytic precursor to MILSB/SOWSB, viz. only half the antimony atoms have replaced a chlorine with a bridging oxide linkage.

SOWSB was prepared by the action of pyridine and antimony(III) chloride in dichloromethane. Photolysis of a mixture of antimony(III) chloride and ferrocene in the presence of oxygen lead to the isolation of RHEINSB. A detailed comparison of the dimensions about the oxygen bridged antimony atoms of the three compounds MILSB, SOWSB and RHEINSB is given in Table 4.3 and Table 4.4.

Consideration of Table 4.3 confirms the gross similarity between MILSB and SOWSB. The differences in respect of RHEINSB are readily reconciled in terms of the two quadruply bridging chloride ions, viz. lengthened mean  $\text{Sb}-\text{Cl}_{\text{bb}}$  and  $\text{Sb}-\text{Sb}$ , shortened  $\text{Sb}-\text{O}$  and mean  $\text{Sb}-\text{Cl}_{\text{a}}$ .

Distinction between MILSB and SOWSB is evident upon inspection of the individual  $\text{Sb}-\text{Cl}$  distances given in Table 4.4. For MILSB both the  $\text{Sb}-\text{Cl}_{\text{bb}}$  and  $\text{Sb}-\text{Cl}_{\text{a}}$  distances are symmetric (within  $3\sigma$ ). However, SOWSB exhibits one distinctly asymmetric chlorine bridge

(2.832, 2.952 Å). This can be ascribed to the presence of a weak hydrogen bond between a pyridinium cation and the bridging chlorine (N...Cl 3.32(2) Å). A major structural feature of SOWSB is the existence of a short, strong, hydrogen bond (2.68(1) Å) between the bridging oxygen atom and the nitrogen of a second pyridinium cation. The absence of this interionic hydrogen bond in MILSB results in a closing of the Sb-O-Sb angle by 2.4° with concomitant reduction in the Sb-Sb contact by 0.17 Å, whilst the mean Sb-O distance remains essentially unchanged.





**Table 4.3** Comparison of mean interatomic distances (Å) for  $[\text{Sb}_2\text{OCl}_6]^{2-}$  based species.

Bond Length	MILSB	SOWSB	RHEINSB
Sb-O	1.943(7)	1.949(8)	1.92
Sb-Sb	3.312	3.37	3.457
Sb-Cl <sub>(terminal)</sub>	2.428(5)	2.443(3)	2.373
Sb-Cl <sub>(bridging)</sub>	2.888(5)	2.887(4)	3.200

**Table 4.4** Comparison of interatomic distances (Å) and angles (°) for  $[\text{Sb}_2\text{OCl}_6]^{2-}$  based species.

Bond Dimension		MILSB	SOWSB
Sb-Cl <sub>(terminal)</sub>	Sb1	2.431(5), 2.425(5)	2.437(3), 2.483(3)
	Sb2	2.423(5), 2.432(5)	2.419(3), 2.424(3)
Sb-Cl <sub>(bridging)</sub>	Sb1	2.900(5), 2.920(5)	2.878(4), 2.832(4)
	Sb2	2.868(5), 2.865(5)	2.884(4), 2.952(4)
Sb-O	Sb1	1.941(7)	1.947(8)
	Sb2	1.944(7)	1.949(8)
∠ Sb-O-Sb		117.1(4)	119.5(4)

# MOLECULAR STRUCTURE OF THE ANION $[\text{As}_4\text{O}_7\text{Cl}_{10}]^{2-}$

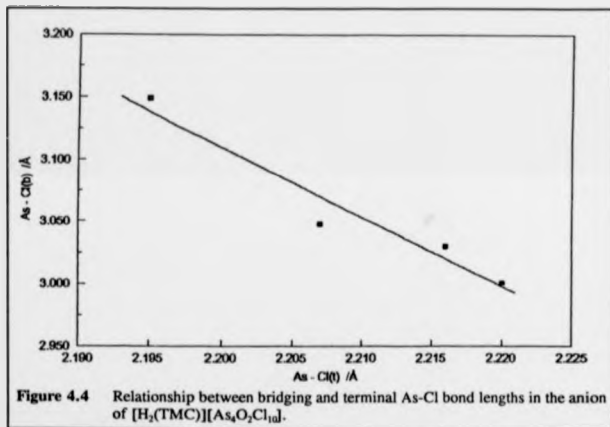
The arsenic trichloride derived anion  $[\text{As}_4\text{O}_7\text{Cl}_{10}]^{2-}$ , shown in Figure 4.5, is situated about a crystallographic two-fold axis. Bond lengths and angles are given in Table 4.5. The quadrangular array of arsenic atoms comprises two  $[\text{Cl}_2\text{As-O-AsCl}_2]$  units with oxygen bridging within each. These are further connected by two quadruply-bridging chlorine atoms. The  $[\text{As}_2\text{OCl}_4]$  moiety is analogous to that seen within  $[\text{Sb}_2\text{OCl}_4]^{2-}$ . The ion has an imposed  $C_2$  symmetry and crudely approximates to an idealised  $D_{2h}$  point group. The four  $\text{As}(\text{Cl}_{\text{quadruply}})_2$  planes have an orthogonal orientation to the  $(\text{As})_4$  and  $(\text{As})_2\text{O}$  planes.

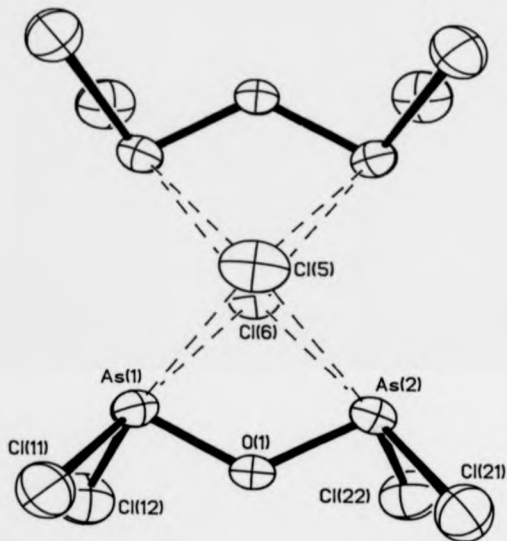
The primary co-ordination sphere around each arsenic atom comprises two terminal chlorine atoms,  $\text{Cl}_{\text{ter}}$ , (mean  $\text{As-Cl}_{\text{ter}}$  2.210) and a bridging oxygen atom (mean  $\text{As-O}$  1.770 Å). The two  $\mu^4$  bridging chlorine atoms,  $\text{Cl}_{\text{qu}}$ , exhibit extended, secondary bonds to each arsenic (mean 3.057 Å). The four chlorine atoms around each arsenic are almost coplanar with a maximum deviation from the best plane of just 0.057 Å (mean 0.036 Å). The As atom lies up to 0.090 Å below this plane, displaced to the side opposite the bridging oxygen atom. The dimensions of the symmetrical As-O-As linkages are comparable to those previously reported: e.g. arsenic(III) oxide, As-O (mean) 1.789 Å,  $\angle$  As-O-As (mean)  $125.2^\circ$ ; <sup>200</sup> *o*-phenylene diarsine oxychloride, As-O 1.787 Å,  $\angle$  As-O-As  $121.8^\circ$ . <sup>201</sup>

The oxygen bridges can be visualised as the product of face sharing between two  $\psi$ -octahedral  $:\text{AsCl}_4\text{O}$  units with bridging chlorines trans to terminal chlorines and the oxygen atom trans to the arsenic 4s lone pair. To complete the tetranuclear array there is edge sharing between two  $\text{As}_2\text{Cl}_4\text{O}$  moieties by the two, already bridging, chlorine atoms. The geometry manifest about arsenic may, alternatively, be ascribed to geometric constraints of the bridging species.

An alternative description of the  $\{\text{As}_4\text{O}_2\text{Cl}_{10}\}^{2-}$  unit would invoke a charge separated model with two neutral  $\text{Cl}_2\text{As-O-AsCl}_2$  molecules together with two chloride ions. The secondary bonded view presented is supported by the observations that:

- a) Each  $\text{As}_2\text{Cl}_4\text{O}$  unit is oriented towards the bridging chlorine atoms.
- b) Covalent character in the  $\text{As-Cl}_{\text{br}}$  bonds leads to the expected inverse relationship between each *trans*-oriented bond length ( $\text{As-Cl}_{\text{br}}$  :  $\text{As-Cl}_{\text{tr}}$ ). This rudimentary correlation is illustrated in Figure 4.4.





**Figure 4.5** Structure of the polyarsa-anion  $[As_4O_2Cl_{10}]^{3-}$ .

Table 4.5 Bond lengths (Å) and angles (°) for the compound  $[H_3(TMC)][As_3O_7Cl_{10}]$ .

Bond lengths (Å)

As(1)-Cl(11)	2.216(3)	As(1)-Cl(12)	2.207(3)
As(1)-O(1)	1.774(4)	As(1)-Cl(5)	3.048(3)
As(1)-Cl(6)	3.030(3)	As(2)-Cl(21)	2.220(3)
As(2)-Cl(22)	2.195(3)	As(2)-Cl(5)	3.149(3)
As(2)-Cl(6)	3.001(3)	As(2)-O(1)	1.766(4)
N(1)-C(1)	1.444(11)	N(1)-C(2)	1.457(10)
N(1)-C(7a)	1.474(10)	N(2)-C(4)	1.473(11)
N(2)-C(3)	1.516(11)	N(2)-C(6)	1.517(10)
C(2)-C(3)	1.556(11)	C(3)-C(4)	1.535(12)
C(6)-C(7)	1.460(13)	C(7)-N(1a)	1.474(10)

Bond angles (deg.)

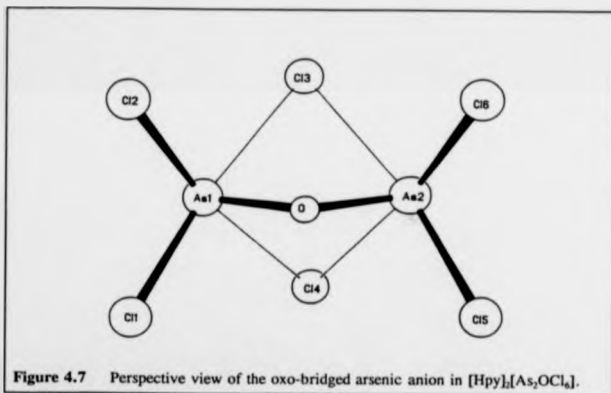
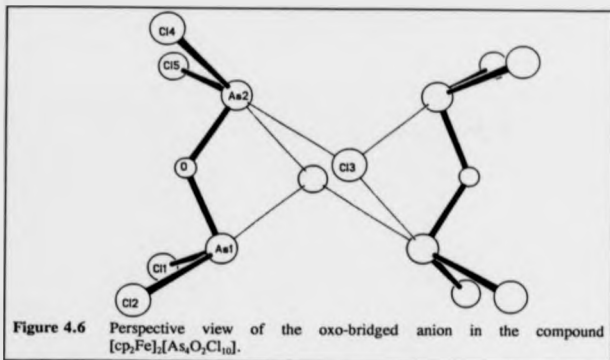
Cl(11)-As(1)-Cl(12)	94.2(1)	Cl(11)-As(1)-Cl(6)	170.7(1)
Cl(12)-As(1)-Cl(5)	169.9(1)	Cl(11)-As(1)-O(1)	94.6(2)
Cl(12)-As(1)-O(1)	93.8(2)	Cl(21)-As(2)-Cl(22)	94.8(1)
Cl(21)-As(2)-Cl(6)	175.2(1)	Cl(22)-As(2)-Cl(5)	164.1(1)
Cl(21)-As(2)-O(1)	93.2(2)	Cl(22)-As(2)-O(1)	96.2(2)
As(1)-O(1)-As(2)	122.2(3)	C(1)-N(1)-C(2)	111.3(6)
C(1)-N(1)-C(7a)	112.5(6)	C(2)-N(1)-C(7a)	104.9(6)
C(4)-N(2)-C(6)	111.9(6)	C(4)-N(2)-C(6)	112.3(7)
C(5)-N(2)-C(6)	107.3(7)	N(1)-C(2)-C(3)	110.8(7)
C(2)-C(3)-C(4)	112.3(7)	N(2)-C(4)-C(3)	110.6(6)
N(2)-C(6)-C(7)	114.8(7)	C(6)-C(7)-N(1a)	115.7(8)

### COMPARISON OF $[\text{As}_4\text{O}_2\text{Cl}_{10}]^{2-}$ WITH RELATED OXYCHLOROANIONS

The tetranuclear anion in  $[\text{H}_2(\text{TMC})][\text{As}_4\text{O}_2\text{Cl}_{10}]$  will be referred to as MILAS. Detailed comparison of this species is warranted with two other, closely related, structures. The first, to be termed SHELDAS, contains the anion  $[\text{As}_4\text{OCl}_{10}]^{2-}$ ,<sup>202</sup> the arsenic analogue of MILSB, and can be regarded as a subunit of MILAS, see Figure 4.6. The second, an isomeric form of MILAS, is the anion reported by Rheingold in the compound  $[\text{Fe}(\eta^5\text{-C}_5\text{H}_5)_2][\text{As}_4\text{O}_2\text{Cl}_{10}]$ .<sup>203</sup> This ion will be described as RHEINAS during this discussion. SHELDAS was isolated from the reaction of arsenic trichloride, pyridinium hydrochloride and water in acetonitrile. RHEINAS was prepared by the action of sunlight on a solution of  $\text{AsCl}_3$  and ferrocene in benzene.

The structure of RHEINAS is shown in Figure 4.7. The anion sits about a crystallographic inversion centre (c.f. a 2-fold axis for MILAS). Although grossly similar to MILAS, the bridging chlorine atoms of RHEINAS make just three secondary  $\text{As}\cdots\text{Cl}_{\text{br}}$  contacts in the range 2.889(2) - 3.062(2) Å. The fourth contact at 3.349 Å, although clearly much weaker, is within 3.60 Å, the summed Van der Waals radii of arsenic and chlorine. Distinction between these two isomers is most readily achieved by comparison of the *trans*  $\text{As}=\text{As}$  distances: for MILAS these are 4.759 and 4.848 Å, for RHEINAS 4.660 and 5.075 Å.

Table 4.6 presents selected dimensions found in the three ions under consideration. The  $\text{As}-\text{O}$  and  $\text{As}=\text{As}$  distances show little variation.



**Table 4.6** Comparison of interatomic distances (Å) for  $[\text{As}_2\text{OCl}_4]^{2-}$  based species.

Bond Length		MILAS	RHEINAS	SHELDAS
As - O		1.744(4), 1.766(4)	1.769(3), 1.766(4)	1.765(1), 1.777(1)
	mean	1.770	1.768	1.771
As - As		3.098	3.110	3.057
As - Cl	As1	2.216(3), 2.207(3)	2.199(2), 2.241(2)	2.265(1), 2.242(1)
	As2	2.220(3), 2.195(3)	2.260(2), 2.242(2)	2.268(1), 2.242(1)
	mean	2.210	2.236	2.254
As - Cl <sub>longer</sub>	As1	3.048(3), 3.030(3)	2.920(2), 3.349(2)	2.836(1), 2.965(1)
	As2	3.149(3), 3.001(3)	2.889(2), 3.062(2)	2.855(1), 2.925(1)
	mean	3.057	3.055	2.895



## TETRA-N-METHYLCYCLAM AND ITS DIPROTONATED CATION

The diprotonated form of TMC was found as counterion to the arsenic and antimony oxo-bridged anions formed following reaction of arsenic and antimony trichloride with the parent macrocycle. As will be seen in the description of the structures, a different sequential configuration about nitrogen was found in each compound. To more fully consider the configurational flexibility of the diprotonated form, the configuration exhibited by the free base was sought. Surprisingly, no crystallographic study had been reported in the literature and so a single crystal structure determination was undertaken.

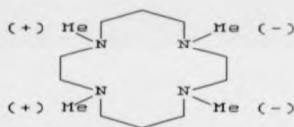
Table 4.7 Basicity constants of selected tetramines at 25.0 °C.

Ligand	$\log K_1$	$\log K_2$	$\log K_3$	$\log K_4$
2,3,2-tet	10.3	9.5	7.3	6.0
cyclam	11.6	10.6	1.6	2.4
TMC	9.7	9.3	3.1	2.6

Table 4.7 shows the basicity constants in respect of the polyamines 2,3,2-tet,<sup>204</sup> cyclam,<sup>205</sup> and TMC.<sup>206</sup> Clearly the cyclic polyamines show a stepped sequence in their protonation profile. This is attributed to the formation of intracationic hydrogen bonds for the macrocycles whilst the linear amine partakes in inter molecular hydrogen bonding with the solvent.

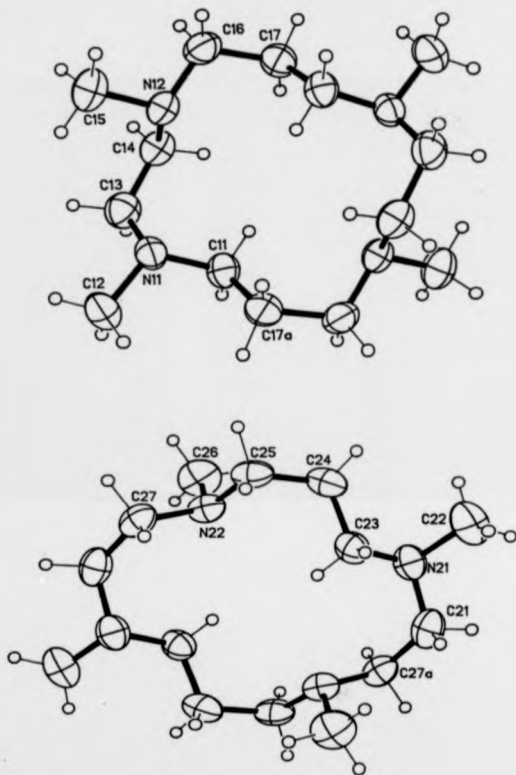
## MOLECULAR STRUCTURE OF TETRA-N-METHYLCYCLAM

The structure of TMC consists of two independent molecules (1 and 2) and these are shown in Figure 4.9; bond lengths and angles are given in Table 4.8. The macrocyclic rings are positioned about the crystallographic inversion centre so placing the four nitrogen atoms of each molecule in a planar array. Consideration of the location of the methyl groups with regard to the  $N_4$  plane would classify each molecule as the trans(IV) isomer. This is shown in Figure 4.8, where the '+' and '-' signs denote the methyl group location above and below the  $N_4$  plane respectively. For molecule 1 the two sets of methyl groups lie  $\pm 1.191$  and  $\pm 0.503$  Å above and below the  $N_4$  plane. For molecule 2 these dimensions are  $\pm 0.641$  and  $\pm 0.265$  Å.



**Figure 4.8** Location of methyl groups relative to the  $N_4$  plane for molecules 1 and 2 of tetramethylcyclam.

Use of the sequential absolute configurations of the nitrogen centres to categorise the two molecules highlights their different stereochemistry. Molecule 1 can be identified as the RSSR (Trans(IV)) isomer and molecule 2 as the RRSS (Trans (III)) isomer.



**Figure 4.9** Views of TMC molecules 1 and 2 with atomic numbering.

Table 4.8 Bond lengths (Å) and angles (°) for tetra-N-methylcyclam.

Bond lengths (Å)

N(11)-C(11)	1.453(2)	N(11)-C(12)	1.448(3)
N(11)-C(13)	1.453(3)	N(12)-C(14)	1.451(3)
N(12)-C(15)	1.454(2)	N(12)-C(16)	1.459(2)
C(11)-C(17a)	1.513(4)	C(13)-C(14)	1.506(3)
C(16)-C(17)	1.521(3)	C(17)-C(11a)	1.513(4)
N(21)-C(21)	1.461(3)	N(21)-C(22)	1.453(4)
N(21)-C(23)	1.454(2)	N(22)-C(25)	1.456(3)
N(22)-C(26)	1.452(4)	N(22)-C(27)	1.456(2)
C(21)-C(27a)	1.509(3)	C(23)-C(24)	1.522(3)
C(24)-C(25)	1.517(3)	C(27)-C(21a)	1.509(3)

Bond angles (deg.)

C(11)-N(11)-C(12)	111.6(1)	C(11)-N(11)-C(13)	111.8(1)
C(12)-N(11)-C(13)	109.7(2)	C(14)-N(12)-C(15)	111.0(2)
C(14)-N(12)-C(16)	111.7(2)	C(15)-N(12)-C(16)	109.6(1)
N(11)-C(11)-C(17a)	113.4(2)	N(11)-C(13)-C(14)	115.7(2)
N(12)-C(14)-C(13)	114.9(2)	N(12)-C(16)-C(17)	114.0(2)
C(16)-C(17)-C(11a)	112.1(2)	C(21)-N(21)-C(22)	109.2(2)
C(21)-N(21)-C(23)	111.6(2)	C(22)-N(21)-C(23)	110.8(2)
C(25)-N(22)-C(26)	110.8(2)	C(25)-N(22)-C(27)	111.8(1)
C(26)-N(22)-C(27)	111.3(2)	N(21)-C(21)-C(27a)	115.8(2)
N(21)-C(23)-C(24)	114.0(2)	C(23)-C(24)-C(25)	111.8(2)
N(22)-C(25)-C(24)	113.0(1)	N(22)-C(27)-C(21a)	115.9(1)

## MOLECULAR STRUCTURE OF DIPROTONATED TETRA-N-METHYLCYCLAM

The diprotonated TMC counter-cation of the anion  $[As_4O_2Cl_{10}]^2$  exhibited a different stereochemical configuration to that seen in the counter-cation of  $[Sb_2OCl_6]^2$ . For the former, the *RSRS* (Trans I) configuration was found with all methyl groups oriented towards the same side of the ring. The ion is illustrated in Figure 4.10, dimensions given in Table 4.5. This cation lies about a crystallographic two-fold axis with the nitrogen atoms approximately  $\pm 0.19$  Å pairwise above and below the  $N_4$  mean plane. The two protons are bound within the ring to two alternate nitrogen atoms at a distance of approximately 1.0 Å. A longer, hydrogen, bond at 2.1 Å exists to the other nitrogen atom such that two six-membered rings are formed. Each proton lies at 1.3 Å from the  $N_4$  centroid and effectively within the mean  $N_4$  plane (actually displaced by 0.07 Å). The  $N^*HN$  planes intersect the  $N_4$  plane at 7.7 Å whilst the methyl groups are displaced from the  $N_4$  plane in pairs at (approx.) 1.0 and 1.5 Å. *Trans* N--N contacts 4.46 and 4.03 Å give an indication of the macrocyclic cavity dimension. Torsion angles around the macrocyclic ring, six *anti* and eight *gauche*, define four true corners to permit classification as [3434].

The asymmetric unit of the unit cell containing  $[Sb_2OCl_6]^2$  contains two independent  $[H_2(TMC)]^{2+}$  half-cations. The slight geometric differences between the two are without chemical significance. The cation is illustrated in Figure 4.11, molecular dimensions are given in Table 4.2. Figures quoted in this description will relate to molecule 1 unless explicitly stated otherwise. In contrast to the *RSRS* isomer found with  $[As_4O_2Cl_{10}]^2$ , in this instance the diprotonated cation has assumed an *RRSS* (Trans III) configuration. The methyl groups are arranged with two above and two below the mean  $N_4$  plane with a pseudo-2-fold axis bisecting the two carbon-carbon bonds of the ethyl linkages. The centrosymmetric space

group requires the four nitrogen atoms of each macrocycle to define a plane. The two protons found are bound within the ring to two alternate nitrogen atoms at a distance (0.92 Å) slightly less than that found for the *RSRS* isomer. The completion of two six-membered rings is achieved through two H-N hydrogen bonds of length 2.22 Å. For the *RRSS* isomer, each proton lies 1.25 Å from the  $N_4$  centroid and almost within the mean  $N_4$  plane (actually  $\pm 0.05$  Å). The  $N^*HN$  planes are, of course, parallel and intersect the  $N_4$  plane at  $5.4^\circ$ . The methyl groups are displaced from the  $N_4$  plane in pairs at (approx.)  $\pm 1.2$  and  $\pm 1.3$  Å. Torsion angles around the macrocyclic ring, eight *anti* and six *gauche*, define one true and one false corner. A [77] classification can be made if the requirement to include only true corners is lifted. In this compound the *Trans* N-N distances are almost equal at 4.33 and 4.28 Å.

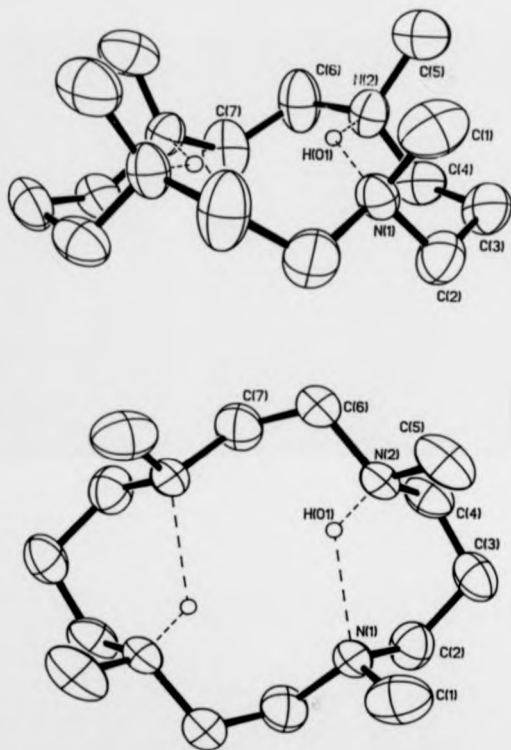


Figure 4.10 Two views of the cation (*RSRS*) in the compound  $[H_2(TMC)][As_4O_7Cl_{10}]$ .

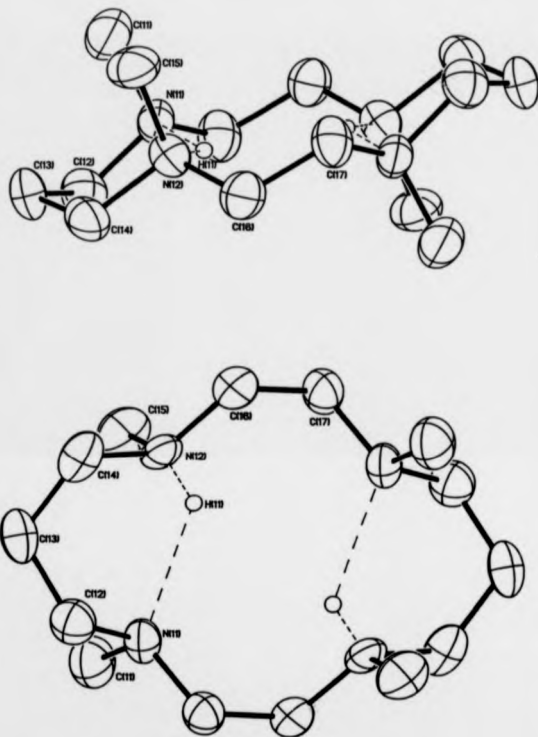


Figure 4.11 Two views of the cation (*RRSS*) in the compound  $[H_2(TMC)][Sb_2OCl_6]$ .



## Structural Comparison of Neutral and Protonated 14N4 Macrocycles

Having characterised the crystal structures of TMC and its diprotonated form, and with the structural characterisations of cyclam and its di- and tetraprotonated forms available in the literature, correlations within this series can now be made. Table 4.9 shows selected structural parameters in respect of the compounds containing the macrocyclic species under consideration. The following observations are made:

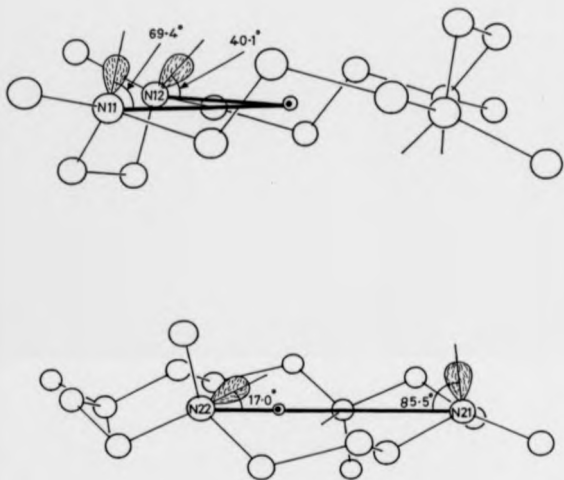
- 1) In all cases except one, the four nitrogen atoms are coplanar. The exception,  $\text{RSRS}[\text{H}_2(\text{TMC})]^{2+}$  shows a deviation of  $\pm 0.19 \text{ \AA}$  from the mean  $\text{N}_4$  plane.
- 2) The C-C distances around the ring show little variation in the range c.  $1.51 - 1.52 \text{ \AA}$ .
- 3) Those  $\text{N}-\text{C}_{\text{ring}}$  bonds associated with protonated nitrogen centres are somewhat longer than those linked to basic (3-coordinate) nitrogen atoms. e.g. there is a difference between the mean values of c.  $0.02 - 0.03 \text{ \AA}$  for diprotonated TMC.
- 4) A similar difference is discernible between the 3- and 4-coordinate nitrogen centres of diprotonated TMC with regard to the  $\text{Me}-\text{N}$  distances. Here the difference between the mean values is c.  $0.05 \text{ \AA}$ .

The two isomeric forms isolated for neutral TMC are neither *exo-* nor *endodentate*, but can be classified as *mesodentate*. The assumed lone pair directions are orthogonally oriented to each other, presumably to minimise electrostatic repulsions. Figure 4.12 illustrates the angles between the nitrogen lone pairs and the N - ring centroid direction. These are  $69.4^\circ$  ( $\text{N}_{11}$ ),

40.1° (N<sub>12</sub>), 85.5° (N<sub>11</sub>), and 17.0° (N<sub>22</sub>). For neutral cyclam, an endodentate geometry is adopted as a consequence of intramolecular hydrogen bonding by alternate amine centres. The remaining two amine hydrogen atoms form weak intermolecular interactions to yield a loosely associated polymeric chain structure.

Diprotonation of TMC yields an endodentate cation with an RRSS or RSSR configuration dependent upon the associated anion. The two hydrogen bonds, at alternate nitrogen atoms, are incorporated into six-membered rings with [H...N]<sup>+</sup> distances c. 2.2 Å. An additional [H...N]<sup>+</sup>, c. 2.7 Å, bifurcates the hydrogen contacts. A similar network of internal hydrogen bonds ([H...N]<sup>+</sup> 2.06 and 2.61 Å) is observed for diprotonated cyclam. It is apparent that the *trans* N-N distances are reduced to c. 4 Å as a result of the bifurcated intramolecular hydrogen bonding in diprotonated TMC and cyclam. By way of contrast, neutral TMC enjoys larger *trans* N-N distances (range 4.83 - 6.09 Å, mean 5.4 Å), i.e. there is a diminution of c. 1 Å in the macrocyclic cavity upon diprotonation.

Protonation of all four nitrogen atoms of cyclam causes the ring conformation to 'flip' from endodentate to exodentate with all NH<sub>3</sub><sup>+</sup> centres directed away from the macrocyclic cavity. Although the analogous tetraprotonated form of TMC has yet to be structurally characterised, it is likely to closely resemble the tetranuclear, exodentate complex with aluminium trimethyl.<sup>187</sup>



**Figure 4.12** Directionality of assumed nitrogen lone pairs in the mesodentate conformations of a) TMC (RSSR), and b) TMC (RRSS).

Table 4.9 Selected bond lengths (Å) of neutral and protonated TMC and cyclam structures.

Compound	Ring Geometry	[N-H] <sup>+</sup>	[H-N] <sup>+</sup>	trans N-N	Me-N (nm)		C-C (nm)		N-C <sub>eq</sub> (nm)		Ref.
					protonated	basic			protonated	basic	
cyclam	endo			4.020, 4.226			1.341			1.461	a
[H <sub>2</sub> cyclam](CO <sub>3</sub> ) <sub>2</sub>	endo	0.91, 0.99	2.06	3.96, 4.22			1.539	1.497	1.467		b
[H <sub>2</sub> cyclam]Cl <sub>2</sub>	exo	1.0		3.827, 4.493			1.511	1.499			a
[H <sub>2</sub> cyclam](ClO <sub>4</sub> ) <sub>2</sub>	exo			3.286, 5.459			1.520	1.505			c
[H <sub>2</sub> cyclam](NaClO <sub>4</sub> ) <sub>2</sub>	exo	1.0		3.221, 5.509			1.536	1.499			d
TMC (R155)	macro			5.097, 5.184			1.515			1.454	e
TMC (R155)	macro			4.326, 6.090			1.453	1.515		1.457	e
[H <sub>2</sub> TMC](AuO <sub>4</sub> Cl <sub>4</sub> ) <sub>2</sub>	endo	1.04	2.12, 2.61	4.031, 4.463	1.916	1.444	1.517	1.495		1.466	e
[H <sub>2</sub> TMC](SS-OC <sub>4</sub> ) <sub>2</sub>	endo	0.92	2.22, 2.75	4.275, 4.326	1.496	1.452	1.501	1.491		1.470	e

References a) <sup>28</sup>, b) <sup>29</sup>, c) <sup>30</sup> d) <sup>30</sup> e) this thesis.

## Molecular Modelling

**Table 4.10** Strain energy calculations ( $\text{kcal mol}^{-1}$ ) for the solid state isomers of TMC and its diprotonated cations.

Molecule	Sequential configuration	Experimental energy	Minimised energy	Distortion energy	RMS deviation /Å
TMC	RSSR (Trans IV)	36.31	33.21	3.10	0.045
TMC	RRSS (Trans III)	42.08	36.81	5.27	0.120
H <sub>2</sub> TMC	RSRS (Trans I)	74.98	60.56	14.42	0.491
H <sub>2</sub> TMC	RRSS (Trans III)	74.05	64.50	9.55	0.424
H <sub>2</sub> TMC	RRSS (Trans III)	73.68	63.95	9.73	0.453

The results of the calculations are given in Table 4.10. The experimental structures of the two forms of the neutral macrocycle show good agreement with the minimised energies. The RRSS isomer is lower in energy than the RSSR at both the experimental and minimised geometries. The energy difference is calculated to be 5.77 and 3.60  $\text{kcal mol}^{-1}$  respectively. This is consistent with the failure to observe an RSSR isomer of a TMC metal complex. The global minimum facilities in PCMODEL<sup>145</sup> failed to discover a minimum lower than those derived from the two independent molecules, the RRSS molecule must therefore be taken as the global minimum.

With regard to the diprotonated species, the two RRSS isomers have very similar conformations; a RMS deviation of just 0.104 Å exists between the non-hydrogen atoms of the two structures. This similarity is again witnessed in the strain energy calculations. Their distortion energy of c. 10 kcal mol<sup>-1</sup> can be considered a good fit.<sup>218</sup>

The N-H...N distances warrant comparison with those previously reported. In the case of the diprotonated TMC molecules these N...N distances varied between 2.78 and 2.91 Å. Reported examples incorporating the system [N...H...N]<sup>+</sup> include the cations hydrogen diquinclidinone<sup>211</sup> and hydrogen-3,6-dimethyl-1,6-diazacyclodecane.<sup>212</sup> Both have N...N separations of approximately 2.6 Å. These agreed well with the specimen molecules [Me<sub>2</sub>NH(CH<sub>2</sub>)<sub>5</sub>NMe<sub>2</sub>]<sup>+</sup> and [Me<sub>2</sub>N-H-NMe<sub>2</sub>]<sup>+</sup>, for which the MMX<sup>142</sup> force field finds minima at almost 2.5 Å. To probe the elongation of this distance with the diprotonated TMC molecules, the RSRS isomer of [H<sub>2</sub>TMC]<sup>2+</sup> was taken to explore the dependency of overall ring strain energy upon the H-bonded N...N separation. It is clear from Figure 4.13 that there is little change in strain energy from a N...N separation of 2.7 Å through to 3.1 Å.

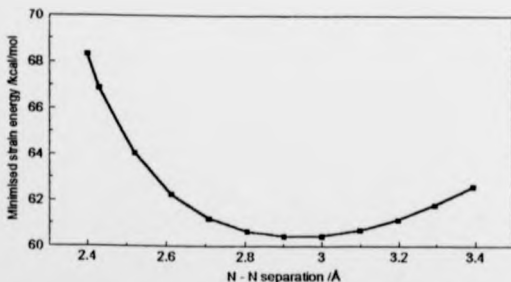


Figure 4.13 Strain energy v. H-bond N-N separation in RSRS [H<sub>2</sub>(TMC)]<sup>2+</sup>.

It has been noted that the diprotonated form of TMC has a cavity reduced by some 1 Å, as measured by the *trans* N-N distance, when compared to the free amine. The energetic penalty involved in distorting the macrocycle conformation to accommodate the intramolecular hydrogen bonding has been investigated. The two isomers of TMC were selected to contrast their differing stereochemistry. Fixing the *trans* N-N distance of RSSR TMC at 4.275 and 4.326 Å, as seen in the two RRSS diprotonated molecules, a distortion energy in excess of 40 kcal mol<sup>-1</sup> was calculated. Conversely, the reverse process of fixing the RRSS *trans* N-N distance at 5.097 and 5.384 Å, those of the RSSR isomer, lead to a distortion energy of just 0.86 kcal mol<sup>-1</sup>. Clearly, the RSSR form of TMC shows insufficient flexibility to adopt the smaller cavity whilst the RRSS form is able to freely alter its cavity size over a wide range.

## CONCLUSIONS

- 1) The initial adducts formed between TMC and  $MCl_3$  (where  $M = As, Sb, Bi$ ), appear to conform to a  $(TMC)_2(MCl_3)_3$  formulation. However, conclusive characterisation has been thwarted by the propensity of these species towards further, ill-defined hydrolysis.
- 2) Controlled hydrolysis of the adducts formed between TMC and  $MCl_3$  ( where  $M = As, Sb$ ) leads to oxychloro anions with a common  $[M_2OCl_4]^{2-}$  structural motif. Closely related anions have previously been isolated via a variety of reaction pathways.
- 3) The two, structurally characterised, compounds containing diprotonated TMC exhibit different sequential stereochemistries about the macrocyclic ring. The configuration chosen appears to be dependent upon the exact nature of the counter anion. Two bifurcated hydrogen bonds are present within the macrocyclic cavity.
- 4) The solid state structure of TMC comprises molecules of two different sequential stereochemistries. Molecular mechanical calculations indicate a difference in the strain energy between the two forms of up to  $5.77 \text{ kcal mol}^{-1}$ .



## EXPERIMENTAL

All reactions and manipulations were carried out as described in Chapter 2. Preparation of solvents and of the trivalent trihalides of arsenic, antimony and bismuth are also described in Chapter 2. Toluene was stored over sodium wire for 7 days prior to 24 h reflux over a sodium/potassium alloy. N-tetramethylcyclam was prepared following the procedure of Barefield and co-workers.<sup>213,214</sup>

**Synthesis of  $[H_2(TMC)][As_4O_2Cl_{10}]$** 

A solution of  $AsCl_3$  (0.14 g, 0.78 mmol) in toluene (20 cm<sup>3</sup>) was placed in a Schlenk vessel of narrow diameter under a dinitrogen atmosphere. A layer of acetonitrile (25 cm<sup>3</sup>) was added with minimal mixing of the layers. To this a solution of TMC (0.20 g, 0.78 mmol) was cautiously layered with minimum turbulence. Finally, whilst the reaction system was maintained under a closed dinitrogen atmosphere,  $H_2O$  (c. 0.03 g, 1.7 mmol) was added by syringe injection into the arm of the Schlenk vessel. Over a period of several days the product slowly deposited as a white, semi-crystalline solid which was collected, washed with *n*-hexane (3 x 20 cm<sup>3</sup>) and pumped *in vacuo*. With patience, a number of crystals, directly suitable for X-ray diffraction studies (0.048 g, 26%), were physically separated from the bulk product. M.p. c. 220 °C (decomp.). Anal. calc. for  $C_{14}H_{24}As_4Cl_{10}N_4O_2$ : C, 17.80; H, 3.63; N, 5.93%. Found: C, 18.12; H, 3.91; N, 6.11%. I.R. (CsI plates, nujol):  $\nu(AsCl)$  348 cm<sup>-1</sup>;  $\nu(As-O-As)$  755;  $\nu_{max}(N^+-H)$  2633 cm<sup>-1</sup>;  $\nu(\text{ligand})$  958, 1154, 1310, 1401 cm<sup>-1</sup>. Mass spec. *m/e* 256. During another experimental run, all efforts were made to provide strictly anhydrous conditions. The initial white precipitate was isolated within two minutes of formation. Anal. calc. for  $C_{28}H_{44}As_4Cl_4N_2$ : C, 31.82; H, 6.41; N, 10.60%. Found: C, 32.00; H, 6.57; N, 10.57%.

#### Synthesis of $[H_2(TMC)][Sb_2OCl_4]$

Following the procedure outlined for the compound  $[H_2(TMC)][As_2O_2Cl_4]$ , an acetonitrile solution of TMC (0.20 g, 0.78 mmol) was cautiously layered over a toluene solution of antimony trichloride (0.18 g, 0.78 mmol) in a narrow Schlenk and  $H_2O$  (c. 0.03 g, 1.7 mmol) allowed to diffuse into the closed dinitrogen atmosphere. Again crystals (0.034 g, 12%) directly suitable for X-ray diffraction studies were physically separated from the white, semi-crystalline bulk product. M.p. c. 210 °C (decomp.). Anal. calc. for  $C_{14}H_{34}Sb_2Cl_4N_4O$ : C, 23.01; H, 4.69; N, 7.67%. Found: C, 23.99; H, 5.21; N, 8.14%. I.R. (CsI plates, nujol):  $\nu(SbCl)$  315, 291  $cm^{-1}$ ;  $\nu(Sb-O-Sb)$  692;  $\nu_{max}(N^+-H)$  2667  $cm^{-1}$ ;  $\nu(\text{ligand})$  964, 1154, 1311, 1403  $cm^{-1}$ . Mass spec.  $m/e$  256

#### Reaction of TMC with bismuth trichloride

In the case of the heaviest group 15 congener no fully characterised product was isolated. As seen with the arsenic and antimony reactions, dropwise addition of a TMC solution to a solution containing bismuth trichloride (a variety of solvents were utilised) immediately deposited a flocculent white precipitate of variable, indeterminate composition. Techniques to augment partial hydrolysis and produce a homogeneous product, as used with arsenic and antimony trichloride, were unsuccessful. M.p. variable. Anal. calc. for  $C_{21}H_{48}BiCl_6N_4$ : C, 23.05; H, 4.65; N, 7.68%. Found: C, 23.23; H, 4.70; N, 7.71%. I.R. (CsI plates, nujol):  $\nu(BiCl)$  304  $cm^{-1}$ ;  $\nu_{max}(N^+-H)$  2658  $cm^{-1}$ ;  $\nu(\text{ligand})$  972, 1065, 1312, 1397  $cm^{-1}$ . Mass spec.  $m/e$  256.

Table 4.11 Crystallographic data for  $[H_2(TMC)][As_8O_2Cl_{10}]$ .

Formula	$[C_{14}H_{14}N_6][As_8O_2Cl_{10}]$
$M_r$	944.6
Crystal class	orthorhombic
Space group	Ibca
$a / \text{\AA}$	15.781(8)
$b / \text{\AA}$	17.898(8)
$c / \text{\AA}$	22.929(13)
$\alpha / ^\circ$	
$\beta / ^\circ$	
$\gamma / ^\circ$	
$V / \text{\AA}^3$	6476
$Z$	8
$D_x / \text{g cm}^{-3}$	1.94
Mo-K $\alpha$ radiation, $\lambda / \text{\AA}$	0.71069
$\mu (\text{Mo-K}\alpha) / \text{cm}^{-1}$	4.94
$T / \text{K}$	290
$F_{000}$	3984
Final R	0.043
Unique observed ( $I/\sigma(I) \geq 2.0$ ) reflections	1746

#### Crystal Structure determination of $[\text{H}_2(\text{TMC})][\text{As}_4\text{O}_3\text{Cl}_{10}]$

The colourless block crystals were mounted, under argon, in Lindemann capillaries. Data were collected with a Siemens R3m four circle diffractometer in  $\omega$ - $2\theta$  mode. Maximum  $2\theta$  was  $50^\circ$  with scan range  $\pm 0.7^\circ(\omega)$  around the  $K_{\alpha 1}$ - $K_{\alpha 2}$  angles, scan speed  $2.5\text{--}15^\circ(\omega) \text{ min}^{-1}$ , depending on the intensity of a 2s pre-scan; backgrounds were measured at each end of the scan for 0.25 of the scan time. The  $hkl$  ranges were: 0/18; 0/20; 0/27. Three standard reflections were monitored every 200 reflections, and showed a slight decrease (3%) during data collection. The data were rescaled to correct for this. Unit cell dimensions and standard deviations were obtained by least-squares fit to 19 reflections ( $2\theta < 28^\circ$ ). The 2872 reflections collected (all unique) were processed using profile analysis; 1746 were considered observed ( $I/\sigma(I) > 2.0$ ). These were corrected for Lorentz, polarization and absorption effects (the last by the Gaussian method); minimum and maximum transmission factors were 0.30 and 0.37. Crystal dimensions were  $0.28 \times 0.09 \times 0.38 \text{ mm}$ . The systematic reflection conditions  $hkl$ ,  $h+k+l = 2n$ ;  $OkI$ ,  $k = 2n$ ;  $hko$ ,  $h = 2n$ , indicate space group  $Ibca$ . The structure was solved by direct methods using SHELXTL (TREF) to locate two arsenic positions (and with hindsight several chlorine positions could have been located). The remaining atoms were then found by successive Fourier syntheses. The anion and cation both lie on two-fold axes. Anisotropic thermal parameters were used for all non-H atoms. Hydrogen atoms were given fixed isotropic thermal parameters,  $U = 0.08 \text{ \AA}^2$ . Those defined by the molecular geometry were inserted at calculated positions and not refined. Final refinement was on  $F$  by least squares methods refining 165 parameters. Largest positive and negative peaks on a final difference Fourier synthesis were of height  $\pm 0.5 \text{ e. \AA}^{-3}$ . A weighting scheme of the form  $W = 1/(\sigma^2(F) + gF^2)$  with  $g = 0.00056$  was used and shown to be satisfactory by a weight analysis. Final  $R = 0.043$ ,  $R_w = 0.051$ ,  $S = 1.31$ ;  $R_{\text{(all reflections)}} = 0.077$ . Maximum shift/error in final cycle was 0.09. Computing was conducted on a DEC Microvax-II using SHELXTL PLUS<sup>147</sup>. Scattering factors in the analytical form and anomalous dispersion factors were taken from reference 148.

Table 4.12 Crystallographic data for  $[H_2(TMC)][Sb_2OCl_4]$ .

Formula	$[C_{14}H_{14}N_4][Sb_2OCl_4]$
$M_r$	722.1
Crystal class	triclinic
Space group	P1
$a / \text{\AA}$	9.603(11)
$b / \text{\AA}$	12.091(11)
$c / \text{\AA}$	12.562(18)
$\alpha / ^\circ$	78.35(10)
$\beta / ^\circ$	72.09(8)
$\gamma / ^\circ$	71.35(5)
$V / \text{\AA}^3$	1311
$Z$	2
$D_c / \text{g cm}^{-3}$	1.94
Mo-K $\alpha$ radiation, $\lambda / \text{\AA}$	0.71069
$\mu (\text{Mo-K}\alpha) / \text{cm}^{-1}$	1.38
$T / \text{K}$	290
$F_{000}$	644
Final R	0.043
Unique observed ( $I/\sigma(I) \geq 2.0$ ) reflections	2782

### Crystal structure determination of $[H_2(TMC)][Sb_2OCl_4]$

A suitable crystal was mounted in a Lindemann capillary. Data were collected with a Siemens R3m four circle diffractometer in  $\omega$ - $2\theta$ . Maximum  $2\theta$  was  $45^\circ$  with scan range  $\pm 0.7^\circ(\omega)$  around the  $K_{\alpha 1}$ - $K_{\alpha 2}$  angles, scan speed was  $2.5$ - $15^\circ(\omega) \text{ min}^{-1}$ , depending on the intensity of a 2s pre-scan; backgrounds were measured at each end of the scan for 0.25 of the scan time. The  $hkl$  ranges were  $0/13$ ,  $-14/14$ ,  $-19/19$ . Three standard reflections were monitored every 200 reflections, and showed a slight decrease during data collection. The data were rescaled to correct for this. Unit cell dimensions and standard deviations were obtained by least-squares fit to 18 reflections ( $20 < 2\theta < 22^\circ$ ). The reflections collected were processed using profile analysis to give 3452 unique reflections ( $R_{\text{int}} = 0.0216$ ), of which 2782 were considered observed ( $I/\sigma(I) > 2.0$ ). These were corrected for Lorentz, polarization and absorption effects (by the Gaussian method); minimum and maximum transmission factors were 0.76 and 0.90. Crystal dimensions were  $0.35 \times 0.25 \times 0.12 \text{ mm}$ . No systematic reflection conditions indicate space group  $P1$  or  $P1$ .  $P1$  was chosen and deemed satisfactory by successful refinement. The structure was solved by direct methods using SHELXTL (TREF) to locate two Sb atoms. Remaining atoms were found by successive Fourier syntheses. The asymmetric unit contains two independent, centrosymmetric half-cations and one anion. Anisotropic thermal parameters were used for all non-H atoms. The unique proton of one cation was identified on a difference Fourier synthesis and its coordinates refined, that of the second cation was not located, possibly due to disorder between two positions. Other hydrogen atoms were given fixed isotropic thermal parameters,  $U = 0.08 \text{ \AA}^2$ , inserted at calculated positions and not refined. Final refinement was on  $F$  by least squares methods refining 244 parameters. Largest positive and negative peaks on a final difference Fourier synthesis were of height  $\pm 1.0 \text{ el. \AA}^3$ . A weighting scheme of the form  $W = 1/\sigma^2(F) + gF^2$  with  $g = 0.00052$  was used and shown to be satisfactory by a weight analysis. Final  $R = 0.043$ ,  $R_w = 0.045$ ,  $S = 1.7352$ ;  $R_{\text{int}} = 0.056$ . Maximum shift/error in final cycle was 0.036. Computing was conducted on a DEC Microvax-II using SHELXTL PLUS.<sup>147</sup> Scattering factors in the analytical form and anomalous dispersion factors taken from reference 148.

**Table 4.13** Crystallographic data for tetramethylcyclam.

Formula	$C_{14}H_{12}N_4$
$M_r$	256.4
Crystal class	triclinic
Space group	P1
$a / \text{\AA}$	8.467(4)
$b / \text{\AA}$	10.057(5)
$c / \text{\AA}$	10.637(5)
$\alpha / ^\circ$	67.68(3)
$\beta / ^\circ$	75.38(4)
$\gamma / ^\circ$	76.34(4)
$V / \text{\AA}^3$	800.75
$Z$	2
$D_x / \text{g cm}^{-3}$	1.06
Mo-K $\alpha$ radiation, $\lambda / \text{\AA}$	0.71069
$\mu_{\text{obs}}(\text{Mo-K}\alpha) / \text{cm}^{-1}$	0.6
$T / \text{K}$	260
$F_{\text{calc}}$	
Final R	0.047
Unique observed ( $I/\sigma(I) \geq 2.0$ ) reflections	2140

#### Crystal structure determination of tetramethylcyclam

Colourless block crystals were obtained from the melt and mounted, under dinitrogen, in a Lindemann capillary. Data were collected with a Siemens R3m four circle diffractometer in  $\omega$ - $2\theta$  mode. The crystal was held at 260 K with an Oxford Cryosystems Cryostream Cooler. Maximum  $2\theta$  was  $50.11^\circ$  with scan range  $\pm 0.7^\circ(\omega)$  around the  $K_{\alpha 1}$ - $K_{\alpha 2}$  angles, scan speed  $2.15^\circ(\omega) \text{ min}^{-1}$ , depending on the intensity of a  $2\theta$  pre-scan; backgrounds were measured at each end of the scan for 0.25 of the scan time. The hkl ranges were: -10/10, -11/11 -12/12. Three standard reflections were monitored every 200 reflections, and showed a slight decrease during data collection. The data were rescaled to correct for this. Unit cell dimensions and standard deviations were obtained by least-squares fit to 12 reflections ( $24 < 2\theta < 26^\circ$ ). The 3166 reflections collected were processed using profile analysis to give 2830 unique reflections ( $R_{\text{int}} = 0.0685$ ), of which 2140 were considered observed ( $I/\sigma(I) > 2.0$ ). These were corrected for Lorentz, polarization and absorption effects (the last by the Gaussian method); minimum and maximum transmission factors were 0.973 and 0.987. Crystal dimensions were  $0.17 \times 0.19 \times 0.40 \text{ mm}$ . No systematic reflection conditions indicate space group P1 or P1. P1 was chosen and deemed correct by successful refinement. The structure was solved by direct methods using SHELXTL (TREF). Refinement was by E-map expansion and successive Fourier syntheses. The structure consists of two independent, centrosymmetric molecules. Anisotropic thermal parameters were used for all non-H atoms. Hydrogen atoms were given fixed isotropic thermal parameters,  $U = 0.08 \text{ \AA}^2$ . Those defined by the molecular geometry were inserted at calculated positions and not refined. Final refinement was on F by least squares methods refining 291 parameters. Largest positive and negative peaks on a final difference Fourier synthesis were of height  $\pm 0.13 \text{ e. \AA}^{-3}$ . A weighting scheme of the form  $W = 1/(\sigma^2(F) + gF^2)$  with  $g = 0.00400$  was used and shown to be satisfactory by a weight analysis. Final  $R = 0.047$ ,  $R_w = 0.052$ ,  $S = 0.8945$ ;  $R_{\text{int}} = 0.070$ . Maximum shift/error in final cycle was 0.008. Computing was conducted on a DEC Microvax-II with SHELXTL PLUS<sup>147</sup>. Scattering factors in the analytical form and anomalous dispersion factors taken from reference 148.



## **CHAPTER FIVE**

### **STABILISATION OF ANHYDROUS GROUP 3 CATIONIC SPECIES BY OXAMACROCYCLIC LIGANDS**

## INTRODUCTION

These studies set out to investigate the applicability of antimony pentachloride as a halide abstraction agent with the pre-lanthanide trichlorides of scandium, yttrium and lanthanum. This would provide a direct route to anhydrous species with a pre-determined cationic charge. Oxygen crown ethers were used as a means of stabilising the cations formed, so permitting the isolation of charge separated, crown ether encapsulated lanthanide cations as crystalline solids.

### Antimony pentachloride as a halide abstraction agent

In the liquid phase, Raman spectroscopy<sup>215</sup> shows antimony pentachloride to enjoy a trigonal bipyramidal structure with the antimony atom somewhat displaced above the equatorial plane. In the gaseous phase the molecule exists as a monomeric, trigonal bipyramid,<sup>216</sup> with equatorial and axial bond lengths of 2.43 Å and 2.31 Å respectively. These distances correlate well with those of the crystal structure determination which found an equatorial bond length of 2.29 Å and an axial bond length of 2.34 Å.<sup>216</sup>

Antimony pentachloride is a voracious Lewis acid, seeking electron lone pairs from both neutral and ionic species. When reacted with other halides (both organic and inorganic), antimony pentachloride is often able to compete successfully with the resultant cation and fully remove the halide anion, thereby forming a hexahaloantimonate(V) salt. This capability for halide abstraction extends to the pseudohalide anions  $\text{CN}^-$ ,  $\text{N}_3^-$ ,  $\text{NCO}^-$ , and  $\text{NCS}^-$ .<sup>217</sup>

Groenwald has explored the halide abstraction potential of antimony pentachloride in the presence of many metal halides;

$MCl$  where  $M = Li, K, Rb, Cs, Ag, Au$ ; <sup>218</sup>

$MCl_2$  where  $M = Be, Mg, Ca, Cd, Mn, Fe, Co, Cu$ ; <sup>219</sup>

$MCl_3$  where  $M = Al, In, V, La, Fe, Ti, Bi$ ; <sup>220</sup>

The presence of a suitable donor solvent was found to be essential for stabilisation of the resulting cation. The suitability of acetonitrile is well established. Other solvents that have been used include pyridine, phosphorus oxychloride, nitromethane, various carbonyl ligands, and ethers. The, sometimes unique, ability of antimony pentachloride to abstract halide ions and form isolable salts is well illustrated by the range of titanium cations  $[TiCl_3(MeCN)_3]^{1+}$ , <sup>221</sup>  $[[TiCl(\mu-O)(12O4)]_2]^{2+}$ , <sup>222</sup>  $[TiCl_2(MeCN)_4]^{2+}$ , <sup>223</sup> and  $[cp^*Ti(MeCN)_3]^{1+}$ , <sup>224</sup> all characterised as the hexachloroantimonate(V) salts.

When antimony pentachloride is reacted with a halide-containing compound, three possible outcomes to the potential halide transfer reaction can be envisaged:

- 1) No reaction, the halide-containing compound fails to release a halide ion.
- 2) Partial transfer, the halide ion forms a bridge between the antimony and the other centre.
- 3) Halide transfer, formation of the hexahaloantimonate(V) salt.

Clearly, the prevailing result hinges upon the competition for halide ions between  $SbCl_5$  and the conjugate acid of the halide donor. This contest is influenced by several parameters:

1) Stability of the resultant cation.

*e.g.* With organic halo-compounds, halide abstraction only occurs where the concomitant organic cation is sufficiently stable *e.g.*  $\text{Ph}_2\text{CCl}$  and  $\text{Ph}_3\text{C}_3\text{Cl}$ .<sup>225, 226</sup>

For acid chlorides,  $\text{RCOCl}$ , halide abstraction was found where  $\text{R} = \text{Me}$  or  $\text{Me}_2\text{CH}$ , but adduct formation,  $\text{RCIC}=\text{O} \rightarrow \text{SbCl}_5$ , where  $\text{R} = \text{Et}$  or  $\text{Ph}$ .<sup>227, 228</sup>

2) Solvent used, solvation of the cation

*e.g.* The effect of the solvent used is seen in the reaction of antimony pentachloride and *p*-toluoyl chloride.<sup>229</sup> In carbon tetrachloride the adduct, with the carbonyl as electron pair donor, is formed. In chloroform, an ionic product is produced following halide transfer. Furthermore, dissolution of the adduct in  $\text{CHCl}_3$  allows isolation of the salt and *vice versa*.

3) Relative concentrations of the reactants

*e.g.* For the reaction of bismuth trichloride and magnesium chloride, the bismuth halide acceptor characteristics leading to chloride-bridged, polynuclear bismuth(III) species can be manipulated by adjustment of the reagent stoichiometry.<sup>230</sup>

The use of antimony pentachloride as a convenient route to cationic species suffers from two specific disadvantages:

- 1) Equilibrium - The possibility of a significant reverse reaction being established due to the abstracted halide remaining accessible to the cation formed.
- 2) Oxidation - Antimony in its fifth oxidation state is a potent oxidant.<sup>231</sup>

Other methods for removal of a halide ion include:

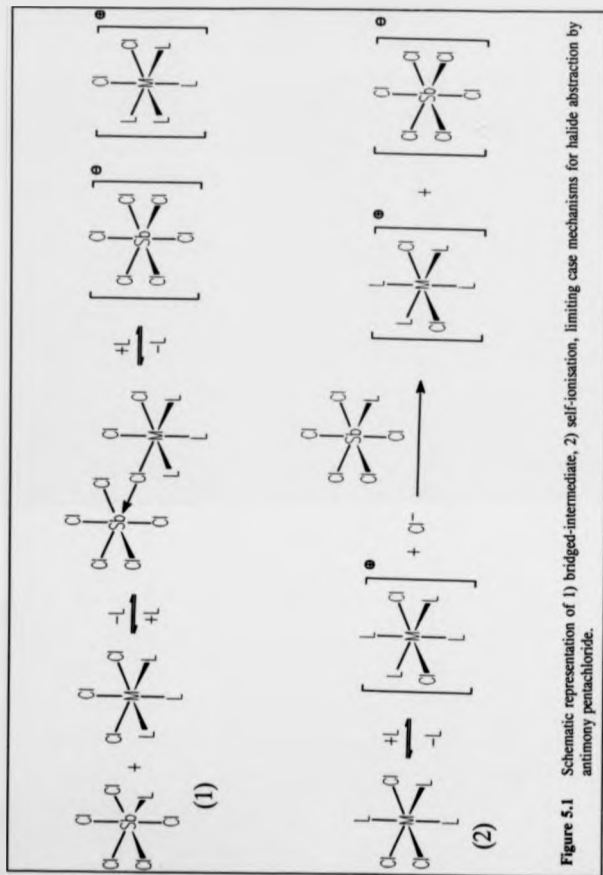
- 1) Reaction with  $\text{AgBPh}_4$ .
- 2) Reaction with  $\text{AgPF}_6$ .

These approaches avoid equilibria by precipitation of the halide ion as the silver salt. However, salts of the hexachloroantimonate ion often show greater hydrolytic and thermal stability, and are also significantly soluble in a wider range of organic solvents than other anions.<sup>254</sup>

### MECHANISM

Quantitative elucidation of the mechanistic pathway followed by the chloride abstraction reaction of antimony pentachloride has yet to be reported. However, it is possible to speculate upon the existence of two limiting cases as shown in Figure 5.1. The typical system modelled relates to a metal trichloride dissolved in acetonitrile. In this medium, solvent molecules coordinated to both the halide donor and the antimony centre are fully labile and of little consequence to the overall reaction.

- 1) **Bridged-Intermediate** - Here, the antimony-coordinated solvent ligand is replaced by a chloride that temporarily bridges the two Lewis acid centres. Cleavage of this bridged moiety moves the chloride ion onto the antimony molecule to form fully charge separated ions.
- 2) **Self-ionisation** - Loss of chloride ions by the halide donor may become significant if the, otherwise negligible, equilibrium reaction is perturbed. Removal of the free chloride ions from this system by the antimony would drive the self-ionisation reaction towards completion.



It may be, of course, that both routes are available and that the specific conditions peculiar to any given system, *e.g.* solvent, halide donor, co-ligands, temperature *etc.*, will allow one pathway to predominate. Alternatively, a hybrid mechanism could be preferred: It is apparent that the two schemes become equivalent in a concerted process where the halide donor *begins* to lose a chloride ion which is then taken up by the antimony.

### Lanthanide compounds containing oxygen crown ethers

Although a substantial lanthanide coordination chemistry exists with the crown ethers, existing complexes generally have water bound in some way, or they do not contain a metal-bound ligand which is easily replaceable by an organic group. This inhibits the use of these complexes as novel substrates for organometallic synthetic reactions. Preparation of anhydrous crown ether chloride complexes would facilitate entry into a novel organo-f-element chemistry. Rare Earth complexes with neutral macrocyclic ligands have been reviewed up to the end of 1983.<sup>232</sup>

Isolation of directly coordinated lanthanide chloride crown ether complexes has been described as less than straightforward.<sup>233</sup> A marked preference for coordination of water molecules or retention of the anion in the primary coordination sphere is displayed. The continued attachment to, even non-coordinating, anions is seen to good effect in the crystal structure of  $[\text{Eu}(\text{ClO}_4)(222)](\text{ClO}_4)_2$ .<sup>234</sup> Here the europium(III) ion is ten-coordinate, linked to the eight donor atoms of the cryptand and to two oxygen atoms of a perchlorate ion which reach into the cryptate cavity.

Lanthanide nitrates yield 1:1 complexes with 12O4, those of the larger ions (La(III) to Pr(III)) being hygroscopic. Reaction of 12O4 with hydrated europium nitrate produces the anhydrous, ten coordinate product  $[\text{Eu}(\text{NO}_3)_2(12\text{O}_4)]$ .<sup>233</sup> With the poorer donor perchlorate salts, 2:1 stoichiometries have been observed.<sup>238</sup> Hydrated lutetium trichloride and 12O4 yields the compound  $[\text{Lu}(\text{H}_2\text{O})_9]\text{Cl}_3 \cdot 1\frac{1}{2}(12\text{O}_4) \cdot 2\text{H}_2\text{O}$  with the crown hydrogen bonded to the coordinated water molecules.<sup>237</sup> In contrast, the hydrated europium trichloride forms  $[\text{Eu}(\text{H}_2\text{O})_9(12\text{O}_4)]\text{Cl}_3 \cdot 2\text{H}_2\text{O}$  with all ethereal oxygen atoms directly bound to the metal.<sup>238</sup>

Although direct coordination has been established for 12O4 and 18O6, only second-sphere, hydrogen bonded complexes of 15O5 with hydrated lanthanide trihalides have been isolated. Directly bound 15O5 complexes have been formed and structurally characterised under anhydrous conditions, e.g.  $[\text{Eu}(\text{NO}_3)_3(15\text{O}_5)]$ .<sup>239</sup> A study of 15O5 and hydrated samarium perchlorate found both complexed and hydrogen bonded polyethers in the same structure.<sup>240</sup>

Treatment of hydrated lanthanide nitrates with 18O6 in hot acetone has produced three types of analytically pure complex according to the stoichiometry and precise metal used. Structural determination has shown the complex  $[\text{Nd}(\text{NO}_3)_3(18\text{O}_6)]$  to involve coordination by all crown oxygen atoms, together with all three nitrate ions as bidentate chelators.<sup>241</sup> In the complex  $[\text{Gd}(\text{NO}_3)_3(\text{H}_2\text{O})_3] \cdot 18\text{O}_6$ , the crown is not coordinated to the metal ion but is linked to the  $[\text{Gd}(\text{NO}_3)_3(\text{H}_2\text{O})_3]$  molecule by O-HO bonds.<sup>242</sup> Metal bound 18O6 complexes of hydrated lanthanide chlorides are readily obtained using anhydrous solvent systems. Nevertheless, water molecules also remain in the primary coordination sphere, as seen for  $[\text{GdCl}(\text{H}_2\text{O})_5(18\text{O}_6)]\text{Cl}_2 \cdot 2\text{H}_2\text{O}$ .<sup>243</sup>



A Cambridge Structural Database survey of all crystallographically characterised crown ether complexes of the metals used in the present studies can be summarised thus:

#### Scandium

Only two examples of a crown ether-scandium(III) complex have been reported in the literature;  $\text{Sc}(\text{NO}_3)_3 \cdot 18\text{O}6 \cdot 3\text{H}_2\text{O}^{344}$  and  $\text{Sc}(\text{NO}_3)_3 \cdot \text{bz}15\text{O}5 \cdot 2\text{H}_2\text{O}^{345}$ . In both of these the scandium is held in proximity of the crown by hydrogen bonding involving coordinated water molecules.

#### Yttrium

Of the nine compounds reported, six involve direct association between the ether donor atoms and yttrium. Of this six, two are neutral species with tris-coordination by either thiocyanate or nitrate, and the other four cationic species have water molecules in the metal primary coordination sphere.

#### Lanthanum

Ten characterisations have been published involving lanthanum, and nine of these exhibited direct crown-metal binding. Eight of the characterisations comprised neutral molecules with coordination by three bidentate nitrate ions. The other two compounds proved to be cationic structures, both with water molecules bound to the lanthanum centre.

## RESULTS AND DISCUSSION

The anhydrous chlorides of scandium(III), yttrium(III), and lanthanum(III) have been used in the reaction system  $\text{MCl}_3/\text{SbCl}_5/\text{crown ether}/\text{MeCN}$ . Halide abstraction by antimony pentachloride has provided  $\text{MCl}_{3-n}^{n+}$  species ( $n = 1, 2, 3$ ) prior to a subsequent complexation reaction with polyoxamacrocycles. For those compounds isolated in the solid state, characterisation was effected by means of melting point, elemental analysis,  $^{13}\text{C}$  and  $^1\text{H}$  nuclear magnetic resonance, electronic absorption spectroscopy, and infra red spectroscopy. For three compounds, crystals suitable for X-ray diffraction were secured and two structures were satisfactorily refined. The results reported are summarised in Table 5.1.

**Table 5.1** Summary of reactions conducted between rare earth trichlorides, crown ethers and antimony pentachloride.

Cation*	1204	1505	bz1505	1806
$[\text{ScCl}_2]^+$	isolated and characterised	isolated and characterised - crystal structure part-determined	crystal structure determined	crystal structure determined
$[\text{ScCl}]^{2+}$	not detected	NMR evidence		NMR evidence
$\text{Sc}^{3+}$	not detected	NMR evidence		NMR evidence
$\text{Y}^{3+}$	isolated and characterised			isolated and characterised
$\text{La}^{3+}$	isolated and characterised			isolated and characterised

\* Solvation of 2+ and 3+ cations by acetonitrile molecules has been omitted for clarity.

### Reactions without crown ethers

Preliminary work endeavoured to secure the cationic species with just acetonitrile available to provide coordinative saturation. Although the generation of hexachloroantimonate salts was intimated by electronic and infra red spectroscopy, the acute sensitivity of these compounds to traces of air/moisture precluded the attainment of satisfactory elemental analyses. In the case of the reaction of scandium trichloride with one equivalent antimony pentachloride, clear, needle crystals were reproducibly isolable. Nevertheless, it proved impossible to prevent their decomposition once removed from the solvent, even when kept under moderate (Schlenk line) vacuum.

### Hydronium-crown ether complexes

Despite the apparent panacea of using oxygen crown ethers to surround the ionic species being prepared and thereby ameliorate their intense sensitivity, initial work was beset by the incursion of an unexpected side-product. The crown ethers are known to have an affinity for the hydronium ion.<sup>30a,367</sup> Regrettably, this surpasses that for the cationic metaño species under investigation. Initial recrystallisations of the reaction mixture produced the salt  $[H_3O(18O6)]^+ [SbCl_6]^-$  as beautiful pale yellow crystals. These were characterised by  $^1H$  NMR and elemental analysis. By repeated syntheses with increased diligence it was first possible to detect the presence of a crown complex in addition to that of the hydronium ion. This new species had an NMR signal, ascribed to the crown  $CH_2$  backbone, just 10% that of the crown-hydronium complex. Since the reaction had been conducted with every precaution to avoid the ingress of air/moisture, isolation of the crown ether-metal cation complex still appeared to be a formidable objective. Formation of the desired product with negligible contamination by hydronium species was eventually achieved using a *minimalist* approach; as little solvent as possible (*circa* 10 cm<sup>3</sup>), all reagents added directly to a single reaction vessel within a dinitrogen glove-box and recrystallisation directly from the reaction solvent, where possible. Application of these techniques has permitted synthesis of the required scandium, yttrium and lanthanum anhydrous, cationic crown ether complexes in high yield.

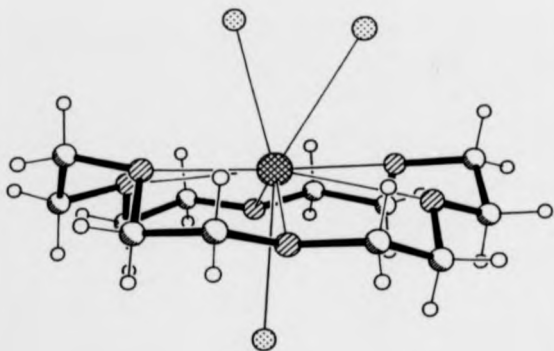
## 18-Crown-6 Complexes

Products were isolated using all three metal trichlorides as starting species. For scandium the nature of the monocationic compound was confirmed by a single crystal X-ray diffraction study. Evidence for di- and tri-cationic species is discussed under the section concerning NMR studies. For yttrium and lanthanum, reactions with one and two equivalents of antimony pentachloride failed to produce full dissolution of the anhydrous halide and were not pursued further. Use of four equivalents of antimony pentachloride lead to elemental analyses consistent with the formulation  $M \cdot (18O6) \cdot 3MeCN \cdot 3SbCl_5$ . By analogy with the reported structure of  $[La(18O6)(NO_3)_3]$ ,<sup>342</sup> a nine coordinate metal centre is postulated with equatorial hexa-coordination by the crown and the acetonitrile ligands occupying sites, two above and one below the mean  $O_6$  plane. This arrangement is illustrated in Figure 5.2.

### NMR Studies

#### 1) Room temperature

For the 3:1 yttrium and lanthanum complexes, the room temperature  $^1H$  and  $^{13}C$  spectra ( $CD_3CN$ ) show simple singlets, shifted downfield from those of the free ligand in the same medium. The downfield shift of the lanthanum complex,  $\delta$  4.06, compared to that reported for  $[La(18O6)(NO_3)_3]$ ,  $\delta$  3.80,<sup>342</sup> is in accordance with coordination by three nitrate ions in the latter compound. The same simple signal was observed for the 1:1 scandium complex. Treatment of scandium trichloride with two equivalents of antimony pentachloride produced a  $^1H$  spectrum showing a singlet at the same shift as that seen in the 1:1 spectrum, an AA'BB' multiplet centred somewhat downfield, and a further singlet moved further still downfield.



**Figure 5.2** Likely structure of the complexes  $[M(18O6)(MeCN)_3]^{3+}$ ,  $M = Y, La$  (donor nitrogen atoms only shown for MeCN molecules).

Although impaired by overlap of the signals, a crude estimate of the integral shows the singlet to multiplet to singlet ratio to be 1:2:1. The three singlets seen in the  $^{13}C$  spectrum confirm the presence of three species. A simple, single line spectrum, downfield from the 2:1 multiplet, returns for the 3:1 reaction. Figure 5.3 shows the  $^1H$  spectra obtained for the three reaction stoichiometries. These results can be rationalised by ascribing the sequential downfield shift to increasing formal charge on the scandium ion as further chloride ions are abstracted by antimony. In the case of the 2:1 reaction, a redistribution occurs such that for

every eight antimony atoms three are associated with a single  $[\text{Sc}(\text{18O6})]^{3+}$ , four are associated with two  $[\text{ScCl}(\text{18O6})]^{2+}$ , and one is associated with a single  $[\text{ScCl}_2(\text{18O6})]^+$  (additional acetonitrile ligands ignored for simplicity).

## 2) Low temperature

The X-ray structural determination (see next section) of  $[\text{ScCl}_2(\text{18O6})][\text{SbCl}_4]$  suggested that the simple singlet seen in the room temperature NMR spectrum of this compound might benefit from low temperature investigations. In particular, it might be expected that if penta-coordination is present in the solution state, then the energy barrier allowing time-averaged equivalence could become sufficient to make the process slow on the NMR timescale. Initial spectra run in  $\text{CD}_3\text{CN}$ , showed a noticeable broadening but no fragmentation of the single signal. Fortunately, sufficient of the compound could be dissolved in acetone- $d_6$  to access temperatures below 200K. The experiments found two, separate processes being slowed down sufficiently to allow resolution of individual resonances.

The first, shown in Figure 5.4, commences at approximately 235 K and involves a smaller peak moving upfield from the main signal. Integration suggests a 5:1 ratio. This feature is consistent with the ligand structure as determined by X-ray diffraction; coordination by five oxygen atoms leaves just four hydrogen atoms  $\beta$  to the excluded ether oxygen *i.e.* a 5:1 ratio. Non-coordination should result in an upfield shift, towards that of the free-ligand, for the  $\beta$ -hydrogen atoms, exactly as observed.



Figure 5.3  $^1\text{H}$  NMR spectra obtained by reaction of scandium(III) chloride/1806 with one, two and three equivalents antimony pentachloride.

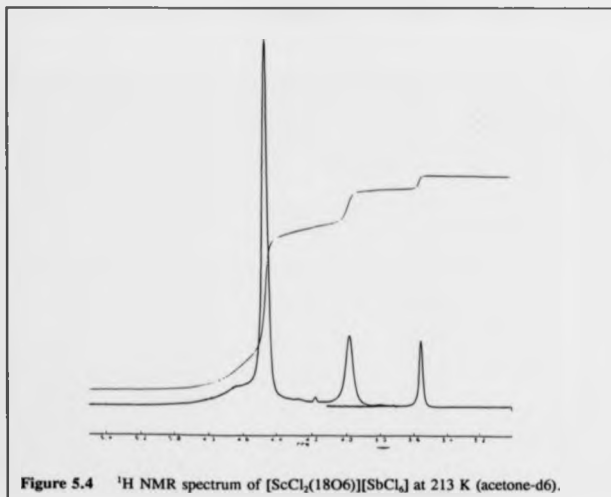
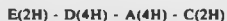
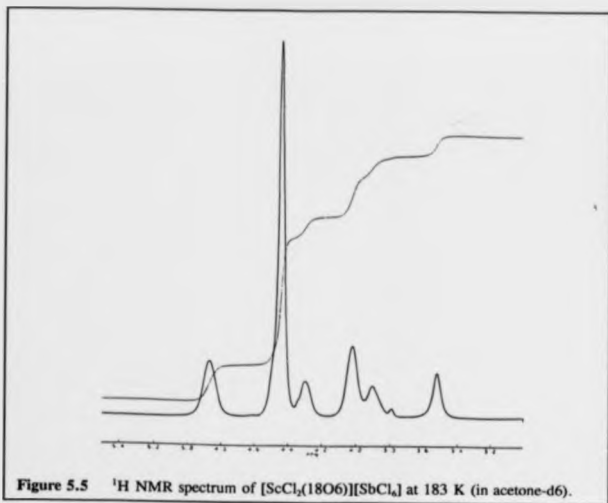


Figure 5.4  $^1\text{H}$  NMR spectrum of  $[\text{ScCl}_2(18\text{O}6)][\text{SbCl}_6]$  at 213 K (acetone- $d_6$ ).

The second, more complicated process yields five broadly resolved signals. Integration of these peaks suggests a ratio 4:12:2:4:2, designated A, B, C, D, E in Figure 5.5. In an effort to gain a deeper insight into the cause of this second separation, the Nuclear Overhauser Effect was sequentially applied. This determined that the hydrogen atoms producing the signals were oriented in space such that their relative positions can be represented as (relative intensity in brackets):







Unexpectedly, signal B(12H) was found not to be in the proximity of the others. This allows for the possibility that there may be more than one independent species present in solution, interconverting above 200 K. In view of the difficulties associated with conducting sophisticated NMR experiments at low temperature and at low concentration, the exact nature of the solution state species present remains undecided.

### Molecular structure of $[\text{ScCl}_2(18\text{O}6)][\text{SbCl}_4]$

The structure of this compound comprises discrete scandium cations  $[\text{ScCl}_2(18\text{O}6)]^+$  and  $\text{SbCl}_4^-$  counteranions. Two crystallographically independent molecules are present although the slight variations in bond lengths and angles are without chemical significance. The structure of the cation (molecule 1) is shown in Figure 5.6, bond lengths and angles in Table 5.2. The anions exhibit almost regular octahedral geometry with Sb-Cl (mean) 2.339 Å,  $\angle \text{Cl-Sb-Cl}$  (mean) 90.0 and 178.8°. The two important, gross structural features of the cation are:

- 1) A linear  $\text{ScCl}_2^+$  unit has been threaded through the crown cavity.
- 2) Only five of the ethereal oxygen atoms coordinate to the scandium cation.

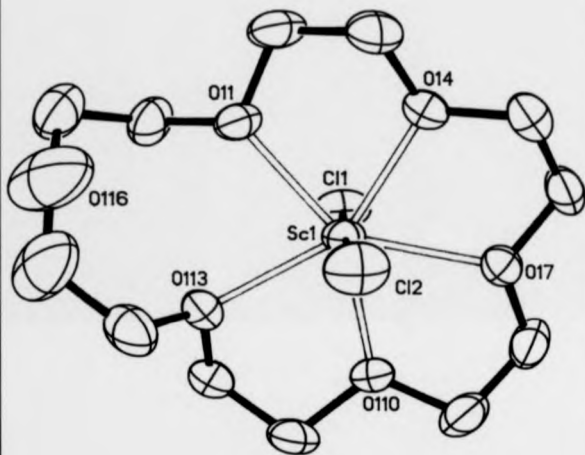
The five coordinated oxygen atoms define a plane with deviations of +0.051, -0.145, +0.070, -0.150, +0.174 Å. The scandium atom lies in this plane with a deviation of just 0.005 Å and metal-oxygen bond lengths in the range 2.190-2.229 Å. The  $\text{ScCl}_2^+$  unit is nearly linear with  $\angle \text{Cl-Sc-Cl}$  176.5(1)° and lies perpendicular to the  $\text{O}_5$  plane. This yields a close-to-ideal pentagonal bipyramidal coordination geometry about scandium. The flexibility of the aliphatic macrocycle is highlighted by its 'shrink-wrapping' of the scandium ion in the present structure.<sup>24</sup> The constriction of its effective cavity no doubt enables improved bonding by the coordinating oxygen atoms. However, the Sc-O bond lengths display no discernable shortening and appear to be unexceptional.<sup>25</sup> The excluded oxygen atom lies well outside the  $\text{O}_5$  mean plane (1.30 Å) and, with Sc-O separation of 4.137 Å, is clearly not involved in metal coordination. The segment of the ring containing the scandium-bonded oxygen atoms adheres to the usual symmetric *crown* conformation with all *gauche* O-C-C-O dihedral angles (range 49.7 - 55.1°) and *anti* C-O-C-C (range 164.5-178.8°). For the

irregular section of the ring, torsion angles involving the non-coordinated oxygen, *e.g.* 76.9, 113.4, 67.1 and 108.1° for O116, give an insight into the extent of distortion.

Comparison with the magnesium(II) complex of 18O6 is warranted ( $\text{Sc}^{3+}$  and  $\text{Mg}^{2+}$  are isoelectronic and have six-coordinate ionic radii of 88.5 and 86.0 Å respectively<sup>249</sup>). In  $[\text{MgCl}_2(18\text{O}6)]$ ,<sup>250</sup> the macrocycle adopts a similarly unsymmetrical conformation to bind the metal in a pentadentate, pseudo-coplanar array (Mg-O 2.15-2.33 Å). The sixth oxygen enjoys a non-bonded position some 4.4 Å from the magnesium atom. The hydrated sodium thiocyanate complex of 18O6 again displays a pentagon of five oxygen atoms around the metal ion. However, the sodium ion maintains coordination with the remaining oxygen atom by utilising an axial site. The resultant pseudo pentagonal bipyramidal structure is completed with a coordinated water molecule.

The present structure provides only the third example of a seven coordinate scandium(III) species. The previous examples are  $[\text{Sc}(\text{dapac})(\text{H}_2\text{O})_2][\text{NO}_3]_2[\text{OH}]$ , mean Sc-O 2.110 Å [dapac = 2,6-diacetylpyridine bis(semicarbazone)],<sup>251</sup> and  $[(\text{H}_2\text{O})_3\text{Sc}(\mu\text{-OH})_2\text{Sc}(\text{H}_2\text{O})_2][\text{C}_6\text{H}_5\text{SO}_3]_4 \cdot 4\text{H}_2\text{O}$  ( $\text{C}_6\text{H}_5\text{SO}_3^-$  = benzenesulfonate anion),<sup>252</sup> mean Sc-O ( $\text{H}_2\text{O}$ ) axial 2.146, equatorial 2.227 and Sc-O (OH bridge) 2.072 Å.

The Sc-Cl bond distances, 2.402(3) and 2.418(3) Å, are similar to those in  $[\text{ScCl}_2(\text{THF})_2]$  (mean 2.41)<sup>253</sup> and so appear unaffected by the formal charge residing on the scandium ion in the current structure.



**Figure 5.6** Molecular structure of the cation  $[\text{ScCl}_2(18\text{O}6)]^+$  (molecule 1).

**Table 5.2** Bond lengths (Å) and angles (°) for  $[\text{SbCl}_6(18\text{O}6)]/[\text{SbCl}_4]$ .

TABLE 2. Seed lengths ( $\mu$ )

SH(1)-(C11)	2.339(5)	SH(1)-(C12)	2.270(4)
SH(1)-(C12)	2.332(5)	SH(1)-(C14)	2.245(5)
SH(1)-(C14)	2.332(5)	SH(1)-(C15)	2.281(4)
SH(2)-(C21)	2.344(3)	SH(2)-(C22)	2.307(4)
SH(2)-(C22)	2.322(3)	SH(2)-(C23)	2.346(4)
SH(2)-(C23)	2.346(3)	SH(2)-(C24)	2.337(3)
SH(3)-(C31)	2.346(3)	SH(3)-(C32)	2.337(3)
SH(3)-(C32)	2.337(3)	SH(3)-(C33)	2.341(3)
SH(3)-(C33)	2.341(3)	SH(3)-(C34)	2.341(3)
SH(4)-(C41)	2.221(5)	SH(4)-(C42)	2.410(5)
SH(4)-(C42)	2.221(5)	SH(4)-(C43)	2.410(5)
SH(4)-(C43)	2.221(5)	SH(4)-(C44)	2.410(5)
SH(4)-(C44)	2.221(5)	SH(4)-(C45)	2.410(5)
SH(4)-(C45)	2.221(5)	SH(4)-(C46)	2.410(5)
SH(4)-(C46)	2.221(5)	SH(4)-(C47)	2.410(5)
SH(4)-(C47)	2.221(5)	SH(4)-(C48)	2.410(5)
SH(4)-(C48)	2.221(5)	SH(4)-(C49)	2.410(5)
SH(4)-(C49)	2.221(5)	SH(4)-(C50)	2.410(5)
SH(4)-(C50)	2.221(5)	SH(4)-(C51)	2.410(5)
SH(4)-(C51)	2.221(5)	SH(4)-(C52)	2.410(5)
SH(4)-(C52)	2.221(5)	SH(4)-(C53)	2.410(5)
SH(4)-(C53)	2.221(5)	SH(4)-(C54)	2.410(5)
SH(4)-(C54)	2.221(5)	SH(4)-(C55)	2.410(5)
SH(4)-(C55)	2.221(5)	SH(4)-(C56)	2.410(5)
SH(4)-(C56)	2.221(5)	SH(4)-(C57)	2.410(5)
SH(4)-(C57)	2.221(5)	SH(4)-(C58)	2.410(5)
SH(4)-(C58)	2.221(5)	SH(4)-(C59)	2.410(5)
SH(4)-(C59)	2.221(5)	SH(4)-(C60)	2.410(5)
SH(4)-(C60)	2.221(5)	SH(4)-(C61)	2.410(5)
SH(4)-(C61)	2.221(5)	SH(4)-(C62)	2.410(5)
SH(4)-(C62)	2.221(5)	SH(4)-(C63)	2.410(5)
SH(4)-(C63)	2.221(5)	SH(4)-(C64)	2.410(5)
SH(4)-(C64)	2.221(5)	SH(4)-(C65)	2.410(5)
SH(4)-(C65)	2.221(5)	SH(4)-(C66)	2.410(5)
SH(4)-(C66)	2.221(5)	SH(4)-(C67)	2.410(5)
SH(4)-(C67)	2.221(5)	SH(4)-(C68)	2.410(5)
SH(4)-(C68)	2.221(5)	SH(4)-(C69)	2.410(5)
SH(4)-(C69)	2.221(5)	SH(4)-(C70)	2.410(5)
SH(4)-(C70)	2.221(5)	SH(4)-(C71)	2.410(5)
SH(4)-(C71)	2.221(5)	SH(4)-(C72)	2.410(5)
SH(4)-(C72)	2.221(5)	SH(4)-(C73)	2.410(5)
SH(4)-(C73)	2.221(5)	SH(4)-(C74)	2.410(5)
SH(4)-(C74)	2.221(5)	SH(4)-(C75)	2.410(5)
SH(4)-(C75)	2.221(5)	SH(4)-(C76)	2.410(5)
SH(4)-(C76)	2.221(5)	SH(4)-(C77)	2.410(5)
SH(4)-(C77)	2.221(5)	SH(4)-(C78)	2.410(5)
SH(4)-(C78)	2.221(5)	SH(4)-(C79)	2.410(5)
SH(4)-(C79)	2.221(5)	SH(4)-(C80)	2.410(5)
SH(4)-(C80)	2.221(5)	SH(4)-(C81)	2.410(5)
SH(4)-(C81)	2.221(5)	SH(4)-(C82)	2.410(5)
SH(4)-(C82)	2.221(5)	SH(4)-(C83)	2.410(5)
SH(4)-(C83)	2.221(5)	SH(4)-(C84)	2.410(5)
SH(4)-(C84)	2.221(5)	SH(4)-(C85)	2.410(5)
SH(4)-(C85)	2.221(5)	SH(4)-(C86)	2.410(5)
SH(4)-(C86)	2.221(5)	SH(4)-(C87)	2.410(5)
SH(4)-(C87)	2.221(5)	SH(4)-(C88)	2.410(5)
SH(4)-(C88)	2.221(5)	SH(4)-(C89)	2.410(5)
SH(4)-(C89)	2.221(5)	SH(4)-(C90)	2.410(5)
SH(4)-(C90)	2.221(5)	SH(4)-(C91)	2.410(5)
SH(4)-(C91)	2.221(5)	SH(4)-(C92)	2.410(5)
SH(4)-(C92)	2.221(5)	SH(4)-(C93)	2.410(5)
SH(4)-(C93)	2.221(5)	SH(4)-(C94)	2.410(5)
SH(4)-(C94)	2.221(5)	SH(4)-(C95)	2.410(5)
SH(4)-(C95)	2.221(5)	SH(4)-(C96)	2.410(5)
SH(4)-(C96)	2.221(5)	SH(4)-(C97)	2.410(5)
SH(4)-(C97)	2.221(5)	SH(4)-(C98)	2.410(5)
SH(4)-(C98)	2.221(5)	SH(4)-(C99)	2.410(5)
SH(4)-(C99)	2.221(5)	SH(4)-(C100)	2.410(5)
SH(4)-(C100)	2.221(5)	SH(4)-(C101)	2.410(5)
SH(4)-(C101)	2.221(5)	SH(4)-(C102)	2.410(5)
SH(4)-(C102)	2.221(5)	SH(4)-(C103)	2.410(5)
SH(4)-(C103)	2.221(5)	SH(4)-(C104)	2.410(5)
SH(4)-(C104)	2.221(5)	SH(4)-(C105)	2.410(5)
SH(4)-(C105)	2.221(5)	SH(4)-(C106)	2.410(5)
SH(4)-(C106)	2.221(5)	SH(4)-(C107)	2.410(5)
SH(4)-(C107)	2.221(5)	SH(4)-(C108)	2.410(5)
SH(4)-(C108)	2.221(5)	SH(4)-(C109)	

TABLE 3. Bond angles (deg.)

01121	011013	01101	870.4621	011011	011011	01101	870.1172
01122	011013	011013	872.4621	011012	011013	01101	870.1172
01123	011013	011013	874.4621	011013	011013	01101	870.1172
01124	011013	011013	876.4621	011014	011013	01101	870.1172
01125	011013	011013	878.4621	011015	011013	01101	870.1172
01126	011013	011013	880.4621	011016	011013	01101	870.1172
01127	011013	011013	882.4621	011017	011013	01101	870.1172
01128	011013	011013	884.4621	011018	011013	01101	870.1172
01129	011013	011013	886.4621	011019	011013	01101	870.1172
01130	011013	011013	888.4621	011020	011013	01101	870.1172
01131	011013	011013	890.4621	011021	011013	01101	870.1172
01132	011013	011013	892.4621	011022	011013	01101	870.1172
01133	011013	011013	894.4621	011023	011013	01101	870.1172
01134	011013	011013	896.4621	011024	011013	01101	870.1172
01135	011013	011013	898.4621	011025	011013	01101	870.1172
01136	011013	011013	900.4621	011026	011013	01101	870.1172
01137	011013	011013	902.4621	011027	011013	01101	870.1172
01138	011013	011013	904.4621	011028	011013	01101	870.1172
01139	011013	011013	906.4621	011029	011013	01101	870.1172
01140	011013	011013	908.4621	011030	011013	01101	870.1172
01141	011013	011013	910.4621	011031	011013	01101	870.1172
01142	011013	011013	912.4621	011032	011013	01101	870.1172
01143	011013	011013	914.4621	011033	011013	01101	870.1172
01144	011013	011013	916.4621	011034	011013	01101	870.1172
01145	011013	011013	918.4621	011035	011013	01101	870.1172
01146	011013	011013	920.4621	011036	011013	01101	870.1172
01147	011013	011013	922.4621	011037	011013	01101	870.1172
01148	011013	011013	924.4621	011038	011013	01101	870.1172
01149	011013	011013	926.4621	011039	011013	01101	870.1172
01150	011013	011013	928.4621	011040	011013	01101	870.1172
01151	011013	011013	930.4621	011041	011013	01101	870.1172
01152	011013	011013	932.4621	011042	011013	01101	870.1172
01153	011013	011013	934.4621	011043	011013	01101	870.1172
01154	011013	011013	936.4621	011044	011013	01101	870.1172
01155	011013	011013	938.4621	011045	011013	01101	870.1172
01156	011013	011013	940.4621	011046	011013	01101	870.1172
01157	011013	011013	942.4621	011047	011013	01101	870.1172
01158	011013	011013	944.4621	011048	011013	01101	870.1172
01159	011013	011013	946.4621	011049	011013	01101	870.1172
01160	011013	011013	948.4621	011050	011013	01101	870.1172
01161	011013	011013	950.4621	011051	011013	01101	870.1172
01162	011013	011013	952.4621	011052	011013	01101	870.1172
01163	011013	011013	954.4621	011053	011013	01101	870.1172

[illegible]

## Pentaoxamacrocyclic complexes

### Introduction

After elucidating the structure of  $[\text{ScCl}_2(18\text{O}6)]^+$ , curiosity was aroused regarding the nature of the cation  $[\text{ScCl}_2(15\text{O}5)]^+$ . Would the almost regular pentagonal bipyramidal metal geometry persist, or would other factors come into play? The type of macrocycle studied was then extended to include an aromatic functionalisation. Some trepidation was initially warranted; the oxidising power of antimony(V) has previously been used to generate cation radicals formed from aromatic hydrocarbons.<sup>254</sup> Indeed, following this work with scandium(III), preliminary studies using halide donors from other groups seem to indicate that the success within group III may not enjoy general applicability.<sup>255</sup>

### Results and Discussion

The 1:1 compounds  $[\text{ScCl}_2(\text{L})][\text{SbCl}_4]$  ( $\text{L} = 15\text{O}5$  and  $\text{Bz}15\text{O}5$ ) were isolated in the solid state as crystalline materials. The spectroscopic analyses were consistent with the formulation derived from elemental analysis. When formed as crystals these compounds proved impervious to brief exposure to the open atmosphere. Solution state manipulation was, as usual, hampered by the ready formation of the hydronium-crown ether complex. The compound prepared with 15O5 was treated with one and two additional equivalents of antimony pentachloride with a view to detecting species of higher cationic charge. As suggested by the yellow colour of  $[\text{ScCl}_2(\text{Bz}15\text{O}5)][\text{SbCl}_4]$ , the u.v./visible spectrum of this compound shows a tailing into the visible region. In the light of subsequent crystallographic evidence, it may be that this absorption is a consequence of a chlorine-aromatic ring  $n \rightarrow \pi^*$  interaction.

## NMR studies

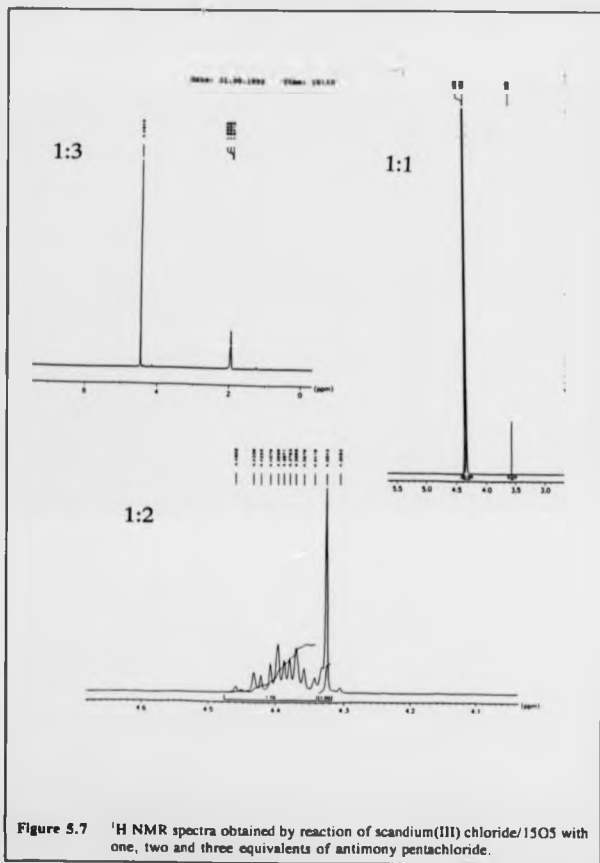
### 1) 15-crown-5

The room temperature  $^1\text{H}$  and  $^{13}\text{C}$  spectra ( $\text{CD}_3\text{CN}$ ) were simple singlets, shifted downfield from those of the free ligand in the same medium. In contrast to the results obtained with 18O6, a singlet persisted in the  $^1\text{H}$  spectrum even down to 177K (acetone- $d_6$ ). This is commensurate with all oxygen atoms being engaged in metal coordination, and hence minimal energy barriers between the ligand conformers.

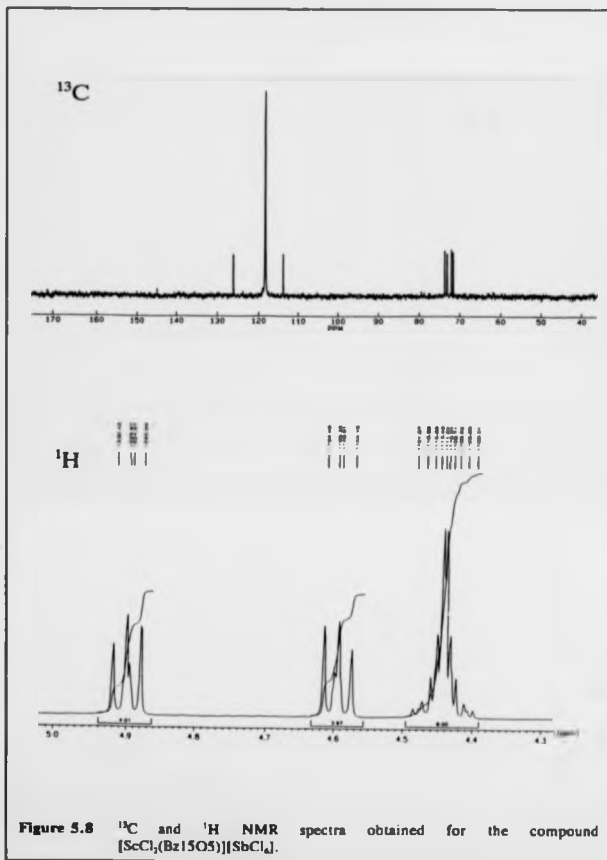
Treatment of scandium trichloride with two and three equivalents of antimony pentachloride produced results directly analogous to those reported with 18O6. The 2:1 reaction yields a  $^1\text{H}$  spectrum showing a singlet at the same shift as that seen in the 1:1 spectrum and an AA'BB' multiplet somewhat downfield from the singlet. Integration shows the singlet to multiplet ratio to be 1:1.7. The two singlets seen in the  $^{13}\text{C}$  spectrum confirm the presence of two species. In contrast to the 18O6 2:1 spectrum, no further singlet is in evidence. A simple, single line spectrum, downfield from the 2:1 multiplet, returns for the 3:1 reaction. Figure 5.7 shows the  $^1\text{H}$  spectra obtained for the three reaction stoichiometries.

### 2) Bz15-crown-5

Room temperature spectra have been run for this compound in  $\text{CD}_3\text{CN}$  (see Figure 5.8). The  $^1\text{H}$  spectrum comprises a singlet for the aromatic protons and two AA'BB' multiplets. The 1:2:2 integration is compatible with the expected ratio, assuming a mirror plane runs through the molecule. It may be observed that one independent AA'BB' system has an A B separation of approximately  $\delta$  0.3, whilst the other separation is just  $\delta$  0.005. The  $^{13}\text{C}$  spectrum is consistent with this interpretation; four signals around  $\delta$  70, and three signals, one very weak, in the aromatic region of the spectrum.

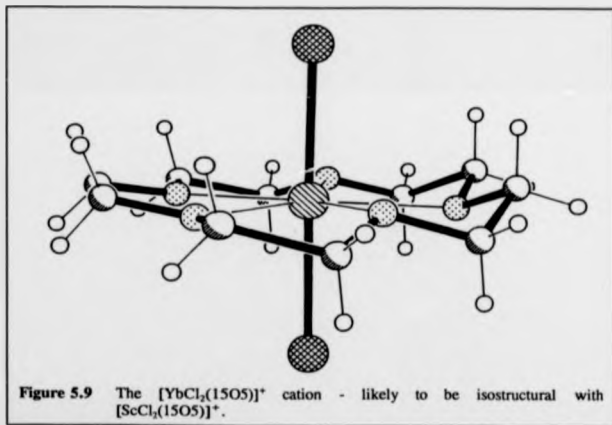






# MOLECULAR STRUCTURE OF $[\text{ScCl}_2(1505)][\text{SbCl}_6]$

The growth of excellent diffraction quality crystals and the collection of a high quality data set bode well for the solution of this structure. Unfortunately, progress to-date has been symied by the high symmetry space group,  $P4_2c$ , and the location of the antimony and scandium atoms on sites of symmetry 222 and 4. Clearly, high disorder of the macrocyclic ring is required to exist around the scandium. At the current level of refinement,  $R = 0.22$ , the scandium atoms have been found to conform to a linear  $\text{ScCl}_2^+$  group. The remaining electron density is radially distributed, normal to the  $\text{Sc-Cl}$  vector, at a distance of  $2.1-2.2$  Å from the scandium atom. It is doubtful whether further work, *e.g.* use of a rigid 1505 group as a model for determination of partial occupancy, will proved meaningful  $\text{Sc-O}$  bond distances.



A structure exhibiting the pentagonal bipyramidal linear  $\text{MCl}_2^+/\text{O}_5$  crown ether topology has been reported, where  $\text{M}$  = ytterbium,<sup>25a</sup> and is shown in Figure 5.9 This serves to confirm the stability of the pentagonal bipyramidal structural motif. Consideration of the relevant ionic radii<sup>17b, 24b</sup> (see Table 5.3 ) indicates that analogous complexes may only be accessible to yttrium and lanthanum with displacement of the metal out of the  $\text{O}_5$  plane.

**Table 5.3** Ionic radius comparison (Å) for  $\text{M}^{3+}$  ( $\text{M}$  = Sc, Y, La, Yb).

Metal	Coordination number		
	6	7	8
Sc	0.86		1.01
Yb	1.01	1.07	1.13
Y	1.04	1.10	1.16
La	1.17	1.24	1.30

## MOLECULAR STRUCTURE OF $[\text{ScCl}_2(\text{Bz15O5})][\text{SbCl}_4]$

Transfer of a chloride ion from scandium trichloride to antimony pentachloride has produced the compound  $[\text{ScCl}_2(\text{Bz15O5})][\text{SbCl}_4]$ , comprising discrete, mono-charged ions. Two views of the cation structure are shown in Figure 5.10 and Figure 5.11, bond lengths and angles are given in Table 5.3. The octahedral geometry adopted by the hexachloroantimonate anion is close to ideal, Sb-Cl (mean) 3.335 Å,  $\angle$  Cl-Sb-Cl (mean) 90.0 and 178.7° (mean). Inexplicably, refinement of the anion left just Cl5 with an unusually large  $U_{11}$  thermal parameter. The thermal ellipsoids shown in Figure 5.12 serve to visualise this irregularity. The most notable feature of the cation is the threading through the crown cavity of an almost linear  $\text{ScCl}_2^+$  moiety exactly as seen in the analogous complex with 18-crown-6. All ethereal oxygen atoms are coordinated to the scandium ion, in a regular fashion, Sc-O (mean) 2.19 Å. The scandium sits in the  $\text{O}_5$  mean plane (just 0.008 Å displacement) and with chloride ions assuming a coordination site above and below this plane, a regular pentagonal bipyramidal geometry is adopted about the metal ion (see Figure 5.11). The ion conforms to a pseudo mirror symmetry about the plane running through O7, Sc1, Cl7 and the aromatic ring centroid. The dihedral angle defined by these four centres is 179.8°.

Viewing the cation parallel to the  $\text{O}_5$  mean plane it is immediately apparent that the benzene ring is markedly tilted towards one of the chlorine atoms. The interplanar angle of 24.9° is noticeably larger than that seen in other Bz15O5 complexes, e.g.  $[\text{Ca}(\text{NCS})_2(\text{Bz15O5})(\text{MeOH})]$ , 6°;  $[\text{Ca}(\text{NCS})_2(\text{Bz15O5})(\text{H}_2\text{O})]$ , 7°;  $[\text{Hg}(\text{NCS})_2(\text{Bz15O5})]$ , 22°. <sup>297</sup> It is possible to consider this in terms of an  $n \rightarrow \pi^*$  interaction between the chlorine atom and the aromatic ring. Further geometric parameters that can aid this interpretation are:

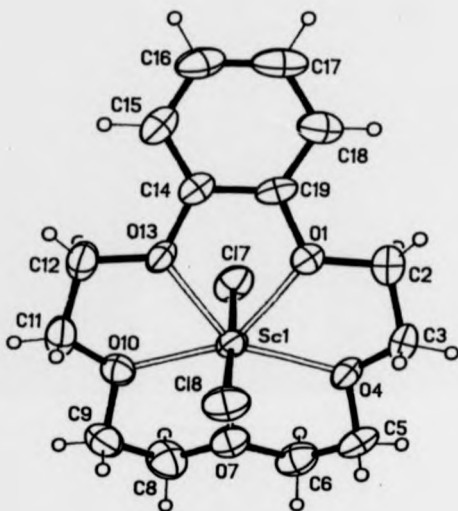
- 1) The chlorine atom, Cl7, is at a distance from the aromatic carbon atoms ranging from 3.444 to 5.081 Å.
- 2) The benzene ring centroid lies at a distance of 4.408 Å from chlorine atom Cl7.
- 3) Although chlorine atom Cl8 is almost normal to the O<sub>3</sub> plane (89.0°), Cl7 is slightly tilted towards the aromatic ring and lies at an angle of 86.3° to the mean ethereal plane.

Within the macrocycle, bond lengths and angles are similar to those observed in other such complexes. The usual shortening of the aliphatic C-C bond lengths, compared to the standard value of 1.524 Å is apparent.<sup>218</sup> Similar aliphatic C-C bond lengths were reported for the crystal structure of Bz15O5 conducted at 123 K.<sup>239</sup> The retention of significant atomic mean-square amplitudes of vibration at this low temperature enforces the possibility that the apparent C-C shortening is due to librational motion. The regular conformation of the macrocycle in the present complex exhibits aliphatic O-C-C-O torsion angles in the range 49.4-51.6. These are somewhat reduced from an 'ideal' *gauche* angle of 60° but may permit improved binding to the metal ion. The C-O-C-C torsion angles, mean 174.1, comply well with the *anti* preference often manifest by oxacrowns.

The five ether oxygen atoms closely define a plane (maximum deviation 0.078 Å) with a slight ripple effect upon passing from O7 back to the aromatic ring. The scandium ion is very slightly displaced away from the O<sub>3</sub> centroid by 0.033 Å. Consideration of the individual metal-oxygen distances confirms a small displacement of the scandium away from the two oxygen atoms nearest to the aromatic ring. This phenomenon is also seen in the compound [Mg(NCS)<sub>2</sub>(Bz15O5)] where, again, the metal ion is slightly displaced away from the aromatic end of the equatorially oriented macrocycle.<sup>217</sup>

The two carbon atoms, C14 and C19, forming the bridgehead between the aromatic and aliphatic rings of the macrocycle show somewhat irregular bond angles. The angles internal to the benzene ring are close to the expected  $120^\circ$ , however the two associated oxygen atoms are drawn together so increasing the exocyclic angle about C19 and C14 to a mean value of  $124.1^\circ$ . Nevertheless, C19 and C14 enjoy a sum of angles totalling  $120^\circ$  as indeed do all carbon atoms of the benzene ring. Further confirmation of the unadulterated nature of the aromaticity comes from the  $C_6$  plane with a mean deviation of just  $0.006 \text{ \AA}$ . Alterations in the aromatic C-C bond lengths are without statistical significance. Detection of this perturbation in other Bz15O5 complexes is hampered where the rest of the benzene ring is found to be non-ideal. However, a clear example is available in the structure of  $[\text{Ca}(\text{NCS})_2(\text{Bz15O5})(\text{MeOH})]$ .<sup>257</sup>

By way of contrast, Bz15O5 complexation of the isoelectronic sodium ion shows a quite different structure in  $[\text{Na}(\text{Bz15O5})(\text{H}_2\text{O})]^+$  to that seen in  $[\text{ScCl}_2(\text{Bz15O5})]^+$ .<sup>260</sup> Bz15O5 fails to form a girdle about the sodium ion; the arrangement of oxygen atoms forming the solvation sphere around the sodium ion may be described as a distorted pentagonal pyramid, the base of which is formed by the ethereal oxygen atoms.



**Figure 5.10** Molecular structure of  $[\text{ScCl}_2(\text{Bz15O5})]^+$ , viewed down onto  $\text{O}_3$  plane.

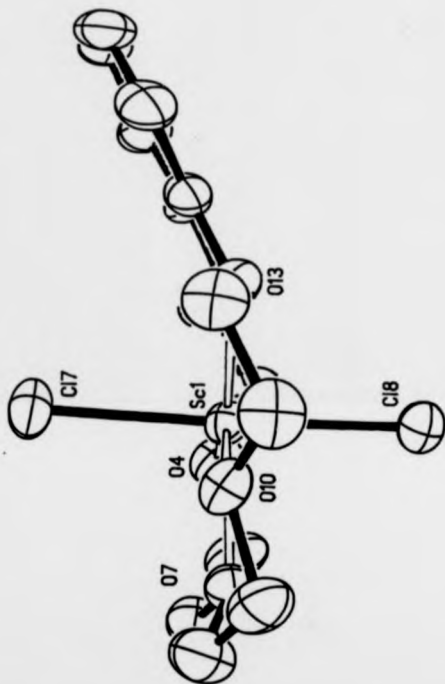


Figure 5.11 Molecular structure of  $[\text{ScCl}_2(\text{Bz15O5})]^+$ , viewed parallel to  $\text{O}_3$  plane.



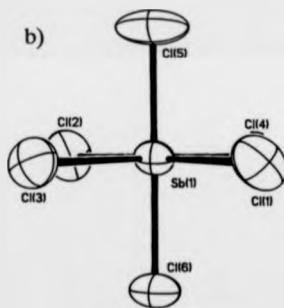
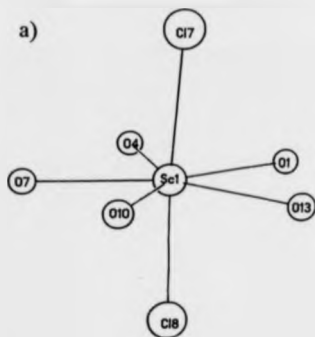


Figure 5.12 Diagrams showing a) scandium coordination geometry, b) hexachloroantimonate(V), in the compound  $\{\text{ScCl}_3(\text{BzISO}_5)\}[\text{SbCl}_6]$ .

Table 5.4 Bond lengths (Å) and angles (°) for [ScCl<sub>2</sub>(BzISO<sub>5</sub>)](SbCl<sub>4</sub>).

Bond lengths (Å)			
Sb(1)-Cl(1)	2.365(2)	Sb(1)-Cl(2)	2.360(2)
Sb(1)-Cl(3)	2.362(2)	Sb(1)-Cl(4)	2.370(2)
Sb(1)-Cl(5)	2.319(2)	Sb(1)-Cl(6)	2.359(2)
Sc(1)-Cl(7)	2.395(2)	Sc(1)-Cl(8)	2.395(2)
Sc(1)-O(1)	2.206(4)	Sc(1)-O(4)	2.172(4)
Sc(1)-O(7)	2.166(4)	Sc(1)-O(10)	2.171(4)
Sc(1)-O(13)	2.224(4)	O(1)-C(2)	1.459(7)
O(1)-C(19)	1.389(6)	O(4)-C(3)	1.422(7)
O(4)-C(5)	1.446(7)	O(7)-C(6)	1.441(8)
O(7)-C(8)	1.431(8)	O(10)-C(9)	1.452(8)
O(10)-C(11)	1.436(8)	O(13)-C(12)	1.456(7)
O(13)-C(14)	1.399(7)	C(2)-C(3)	1.499(9)
C(5)-C(6)	1.487(10)	C(8)-C(9)	1.487(10)
C(11)-C(12)	1.495(9)	C(14)-C(15)	1.374(8)
C(14)-C(19)	1.374(8)	C(15)-C(16)	1.367(9)
C(16)-C(17)	1.382(10)	C(17)-C(18)	1.393(9)
C(18)-C(19)	1.391(8)		
Bond angles (deg.)			
Cl(1)-Sb(1)-Cl(2)	178.8(1)	Cl(1)-Sb(1)-Cl(3)	90.5(1)
Cl(2)-Sb(1)-Cl(3)	90.2(1)	Cl(1)-Sb(1)-Cl(4)	90.4(1)
Cl(2)-Sb(1)-Cl(4)	88.9(1)	Cl(3)-Sb(1)-Cl(4)	178.6(1)
Cl(1)-Sb(1)-Cl(5)	90.1(1)	Cl(2)-Sb(1)-Cl(5)	90.9(1)
Cl(3)-Sb(1)-Cl(5)	89.8(1)	Cl(4)-Sb(1)-Cl(5)	91.3(1)
Cl(1)-Sb(1)-Cl(6)	88.9(1)	Cl(2)-Sb(1)-Cl(6)	90.2(1)
Cl(3)-Sb(1)-Cl(6)	89.3(1)	Cl(4)-Sb(1)-Cl(6)	89.6(1)
Cl(5)-Sb(1)-Cl(6)	178.6(1)	Cl(7)-Sc(1)-Cl(8)	175.5(1)
Cl(7)-Sc(1)-O(1)	87.6(1)	Cl(8)-Sc(1)-O(1)	89.8(1)
Cl(7)-Sc(1)-O(4)	90.0(1)	Cl(8)-Sc(1)-O(4)	92.7(1)
O(1)-Sc(1)-O(4)	72.1(1)	Cl(7)-Sc(1)-O(7)	95.4(1)
Cl(8)-Sc(1)-O(7)	88.8(1)	O(1)-Sc(1)-O(7)	144.8(2)
O(4)-Sc(1)-O(7)	72.8(1)	Cl(7)-Sc(1)-O(10)	88.4(1)
Cl(8)-Sc(1)-O(10)	91.5(1)	O(1)-Sc(1)-O(10)	142.8(2)
O(4)-Sc(1)-O(10)	144.9(2)	O(7)-Sc(1)-O(10)	72.4(2)
Cl(7)-Sc(1)-O(13)	87.2(1)	Cl(8)-Sc(1)-O(13)	88.5(1)
O(1)-Sc(1)-O(13)	70.2(1)	O(4)-Sc(1)-O(13)	142.3(1)
O(7)-Sc(1)-O(13)	144.9(1)	O(10)-Sc(1)-O(13)	72.6(1)
Sc(1)-O(1)-C(2)	117.3(3)	Sc(1)-O(4)-C(3)	115.7(3)
C(2)-O(1)-C(19)	118.0(4)	Sc(1)-O(7)-C(6)	115.0(3)
Sc(1)-O(4)-C(5)	116.6(3)	C(3)-O(4)-C(5)	116.1(5)
Sc(1)-O(7)-C(8)	116.2(3)	Sc(1)-O(10)-C(9)	117.0(4)
C(6)-O(7)-C(8)	115.2(5)	Sc(1)-O(13)-C(12)	115.6(3)
Sc(1)-O(10)-C(9)	116.0(3)	C(9)-O(10)-C(11)	115.2(4)
Sc(1)-O(13)-C(12)	115.5(3)	Sc(1)-O(13)-C(14)	115.2(3)
C(12)-O(13)-C(14)	117.7(4)	O(1)-C(2)-C(3)	105.0(5)
O(4)-C(3)-C(2)	106.8(5)	O(4)-C(5)-C(6)	106.8(5)
O(7)-C(6)-C(5)	105.9(5)	O(7)-C(8)-C(9)	105.5(5)
O(10)-C(9)-C(8)	105.6(5)	O(10)-C(11)-C(12)	106.4(5)
O(13)-C(12)-C(11)	106.7(5)	O(13)-C(14)-C(15)	124.2(5)
O(13)-C(14)-C(19)	114.4(5)	C(15)-C(14)-C(19)	121.4(5)
C(14)-C(15)-C(16)	118.2(6)	C(15)-C(16)-C(17)	121.7(6)
C(16)-C(17)-C(18)	120.1(6)	C(17)-C(18)-C(19)	117.9(6)
O(1)-C(19)-C(14)	115.3(5)	O(1)-C(19)-C(18)	124.0(5)
C(14)-C(19)-C(18)	120.6(5)		

## 12-crown-4 complexes

The size of the cavity in 12O4 has been estimated to be less than 1.8 Å in diameter.<sup>201</sup> It was therefore likely that using this tetraoxa donor as a chelating agent would yield compounds with a 'half-sandwich' topology. The conformation of 12O4 in its complexes is predominantly of  $C_4$  symmetry. This conformation directs all four oxygen atoms to the same side of the crown molecule, well oriented for metal complexation. The free crown ether exhibits  $C_4$  symmetry with two oxygen atoms directed to opposite sides of the crown ether. This 'two-up two-down' bridging arrangement is often manifest where the structure shows an extensive intermolecular hydrogen bonding network.

The reactions reported here used the simple 1:1 metal chloride to crown stoichiometry. Again, immediate reaction by yttrium and lanthanum necessitated the use of three equivalents of antimony pentachloride. The spectroscopic evidence clearly points to the formation of the hexachloroantimonate(V) salts with coordination by the crown ether and additional acetonitrile molecules. For lanthanum and yttrium a nine-coordinate species is proposed:  $[M(12O4)(MeCN)_3][SbCl_6]$ . In the case of scandium, with one equivalent of antimony pentachloride, the compound  $[ScCl_2(MeCN)(12O4)][SbCl_6]$  matches the analytical data most closely. The elemental analyses in respect of the scandium and yttrium complexes were not entirely satisfactory although clearly, to a first approximation, the formulation proposed is likely to be correct.

### NMR studies

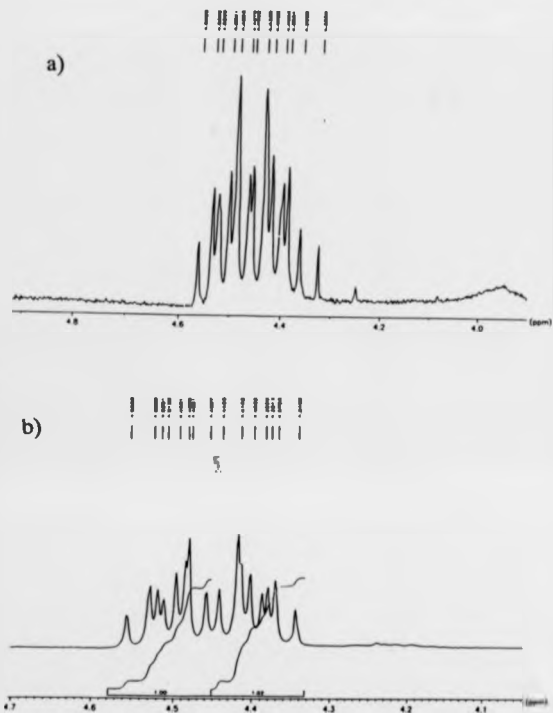
#### 1) Yttrium and lanthanum compounds

For the complex  $[La(12O4)(MeCN)_3]^+$ , an AA'BB' multiplet was observed in the <sup>1</sup>H spectrum some δ 0.5 downfield from the position of the free ligand. This is in full accord with the cationic half-sandwich formulation. In the case of the analogous yttrium complex, the situation is somewhat more complicated in that the individual couplings of the AA'BB'

multiplet are not resolved. Two broadened 'humps' are observed, otherwise similar to the result seen with lanthanum. This suggests the presence of a relatively slow dynamic process. In contrast,  $^{13}\text{C}$  NMR finds a typically sharp, single signal as seen in all the complexes under discussion.

## 2) Scandium species

The 1:1 antimony to scandium complex again revealed an AA'BB' multiplet, now moved downfield by around  $\delta$  0.9 from the free ligand position. This further movement compared to that observed for the  $[\text{M}(\text{12O4})(\text{MeCN})_3]^{3+}$  ( $\text{M} = \text{Y, La}$ ) is quite remarkable and must lead to the postulation that the scandium may exist in solution as  $[\text{Sc}(\text{12O4})(\text{MeCN})_3]^{3+}$ , presumably as a result of self-ionisation. Further support for this suggestion comes from the NMR spectra of the 3:1 complex. The 1:1 and 3:1 spectra are compared in Figure 5.13. Whilst the AA'BB' pattern is retained with the 3:1  $^1\text{H}$  spectrum (still facial coordination), a subtle widening of the separation between the central signals, and some alterations in the relative intensities within the multiplets can be seen. However, no significant change in the median chemical shift is observed. The shifts of the  $^{13}\text{C}$  spectra also remain unaltered whether one or three equivalents of antimony pentachloride are present. On balance it is likely that no alteration in the scandium cationicity has occurred and that the slight AA'BB' pattern changes stem from adjusted interionic/intermolecular interactions. On this basis, the presence of  $[\text{Sc}(\text{12O4})(\text{MeCN})_3]^{3+}$  as a result of self-ionisation best fits the observed NMR results. Solid state infra-red evidence shows the existence of two small bands under  $400\text{ cm}^{-1}$ . If assigned to  $\nu(\text{Sc-Cl})$  modes then the self-ionisation indicated by NMR is not retained in the absence of the acetonitrile solution.



**Figure 5.13**  $^1\text{H}$  NMR spectra resulting from the reaction of scandium(III) chloride and 12O4 with a) one, b) three equivalents antimony pentachloride.

## CONCLUSIONS AND FUTURE WORK

- 1) Addition of antimony pentachloride, in acetonitrile, to the trichlorides of scandium, yttrium and lanthanum has provided a direct route to anhydrous cationic species.
- 2) When encapsulated by a polyoxamacrocyclic, these cations are readily handled crystalline solids, impervious to brief atmospheric exposure.
- 3) In the case of scandium, the cationic charge is readily governed by addition of 1, 2, or 3 equivalents of antimony pentachloride. Analogous behaviour may exist for yttrium and lanthanum. Generation of the *tris*-THF adduct as a precursor may obviate the need for excess antimony pentachloride.
- 4) The 'thread through' trigonal bipyramidal  $[MCl_2 \text{ oxacrown}]^+$  structure seems to be widely adopted, presumably as a result of its stability.
- 5) It seems possible that a  $\pi \rightarrow \pi^*$  interaction may provide additional stability for macrocyclic ligands incorporating an aromatic ring.
- 6) The compounds incorporating 12O4 are most certainly of half-sandwich topology. An additional equivalent of the crown ether, in the case of the trications, may well provide full sandwich complexes. This 2:1 ligand to substrate stoichiometry may also bear fruit with 15O5 and Bz15O5.

- 7) Larger macrocycles such as 24O8 and 30O10 are likely to provide some interest. Of particular attraction would be the use of a 1:2 ligand to substrate stoichiometry. These large rings have been known to encapsulate more than one metal centre.
- 8) Further functionalisation of the macrocycle may be possible whilst maintaining due regard for the oxidative powers of antimony pentachloride. Some thiaether donors within the ring would supply a useful contrast to the oxaeether. Alternatively, it may be necessary to maintain the fundamental crown ether binding but to augment this with a suitable pendent arm.
- 9) The bicyclic cryptand polyethers could present a useful development in the encapsulation of these cationic species.
- 10) Following the success with the trichlorides of scandium, yttrium, and lanthanum, all Rare Earth metal chlorides should now be utilised to test the generality of this halide exchange reaction.
- 11) The organometallic chemistry of these cations is ready for investigation *i.e.* reaction with suitable carbanions.

## EXPERIMENTAL

All procedures were conducted using standard Schlenk techniques and an inert dinitrogen atmosphere except where stated to the contrary. Solvents were prepared as outlined in previous chapters.

'Analar' grade scandium trichloride hydrate, anhydrous yttrium trichloride and anhydrous lanthanum trichloride were obtained from Aldrich Chemical Co. Gillingham. The yttrium and lanthanum trichlorides were used directly without further purification. Scandium trichloride hydrate was dehydrated before use as described in chapter 3. Antimony pentachloride was used as obtained from BDH Ltd., Poole.

#### Synthesis of $[\text{ScCl}_2(18\text{O}6)][\text{SbCl}_6]$

Addition of an acetonitrile solution (10 cm<sup>3</sup>) of antimony pentachloride (0.122 g, 0.408 mmol) to an acetonitrile solution (5 cm<sup>3</sup>) of scandium trichloride *tris*(THF) (0.150 g, 0.408 mmol) provided, after stirring, a clear solution. 18O6 (0.108 g, 0.409 mmol) was then added directly to the reaction mixture. After standing overnight, controlled reduction of the solvent volume over 3 h produced a large crop of colourless block crystals (yield 0.25 g, 86%). M.p. 163-164°C Anal. calc. for  $\text{C}_{12}\text{H}_{24}\text{Cl}_9\text{O}_6\text{SbSc}$ : C, 20.17; H, 3.38; Cl, 39.71 %. Found: C, 20.22; H, 3.45; Cl, 39.58 %. NMR (250 MHz,  $\text{CD}_3\text{CN}$ )  $\delta$ , ppm:  $^1\text{H}$  4.25 [24 H, s,  $\text{CH}_2$  (ligand)],  $^{13}\text{C}$  73.49 [ $\text{CH}_2$ ]. I.R. (Cal plates, nujol):  $\nu(\text{SbCl})$  347 cm<sup>-1</sup>;  $\nu(\text{ScCl})$  399, 291 cm<sup>-1</sup>;  $\nu(\text{ligand})$  1086, 961, 832 cm<sup>-1</sup>. U.v./vis  $\lambda_{\text{max}}$  (MeCN) 36 980 cm<sup>-1</sup>.



#### Synthesis of $[\text{ScCl}_2(1505)][\text{SbCl}_4]$

A methodology directly analogous to that used for the 1806 complex provided diffraction quality crystals directly from the reaction mixture (yield 0.17 g, 62%). Reagents used: antimony pentachloride (0.122 g, 0.408 mmol), scandium trichloride *tris*(THF) (0.150 g, 0.408 mmol), and 1505 (0.090 g, 0.409 mmol). Anal. calc. for  $\text{C}_{10}\text{H}_{20}\text{Cl}_2\text{O}_3\text{SbSc}$ : C, 17.91; H, 3.01%. Found: C, 18.04; H, 3.08%. NMR (250 MHz,  $\text{CD}_3\text{CN}$ )  $\delta$ , ppm:  $^1\text{H}$  4.33 [20 H, s,  $\text{CH}_2$  (ligand)],  $^{13}\text{C}$  73.49 [ $\text{CH}_2$ ]. I.R. (CaI plates, nujol):  $\nu(\text{SbCl})$  346,  $\text{cm}^{-1}$ ;  $\nu(\text{ScCl})$  427, 291  $\text{cm}^{-1}$ ;  $\nu(\text{ligand})$  1062, 964, 827  $\text{cm}^{-1}$ . U.v./vis  $\lambda_{\text{max}}$  (MeCN) 36 900  $\text{cm}^{-1}$ .

#### Synthesis of $[\text{ScCl}_2(\text{Bz}1505)][\text{SbCl}_4]$

A similar method to that used for the 1806 complex was used. Diffraction quality crystals were obtained directly from the reaction mixture by concentrating the solution over the course of several hours (yield 0.25 g, 85%). Reagents used: antimony pentachloride (0.122 g, 0.408 mmol), scandium trichloride *tris*(THF) (0.150 g, 0.408 mmol), and 1505 (0.109 g, 0.408 mmol). Anal. calc. for  $\text{C}_{14}\text{H}_{20}\text{Cl}_2\text{O}_3\text{SbSc}$ : C, 23.40; H, 2.81%. Found: C, 23.31; H, 2.75%. NMR (250 MHz,  $\text{CD}_3\text{CN}$ )  $\delta$ , ppm:  $^1\text{H}$  7.317, [4 H, s, (aromatic)], 4.900, 4.593, 4.444, 4.440 [16 H, two AA'BB' multiplets, ( $\text{CH}_2$ )],  $^{13}\text{C}$  144.89, 126.16, 113.78 [aromatic]; 73.74, 73.15, 72.08, 71.67 [ $\text{CH}_2$ ]. I.R. (CaI plates, nujol):  $\nu(\text{SbCl})$  359, 331  $\text{cm}^{-1}$ ;  $\nu(\text{ScCl})$  418, 406, 287  $\text{cm}^{-1}$ ;  $\nu(\text{ligand})$  1238, 1058, 755  $\text{cm}^{-1}$ . U.v./vis  $\lambda_{\text{max}}$  (MeCN) 33 470  $\text{cm}^{-1}$ , 29 400  $\text{cm}^{-1}$  (shoulder).

#### Synthesis of $[\text{ScCl}_2(\text{MeCN})(1204)][\text{SbCl}_4]$

Antimony pentachloride (0.220 g, 0.736 mmol) in acetonitrile (10  $\text{cm}^3$ ) was added to an acetonitrile solution (5  $\text{cm}^3$ ) of scandium trichloride *tris*(THF) (0.27 g, 0.735 mmol), followed by 1204 (0.129 g, 0.733 mmol). The clear solution was allowed to stand overnight.

Controlled reduction of solvent volume over several hours failed to produce crystalline material. After removal of all solvent *in vacuo*, the resultant white powder was washed with toluene (3 x 10 cm<sup>3</sup>), hexane (2 x 5 cm<sup>3</sup>), and dried under vacuum (yield 0.35 g, 71%). Anal. calc. for C<sub>10</sub>H<sub>14</sub>Cl<sub>3</sub>NO<sub>6</sub>SbSc: C, 17.98; H, 2.85; N, 2.10%. Found: C, 15.83; H, 2.69; N, 2.07%. NMR (250 MHz, CD<sub>3</sub>CN)  $\delta$ , ppm: <sup>1</sup>H 4.25 [24 H, s, CH<sub>2</sub> (ligand)], <sup>13</sup>C 73.49 [CH<sub>2</sub>]. I.R. (CsI plates, nujol):  $\nu$ (SbCl) 342 cm<sup>-1</sup>;  $\nu$ (ScCl) 424, 322 cm<sup>-1</sup>;  $\nu$ (CN) 2300, 2283 cm<sup>-1</sup>. U.v./vis  $\lambda_{\text{max}}$  (MeCN) 37 010 cm<sup>-1</sup>.

#### Synthesis of [Y(MeCN)<sub>6</sub>(18O6)][SbCl<sub>6</sub>]

An acetonitrile solution (35 cm<sup>3</sup>) of antimony pentachloride (1.53 g, 5.12 mmol) was added to an acetonitrile solution (40 cm<sup>3</sup>) of yttrium trichloride (0.25 g, 1.28 mmol). This was stirred and warmed to 50°C for 2 h prior to the addition of 18O6 (0.338 g, 1.28 mmol) in acetonitrile (25 cm<sup>3</sup>). After further stirring overnight all volatiles were removed *in vacuo*. The product was washed with toluene (5 x 20 cm<sup>3</sup>) and hexane (2 x 10 cm<sup>3</sup>) to produce a fine white powder (yield 1.4 g, 74%). Anal. calc. for C<sub>18</sub>H<sub>31</sub>Cl<sub>18</sub>N<sub>3</sub>O<sub>6</sub>Sb<sub>3</sub>Y: C, 14.60; H, 2.23; N, 2.84%. Found: C, 14.34; H, 2.28; N, 2.71%. NMR (250 MHz, CD<sub>3</sub>CN)  $\delta$ , ppm: <sup>1</sup>H 4.178 [24 H, s, CH<sub>2</sub> (ligand)], <sup>13</sup>C 72.695 [CH<sub>2</sub>]. I.R. (CsI plates, nujol):  $\nu$ (SbCl) 342 cm<sup>-1</sup>;  $\nu$ (CN) 2302, 2275 cm<sup>-1</sup>; U.v./vis  $\lambda_{\text{max}}$  (MeCN) 36 930 cm<sup>-1</sup>.

#### Synthesis of [Y(MeCN)<sub>6</sub>(12O4)][SbCl<sub>6</sub>]

A methodology similar to that for the 18O6 complex was used. Reagent quantities were antimony pentachloride (1.60 g, 5.35 mmol), yttrium trichloride (0.25 g, 1.28 mmol), and 12O4 (0.225 g, 1.28 mmol). A fine white powder was obtained after washing thoroughly with toluene (yield 1.0 g, 66%). Anal. calc. for C<sub>18</sub>H<sub>31</sub>Cl<sub>18</sub>N<sub>3</sub>O<sub>4</sub>Sb<sub>3</sub>Y: C, 14.66; H, 2.10; N, 4.75%. Found: C, 14.13; H, 1.99; N, 5.92%. NMR (250 MHz, CD<sub>3</sub>CN)  $\delta$ , ppm: <sup>1</sup>H 4.295,

4-061 [16 H, two broad signals, CH<sub>2</sub> (ligand)], <sup>13</sup>C 70-480 [CH<sub>2</sub>]. I.R. (Csl plates, nujol):  $\nu(\text{SbCl})$  342 cm<sup>-1</sup>;  $\nu(\text{CN})$  2311, 2284 cm<sup>-1</sup>; U.v./vis  $\lambda_{\text{max}}$  (MeCN) 37 010 cm<sup>-1</sup>.

#### Synthesis of [La(MeCN)<sub>7</sub>(18O6)][SbCl<sub>4</sub>]

An acetonitrile solution (35 cm<sup>3</sup>) of antimony pentachloride (1.25 g, 4.18 mmol) was added to a suspension of lanthanum trichloride (0.250 g, 1.02 mmol) in acetonitrile (40 cm<sup>3</sup>). Heating to 70°C for 20 minutes provided a clear solution to which 18O6 (0.270 g, 1.03 mmol) was added directly. After stirring overnight, slow reduction of the solvent volume over several hours failed to produce crystalline material. After all volatiles were removed *in vacuo*, the product was washed with toluene (5 x 10 cm<sup>3</sup>) and hexane (2 x 10 cm<sup>3</sup>) to produce a fine white powder (yield 1.1 g, 70%). Anal. calc. for C<sub>18</sub>H<sub>31</sub>Cl<sub>18</sub>N<sub>6</sub>O<sub>6</sub>Sb<sub>1</sub>La: C, 14.15; H, 2.23; N, 2.74%. Found: C, 14.14; H, 2.24; N, 2.66%. NMR (250 MHz, CD<sub>3</sub>CN)  $\delta$ , ppm: <sup>1</sup>H 4-063 [24 H, s, CH<sub>2</sub> (ligand)], <sup>13</sup>C 72-579 [CH<sub>2</sub>]. I.R. (Csl plates, nujol):  $\nu(\text{SbCl})$  342 cm<sup>-1</sup>;  $\nu(\text{CN})$  2298, 2268 cm<sup>-1</sup>; U.v./vis  $\lambda_{\text{max}}$  (MeCN) 36 980 cm<sup>-1</sup>.

#### Synthesis of [La(MeCN)<sub>7</sub>(12O4)][SbCl<sub>4</sub>]

A similar methodology to that for the 18O6 complex was used. Reagent quantities were antimony pentachloride (1.20 g, 4.01 mmol), lanthanum trichloride (0.250 g, 1.02 mmol), and 12O4 (0.180 g, 1.03 mmol). A fine white powder was obtained after washing thoroughly with toluene (yield 1.1 g, 71%). Anal. calc. for C<sub>18</sub>H<sub>31</sub>Cl<sub>18</sub>N<sub>6</sub>O<sub>4</sub>Sb<sub>1</sub>La: C, 14.19; H, 2.05; N, 4.60%. Found: C, 14.25; H, 2.08; N, 4.93%. NMR (250 MHz, CD<sub>3</sub>CN)  $\delta$ , ppm: <sup>1</sup>H 4-146, 3-978 [16 H, midpoints of AA'BB' multiplet, CH<sub>2</sub> (ligand)], <sup>13</sup>C 69-163 [CH<sub>2</sub>]. I.R. (Csl plates, nujol):  $\nu(\text{SbCl})$  342 cm<sup>-1</sup>;  $\nu(\text{CN})$  2303, 2275 cm<sup>-1</sup>. U.v./vis  $\lambda_{\text{max}}$  (MeCN) 36 890 cm<sup>-1</sup>.

Table 5.5 Crystallographic data for  $[\text{ScCl}_2(18\text{O}6)][\text{SbCl}_4]$ .

Formula	$\text{C}_{12}\text{H}_{24}\text{Cl}_4\text{O}_6\text{SbSc}$
$M_r$	714.6
Crystal class	triclinic
Space group	P1
$a/\text{\AA}$	7.363(2)
$b/\text{\AA}$	18.822(6)
$c/\text{\AA}$	19.164(6)
$\alpha/^\circ$	105.38(3)
$\beta/^\circ$	100.18(3)
$\gamma/^\circ$	90.90(3)
$V/\text{\AA}^3$	2514.8
$Z$	4
$D_x/\text{g cm}^{-3}$	1.89
Mo-K $\alpha$ radiation, $\lambda/\text{\AA}$	0.71069
$\mu_{\text{(calc.)}}/\text{cm}^{-1}$	22.2
$T/\text{K}$	290
$F_{\text{(calc.)}}$	1408
Final R	0.056
Unique observed ( $I/\sigma(I) \geq 2.0$ ) reflections	6663

#### Crystal structure determination of $[\text{ScCl}_2(18\text{O}6)][\text{SbCl}_4]$

Crystals were obtained from MeCN. A colourless block was mounted, under Ar, in a Lindemann capillary. Data were collected with a Siemens R3m four circle diffractometer in  $\omega$ - $2\theta$  mode. Maximum  $2\theta$  was  $50^\circ$  with scan range  $\pm 0.7^\circ(\omega)$  around the  $K_{\alpha 1}$ - $K_{\alpha 2}$  angles, scan speed was  $2.5\text{--}15^\circ(\omega) \text{ min}^{-1}$ , depending on the intensity of a  $2\theta$  pre-scan; backgrounds were measured at each end of the scan for 0.25 of the scan time. The  $hkl$  ranges were  $0/8$ ,  $-22/22$ ,  $-22/22$ . Three standard reflections were monitored every 200 reflections, and showed a slight variation during data collection. The data were rescaled to correct for this. Unit cell dimensions and standard deviations were obtained by a least-squares fit to 26 reflections ( $3 < 2\theta < 27^\circ$ ). The 9620 reflections collected were processed using profile analysis to give 8870 unique reflections ( $R_{\text{int}} = 0.0229$ ), of which 6663 were considered observed ( $I/\sigma(I) > 2.0$ ). These were corrected for Lorentz and polarization effects. The crystal was destroyed before an absorption correction could be made. No systematic reflection conditions indicate space group  $P1$  or  $PT$ .  $P1$  was chosen and deemed satisfactory by successful refinement. The structure was solved by direct methods using SHELXTL (TREF) to locate one Sb atom, two Sb half-atoms and two Sc atoms. Remaining atoms were then found by successive Fourier syntheses. The asymmetric unit contains an anion, two independent, centrosymmetric half-anions and two independent cations. Anisotropic thermal parameters were used for all non-H atoms. Hydrogen atoms were given fixed isotropic thermal parameters,  $U = 0.08 \text{ \AA}^2$ . Those defined by the molecular geometry were inserted at calculated positions and not refined. Final refinement was on  $F$  by least squares methods refining 509 parameters including an isotropic extinction parameter. Largest positive and negative peaks on a final difference Fourier synthesis were of height  $+0.8$ ,  $-1.8 \text{ el. \AA}^{-3}$ . A weighting scheme of the form  $W = 1/\sigma^2(F) + g(F^2)$  with  $g = 0.003625$  was used and shown to be satisfactory by a weight analysis. Final  $R = 0.056$ ,  $R_w = 0.063$ ,  $S = 1.0903$ ;  $R_{\text{all reflections}} = 0.0756$ . Maximum shift/error in final cycle was 0.084. Computing was conducted on a DEC Microvax-II with SHELXTL PLUS.<sup>147</sup> Scattering factors in the analytical form and anomalous dispersion factors taken from reference 148.

Table 5.6 Crystallographic data for  $[\text{ScCl}_2(\text{BzISO}_5)][\text{SbCl}_6]$ .

Formula	$\text{C}_{14}\text{H}_9\text{Cl}_3\text{O}_5\text{SbSc}$
$M_r$	718.6
Crystal class	orthorhombic
Space group	Pbca
$a/\text{\AA}$	17.015(10)
$b/\text{\AA}$	13.296(8)
$c/\text{\AA}$	22.236(12)
$\alpha/^\circ$	
$\beta/^\circ$	
$\gamma/^\circ$	
$V/\text{\AA}^3$	5030.5
$Z$	8
$D_c/\text{g cm}^{-3}$	2.12
Mo-K $\alpha$ radiation, $\lambda/\text{\AA}$	0.71069
$\mu(\text{Mo-K}\alpha)/\text{cm}^{-1}$	23.3
$T/\text{K}$	290
$F_{(000)}$	3144
Final R	0.039
Unique observed ( $I/\sigma(I) \geq 2.0$ ) reflections	3282

#### Crystal structure determination of $[\text{SeCl}_2(\text{Bz1505})][\text{SbCl}_6]$

A yellow block crystal was obtained from acetonitrile and mounted, under argon, in a Lindemann capillary. Data were collected with a Siemens R3m four circle diffractometer in  $\omega$ - $2\theta$  mode. Maximum  $2\theta$  was  $50^\circ$  with scan range  $\pm 0.7^\circ(\omega)$  around the  $K_{\alpha 1}$ - $K_{\alpha 2}$  angles, scan speed  $1.5 - 15^\circ(\omega) \text{ min}^{-1}$ , depending on the intensity of a  $2\theta$  pre-scan; backgrounds were measured at each end of the scan for 0.25 of the scan time. The  $hkl$  ranges were 0/15, 0/20, 0/26. Three standard reflections were monitored every 200 reflections, and showed up to 10% decrease which necessitated recentering during data collection. The data were rescaled to correct for this. Unit cell dimensions and standard deviations were obtained by least-squares fit to 14 reflections ( $15 < 2\theta < 30^\circ$ ). The 5302 reflections collected were processed using profile analysis to give 4452 unique reflections ( $R_{\text{int}} = 0.074$ ), of which 3282 were considered observed ( $I/\sigma(I) > 2.0$ ). These were corrected for Lorentz, polarization and absorption effects (by the Gaussian method); minimum and maximum transmission factors were 0.385 and 0.629. Systematic reflection conditions  $hk0$ ,  $k=2n$ ;  $0kl$ ,  $l=2n$ ;  $h0l$ ,  $h=2n$ , indicate space group  $Pbca$ . The antimony atom was located by the Patterson interpretation section of SHELXTL and the light atoms then found by E-map expansion and successive Fourier syntheses. The asymmetric unit contains one ion pair. Anisotropic thermal parameters were used for all non-H atoms. Hydrogen atoms were given fixed isotropic thermal parameters,  $U = 0.08 \text{ \AA}^2$ . Those defined by the molecular geometry were inserted at calculated positions and successfully refined. Final refinement was on F by least squares methods refining 262 parameters. Largest positive and negative peaks on a final difference Fourier synthesis were of height  $\pm 0.6 \text{ e. \AA}^{-3}$ . A weighting scheme of the form  $W = 1/(\sigma^2(F) + gF^2)$  with  $g = 0.002$  was used and shown to be satisfactory by a weight analysis. Final  $R = 0.0388$ ,  $R_w = 0.0443$ ,  $S = 0.97$ ;  $R_{\text{int}} = 0.059$ . Maximum shift/error in final cycle was 0.001. Computing was conducted on a DEC Microvax-II with SHELXTL PLUS.<sup>147</sup> Scattering factors in the analytical form and anomalous dispersion factors taken from reference 148.

## REFERENCES

1. G. B. Kauffman, *J. Chem. Educ.*, 1976, **53**, 445.
2. A. Werner, *Z. Anorg. Allgem. Chem.*, 1893, **3**, 267.
3. G. B. Kauffman, *Adv. Chem. Ser.*, 1967, **62**, ix.
4. J. Van Alphen, *Rec. Trav. Chim.* 1937, **56**, 343.
5. N. F. Curtis, *J. Chem. Soc.*, 1960, 4409.
6. M. Casabo, L. Mestres, L. Escriche, F. Texidor, C. Perez-Jimenez, *J. Chem. Soc., Dalton Trans.*, 1991, 1969.
7. C. J. Pedersen, *Org. Synth.*, 1972, **52**, 66.
8. D. J. Cram, *Angew. Chem. Int. Ed. Engl.*, 1988, **27**, 89.  
J.-M. Lehn, *Angew. Chem. Int. Ed. Engl.*, 1988, **27**, 1009.  
C. J. Pedersen, *Angew. Chem. Int. Ed. Engl.*, 1988, **27**, 1021.
9. J. J. Christensen, D. J. Eatough, R. M. Izatt, *Chem. Rev.*, 1974, **74**, 351.
10. D.K. Cabbiness, D.W. Margerum; *J. Am. Chem. Soc.*, 1969, **91**, 6540.
11. F.P. Hinz, D.W. Margerum; *Inorg. Chem.*, 1974, **13**, 2941.
12. A. Evers and R. D. Hancock, *Inorg. Chim. Acta.*, 1989, **160**, 245.
13. D. H. Busch, K. Farmery, V. Goedken, V. Katovic, A. C. Melnyk, C. R. Sperati, N. Tokel, *Adv. Chem. Ser.*, 1971, **100**, 44.
14. T. E. Jones, L. L. Zimmer, L. L. Diaddario, D. B. Rorabacher, L. A. Ochrymowycz, *J. Am. Chem. Soc.*, 1975, **97**, 7163.
15. T.E. Jones, L.S.W.L. Sokol, D.B. Rorabacher, M.D. Glick; *J. Chem. Soc., Chem. Commun.*, 1979, 140.
16. C. J. Pedersen, *J. Amer. Chem. Soc.*, 1970, **92**, 391.
17. R. M. Izatt, D. P. Nelson, J. H. Rytting, B. L. Haymore, J. J. Christensen, *J. Amer. Chem. Soc.*, 1971, **93**, 1619.
18. R. M. Izatt, J. S. Bradshaw, S. A. Nielsen, J. D. Lamb, J. J. Christensen, *Chem. Rev.*, 1985, **85**, 271.
19. R. M. Izatt, D. J. Eatough, J. J. Christensen, *Structure and Bonding*, 1973, **16**, 161.



20. R. T. Myers, *Inorg. Nucl. Chem. Lett.*, 1980, *16*, 329.
21. K. Henrick, P. A. Tasker, L. F. Lindoy, *Prog. Inorg. Chem.*, 1985, *33*, 1.
22. G. Schwarzenbach, *Helv. Chim. Acta.*, 1952, *35*, 2344.
23. J. J. R. Frauso da Silva, *J. Chem. Educ.*, 1983, *60*, 390.
24. R. D. Hancock, *Acc. Chem. Res.*, 1990, *23*, 253.
25. R. C. Luckay, R. D. Hancock, *J. Chem. Soc., Dalton Trans.*, 1991, 1491.
26. R. D. Hancock, *Progr. Inorg. Chem.*, 1989, *37*, 187.
27. N. F. Curtis, *J. Chem. Soc.*, 1960, 4409.
28. M. C. Thompson, D. H. Busch, *J. Am. Chem. Soc.*, 1964, *86*, 3651.
29. B. Bosnich, C. K. Poon and M. L. Tobe, *Inorg. Chem.*, 1965, *4*, 1102.
30. D. H. Busch, *Acc. Chem. Res.*, 1978, *11*, 392.
31. V. L. Goedken, J. J. Pluth, S.-M. Peng, B. Burston, *J. Am. Chem. Soc.*, 1976, *98*, 8014.
32. V. L. Goedken, S.-M. Peng, J. Molin-Norris, Y. Park, *J. Am. Chem. Soc.*, 1976, *98*, 8391.
33. F. A. Cotton, J. Czuchajowska, L. R. Falvello, X. Feng, *Inorg. Chim. Acta*, 1990, *172*, 135.
34. C. Floriani, S. Ciurli, A. Chiesi-Villa, C. Guastini, *Angew. Chem. Int. Ed. Engl.*, 1987, *26*, 70.
35. F. A. Cotton, J. Czuchajowska, *Polyhedron*, 1990, *9*, 2553.
36. P. Chaudhuri, K. Wieghardt, *Prog. Inorg. Chem.*, 1987, *35*, 329.
37. R. B. Lauffer, *Chem. Rev.*, 1987, *87*, 901.
38. R. Ramasamy, I. Lazar, E. Brucher, A. D. Sherry, C. R. Malloy, *FEBS Letts.*, 1991, *280*, 121.
39. D. Parker, *Chem. Soc. Rev.*, 1990, *19*, 271.
40. K. Wieghardt, S. Brodka, E. M. Peters, K. Peters, A. Simon, *Z. Naturforsch.*, 1987, *42b*, 279.
41. C. J. Pedersen, *J. Amer. Chem. Soc.*, 1967, *89*, 7017.
42. M. Mercer, M. R. Truter, *J. Chem. Soc., Dalton Trans.*, 1973, 2469.
43. M. Truter, *Struct. Bonding*, 1973, *16*, 71.

44. E. Maverick, P. Seiler, W. B. Schweizer, J. D. Dunitz, *Acta Crystallogr., Sect. B*, 1980, *B36*, 615.
45. J. D. Dunitz, P. Seiler, *Acta Crystallogr., Sect. B*, 1974, *B30*, 2339.
46. J. Dale, *Acta Chem. Scand.*, 1973, *27*, 1115.
47. J. Dale, P. O. Kristiansen, *Acta Chem. Scand.*, 1972, *26*, 1471.
48. G. Wipff, P. Weiner, P. Kollman, *J. Am. Chem. Soc.*, 1982, *104*, 3249.
49. S. G. Bott, H. Prinz, A. Alvanipour, J. L. Atwood, *J. Coord. Chem.*, 1987, *16*, 303.
50. H. Prinz, S. G. Bott, J. L. Atwood, *J. Am. Chem. Soc.*, 1986, *108*, 2113.
51. S. G. Bott, U. Kynast, J. L. Atwood, *J. Incl. Phenom.*, 1985, *2*, 367.
52. B. Dietrich, J.-M. Lehn, J. P. Sauvage, *Tetrahedron Lett.*, 1969, 2885.
53. B. Dietrich, J.-M. Lehn, J. P. Sauvage, *Tetrahedron Lett.*, 1969, 2889.
54. H. E. Simmons, C. H. Park, *J. Am. Chem. Soc.*, 1968, *90*, 2428.
55. B. Metz, D. Moras, R. Weiss, *J. Chem. Soc. Perkin Trans. 2*, 1976, 423.
56. D. Moras, B. Metz, R. Weiss, *Acta Crystallogr., Series B*, 1973, *B29*, 396.
57. D. Moras, B. Metz, R. Weiss, *Acta Crystallogr., Series B*, 1973, *B29*, 383.
58. B. Metz, D. Moras, R. Weiss, *J. Chem. Soc., Chem. Commun.*, 1970, 217.
59. B. Metz, D. Moras, R. Weiss, *J. Chem. Soc., Chem. Commun.*, 1971, 444.
60. B. Metz, R. Weiss, *Inorg. Chem.*, 1974, *13*, 2094.
61. E. Mei, A. I. Popov, J. L. Dye, *J. Am. Chem. Soc.*, 1977, *99*, 6532.
62. E. P. Kyba, C. W. Hudson, M. J. McPhaul, A. M. John, *J. Am. Chem. Soc.*, 1977, *99*, 8053.
63. T. A. DelDonno, W. Rosen, *J. Am. Chem. Soc.*, 1977, *99*, 8051.
64. C. A. McAuliffe, *Comprehensive Coordination Chemistry*, Pergamon Press, 1987, *2*, 1003.
65. R. E. Davis, C. W. Hudson, E. P. Kyba, *J. Am. Chem. Soc.*, 1978, *100*, 3643.
66. W. Mansfield, *Ber.*, 1886, *19*, 696.
67. W. Rosen, D. H. Busch, *J. Chem. Soc. Chem. Commun.*, 1969, 148.

68. W. Rosen, D. H. Busch, *Inorg. Chem.*, 1970, 9, 262.
69. D. St C. Black, I. A. McLean, *Aust. J. Chem.*, 1969, 22, 3961.
70. J. Butler, R. M. Kellog, *J. Chem. Soc., Chem. Commun.*, 1980, 466.
71. J. Butler, R. M. Kellog, *J. Org. Chem.*, 1981, 46, 4481.
72. J. Butler, R. M. Kellog, *Org. Synth.*, 1987, 65, 150.
73. T. Weiss, G. Klar, *Z. Naturforsch. B Anorg. Chem.*, 1979, 34B, 448.
74. S. J. Loeb, G. K. H. Shimizu, *J. Chem. Soc., Chem Commun.*, 1991, 1119.
75. S. E. Livingstone, *Quart. Rev.*, 1965, 16, 386.
76. M. A. Ali, S. E. Livingstone, *Coord. Chem. Rev.*, 1974, 13, 101.
77. C. A. McAuliffe, *Adv. Inorg. Radiochem.*, 1975, 17, 165.
78. C. G. Kuehn, S. S. Isied, *Prog. Inorg. Chem.*, 1980, 27, 153.
79. S. G. Murray, F. R. Hartley, *Chem. Rev.*, 1981, 81, 365.
80. A. G. Orpen, N. G. Connelly, *J. Chem. Soc., Chem., Commun.*, 1985, 1310.
81. S. R. Cooper, S. C. Rawle, *Struct. Bonding*, 1990, 72, 1.
82. H.-J. Kuppers, K. Wiegardt, B. Nuber, J. Weiss, *Z. Anorg. Allg. Chem.*, 1989, 577, 155.
83. A. J. Blake, M. Schroder, *Adv. Inorg. Chem.*, 1990, 35, 1.
84. S. R. Cooper, *Acc. Chem. Res.*, 1988, 21, 141.
85. M. Schroder, *Pure Appl. Chem.*, 1988, 60, 517.
86. R. S. Glass, G. S. Wilson, W. N. Setzler, *J. Am. Chem. Soc.*, 1980, 102, 5068.
87. W. N. Setzler, C. A. Ogle, G. S. Wilson, R. S. Glass, *Tetrahedron*, 1981, 37, 2743.
88. H.-J. Kuppers, B. Nuber, J. Weiss, S. R. Cooper, *J. Chem. Soc., Chem., Commun.*, 1990, 979.
89. W. N. Setzler, C. A. Ogle, G. S. Wilson, R. S. Glass, *Inorg. Chem.*, 1983, 22, 266.
90. J. A. Clarkson, R. Yaghasan, P. J. Blower, S. C. Rawle, S. C. Cooper, *J. Chem. Soc., Chem. Commun.*, 1989, 1244.

91. A. J. Blake, R. O. Gould, A. J. Holder, T. I. Hyde, G. Reid, M. Schroder, *J. Chem. Soc., Dalton Trans.*, 1990, 1759.
92. G. H. Robinson, S. A. Sangokoya, *J. Am. Chem. Soc.*, 1988, *110*, 1494.
93. G. R. Brubaker, D. W. Johnson, *Inorg. Chem.*, 1984, *23*, 1591.
94. G. H. Robinson, S. A. Sangokoya, *J. Am. Chem. Soc.*, 1988, *110*, 1494.
95. A. J. Blake, M. Schroder, *Adv. Inorg. Chem.* 1990, *35*, 45.
96. V. B. Pett, L. L. Diaddario, E. R. Dockal, P. W. Corfield, C. Ceccarelli, M. D. Glick, L. A. Ochrymowycz, D. B. Rorabacher, *Inorg. Chem.*, 1983, *22*, 3661.
97. R. E. Simone, M. D. Glick, *J. Am. Chem. Soc.*, 1976, *98*, 762.
98. N. W. Alcock, N. Herron, P. Moore, *J. Chem. Soc., Dalton Trans.*, 1978, 394.
99. N. W. Alcock, N. W. Herron, P. Moore, *J. Chem. Soc., Chem. Commun.*, 1976, 886.
100. N. Galesic, M. Heroeg, D. Sevdic, *Acta Cryst.*, 1986, *c42*, 565.
101. R. E. Wolf, J. R. Hartman, J. M. E. Storey, B. M. Foxman, S. R. Cooper, *J. Am. Chem. Soc.*, 1987, *109*, 4328.
102. A. J. Blake, J. A. Greig, M. Schroder, *Adv. Inorg. Chem.*, 1990, *35*, 58.
103. P. W. R. Corfield, C. Ceccarelli, M. D. Glick, I. W. Moy, L. A. Ochrymowycz, D. B. Rorabacher, *J. Am. Chem. Soc.*, 1985, *107*, 2399.
104. W. N. Setzer, Y. Tang, G. J. Grant, D. G. VanDerveer, *Inorg. Chem.*, 1992, *31*, 1116.
105. A. J. Blake, R. O. Gould, G. Reid, M. Schroder, *J. Chem. Soc., Chem. Commun.*, 1990, 974.
106. R. O. Gould, A. J. Lavery, M. Schroder, *J. Chem. Soc., Chem. Commun.*, 1985, 1492.
107. J. A. Hartman, E. J. Hints, S. R. Cooper, *J. Am. Chem. Soc.*, 1986, *108*, 1208.
108. R. D. Rogers, L. Nunez, *J. Coord. Chem.*, 1990, *21*, 111.
109. J. E. Richman, T. J. Atkins, *J. Am. Chem. Soc.*, 1974, *96*, 2268.
110. M. C. Thompson, D. H. Busch, *J. Am. Chem. Soc.*, 1964, *86*, 3651.
111. N. W. Alcock, P. Moore, C. J. Reader, S. M. Roe, *J. Chem. Soc., Dalton Trans.*, 1988, 2959.

112. J. J. Christensen, D. J. Eatough, R. M. Izatt, *Chem. Rev.*, 1974, **74**, 351.
113. P. Chaudhuri, K. Weighardt, *Prog. Inorg. Chem.*, 1987, **35**, 329.
114. J.-M. Lehn, *Structure and Bonding*, 1973, **16**, 1.
115. *Coordination Chemistry of Macrocyclic Compounds*, Ed. G. A. Melson, Plenum Press, 1979.
116. N. F. Curtis, *Coord. Chem. Rev.*, 1968, **3**, 3.
117. G. W. Gokel, H. D. Durst, *Synthesis*, 1976, **8**, 168.
118. D. Sellmann, L. Zapf, *Angew. Chem., Int. Ed. Engl.*, 1984, **23**, 807.
119. P. J. Blower, S. R. Cooper, *Inorg. Chem.*, 1987, **26**, 2009.
120. W. Rosen, D. H. Busch, *Inorg. Chem.*, 1974, **13**, 2591.
121. G. H. Searle, R. J. Geue, *Aust. J. Chem.*, 1984, **37**, 959.
122. E. K. Barefield, G. Freeman, *Inorganic Syntheses*, 1980, **20**, 108.
123. C. J. Pedersen, *Organic Syntheses*, 1972, **52**, 66.
124. G. H. Robinson, H. Zhang, J. L. Atwood, *Organometallics*, 1987, **6**, 887.
125. K. Wiegardt, M. Kleine-Boymann, B. Nuber, J. Weiss, *Inorg. Chem.* 1986, **25**, 1654.
126. N. W. Alcock, M. Ravindran, S. M. Roe, G. R. Willey, *Inorg. Chim. Acta*, 1990, **167**, 115.
127. N. W. Alcock, M. Ravindran, G. R. Willey, *J. Chem. Soc. Chem. Commun.*, 1989, 1063.
128. N. W. Alcock, M. Ravindran, G. R. Willey, *Acta Crystallogr.*, 1993, accepted for publication.
129. E. Hough, D. G. Nicholson, A. K. Vasudevan, *J. Chem. Soc. Dalton Trans.*, 1987, 427.
130. M. G. B. Drew, D. G. Nicholson, I. Syka, A. Vasudevan, *Inorg. Chim. Acta*, 1990, **171**, 11.
131. H.-J. Kuppers, K. Wiegardt, Y.-H. Tsay, C. Krugger, B. Nuber, J. Weiss, *Angew. Chem. Int. Ed. Engl.*, 1987, **26**, 575.
132. A. J. Blake, J. A. Greig, M. Schroder, *J. Chem. Soc. Dalton Trans.*, 1991, 529.
133. M. G. B. Drew, J. M. Kiasnyi and G. R. Willey, *J. Chem. Soc., Dalton Trans.*, 1982, 1729.

134. M. Schmidt, R. Bender and Ch. Burschka, *Z. Anorg. Allg. Chem.*, 1979, **454**, 160.
135. N. W. Alcock, *Adv. Inorg. Chem. Radiochem.*, 1972, **15**, 4.
136. J. Dale, *Acta Chim. Scand.*, 1973, **27**, 1115.
137. R. E. Wolf, J. R. Hartman, J. M. E. Storey, B. M. Foxman, S. R. Cooper, *J. Am. Chem. Soc.*, 1987, **109**, 4328.
138. E. Juaristi, *J. Chem. Educ.*, 1979, **56**, 438.
139. G. R. Brubaker, D. W. Johnson, *Coord. Chem. Rev.*, 1984, **53**, 1.
140. G. R. Brubaker, D. W. Johnson, *Inorg. Chem.*, 1984, **23**, 1591.
141. W. N. Setzer, Y. Tang, G. J. Grant, D. G. VanDerveer, *Inorg. Chem.*, 1992, **31**, 1116.
142. J. J. Gajewski, K. E. Gilbert, J. McKelvey, *Advances in Molecular Modelling*, 1990, **2**, 65.
143. M. Walter, L. Ramaley, *Anal. Chem.*, 1973, **45**, 165.
144. S. C. Rawle, D. Phil. Thesis, University of Oxford, 1988.
145. Serena Software, Box 3076, Bloomington, Indiana 47402-3076, USA.
146. N. L. Allinger, *J. Am. Chem. Soc.*, 1977, **98**, 8127.
147. G. M. Sheldrick, *SHELXTL PLUS*, user's manual, Nicolet Instrument Co., Madison, Wis, 1986.
148. *International Tables for X-Ray Crystallography*, Kynoch Press, Birmingham, 1974, vol. 4 (present distributor Kluwer Academic Publishers, Dordrecht).
149. R. E. DeSimone, M. D. Glick, *J. Am. Chem. Soc.*, 1975, **97**, 942.
150. R. E. Simone, M. D. Glick, *J. Coord. Chem.*, 1976, **5**, 181.
151. R. E. Simone, T. M. Tighe, *J. Inorg. Nucl. Chem.*, 1976, **38**, 1623.
152. M. Ciampolini, C. Mealli, N. Nardi, *J. Chem. Soc. Dalton Trans.*, 1980, 376.
153. R. G. Pearson, *J. Am. Chem. Soc.*, 1963, **85**, 3533.
154. H.-J. Kuppers, K. Weighardt, *Polyhedron*, 1989, **8**, 1770.
155. K. L. Baker, G. W. A. Fowles, *Proc. Chem. Soc. London*, 1964, 362.
156. H. S. Ahuja, S. C. Jain, R. Rivest, *J. Inorg. Nucl. Chem.*, 1968, **30**, 2459.

157. A. D. Westland, L. Westland, *Can. J. Chem.*, 1965, **43**, 426.
158. K. L. Baker, G. W. A. Fowles, *J. Chem. Soc.*, 1964, 4330.
159. R. J. H. Clark, W. Errington, *Inorg. Chem.*, 1966, **5**, 650.
160. D. L. Hughes, G. J. Leigh, D. G. Walker, *J. Chem. Soc. Dalton Trans.*, 1989, 1413.
161. A. J. Blake, R. O. Gould, A. J. Holder, T. I. Hyde, M. O. Odulate, M. Schroder, *J. Chem. Soc. Chem. Commun.*, 1987, 118.
162. The terminologies used to describe the strain energies were defined in Chapter 2.
163. R. J. H. Clark, *Spectrochimica Acta*, 1965, **21**, 955.
164. M. W. Duckworth, G. W. A. Fowles, P. T. Greene, *J. Chem. Soc. A*, 1967, 1592.
165. R. J. H. Clark, G. Natile, *Inorg. Chim. Acta*, 1970, **4**, 533.
166. P. C. Crouch, G. W. A. Fowles, R. A. Walton, *J. Chem. Soc. A*, 1968, 2172.
167. A. Belforte, F. Calderazzo, P. F. Zanazzi, *Gazz. Chim.*, 1985, **115**, 71.
168. H.-J. Kuppers, B. Nuber, J. Weiss, S. R. Cooper, *J. Chem. Soc. Chem. Commun.*, 1990, 979.
169. M. R. Caira, B. J. Gellatly, *Acta Crystallogr.* 1980, **B36**, 1198.
170. J. E. Drake, J. Vekris, J. S. Wood, *J. Chem. Soc. (A)*, 1968, 1000.
171. J. Coetzer, *Acta Crystallogr.* 1970, **B26**, 872.
172. L. V. Boas, J. C. Pessoa, in *Comprehensive Coordination Chemistry*, 1987, **3**, 453, Pergamon Press, Oxford.
173. J. K. Money, J. C. Huffman, G. Christou, *Inorg. Chem.*, 1985, **24**, 3297.
174. T. S. Khodashova, M. A. Porai-Koshits, V. S. Sergienko, L. A. Butman, Y. A. Buslaev, V. V. Kovalev, A. A. Kuznetsova, *Koord. Khim.*, 1978, **4**, 1909.
175. S. Gambarotta, A. Chiesi-Villa, C. Guatini, *Inorg. Chem.*, 1988, **27**, 99.
176. R. D. Shannon, *Acta Crystallogr.*, 1976, **A32**, 751.
177. J. R. Nicholson, J. C. Huffman, D. M. Ho, G. Christou, *Inorg. Chem.* 1987, **26**, 3030.
178. L. E. Manzer, *Inorganic Syntheses*, 1982, **21**, 135.

179. E. K. Barefield, F. Wagner, *Inorg. Chem.*, 1973, **12**, 2435.
180. M. J. D'Aniello, M. T. Mocella, A. F. Wagner, E. K. Barefield, I. C. Paul, *J. Am. Chem. Soc.*, 1975, **97**, 192.
181. F. Wagner, E. K. Barefield, *Inorg. Chem.*, 1976, **15**, 408.
182. F. Wagner, M. T. Mocella, M. J. D'Aniello, A. H. J. Wang, E. K. Barefield, *J. Am. Chem. Soc.*, 1974, **96**, 2625.
183. R. Buxtorf, T. A. Kaden, *Helv. Chim. Acta*, 1974, **57**, 1035.
184. M. Micheloni, P. Paoletti, S. Burki, T. A. Kaden, *Helv. Chim. Acta*, 1982, **65**, 587.
185. P. Moore, J. Sachinidis, G. R. Willey, *J. Chem. Soc. Chem. Commun.*, 1983, 522.
186. S. F. Lincoln, D. L. Pisaniello, J. H. Coates, D. A. Hadi, *Inorg. Chim. Acta*, 1984, **81**, L9.
187. G. H. Robinson, H. Zhang, J. L. Atwood, *J. Organomet. Chem.* 1987, **331**, 153.
188. B. Lee, W. T. Pennington, G. H. Robinson, R. D. Rogers, *J. Organomet. Chem.*, 1990, **396**, 269.
189. Chi-Ming Che, Ting-Fong Lai, K. Lau, T. C. W. Mak., *J. Chem. Soc. Dalton Trans.*, 1988, 239.
190. Chi-Ming Che, Kwok-Yin Wong, T. C. W. Mak, *J. Chem. Soc., Chem. Commun.*, 1985, 546.
191. S. F. Lincoln, T. W. Hambley, D. L. Pisaniello, J. H. Coates, *Aust. J. Chem.*, 1984, **37**, 713.
192. M. Kato, T. Ito, *Bull. Chem. Soc. Jpn.*, 1986, **59**, 285.
193. T. W. Hambley, *J. Chem. Soc. Dalton Trans.*, 1986, 565.
194. I. S. Crick, B. F. Hoskins, P. A. Tregloan, *Inorg. Chim. Acta*, 1986, **114**, L33.
195. I. S. Crick, R. W. Gable, B. F. Hoskins, P. A. Tregloan, *Inorg. Chim. Acta*, 1986, **111**, 35.
196. F. Wagner, M. T. Mocella, M. J. D'Aniello, A. H. Wang, E. K. Barefield, *J. Am. Chem. Soc.*, 1974, **96**, 2625.
197. E. K. Barefield, G. M. Freeman, D. G. Van Derveer, *Inorg. Chem.*, 1986, **25** 552.



198. M. Hall, D. B. Sowerby, *J. Chem. Soc. Chem. Commun.*, 1979, 1134.
199. A. L. Rheingold, A. G. Landers, *J. Chem. Soc. Chem. Commun.*, 1979, 143.
200. F. Pertlik, *Monatsh. Chem.* 1975, 106, 755.
201. J. C. Dewan, K. Hendrick, A. H. White, S. B. Wild, *Aust. J. Chem.*, 1975, 28, 15.
202. J. Kaub, W. S. Sheldrick, *Z. Naturforsch.*, 1984, 39b, 1252.
203. M. R. Churchill, A. G. Landers, A. L. Rheingold, *Inorg. Chem.*, 1981, 20, 849.
204. D. C. Weatherburn, E. J. Billo, J. P. Jones, D. W. Margerum, *Inorg. Chem.*, 1970, 9, 1557.
205. M. Micheloni, A. Sabatini, P. Paoletti, *J. Chem. Soc. Perkin II*, 1978, 828.
206. G. H. Robinson, S. A. Sangokoya, W. T. Pennington, M. R. Self, R. D. Rogers, *J. Coord. Chem.* 1989, 19, 287.
207. C. Nave, M. R. Truter, *J. Chem. Soc. Dalton Trans.*, 1974, 2351.
208. M. Studer, A. Riesen, T. A. Kaden, *Helv. Chim. Acta*, 1989, 72, 1253.
209. A. J. Blake, J. A. Greig, M. Schroder, *Acta Crystallogr.*, 1990, C46, 322.
210. F. A. Momany, R. Rone, *J. Computational Chem.*, 1992, 13, 888.
211. J. Roziere, C. Belin, M. S. Lehman, *J. Chem. Soc. Chem. Commun.*, 1982, 388.
212. R. W. Alder, P. Eastment, N. M. Hext, R. E. Moss, A. G. Orpen, J. M. White, *J. Chem. Soc. Chem. Commun.*, 1988, 1528.
213. E. K. Barefield, F. Wagner, *Inorg. Chem.*, 1973, 12, 2435.
214. E. K. Barefield, F. Wagner, A. W. Herlinger, A. R. Dahl, *Inorg. Synth.*, 1976, 16, 220.
215. K. A. Jensen, *Z. Anorg. Chem.*, 1943, 250, 264.
216. S. M. Ohlberg, *J. Am. Chem. Soc.*, 1959, 81, 811.
217. U. Muller: *Z. Anorg. Allg. Chem.*, 1976, 422, 141.
218. A. P. Zurr, W. L. Groenwald, *Rec. Trav. Chim. Pays Bas*, 1967, 86, 108.
219. J. Reedyk, A. P. Zurr, W. L. Groenwald, *Rec. Trav. Chim. Pays Bas*, 1967, 86, 1127.
220. A. P. Zurr, J. J. Van Houte, W. L. Groenwald, *Rec. Trav. Chim. Pays Bas*, 1968, 87, 755.

221. P. P. K. Claire, G. R. Willey, M. G. B. Drew, *J. Chem. Soc., Chem. Commun.*, 1987, 1100.
222. G. R. Willey, J. Palin, N. W. Alcock, *J. Chem. Soc. Dalton Trans.*, 1992, 1117.
223. G. R. Willey, J. Palin, unpublished results, 1992.
224. G. R. Willey and others, unpublished work, 1991.
225. J. Holmes, R. Pettit, *J. Org. Chem.*, 1963, 28, 1695.
226. H. Volz, *Tetrahedron Lett.*, 1964, 28, 1899.
227. G. A. Olah, S. J. Kuhn, W. S. Tolygesi, E. B. Baker, *J. Am. Chem. Soc.*, 1962, 84, 2733.
228. J. M. Le Carpentier, R. Weiss, *J. Chem. Soc. Chem. Comm.*, 1968, 598.
229. B. Chevrier, J. M. Le Carpentier, R. Weiss, *J. Am. Chem. Soc.*, 1972, 94, 5718.
230. G. R. Willey, H. Collins, M. G. B. Drew, *J. Chem. Soc. Dalton Trans.*, 1991, 961.
231. G. W. Powell, A. Ledwith, A. C. White, H. J. Woods, *J. Chem. Soc. (B)*, 1970, 227.
232. J.-C. G. Bunzli, D. Wessner, *Coord. Chem. Rev.*, 1984, 60, 191.
233. R. D. Rogers, R. D. Etzenhouser, J. S. Murdoch, E. Reyes, *Inorg. Chem.*, 1991, 30, 1445.
234. M. Ciampolini, P. Dapporto, N. Nardi, *J. Chem. Soc. Chem. Commun.*, 1978, 788.
235. J.-C. Bunzli, B. Klein, D. Wessner, N. W. Alcock, *Inorg. Chim. Acta*, 1982, 59, 269.
236. J.-C. G. Bunzli, D. Wessner, *Inorg. Chim. Acta*, 1980, 44, L55.
237. R. D. Rogers, *J. Coord. Chem.*, 1988, 16, 415.
238. R. D. Rogers, A. N. Rollins, M. M. Benning, *Inorg. Chem.*, 1988, 27, 3826.
239. J.-C. G. Bunzli, B. Klein, G. Chapuis, K. J. Schenk, *Inorg. Chem.*, 1982, 21, 808.
240. T. J. Lee, H.-R. Sheu, T. I. Chiu, C. T. Chang, *Inorg. Chim. Acta*, 1984, 94, 43.
241. J.-C. G. Bunzli, B. Klein, D. Wessner, *Inorg. Chim. Acta*, 1980, 44, L147.

242. J. D. J. Backer-Dirks, J. E. Cooke, A. M. R. Galas, J. S. Ghotra, C. J. Gray, F. A. Hart, M. B. Hursthouse, *J. Chem. Soc., Dalton Trans.*, 1980, 2191.
243. R. D. Rogers, L. K. Kurihara, *Inorg. Chem.*, 1987, 26, 1498.
244. J. Zhong-Sheng, L. Yong-Sheng, Z. Shu-Gong, Y. Feng-Lan, N. Jia-Zan, *Acta Chim. Sinica*, 1987, 45, 1048.
245. T. Minyu, G. Xinmin, T. Ning, Z. Jinping, *Gaddeng Xuexiao Huaxue Xuebao* (Chem. J. Chin. Univ.), 1988, 45, 1217.
246. J. L. Atwood, S. G. Bott, C. M. Means, W. W. Coleman, H. Zhang, M. T. May, *Inorg. Chem.*, 1990, 29, 467.
247. R. D. Rogers, A. H. Bond, W. G. Hipple, A. N. Rollins, R. F. Henry, *Inorg. Chem.*, 1991, 30, 2671.
248. K. M. Dohsee, H. R. Wierman, T. J. R. Weakley, *J. Am. Chem. Soc.*, 1992, 114, 5165.
249. R. D. Shannon, *Acta Crystallogr.*, 1976, A32, 751.
250. N. R. Strel'tsova, L. V. Ivakina, P. A. Storozhenko, B. M. Bulychev, V. K. Bel'skii, *Sov. Phys. Dokl. (Engl. Transl.)*, 1986, 31, 943.
251. D. D. McRitchie, R. C. Palenik, G. J. Palenik, *Inorg. Chim. Acta*, 1976, 20, L27.
252. F. Matsumoto, Y. Ohki, Y. Suzuki, A. Ouchi, *Bull. Chem. Soc. Jpn.*, 1989, 62, 2081.
253. J. L. Atwood, K. D. Smith, *J. Chem. Soc. Dalton Trans.*, 1974, 921.
254. O. W. Howarth, G. K. Fraenkel, *J. Am. Chem. Soc.*, 1966, 88, 4514.
255. J. Palin, M. D. Rudd, unpublished results, 1992.
256. D. A. Atwood, S. G. Bott, J. L. Atwood, *J. Coord. Chem.*, 1987, 17, 93.
257. J. D. Owen, *J. Chem. Soc. Dalton Trans.*, 1978, 1418.
258. F. H. Allen, O. Kennard, D. G. Watson, L. Brammer, A. G. Orpen, R. Taylor, *J. Chem. Soc. Perkin Trans. II*, 1987, S1.
259. I. R. Hanson, *Acta Crystallogr.* 1978, B34, 1026.
260. M. A. Bush, M. R. Truter, *J. Chem. Soc. Perkin II*, 1972, 341.
261. C. J. Pedersen, *J. Am. Chem. Soc.*, 1967, 89, 7017.

# APPENDIX

## $\text{SbCl}_3 \cdot 9\text{S}_3$

Atom coordinates ( $\times 10^4$ ) and isotropic thermal parameters

Atom	x	y	z	U	( $\text{\AA}^2 \times 10^{-3}$ )
Sb(1)	4589.1(8)	4011.5(6)	-994.8(3)	31(1)*	
Cl(1)	2130(3)	5250(3)	-1538(2)	48(1)*	
Cl(2)	4807.2(35)	3016.5(24)	-2339.0(13)	41(1)*	
Cl(3)	6847(4)	5508(3)	-1295(2)	50(1)*	
S(1)	6703.0(29)	4118.5(27)	836.2(14)	38(1)*	
S(2)	5498(14)	3479(9)	1696(6)	43(3)*	
S(3)	4047(13)	2574(9)	1470(7)	45(3)*	
S(4)	2446.4(31)	3172.8(22)	742.8(14)	34(1)*	
S(5)	1590(13)	4627(9)	1224(5)	37(3)*	
C(6)	1588(12)	5818(9)	667(5)	34(3)*	
S(7)	3651.7(33)	6287.0(23)	230.4(14)	36(1)*	
C(8)	5005(13)	6526(9)	1123(7)	47(4)*	
C(9)	6748(13)	5844(10)	1042(6)	43(3)*	

\* Equivalent isotropic U defined as one third of the trace of the orthogonalized  $U_{ij}$  tensor

## $(\text{SbCl}_3) \cdot 18\text{S}_6$

Atom coordinates ( $\times 10^4$ ) and isotropic thermal parameters

Atom	x	y	z	U	( $\text{\AA}^2 \times 10^{-3}$ )
Sb(1)	1711.3(6)	496.5(6)	2136.2(4)	41(1)*	
Cl(1)	-1625(2)	-815(3)	891(2)	67(1)*	
Cl(2)	683(3)	-936(3)	3655(2)	69(1)*	
Cl(3)	1086(3)	3296(3)	3237(3)	97(1)*	
S(1)	5398(2)	1353(2)	3832(2)	51(1)*	
C(2)	5974(10)	-263(11)	3074(7)	74(5)*	
C(3)	4436(12)	-2225(10)	2741(7)	74(5)*	
S(4)	2263(3)	-2856(3)	1559(2)	62(1)*	
C(5)	3022(10)	-2506(9)	228(6)	60(4)*	
C(6)	3386(9)	-3977(9)	-333(6)	55(4)*	
S(7)	4271(2)	-3586(3)	-1627(2)	60(1)*	
C(8)	2253(10)	-3849(11)	-2751(7)	76(4)*	
C(9)	2648(11)	-3525(11)	-3925(7)	82(4)*	

\* Equivalent isotropic U defined as one third of the trace of the orthogonalized  $U_{ij}$  tensor

**BiCl<sub>3</sub>·12S4**Atom coordinates ( $\times 10^4$ ) and isotropic thermal parameters

Atom	x	y	z	U ( $\text{\AA}^2 \times 10^3$ )
Bi(1)	501.8(5)	2332.3(3)	2164.1(2)	27(1)*
Cl(1)	1754(4)	2394(2)	741(2)	53(1)*
Cl(2)	-1449(4)	3877(2)	1623(2)	43(1)*
Cl(3)	-1723(4)	974(2)	1469(2)	49(1)*
S(1)	3099(3)	3953(2)	2867(2)	31(1)*
S(4)	-245(3)	3279(2)	3889(2)	39(1)*
S(7)	737(4)	694(2)	3756(2)	42(1)*
S(10)	3942(4)	1368(2)	2742(2)	37(1)*
C(2)	2880(14)	4318(8)	3984(7)	40(4)*
C(3)	1009(16)	4422(7)	4046(8)	47(4)*
C(5)	724(15)	2484(7)	4822(7)	40(4)*
C(6)	89(15)	1396(8)	4665(7)	46(4)*
C(8)	2990(15)	479(8)	4191(7)	44(4)*
C(9)	4188(15)	1249(8)	3931(8)	51(4)*
Cl(11)	5354(14)	2410(7)	2608(8)	44(4)*
C(12)	5223(13)	3381(7)	3094(7)	39(4)*

\* Equivalent isotropic U defined as one third of the trace of the orthogonalised  $U_{ij}$  tensor

**BiCl<sub>3</sub>·18S6**Atom coordinates ( $\times 10^4$ ) and isotropic thermal parameters

Atom	x	y	z	U ( $\text{\AA}^2 \times 10^3$ )
Bi	3520.6(3)	3520.6(3)	3520.6(3)	28(1)*
S(1)	5126(2)	3399(2)	4654(2)	42(1)*
S(2)	3374(2)	2549(2)	5171(2)	43(1)*
Cl(1)	3817(3)	2011(2)	3116(2)	46(1)*
Cl(1)	6047(8)	3324(9)	4018(9)	41(5)*
C(2)	5048(9)	2366(10)	5003(10)	51(6)*
C(3)	4373(11)	2321(11)	5629(10)	60(6)*
C(4)	2918(10)	3197(9)	5940(9)	48(5)*

\* Equivalent isotropic U defined as one third of the trace of the orthogonalised  $U_{ij}$  tensor

**BiCl<sub>3</sub>·15S5-½MeCN**

Atom coordinates (x10<sup>4</sup>) and isotropic thermal parameters

Atom	x	y	z	U (Å <sup>2</sup> ×10 <sup>3</sup> )
Bi(1)	1681.0(5)	2940.3(5)	1920.2(3)	33(1)*
Bi(2)	6579.9(5)	1430.2(5)	616.1(3)	33(1)*
Cl(11)	2885(4)	2221(4)	2283(2)	59(3)*
Cl(12)	779(4)	1886(4)	2357(2)	55(3)*
Cl(13)	1749(4)	1934(4)	1271(2)	61(3)*
Cl(21)	5951(3)	151(4)	227(2)	47(2)*
Cl(22)	6873(4)	540(4)	1308(2)	54(2)*
Cl(23)	7878(4)	970(5)	245(3)	61(3)*
S(11)	2581(3)	4411(4)	2462(2)	39(2)*
S(12)	604(3)	4299(4)	2471(2)	41(2)*
S(13)	-46(4)	3116(4)	1565(2)	45(2)*
S(14)	1348(3)	4499(4)	1261(2)	46(2)*
S(15)	3131(3)	3659(4)	1450(2)	48(2)*
C(11)	1925(14)	5166(15)	2728(7)	44(9)*
C(12)	1155(12)	5273(12)	2481(8)	33(8)*
C(13)	-178(14)	4566(17)	2110(9)	63(11)*
C(14)	-592(13)	3760(16)	1923(9)	54(10)*
C(15)	-86(14)	3808(15)	1065(7)	45(9)*
C(16)	724(15)	3953(18)	905(9)	65(12)*
C(17)	2187(18)	4725(20)	953(9)	84(15)*
C(18)	2814(16)	4052(18)	932(10)	75(13)*
C(19)	3529(13)	4599(15)	1758(9)	59(11)*
C(110)	2965(13)	5097(15)	2024(8)	51(10)*
S(21)	5063(4)	2244(5)	51(2)	61(3)*
S(22)	4973(4)	1281(4)	1061(2)	43(2)*
S(23)	6035(3)	3112(4)	1286(2)	41(2)*
S(24)	7854(4)	2626(5)	1001(2)	52(3)*
S(25)	6919(4)	2518(5)	-23(3)	67(3)*
C(21)	4405(13)	2554(15)	495(7)	40(9)*
C(22)	4193(14)	1734(17)	759(9)	65(12)*
C(23)	4968(16)	1832(15)	1573(8)	58(11)*
C(24)	5140(12)	2815(16)	1559(7)	46(10)*
C(25)	6770(12)	2763(15)	1682(7)	43(6)*
C(26)	7570(12)	3057(16)	1524(8)	55(10)*
C(27)	7731(24)	3612(20)	669(10)	128(19)*
C(28)	7672(19)	3541(21)	217(12)	105(18)*
C(29)	6032(18)	3633(17)	21(13)	100(16)*
C(210)	5397(17)	3237(20)	-138(16)	129(23)*
N(001)	10189(19)	-158(18)	768(11)	95(15)*
C(001)	9834(25)	283(23)	992(11)	86(18)*
C(002)	9331(26)	749(26)	1258(13)	132(21)*

\* Equivalent isotropic U defined as one third of the trace of the orthogonalised U<sub>ij</sub> tensor

[VOCl<sub>2</sub>(9S3)]

Atom coordinates (x10<sup>4</sup>) and isotropic thermal parameters

Atom	x	y	z	U
V(1)	7453.4(9)	2338.2(11)	7750.2(8)	33(1)*
O(1)	7483(4)	3082(8)	8774(3)	56(2)*
Cl(11)	8037.4(17)	3565.1(18)	7747.7(14)	52(1)*
Cl(12)	8704(2)	872(2)	7244(2)	50(1)*
Cl(13)	6408.9(17)	3873.7(17)	7735.2(14)	46(1)*
C(12)	6660(7)	4518(7)	6694(5)	42(3)*
C(13)	6647(7)	3834(6)	6884(6)	45(3)*
H(14)	7510.8(14)	2705.0(16)	6020.4(12)	31(1)*
C(15)	6678(6)	1428(6)	5640(5)	43(3)*
C(16)	5688(8)	1440(7)	6150(8)	39(3)*
H(17)	5584.8(18)	1327.7(18)	7382.4(14)	38(1)*
C(18)	8003(4)	2188(7)	7873(5)	47(3)*
C(19)	5085(6)	2337(7)	7562(6)	50(3)*
V(2)	2890.3(9)	2879.2(9)	4822.5(8)	24(1)*
O(2)	2375(4)	2841(4)	3603(3)	42(2)*
Cl(21)	3982.5(18)	2727.7(18)	5049.4(13)	40(1)*
Cl(22)	3883.8(16)	1113.1(16)	4613.0(15)	46(1)*
H(21)	1207.7(15)	3928.3(18)	4990.9(13)	34(1)*
C(22)	877(4)	3547(7)	6175(5)	42(3)*
C(23)	1954(6)	3584(6)	6759(5)	40(3)*
H(24)	2508.7(14)	2340.1(15)	6382.6(12)	31(1)*
C(25)	1431(8)	1428(6)	6591(5)	38(3)*
C(26)	1228(6)	495(6)	5831(5)	40(3)*
H(27)	1083.7(18)	1332.4(18)	6734.4(13)	34(1)*
C(28)	-126(4)	2148(6)	4821(6)	35(3)*
C(29)	26(6)	2255(6)	4578(5)	41(3)*

\* Equivalent isotropic U defined as one third of the trace of the orthogonalized U<sub>ij</sub> tensor

[H<sub>2</sub>(TMC)][Sb<sub>2</sub>OCl<sub>4</sub>]

Atom coordinates (x10<sup>4</sup>) and isotropic thermal parameters

Atom	x	y	z	U
Sb(1)	11100.1(7)	-3824.2(6)	-1210.0(6)	37(1)*
Sb(2)	10739.0(7)	-1376.8(6)	-3213.7(5)	34(1)*
Cl(1)	10059(2)	521(2)	-2658(3)	52(1)*
Cl(2)	8254(2)	-1990(3)	-1442(3)	58(1)*
Cl(3)	10547(3)	-2746(3)	55(2)	51(1)*
Cl(4)	11603(2)	-3825(3)	-3863(3)	61(1)*
Cl(5)	13167(3)	-1107(3)	-4445(2)	55(1)*
Cl(6)	13709(3)	-4452(3)	-1108(3)	64(1)*
O(1)	11626(7)	-2114(6)	-2050(5)	35(2)*
H(11)	4867(8)	1368(8)	-1405(7)	35(4)*
H(12)	3798(9)	-697(8)	-748(7)	36(4)*
C(11)	3548(13)	2342(11)	-1397(11)	57(6)*
C(12)	5465(12)	923(10)	-2498(9)	49(5)*
C(13)	4441(14)	218(11)	-2731(9)	54(6)*
C(14)	4397(12)	-828(11)	-1998(9)	50(5)*
C(15)	2126(11)	-123(11)	-482(11)	51(5)*
C(16)	4209(12)	-1827(9)	-64(9)	48(5)*
Cl(17)	3887(12)	-1721(10)	1145(9)	47(5)*
H(21)	8214(8)	4746(7)	-3523(7)	52(3)*
H(22)	8288(8)	4893(7)	-5255(6)	51(3)*
C(21)	8042(12)	5223(10)	-2475(9)	48(5)*
C(22)	6899(10)	4861(9)	-3484(9)	42(4)*
C(23)	5908(11)	6105(9)	-4108(9)	40(4)*
C(24)	4772(11)	4528(9)	-5247(9)	39(4)*
C(25)	8110(13)	7610(10)	-4738(10)	50(5)*
C(26)	9214(11)	6662(9)	-6423(8)	37(4)*
C(27)	9140(10)	3814(9)	-3481(9)	35(4)*

\* Equivalent isotropic U defined as one third of the trace of the orthogonalized U<sub>ij</sub> tensor

**[H<sub>2</sub>(TMC)][As<sub>4</sub>O<sub>2</sub>Cl<sub>10</sub>]**

Atom coordinates (x10<sup>4</sup>) and isotropic thermal parameters

Atom	x	y	z	u (Å <sup>2</sup> ×10 <sup>3</sup> )
As(1)	4082.2(4)	1445.1(4)	1268.1(4)	38(1)*
As(2)	6043.1(4)	1505.9(4)	1221.7(4)	40(1)*
Cl(11)	3816.4(13)	774.8(11)	1881.0(9)	56(1)*
Cl(12)	3620.3(14)	698.9(12)	170.9(9)	64(1)*
Cl(21)	6739.4(13)	792.2(13)	1852.2(10)	63(1)*
Cl(22)	6481.0(14)	894.0(12)	1448.8(9)	64(1)*
Cl(8)	5000.0	2800.0	2098.8(14)	59(1)*
Cl(4)	5000.0	2800.0	449.8(13)	80(1)*
O(1)	5088(3)	1008(3)	1316(3)	42(2)*
H(1)	6274(4)	-2424(3)	1254(3)	43(2)*
H(2)	5017(4)	-1293(4)	1422(3)	48(2)*
C(1)	6767(6)	-2367(8)	1783(8)	74(4)*
C(2)	6607(8)	-1936(9)	800(4)	81(3)*
C(3)	6409(8)	-1103(4)	940(4)	63(3)*
C(4)	5456(9)	-932(4)	914(3)	87(3)*
C(5)	5240(6)	-847(5)	1981(4)	71(4)*
C(6)	4061(9)	-1224(9)	1358(8)	74(4)*
C(7)	3700(6)	-1820(8)	899(4)	72(4)*

\* Equivalent isotropic U defined as one third of the trace of the orthogonalized U<sub>ij</sub> tensor

**Tetra-N-Methyl-1,4,8,11-Tetraazacyclotetradecane (TMC)**

Atom coordinates (x10<sup>4</sup>) and isotropic thermal parameters

Atom	x	y	z	u (Å <sup>2</sup> ×10 <sup>3</sup> )
N(11)	6387.1(18)	7399.6(15)	-268.1(14)	44(1)*
N(12)	2026.0(18)	8145.1(15)	1287.6(14)	42(1)*
C(11)	4768(3)	8834(2)	-1128(2)	46(1)*
C(12)	7724(3)	6259(2)	-474(3)	65(1)*
C(13)	4872(3)	7160(2)	-498(2)	55(1)*
C(14)	3321(2)	8127(2)	-110(2)	49(1)*
C(15)	2838(2)	6709(2)	2298(2)	58(1)*
C(16)	1891(2)	9194(2)	1548(2)	52(1)*
C(17)	1818(2)	10774(2)	762(2)	51(1)*
N(21)	2459(2)	17480(2)	-4873(2)	50(1)*
N(22)	3430.6(18)	13218.9(16)	-4263.9(14)	45(1)*
C(21)	4103(3)	18445(2)	-9021(2)	55(1)*
C(22)	1378(4)	18343(3)	-3720(3)	77(1)*
C(23)	3167(2)	16142(2)	-3828(2)	48(1)*
C(24)	1803(2)	15237(2)	-3464(2)	56(1)*
C(25)	2474(2)	13624(2)	-3063(2)	51(1)*
C(26)	2343(2)	13130(3)	-8078(2)	68(1)*
C(27)	4874(2)	11868(2)	-3843(2)	49(1)*

\* Equivalent isotropic U defined as one third of the trace of the orthogonalized U<sub>ij</sub> tensor



[ScCl<sub>3</sub>(Bz15O5)][SbCl<sub>4</sub>]

Atom coordinates ( $\times 10^4$ ) and isotropic thermal parameters  
( $\text{\AA}^2 \times 10^3$ )

Atom	x	y	z	U
Sb(1)	1260.4(2)	1709.3(3)	2311.1(2)	39(1)*
Sc(1)	8883.0(6)	2695.3(8)	-70.3(4)	33(1)*
Cl(1)	2417.7(11)	2695.2(14)	2308.6(8)	68(1)*
Cl(2)	117.0(11)	705.2(15)	2330.0(9)	75(1)*
Cl(3)	486.2(12)	3171.6(13)	2424.1(9)	66(1)*
Cl(4)	2020.5(11)	224.1(13)	2218.0(8)	67(1)*
Cl(5)	1173.4(15)	1865.5(15)	1274.6(8)	84(1)*
Cl(6)	1358.9(10)	1591.1(13)	3367.1(7)	60(1)*
Cl(7)	7524.3(8)	2231.6(12)	-117.1(7)	51(1)*
Cl(8)	10264.8(8)	3023.3(12)	06.1(7)	49(1)*
O(1)	8914(2)	2022(3)	836(2)	39(1)*
O(4)	8600(2)	3867(3)	575(2)	44(1)*
O(7)	8748(2)	4083(3)	-570(2)	45(1)*
O(10)	8977(2)	2332(3)	-1020(2)	43(1)*
O(13)	9160(2)	1065(3)	-138(2)	40(1)*
C(2)	8656(4)	2649(5)	1337(3)	56(2)*
C(3)	8889(4)	3639(5)	1167(3)	56(2)*
C(5)	8636(4)	4892(4)	359(3)	60(2)*
C(6)	8334(4)	4882(5)	-269(3)	57(2)*
C(8)	8595(4)	3996(6)	-1201(3)	62(3)*
C(9)	9119(4)	3178(5)	-1418(3)	54(2)*
C(11)	9405(4)	1433(5)	-1163(3)	54(2)*
C(12)	9117(4)	639(5)	-741(3)	49(2)*
C(14)	8889(3)	475(4)	340(3)	37(2)*
C(15)	8756(3)	-543(4)	304(3)	48(2)*
C(16)	8493(4)	-1030(5)	806(3)	56(2)*
C(17)	8342(4)	-522(5)	1336(3)	58(2)*
C(18)	8474(4)	510(5)	1372(3)	52(2)*
C(19)	8758(3)	998(4)	863(3)	39(2)*

\* Equivalent isotropic U defined as one third of the trace of the orthogonalized  $U_{ij}$  tensor

[ScCl<sub>2</sub>(18O6)][SbCl<sub>4</sub>]

Atom coordinates ( $\times 10^4$ ) and isotropic thermal parameters

Atom	x	y	z	U ( $\text{\AA}^2 \times 10^3$ )
Sb(1)	2709.2(8)	2481.7(3)	2348.8(3)	42(1)*
Cl(11)	5340(6)	2442(2)	1838(3)	142(2)*
Cl(12)	145(8)	2940(2)	2928(3)	124(2)*
Cl(13)	1152(7)	1659(2)	1482(2)	151(2)*
Cl(14)	4334(5)	3699(2)	3264(2)	113(2)*
Cl(15)	1747.7(49)	3448.8(15)	1615.3(13)	88(1)*
Cl(16)	3724.2(39)	1911.4(12)	3126.8(11)	66(1)*
Sb(2)	5000	0	5000	38(1)*
Cl(21)	7678(4)	-1888(2)	4735(2)	80(1)*
Cl(22)	5057(5)	624(2)	4694(2)	109(2)*
Cl(23)	3188(6)	-987(2)	4133(2)	149(2)*
Sb(3)	0	5000	0	43(1)*
Cl(31)	146.4(42)	5788.5(16)	1200.8(14)	83(1)*
Cl(32)	-1395(4)	4037(2)	319(2)	82(1)*
Cl(33)	2924.4(26)	4592.3(14)	345.2(17)	80(1)*
Sc(1)	3897.0(17)	1238.2(7)	8755.7(7)	31(1)*
Sc(2)	5539.4(26)	1851.4(12)	8682.9(11)	49(1)*
Cl(2)	2375.2(29)	481.8(12)	9694.2(11)	53(1)*
O(11)	1850(7)	1074(3)	7815(3)	40(2)*
O(14)	2114(7)	2158(3)	8977(3)	44(2)*
O(17)	5152(7)	2051(3)	9805(3)	41(2)*
O(110)	4624(7)	911(3)	8224(3)	40(2)*
O(113)	4307(7)	99(3)	8101(3)	44(2)*
O(116)	494(13)	-452(8)	7251(7)	42(6)*
Cl(12)	261(12)	1650(8)	7834(5)	54(3)*
Cl(13)	220(13)	2007(5)	8614(5)	54(3)*
Cl(19)	2376(12)	2618(5)	9726(5)	56(3)*
Cl(16)	4424(12)	2770(4)	9972(5)	55(3)*
Cl(18)	7085(11)	2031(5)	10105(4)	54(3)*
Cl(19)	7425(12)	1238(5)	9979(4)	54(3)*
Cl(111)	7200(11)	148(4)	8915(5)	53(3)*
Cl(112)	6259(11)	2(4)	8120(5)	49(3)*
Cl(114)	3216(12)	-880(4)	8050(5)	56(3)*
Cl(115)	1833(19)	-802(7)	7396(8)	112(7)*
Cl(117)	298(15)	30(8)	6790(8)	74(4)*
Cl(118)	1441(12)	678(5)	7057(4)	53(3)*
Sc(2)	449.9(19)	3511.7(8)	4003.9(8)	37(1)*
Cl(3)	2884.8(32)	4240.7(12)	5645.9(13)	60(1)*
Cl(4)	-802.2(29)	2753.4(12)	4512.4(12)	55(1)*
O(21)	3177(7)	3360(3)	6829(3)	50(2)*
O(24)	2367(9)	2581(3)	5511(3)	56(2)*
O(27)	-590(9)	2957(3)	4864(3)	55(2)*
O(210)	-1740(8)	4029(3)	5711(3)	55(2)*
O(213)	733(8)	4537(3)	6898(3)	55(2)*
O(216)	4773(12)	4722(3)	7724(3)	56(4)*
Cl(22)	4352(14)	2760(4)	6438(4)	72(4)*
Cl(23)	4317(14)	2628(4)	5835(4)	74(5)*
Cl(29)	3003(17)	2286(6)	1728(8)	78(5)*
Cl(26)	-32(18)	2234(8)	4531(8)	78(5)*
Cl(28)	-2412(14)	3103(4)	4604(4)	72(4)*
Cl(29)	-2582(14)	3898(4)	4952(5)	71(4)*
Cl(211)	-2098(16)	4716(5)	6195(6)	72(4)*
Cl(212)	-1156(14)	6488(5)	5944(5)	67(4)*
Cl(214)	2033(15)	5181(5)	7156(6)	71(4)*
Cl(215)	2349(17)	9201(6)	7851(6)	88(5)*
Cl(217)	4738(14)	4117(7)	8022(6)	90(5)*
Cl(218)	3211(13)	3876(4)	7611(5)	63(4)*

\* Equivalent isotropic U defined as one third of the trace of the orthogonalized U<sub>ij</sub> tensor